



Nanostructured coatings for controlling bacterial biofilms and antibiotic resistance

Kristina Dimitrova Ivanova

A thesis submitted in fulfilment of the requirements for degree of

Doctor of Philosophy

at the

Universitat Politècnica de Catalunya

Supervised by Dr. Tzanko Tzanov

Group of Molecular and Industrial Biotechnology (GBMI)

Department of Chemical Engineering

Universitat Politècnica de Catalunya

Terrassa (Barcelona)

2017

The work carried out during the thesis was financially supported by:



Novel approaches for prevention of biofilms formed on
medical indwelling devices, *e.g. catheters*
FP7-HEALTH-2011-278402

Group of Molecular and Industrial Biotechnology

Terrassa

“My strength is my family”

To the people I love the most,

Stanimir and my parents

Abstract

The accelerated emergence of drug resistant bacteria is one of the most serious problems in healthcare and the difficulties in finding new antibiotics make it even more challenging. To overcome the action of conventional antibiotics bacteria develop effective resistance mechanisms including the formation of biofilms. Biofilms are bacterial communities of cells embedded in a self-produced polymeric matrix commonly found on medical devices such as indwelling catheters. When pathogens adopt this mode of growth on the surface, they effectively circumvent host immune defences and antibiotic therapy, causing severe and life threatening device-related infections.

To reduce the incidence of biofilm-associated infections different strategies, such as often replacement of the device, utilisation of novel materials for its construction and/or design of functional coatings have been suggested. Besides the variable efficiency, they commonly involve the use of large quantities of antibacterials leading to side effects, hypersensitivity, inflammatory responses or emergence of resistance. Thus, new paradigms are urgently needed for more efficient and specific approaches to prevent and treat biofilm infections.

This thesis focuses on the development of advanced nanoscale materials and coatings for controlling clinically relevant bacterial biofilms and the emergence of drug resistance. To this end, acylase and amylase enzymes degrading essential for the biofilm growth components, were innovatively combined into hybrid nanocoatings to impart antibiofilm functionalities onto indwelling medical devices. Alternatively, ultrasound-assisted nanotransformation of antimicrobials was used as a tool for enhancing their antibacterial efficacy and overcoming the intrinsic drug resistant mechanisms in Gram-negative bacteria. These strategies offer new perspectives for prevention and treatment of biofilm infections, limiting the selection and spread of antibiotic resistance.

The first part of the thesis describes the building of enzyme multilayer coatings able to interfere with bacterial quorum sensing (QS) and prevent biofilm establishment on silicone urinary catheters. This was achieved by alternate deposition of negatively charged acylase and oppositely charged polyethylenimine in a Layer-by-Layer (LbL) fashion. The acylase-coated catheters degraded the bacterial signalling molecules and inhibited the QS process of Gram-negative bacteria. These coatings also significantly reduced the biofilm growth on urinary catheters under conditions mimicking the real situation in catheterised patients, without affecting the human cells viability.

Acylase was further combined with the matrix degrading α -amylase enzyme into hybrid multilayer coatings able to interfere simultaneously with bacterial QS signals and biofilm integrity. The LbL assembly of both enzymes into hybrid nanocoatings resulted in stronger biofilm inhibition as a function of acylase or amylase location in the multilayer coating. Hybrid nanocoatings with the QS inhibiting acylase as outermost layer reduced the occurrence of single and multi-species biofilms on silicone catheters *in vitro* and in an *in vivo* animal model.

The thesis also reports on the efficacy of nanomaterials for prevention and eradication of antibiotic resistant biofilms. Multilayer assemblies that contain in their structure and release on demand antibacterial polycationic nanospheres (NSs) were engineered on silicone surfaces. A polycationic aminocellulose (AC) conjugate was first transformed into NSs with enhanced bactericidal activity and then combined with hyaluronic acid to build bacteria-responsive layers on silicone material. When challenged with bacteria these multilayers disassembled gradually inhibiting both planktonic and biofilm modes of bacterial growth.

The same AC NSs were also covalently immobilised on silicone material using epoxy-amine conjugation chemistry. The intact NSs on the silicone material were able to inhibit bacterial colonisation and biofilm growth, suggesting the potential of epoxy-amine curing reaction for generation of stable non-leaching coatings on silicone-based medical devices.

Finally, ultrasound-assisted nanotransformation of clinically relevant antibiotic penicillin G was used as a strategy to boost its activity towards Gram-negative bacteria and their biofilms. The efficient penetration of the spheres within a Langmuir monolayer sustained the theory that NSs are able to cross the membrane and reach the periplasmic space in Gram-negative bacteria where they may exert their bactericidal activity “unrecognised” as a threat by bacteria. In such conditions it is very likely that the selective pressure is reduced and bacteria do not feel the need to defend, expressing resistant phenotypes.

Keywords: enzymes, Layer-by-Layer coatings, sonochemistry, nanospheres, silicone, urinary catheters, quorum quenching, antibacterial activity, biofilm prevention, antibiotic resistance

Table of Contents

Abstract	i
Table of Contents	iii
Abbreviation list	vi
1 Introduction.....	1
2 State-Of-The Art	4
2.1 Bacterial Biofilms Formation	5
2.2 Quorum Sensing in Bacterial Virulence and Biofilm Growth.....	7
2.2.1 Quorum Sensing in Gram-negative Bacteria.....	7
2.2.2 Quorum Sensing in Gram-positive Bacteria	10
2.3 Antibiotic Resistance of Biofilms	12
2.4 Biofilms in Device-Related Infections.....	12
2.5 Current Strategies for Controlling Bacterial Biofilms.....	17
2.6 Layer by Layer assembly: A versatile tool for engineering bacteria resistant materials	18
2.7 Quorum Sensing Inhibitors in Next Generation Antibiofilm Coatings.....	25
2.8 Enzymes in Biofilms Prevention.....	28
2.8.1 Quorum Quenching Enzymes	28
2.8.2 Matrix-degrading Enzymes	29
2.8.3 Enzymes Targeting Bacterial Cells	31
2.8.4 Enzymes Producing Biocides	33
2.9 Nanomaterials for Controlling Bacterial Biofilms	34
2.9.1 Sonochemistry for Synthesis of Nanoparticles	35
2.9.2 Nanoparticles Interaction with Bacteria and Biofilms.....	36
2.9.3 Metal and Metal Oxide Nanoparticles	38
2.9.4 Nanoantibiotics	40
3 Objectives of the Thesis.....	42
4 Materials and Methods.....	45
4.1 Materials and Reagents.....	46
4.2 Bacterial and Human cells	46
4.3 Experimental Methods	47
4.3.1 Enzymatic Degradation of Biofilm Components	47
4.3.2 Enzyme Multilayer Coatings for Prevention of Bacterial Biofilm Formation on Silicone Foley Catheters	48

4.3.3	Nanomaterials for Controlling Planktonic Bacterial Growth and Biofilm Occurrence: Polycationic Aminocellulose Nanospheres.....	57
4.3.4	Covalent Grafting Of Aminocellulose Nanospheres onto Silicone Material for Escherichia Coli Biofilm Prevention	60
4.3.5	Nano-sized Penicillin G for Overcoming Gram-Negative Bacterial Resistance.....	61
5	Results and Discussion.....	67
	68
5.1	Quorum Quenching Acylase in Multilayer Coatings	69
5.1.1	Acylase Induced Degradation of QS Signals	70
5.1.2	Acylase Multilayer Coatings Build-Up onto Silicone and its Characterisation.....	71
5.1.3	Acylase Activity in The Multilayers	74
5.1.4	Functional Properties of the Acylase Multilayer Coatings.....	76
5.1.5	Antibiofilm Efficacy of Acylase Multilayer Coatings in an <i>In Vitro</i> Model of Catheterised Human Bladder.....	79
5.1.6	Biocompatibility Evaluation	80
5.1.7	Conclusions.....	82
5.2	Quorum Quenching and Matrix Degrading Enzymes in Hybrid Multilayer Coatings.....	83
5.2.1	Enzymatic Degradation of Biofilm Matrix Components.....	84
5.2.2	Characterisation of the Multilayer Enzyme Coatings.....	85
5.2.3	Enzymes Activities in the Multilayers	90
5.2.4	Antibiofilm Activity of Enzyme Multilayers in Static Conditions	91
5.2.5	Dynamic Biofilm Inhibition Tests	96
5.2.6	Biocompatibility Tests	99
5.2.7	<i>In Vivo</i> Biofilm Inhibition Tests	100
5.2.8	Conclusions.....	103
5.3	Bacteria-Responsive Multilayer Coatings Comprising Polycationic Nanospheres.....	105
5.3.1	Assembling Of the Multilayer Coatings	106
5.3.2	Characterisation of the Coated Silicone Materials.....	108
5.3.3	Antimicrobial Action upon Bacteria-Induced Degradation of Coatings..	112
5.3.4	Antibiofilm Properties of the Layered Assemblies	114
5.3.5	Conclusions.....	118
5.4	Covalent Grafting Of Aminocellulose Nanospheres onto Silicone Material..	119
5.4.1	Inhibition of <i>E. Coli</i> Biofilms – Proof of Concept.....	120

5.4.2	Incorporation of Cationic Nanospheres onto Silicone Material	121
5.4.3	Functional Properties	124
5.4.4	Conclusions.....	127
5.5	Nano-sized Penicillin G for Overcoming Gram- Negative Bacterial Resistance 128	
5.5.1	Antibacterial Activity of Penicillin G towards Gram-negative Bacteria.....	129
5.5.2	Penicillin Nanospheres Preparation and Characterisation	130
5.5.3	Antibacterial and Antibiofilm Activities	132
5.5.4	Interaction with Bacterial Cell Membrane	135
5.5.5	Cytotoxicity with Mammalian Cells.....	139
5.5.6	Conclusions.....	140
6	Conclusions and Future Plans	142
6.1	Final conclusions	143
6.2	Future Perspectives.....	145
	Bibliography	146
	Appendix: Scientific Contribution	165

Abbreviation list

A

ANOVA	a one way analysis of variance
AgNPs	silver nanoparticles
Agr	accessory gene regulator
ACP	acyl-acyl carrier protein
AHL	acyl-homoserine lactones
ATCC	American type culture collection
AC	aminocellulose
ACNSs	aminocellulose nanospheres
APTES	(3-aminopropyl)triethoxysilane
A. melleus	Aspergillus melleus
AFM	atomic force microscopy
ATR-FTIR	attenuated total reflection-Fourier transform infrared
Als	autoinducers
AIPs	auto-inducing peptides
pro-AIP	auto-inducing peptide precursor

B

BSA	bovine serum albumin
-----	----------------------

C

C. violaceum	Chromobacterium violaceum
C. albicans	Candida albicans
CAUTIs	catheters-associated urinary tract infections
CECT	Spanish type culture collection
CFU	colony-forming unit
CV	crystal violet
C4-DL-HL	N-butyryl-DL-homoserine lactone
C6-DL-HL	N-hexanoyl-DL-homoserine lactone

D

D. pulchra	Delisea pulchra
DHPs	dihydropyrrolones
DMSO	dimethyl sulfoxide
DNA	deoxyribonucleic acid
DNSA	3,5-dinitrosalicylic acid
DMEM	Dulbecco's modified Eagle's medium

DLS	dynamic light scattering
E	
<i>E. faecalis</i>	<i>Enterococcus faecalis</i>
<i>E. coli</i>	<i>Escherichia coli</i>
EtOH	ethanol
EPS	exopolysaccharide
eDNA	extracellular deoxyribonucleic acid
EPM	extracellular polymeric matrix
F	
FITC	fluorescein isothiocyanate
G	
GOPTS	3-(glycidoxypropyl) trimethoxysilane
H	
HPLC	high-performance liquid chromatography
HTP	high-throughput assay
HL	homoserine lactone
HA	hyaluronic acid
HCl	hydrochloric acid
I	
IMDs	indwelling medical devices
K	
<i>K. pneumoniae</i>	<i>Klebsiella pneumoniae</i>
L	
LbL	Layer-by-Layer
LB	Luria Bertani Broth
M	
<i>M. luteus</i>	<i>Micrococcus luteus</i>
MBEC	Minimum Biofilm Eradication Concentration
N	
NaCl	sodium chloride
NAMET	N-acetyl-L-methionine
NaPB	sodium phosphate buffer

NSs	nanospheres
NCs	nanocapsules
NPs	nanoparticles
NB	nutrient broth
O	
(3-oxo-C10-L-HL)	3-oxo-C10-L-HL N-(3-Oxodecanoyl)-L-homoserine lactone
(3-oxo-C12-L-HL)	3-oxo-C12-L-HL N-(3-Oxododecanoyl)-L-homoserine
P	
PBS	phosphate buffered saline
PAA	poly(acrylic acid)
PAH	poly(allylamine hydrochloride)
PE	L- α -Phosphatidylethanolamine phospholipid
PEG	poly(ethylene glycol)
PGA	poly(L-glutamic acid)
PLL	poly(L-lysine)
PMMA	poly(methacrylic acid)
PDMS	polydimethyl/vinylmethyl siloxane
PEO	polyethylene oxide
PEI	polyethyleneimine
(p-NBP)	4-(para-nitrobenzyl) pyridine
PPO	polypropylene oxide
PSS	polystyrene sulfonate
P. mirabilis	Proteus mirabilis
P. aeruginosa	Pseudomonas aeruginosa
Q	
QCM-D	quartz crystal microbalance with dissipation
QQ	quorum quenching
QS	quorum sensing
QSIs	quorum sensing inhibitors
R	
ROS	reactive oxygen species
RT	room temperature
S	
SEM	scanning electron microscopy

SiO ₂ NPs	silica nanoparticles
SDS	sodium dodecyl sulfate
S. aureus	Staphylococcus aureus
S. epidermidis	Staphylococcus epidermidis
S. mutans	Streptococcus mutans

T

TET	tetracycline
TETNPs	tetracycline nanoparticles
TSB	tryptic soy broth

U

UV	ultraviolet
UTIs	urinary tract infections

V

V. fischeri	Vibrio fischeri
V. harveyi	Vibrio harveyi

Z

ZnO	zinc oxide
-----	------------

Figure, Table and Scheme Captions

Figure 2.1 Biofilm growth cycle. Once planktonic bacteria are attached to a surface, the secretion of matrix components begins leading to mature biofilm formation. The biofilm growth cycle finishes when the bacteria and parts of the biofilm structure are dispersed towards the surrounding environment for colonisation of other sites..... 7

Figure 2.2 Quorum sensing in Gram-negative bacteria. A) Bacteria secrete acyl homoserine lactones (AHLs, orange circle) that in threshold concentrations penetrate into the cells and activate the cognate signal receptor, inducing the QS-regulated production of virulence factors and biofilm formation. B) Chemical structure of AHL signalling molecules secreted and detected by most Gram-negative bacteria..... 9

Figure 2.3 Quorum sensing in Gram-positive bacteria. A) Initially, bacteria synthesize auto-inducing peptide (AIP) signals as precursors (pro-AIP) in the cells that are further transformed into mature AIPs (grey rhomboids) during their transportation through membrane transporters. These AIPs then interact with a transmembrane histidine kinase receptor activating the target genes expression via autophosphorylation of the cognate transcriptional regulator. B) Chemical structure of the AIP signals produced by *S. aureus*, *S. mutants* and *B. subtilis*. 11

Figure 2.4 Schematic representation of Foley urinary catheter..... 15

Figure 2.5 A) Schematic representation of the LbL assembling of oppositely charged polyelectrolytes (left). Three major classes of multilayer coatings with antibacterial functionalities have been engineered (right): antiadhesive that inhibits the attachment of pathogens, contact-killing coatings that explore antimicrobial agents on the surface, and biocide-releasing to deliver antibacterials and kill bacteria in the supernatant. PEG-poly(ethylene glycol), purple ellipse (live cells), red ellipse (dead cells)..... 20

Figure 2.6 Enzymatic degradation of AHL signals by lactonase, acylase and oxidoreductase. 29

Figure 2.7 Schematic representation of the mechanisms involved in the NPs (red circles) interaction with free floating and sessile bacterial cells. In mature biofilms the NPs efficiency is altered by the exchange with matrix compounds resulting in NPs aggregation or interfacial interaction with biofilm cells (adapted from [247]). 38

Figure 5.1 A) AHL degradation by acylase assessed with fluorescamine method and B) C6-DL-HL degradation study using the *C. violaceum* CECT 5999..... 71

Figure 5.2 A) Non-treated and APTES-treated silicone sheets after incubation in 1mL of 2 % ninhydrin solution. The formation of characteristic Ruhemann's purple demonstrated the presence of amino groups on the surface. B) ATR–FTIR spectra of non-treated and APTES-treated silicone. Two dominating vibrational modes around 1575 and 1485 cm^{-1} appeared in the FTIR spectra of the APTES-treated samples. ... 72

Figure 5.3 Representative FTIR-ATR spectra of (a) untreated silicone and (b) acylase multilayer coatings. 73

Figure 5.4 AFM (2D and 3D topographic) and water contact angle images of untreated silicone before APTES functionalisation and acylase multilayer coatings. 74

Figure 5.5 Violacein production by *C. violaceum* CECT 5999 in presence of free acylase solution and acylase multilayer coatings on silicone. The control - untreated silicone was set as 100% violacein production. 75

Figure 5.6 A) Initial adhesion of *P. aeruginosa* on untreated silicone and acylase multilayer coatings after 3-h contact ($\times 40$ magnification). B) Fluorescence microscopy images of 24 h-old *P. aeruginosa* biofilms (formed in static conditions) on untreated silicone and acylase multilayer coatings analyzed after Live/Dead staining ($\times 20$ magnification). 77

Figure 5.7 Inhibition of *P. aeruginosa* planktonic growth in the presence of untreated silicone and acylase multilayer coatings. 78

Figure 5.8 Crystal violet assessment of biofilm formation of *P. aeruginosa* on untreated silicone and acylase multilayer coatings after incubation in artificial urine for 1 and 7 days. 79

Figure 5.9 A) Microscopic images of untreated and acylase coated Foley catheters after 7 days incubation in dynamic bladder model system (40x magnification); B) Crystal violet assessment of total biomass formed on urinary catheters: untreated and acylase multilayer coatings on silicone Foley catheter. 80

Figure 5.10 Viability of fibroblasts (BJ5ta) after being in contact with untreated silicone and acylase multilayer coatings: 1 day and 7 days. 81

Figure 5.11 *In vitro* degradation of model exopolysaccharide components of bacterial biofilm matrix by α -amylase. 85

Figure 5.12 A) ATR-FTIR spectra of a) pristine silicone, and multilayer assemblies: b) LbL Acy, c) LbL Amy, d) LbL Hyb-Acy and e) LbL Hyb-Amy; and B) normalised LbL Amy spectra: non-washed (dot line), washed (solid line)..... 86

Figure 5.13 AFM images of A) pristine silicone surface and enzyme-coated silicone: B) LbL Amy, C) LbL Acy, D) LbL Hyb-Acy and E) LbL Hyb-Amy 87

Figure 5.14 A) Cumulative fluorescence intensity vs. time of incubation for: LbL Amy (▪), LbL Acy (●), LbL Hyb-Acy and (Δ)LbL Hyb-Amy (○). B) Microscopic images of FITC labelled LbL Hyb-Amy coatings before (0 days) and after (7 days) incubation in artificial urine. 89

Figure 5.15 A) Quantification of violacein production in presence of acylase and acylase/amylase comprising coatings. B) EPS-induced degradation by α -amylase comprising silicone samples. 91

Figure 5.16 (A) Inhibition (%) of single-species (*P. aeruginosa* and *S. aureus*) and dual-species (*P. aeruginosa* and *E. coli*) biofilm formation on enzyme coated silicone catheters. Stars represent the statistical differences between the different groups of samples; $p < 0.05$. (B) Fluorescence microscopy images of *P. aeruginosa* biofilms grown for 24 h on pristine and enzyme-coated silicone materials analysed after Live/Dead staining. (C) Fluorescence microscopy images of *S. aureus* biofilms grown for 24 h. (D) Fluorescence microscopy images of mixed *P. aeruginosa* and *E. coli* biofilms. The green and red fluorescence images are overlaid in one picture for better comparison of live and dead cells, respectively..... 94

Figure 5.17 Planktonic growth of Gram-negative *P. aeruginosa*, Gram-positive *S. aureus*, and mixed inoculum of *P. aeruginosa* and *E. coli* in the presence of pristine silicone and multilayer enzyme coatings. 95

Figure 5.18 *P. aeruginosa* biofilm growth on pristine silicone and polyethyleneimine/bovine serum albumin (PEI/BSA) multilayer coatings 96

Figure 5.19 Biofilm inhibition tests of *in vitro* catheterized bladder model system. (A) Inhibition of *P. aeruginosa*, *S. aureus*, and mixed species (*P. aeruginosa* and *E. coli*) biofilm formation on enzyme-coated silicone urinary catheters assessed with CV. Stars represent the statistical differences between the different groups of samples; $p < 0.05$. (B) Fluorescence microscopy images of live (green) and dead (red) bacteria in biofilms

grown for 7 days on pristine and enzyme-coated silicone Foley catheter shaft. The green and red fluorescence images are overlaid in one picture for better comparison.99

Figure 5.20 Biofilm formation in *in vivo* rabbit model. A) Representative images of the control catheter and enzymes coated silicone urinary catheters and B) Total biomass formation after 7 days of catheterisation. 101

Figure 5.21 Representative frequency and dissipation changes obtained for the LbL build-up onto amino-functionalised gold surfaces using ACsol (A1) or ACNSs (B1) as polycations and the respective $\Delta D/\Delta F$ plots for the same experiments (A2 and B2). Schematic presentation of these build ups (A3 and B3) based on the obtained data – HA in green, water in red and ACsol/ACNSs in blue. The presented data are for the 7th overtone..... 107

Figure 5.22 A) Representative FTIR spectra of silicone control (silicone-APTES) with dotted line and multilayer assemblies on silicone: HA-ACsol specimens with dashed lines and HA-ACNSs specimens with full lines. B) Water contact angles of HA/AC coatings deposited onto silicone. Statistical difference in the case of $(HA/AC_{sol})_{10}$ is related to the pristine silicone and represented as $**p < 0.01$. Images of water contact angle measurements are given for each specimen. 109

Figure 5.23 (A) AFM images ($5 \times 5 \mu m^2$) of $(HA/ACsol)_{10}$ and $(HA/ACNSs)_{10}$ deposited onto silicone strips. (B) Cross-section and (C) top view of the same samples taken with SEM..... 110

Figure 5.24 SEM images of $(HA/ACNSs)_{100}$ deposited onto silicone: (A) side view, (B) top view, (C) view at 60° with a cut, and (D) magnified zone of the cut. 111

Figure 5.25 Antibacterial activity of silicone coated with HA/ACsol and HA/ACNSs against *P. aeruginosa* as compared to pristine silicone. Statistical differences are represented as $***p < 0.001$ 113

Figure 5.26 Fluorescence microscopy (20x magnification) of $(HA/ACNSs)_{10}$ coating incubated for 6 and 24 h in the absence and presence of *P. aeruginosa*. Scale bars 100 μm 114

Figure 5.27 Fluorescence microscopy images (20x magnification) of *P. aeruginosa* biofilms on non-treated and silicone coated with HA/ACsol and HA/ACNSs, analysed after Live/Dead staining. Scale bars 100 μm 116

Figure 5.28 Photos and fluorescence microscopy images (20x magnification) of the shaft and balloon sections of untreated Foley catheter (top row) and catheter coated with (HA/ACNSs) ₁₀ (bottom row) after a 7 day incubation in a dynamic bladder model system with <i>P. aeruginosa</i> . Scale bars 100 µm.....	117
Figure 5.29 <i>E. coli</i> biofilm formation on polystyrene surface assessed by: A) crystal violet assay (the OD ₅₉₅ is directly proportional to the amount of total biomass formed) and B) Live/dead cells viability kit (ACsol left and AC NS on the right). The green and red fluorescence are overlaid in for better comparison of live and dead cells. Scale bar indicate 100 µm.	121
Figure 5.30 ATR-FTIR spectra of non-treated silicone (blue line), silicone (black line) epoxy silicone treated with ACNSs at pH 6 (red line).	123
Figure 5.31 SEM images of ACNSs functionalised silicone surface at pH 3 and 6. ...	124
Figure 5.32 <i>E. coli</i> biofilm formation on epoxy-treated silicone decorated with ACNSs and unmodified silicone assessed by: A) crystal violet assay (the OD595 is directly proportional to the amount of total biomass formed) and B) Live/dead cells viability kit. The green and red fluorescence images are overlaid for better comparison of live and dead cells. Scale bar indicate 100 µm.....	125
Figure 5.33 <i>P. aeruginosa</i> , <i>E. coli</i> and <i>S. aureus</i> growth after 24 h incubation with Penicillin G.....	129
Figure 5.34 A) Dynamic light scattering, and B) scanning electron microscopy images of nanopenicillin.	131
Figure 5.35 FTIR spectra of lyophilized penicillin, nanopenicillin, surfactant (poloxamer) and oil.	132
Figure 5.36 Antimicrobial activity of 125 µg/mL penicillin and nanopenicillin on <i>E. coli</i> and <i>P. aeruginosa</i> after 24 h contact.	133
Figure 5.37 Fluorescence microscopy live/dead images of 24 h grown <i>P. aeruginosa</i> and <i>E. coli</i> biofilms incubated with 125 µg/mL penicillin, nanopenicillin and control NSs (live cells are represented in green and dead cells in red). Scale bars denote 100 micron.....	134

Figure 5.38 A) Surface pressure-area isotherms (or surface activity) and schematic representation of the nanospheres surface activity upon Langmuir compression; B) Surface pressure-area isotherm of <i>E. coli</i> PE monolayer (the area per molecule in X-axe refers to <i>E. coli</i> PE) in water with 0.5 µg/mL penicillin in solution, nanopenicillin and control NSs and schematic representation of the NSs interaction with the a Langmuir monolayer upon compression; and C) kinetic adsorption process resulting from the incorporation of 0.2 µg/mL (final concentration) penicillin, nanopenicillin and control NSs onto the air/water interface of <i>E. coli</i> PE monolayer at a surface pressure of 30 mN/m and schematic representation of the incorporation of the spheres in the subphase beneath the phospholipid monolayer built at 30 mN/m.	136
Figure 5.39 Relative viabilities (%) of human fibroblasts exposed to 250 µg/mL and 125 µg/mL penicillin and nanopenicillin for 24 h.	139
Table 2.1 Medical devices and biofilm-related diseases.	13
Table 5.1 Protein content on silicone surface.	88
Table 5.2 Viable human fibroblasts (BJ5ta) after 7 days of contact with silicone samples	100
Table 5.3 Antibacterial activity of silicone coated with HA/ACsol and HA/ACNSs against <i>P. aeruginosa</i>	113
Table 5.4 Viable cells within <i>P. aeruginosa</i> and <i>E. coli</i> biofilms before (control) and after applying 125 µg/mL of penicillin, nanopenicillin and control NSs.....	135
Table 5.5 Maximum compression modulus of <i>E. coli</i> PE monolayers with water, penicillin, nanopenicillin and control NSs in the subphase.	138
Scheme 4.1 LbL assembly of acylase on the silicone catheters.	49
Scheme 4.2 Physical glass model of catheterised bladder used in dynamic biofilm inhibition tests.	55
Scheme 4.3 Nanospheres formation via one-step sonochemical process.	57
Scheme 4.4 LbL assembly of aminocellulose nanospheres (ACNSs) on the catheters surface.....	58

Scheme 4.5 Inoculation of Minimum Biofilm Eradication Concentration (MBEC™) High-throughput (HTP) assay kit. A fresh sub-culture of *P. aeruginosa* or *E. coli* was used to create an inoculum with OD₆₀₀ = 0.28. The bacterial suspension was diluted with TSB (1:30) and 22 ml of dilution were added to the trough of the MBEC™-HTP device. The device was placed at 37 °C with shaking to assist the formation of biofilms on the polystyrene pegs. After washing with 0.9 % NaCl, pH 6.5, the lid with the developed biofilm was transferred to another plate containing different concentrations of penicillin G solution and nanospheres..... 65

Scheme 5.1 Strategy used to functionalise silicone material: chemisorption of GOPTS followed by the reaction of epoxy groups with ACNSs using the epoxy-amine curing method and evaluation of the colour of silicone after reaction with p-NBP to assess the efficiency of epoxy immobilisation..... 122

Scheme 5.2 Schematic representation of the interaction of nanopenicillin and penicillin G onto: A) the gram-negative bacterial cell wall and B) the biofilm structure. 141

1 Introduction

For most of the history of microbiology, bacteria have been simply viewed as freely suspended single cells often referred as planktonic. However, towards the end of the 20th century it became clear that bacteria thrive predominantly in surface attached communities of cells embedded within self-produced extracellular polymeric matrix (EPM) known as biofilms [1].

Although traditionally regarded as environmental phenomenon, nowadays biofilm growth is widely considered one of the major virulence attributes of bacteria and fungi that play a pivotal role during the pathogenesis [2, 3]. Biofilm may form on any foreign object inserted into the human body as well as in any place in the body where the host defence is compromised, such as in the lungs of patients with cystic fibrosis, or in chronic wounds with impaired blood supply [4]. When established on sutures, catheters, heart valves, implants, and intrauterine devices the biofilms usually cause severe chronic infection and subsequent tissue destruction, as well as systemic dissemination of the pathogen and dysfunction of the device [5, 6]. Whereas free floating bacterial cells can be eradicated by the action of antibacterials and host immune responses, the biofilm encased communities of bacteria frequently survive the treatment and can cause infection recurrence. In most cases, the treatment of biofilm-related diseases requires surgical removal of the contaminated device and affected areas in combination with intensive antibiotic therapy [7]. However, the innate or acquired resistance of bacteria to antimicrobials and immune defence mechanisms often impairs the conventional therapy resulting in increased time of hospitalization and health care costs, and ultimately in significant mortality and morbidity [8, 9]. Hence, instead of treating the consequences, the efforts are currently directed towards the development of preventive strategies to reduce the high incidence of device-related infections [13].

Various physical and chemical methods including flushing, chlorination, and ultraviolet (UV) disinfection, have been applied to control bacterial contamination and biofilms occurrence on medical devices and equipment [10] [11, 12]. More recently antimicrobial coatings with variable efficiency in preventing biofilms, by either killing the pathogens or inhibiting bacterial growth and reproduction, have been developed [13-18]. Despite some promising results, most antibacterial agents eventually increase the risk of resistance development.

Advances in the biofilm research have led to new insights into the mechanisms of biofilm establishment that marked an important progress in the development of novel strategies to address bacterial biofilm challenge. Enzymatic based approaches have been suggested as a valuable alternative to control biofilms. Enzymes have been

successfully explored for the inhibition of bacterial virulence and surface adherence as well as elimination of clinically relevant biofilms. Whereas the conventional antibiotics exert substantial evolutionary stress on bacterial population by targeting different intracellular components, the antibiofilm active enzymes use other eradicating mechanisms, which reduce the selection for resistance strains. Another very promising approach utilises nanotechnology to form highly efficacious nanostructures of currently available antimicrobials with enhanced functionality. The assemblies of the molecules at nanometer scale have unique properties, differing from those of the free molecules and the bulk materials with the same composition. Nano-size transformation of current bactericides could be considered a straightforward method to improve the treatment of severe infections and viable alternative to reduce the time- and resource-consuming screening for new drugs.

The main goal of this thesis is to develop nanostructured materials for prevention and eradication of bacterial biofilms limiting the selection and spread of drug resistance. To achieve this, innovative platforms of enzymes and NSs for coating of medical devices were designed. Enzymes interfering with bacterial cooperative behaviours and essential biofilm adhesives are innovatively integrated into multilayer nanocoatings expected to reduce the incidence of catheter-associated biofilm infections. Sonochemically engineered NSs of bactericides are proposed as novel tools for eradicating medically relevant bacteria. We opted for altering the form and enhancing the interaction of existing antibacterials with bacterial cells and biofilms to improve the treatment efficiency, instead of screening for new drug entities.

2 State-Of-The Art

2.1 Bacterial Biofilms Formation

Wherever a suitable surface, moisture and nutrients are available, free floating bacteria are likely to exist in the form of complex biofilm structures of cells embedded within the self-produced EPM [19, 20]. Bacterial biofilms are not just passive assembly of cells attached to a substratum or to each other, but rather structured, coordinated, communities with distinct architectures and properties [6, 21]. These sessile bacterial communities are ubiquitous in nature and possess the sophisticated ability to rapidly adapt and propagate in a wide variety of habitats. While in some case biofilms provide significant benefits to the human health forming protective layers on the body tissues against pathogenic microorganisms, more and more evidences highlight their role in the occurrence of life-threatening infections [22]. During the adaptation to biofilm lifestyle hundreds of genes are differentially expressed to introduce changes in phenotypic and genotypic pattern, making the population more resistant to currently available antimicrobials and host immune system. The significance of biofilms for human health has stimulated the efforts to understand the mechanism of biofilm formation in order to open a new axis of customizing measures highly effective against bacteria and their biofilm forms.

The formation of microbial biofilms can be described in three main stages - attachment, growth (maturation), and detachment. Initially, bacteria attach to a living or non-living surface where they proliferate and form a characteristic three dimensional structure, the second stage. During the third stage, planktonic cells detach from the biofilm, as a result of either cell growth or removal of biofilm aggregates, and colonize other sites away from the original site of infection (Figure 2.1) [23]. An important step for biofilm establishment on medical devices is the adherence of free floating cells to the so called "surface conditioning layer". This conditioning layer comprises: biomolecules such as proteins (e.g. fibronectin, fibrinogen, and collagen), lipids, polysaccharides, and inorganic salts that modify the physical and chemical properties of the material and serve as source of nutritive substances and microelements [13]. When bacteria approach that layer, they first interact with the biomolecules through specific receptors and then irreversibly adhere to the surface [24]. Upon attachment, they start to grow and expand, forming small microcolonies of cells of the same species or other bacterial species and microorganisms according to the environmental parameters. Further changes in genes expression allow cells to replicate and establish functional community encased in protective EPM [3].

Biofilm EPM comprises variety of compounds including polysaccharides, proteins, nucleic acids, uronic acid and humic substances that originate from both the bacteria

and surrounding environment [25-27]. Among all, matrix exopolysaccharides (EPS) are integral part of the biofilm structure and provide diverse benefits for bacterial populations within the mature stage [21]. They assist bacteria to strongly adhere to a multitude of different surfaces, provide protection from a wide range of host and environmental factors (e.g. immune effectors, antimicrobials, predators), serve as reservoirs for nutrient acquisition and help the formation of three-dimensional biofilm architecture. Even though being a part of similar microbial communities, it is quite possible that under specific environmental conditions bacteria elaborate multiple EPS with different structure and functional roles [28, 29]. For example, in a response to environmental stressors, e.g. dehydration and osmotic stress, the biofilm forming *Escherichia coli* and *Pseudomonas aeruginosa* species produce significant amounts of colonic acid and alginate, respectively [29-31]. *P. aeruginosa* also utilise the polysaccharides Pel and Psl which are very important for the cells attachment to the surface as well as biofilm firmness and stability. However, the regulation and expression of alginate, Pel and Psl as well as their functional role in the biofilm maturation can vary drastically among the different strains [32].

Mature biofilm is often observed as three dimensional, mushroom- or tower-like, structure of matrix-enclosed cells organised in accordance with their metabolism and aero tolerance [9, 29]. Its architecture is very heterogeneous in space and time, containing microcolonies of cells, separated by water channels allowing the transport of nutrients, oxygen, and even antimicrobial agents [33]. At the last step of biofilm life cycle, bacteria become motile again, disperse from the community to colonise distal sites and initiate new biofilm growth (Figure 2.1) [9, 34]. The biofilm dispersion is in response to the starvation conditions or overcrowding, which take place because of the: i) production of EPM - degrading enzymes, lithic activation of bacteriophages, expression of phosphodiesterase and specific signals, and ii) passive detachment of biofilm fragments or cells mediated by shear forces, abrasion, human factors and predation over bacteria in the biofilm [34].

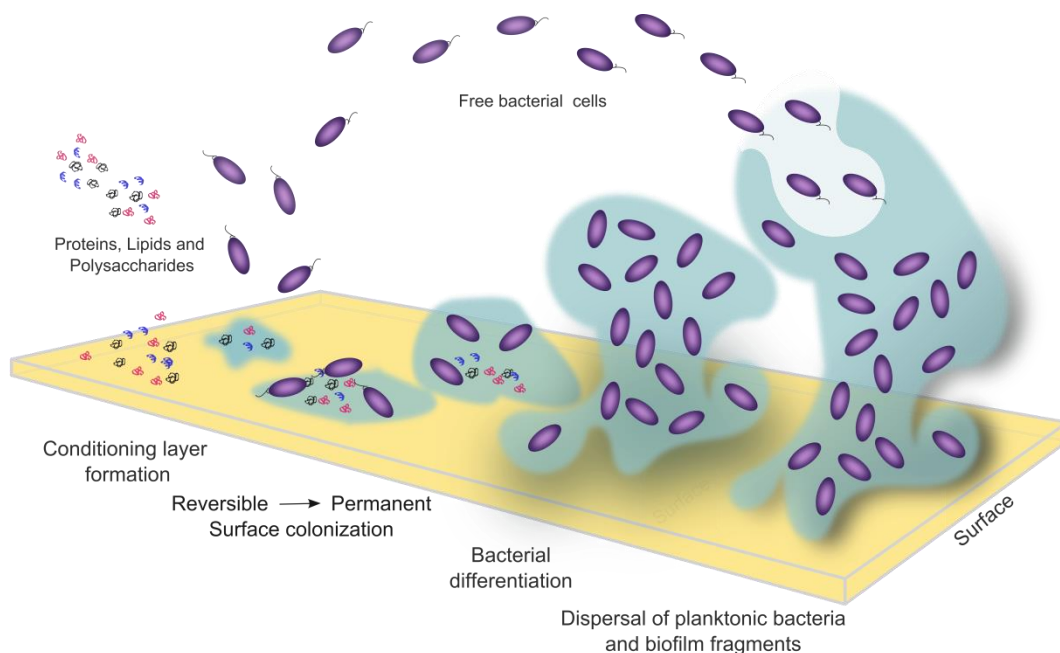


Figure 2.1 Biofilm growth cycle. Once planktonic bacteria are attached to a surface, the secretion of matrix components begins leading to mature biofilm formation. The biofilm growth cycle finishes when the bacteria and parts of the biofilm structure are dispersed towards the surrounding environment for colonisation of other sites.

2.2 Quorum Sensing in Bacterial Virulence and Biofilm Growth

There are growing evidences that pathogens are able to switch from free-swimming cells to a surface-attached lifestyle by sensing the changes in the environmental conditions [35-37]. At certain population density, bacteria sense the presence of other bacterial cells in the surrounding and act as multicellular organisms through the QS process [38]. QS is a communication process mediated by small diffusible hormone like molecules, called autoinducers (AIs). This process differs greatly from microorganism to microorganism, depending on the bacterium group (Gram-positive or Gram-negative), the type of signalling molecules and signal transduction system [38, 39].

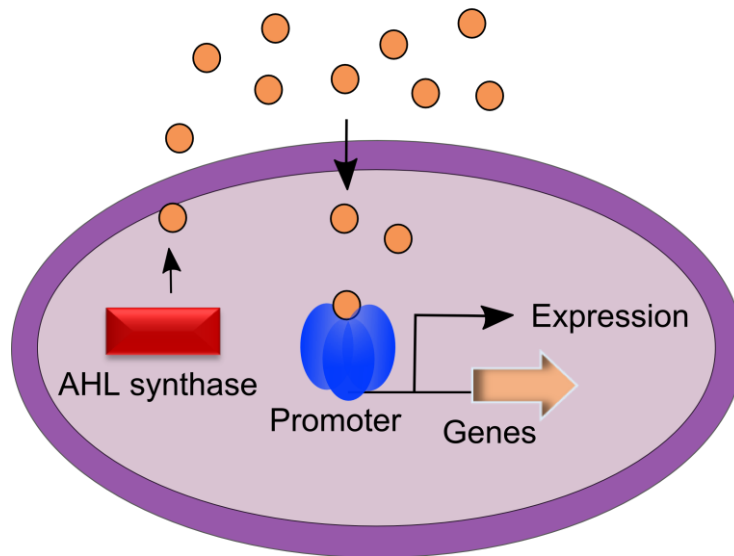
2.2.1 Quorum Sensing in Gram-negative Bacteria

Gram-negative bacteria use acyl-homoserine lactones (AHLs) whereas Gram-positive bacteria utilize peptides or cyclic oligopeptide signals, called autoinducing peptides (AIPs), as the primary signalling molecules (Figure 2.2) [40, 41]. AHLs molecules consist of homoserine lactone (HL) ring and fatty acid side chain, varying in length (C4 to C18), saturation, and oxidation at C3 position (Figure 2.2) [42]. They are produced by intracellular synthases (LuxI homologues of *Vibrio fischeri*) through an acylation reaction of adenosyl-methionine, which is the source for HL formation, and acyl-acyl

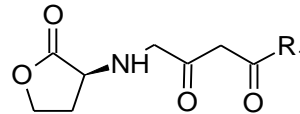
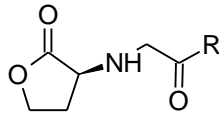
carrier protein (ACP), the source of fatty acid AHL side chain. The AHL signals accumulate in the surrounding environment and when reach high concentrations (i.e. threshold levels) they bind to cognate cytoplasmic transcriptional regulators, which are LuxR type proteins, inducing target genes expression (Figure 2.2A) [43]. This results in the activation of specific quorum responses (e.g. virulence factors production, biofilm formation, bioluminescence and etc.) and positive regulation of the intracellular synthetase by the signals which will then provide more AHLs for the expression of QS-related genes.

The QS signalling systems in some Gram-negative bacteria are usually more complicated than described above. Extensive studies have been carried out to understand the QS pathways of pathogenic *P. aeruginosa*, which exploit four types of QS systems associated with the induction of different virulence phenotypes [44]. Two of these QS systems, known as *las* and *rhl*, are AHL based and use 3-oxo-C12-HSL and C4-HSL signals to regulate the production and secretion of various virulence factors including elastase, exotoxin A, pyocyanin, and biofilm formation [45, 46]. The other systems, named *pqs* and *iqs*, use another class of signalling molecules which are known as 2,2-heptyl-3-hydroxy-4(1H)-quinolone (PQS) and 2-(2-hydroxyphenyl)-thiazole-4-carbaldehyde, respectively [47, 48]. All these systems are hierarchically arranged, being the *las* at the top of the QS control. The sophisticated QS circuit in *P. aeruginosa* is extremely adaptable and can respond to distinct environmental stress cues, providing high flexibility of its pathogenesis [49]. Despite the complex QS network in *P. aeruginosa*, most pathogenic Gram-negative species possesses a single AI based QS system that comprise one type AHL synthase and cognate transcription regulator.

A



● Acyl-homoserine lactones (AHLs)



R=C₃H₇

P. aeruginosa; *Aeromonas hydrophila*; *V. fischeri*; *Erwinia carotovora*; *Erwinia chrysanthemi* [45, 50]

R=C₃H₆OH

Vibrio harveyi [51]

R= C₅H₁₁

Chromobacterium violaceum;
Pseudomonas aureofaciens; *Yersinia pseudotuberculosis* [52-54]

R=C₇H₁₅

V. fischeri; *Burkholderia cenocepacia* [55, 56]

R₁=C₃H₇

V. fischeri; *Erwinia carotovora*; *Erwinia chrysanthemi* [55, 57, 58]

R₁=C₅H₇

Agrobacterium tumefaciens [59]

R₁=C₇H₁₅

Pseudomonas putida; *Yersinia pestis* [60, 61]

R₁=C₉H₁₉

P. aeruginosa [45]

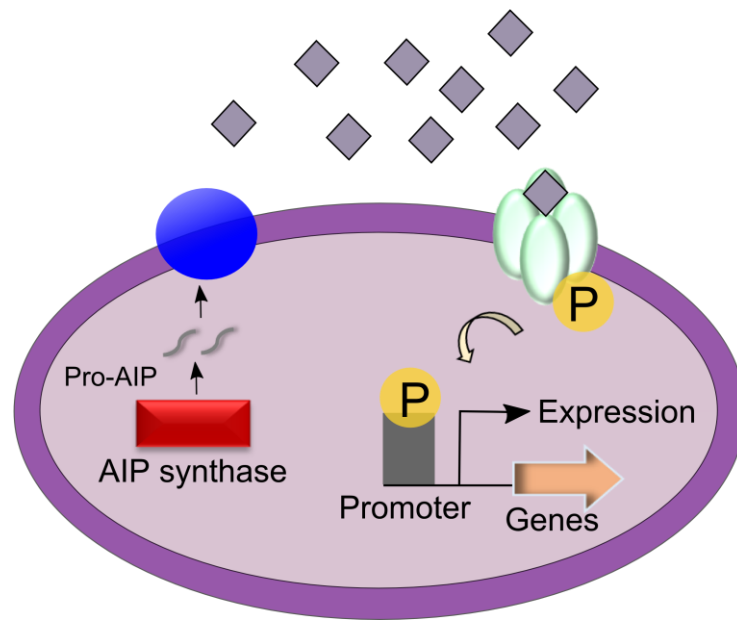
Figure 2.2 Quorum sensing in Gram-negative bacteria. A) Bacteria secrete acyl homoserine lactones (AHLs, orange circle) that in threshold concentrations penetrate into the cells and activate the cognate signal receptor, inducing the QS-regulated production of virulence factors and biofilm formation. B) Chemical structure of AHL signalling molecules secreted and detected by most Gram-negative bacteria.

2.2.2 Quorum Sensing in Gram-positive Bacteria

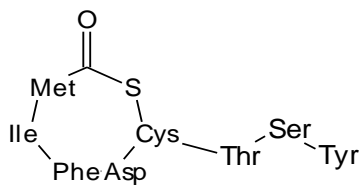
Gram-positive bacteria use linear or cyclic AIPs, as the primary means of signalling molecules and two component signal transduction systems as the main quorum mechanism (Figure 2.3) [62]. AIP signals are synthesised in bacterial cells as precursors (pro-AIP) and excreted through specialized membrane-bound AIP transporters. During the pro-AIPs transportation through the membrane these transporters process the signal in sizes that vary from 5 to 17 amino acids [63, 64]. At threshold concentrations, the already mature AIP signals specifically bind to and activate two-component histidine kinase receptor located in the cell membrane of Gram-positive bacteria. The activation of the histidine kinase then results in phosphorylation of cognate response regulator protein, which modulates the target genes expression of a wide range of bacterial phenotypes (Figure 2.3) [33]. Several AIP based QS signal transduction systems have been well studied such as the accessory gene regulator (*agr*) system of *Staphylococcus aureus* and *agr*-like system of *Enterococcus faecalis*. The *agr* signalling system in *S. aureus* uses four different types of thiolactone-containing peptides, namely AIP I, AIP II, AIP III and AIP IV and represent an attractive target for the attenuation of QS regulated virulent behaviours (Figure 2.3).

Besides being able to communicate with members of the same species via AHLs or AIPs signals, bacteria may also communicate with members of other species, using specific signal molecules, known as AIs-2 [65-67]. These signals are obtained from 4,5-dihydroxy-2,3-pentanedione, produced by LuxS enzyme and consequently recognized by the interspecies LuxP and LsrB receptors found in *V. harveyi* and *Salmonella typhimurium*, respectively [38].

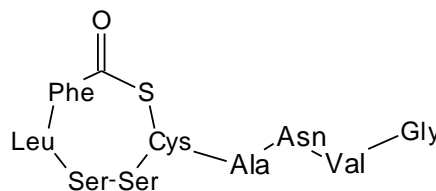
A



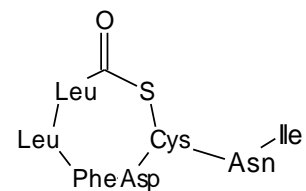
◆ **Auto-inducing peptides (AIPs)**



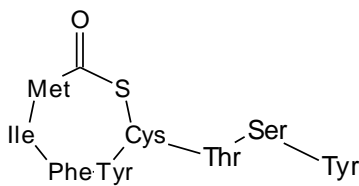
AIP-I



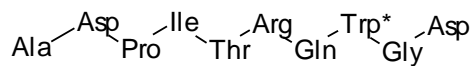
AIP-II



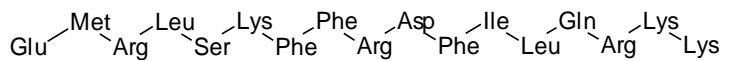
AIP-III



AIP-IV



ComX (*B. subtilis*) [68]



CSP (*Streptococcus mutans*) [69]

Figure 2.3 Quorum sensing in Gram-positive bacteria. A) Initially, bacteria synthesize auto-inducing peptide (AIP) signals as precursors (pro-AIP) in the cells that are further transformed into mature AIPs (grey rhomboids) during their transportation through membrane transporters. These AIPs then interact with a transmembrane histidine kinase receptor activating the target genes expression via autophosphorylation of the cognate transcriptional regulator. B) Chemical structure of the AIP signals produced by *S. aureus*, *S. mutants* and *B. subtilis*.

2.3 Antibiotic Resistance of Biofilms

QS-regulated gene expression events in the pathogens have an important role for cells organisation into sophisticated communities able to sustain long-term exposure to high antibiotic concentrations and therefore cause severe chronic infections [7, 35]. Biofilm insusceptibility is multifactorial interplay of physical, physiological and adaptive tolerance mechanisms of: i) impaired penetration of antibiotics and antiseptics through the biofilm matrix, ii) horizontal gene transfer of resistance plasmids in the extracellular deoxyribonucleic acid (eDNA), iii) decreased bacterial growth and increased nutrient limitations, and iv) adaptive stress responses and formation of multi-resistant strains [70].

The decreased bactericidal effect of aminoglycoside antibiotics, for instance, have been explained with the limited diffusion of positively charged antibiotic molecules due to their sequestration by the oppositely charged matrix polysaccharides and eDNA [71, 72]. Furthermore, environmental gradients of nutrients, metabolites, pH, oxygen and slow bacterial growth are thought the reason for resistance to β -lactams penicillin and ampicillin, a class of broad-spectrum antibiotics effective only towards dividing bacteria, but not very active against the slow or no growing bacteria within the depths of mature biofilms [73]. The limited availability of oxygen also allows *P. aeruginosa* to survive the treatment with tobramycin and ciprofloxacin [74]. The juxtaposition of one or more species within the EPM is great advantage for the horizontal transmission of resistant genes and the increased mutation frequency [75-77]. Bacteria within the community easily acquire resistance and may inactivate the antibiotics via the inhibition of cell wall synthesis and protein production, alteration of drug targets, and overexpression of efflux pumps [77, 78].

Nevertheless, the existence of small subpopulation of dormant cells, called persisters, is considered to elucidate most of the biofilm specific tolerance towards antimicrobials [7]. These cells were found in both planktonic and biofilm forms. They are not considered resistant mutants, but possess great potential to avoid the killing by most of the currently used in practice antibiotics and resume their growth once the therapy is withdrawn acting as reservoirs for infection recurrence [29].

2.4 Biofilms in Device-Related Infections

Microbial biofilms are at the root of many chronic and recurrent infections and their formation have been estimated to account for 80 % of all microbial infections currently treated in hospitals [79]. A number of diseases including otitis, sepsis, endocarditis,

osteomyelitis, prostatitis, recurrent urinary tract infections and tooth decay are associated with drug resistant biofilm occurrence (Table 2.1) [9]. These biofilms may be composed of single or mixture of bacterial and fungal species which are frequently in a continuous interplay to accelerate the persistence of the infection [80, 81]. Gram-negative *P. aeruginosa*, *E. coli* and *Klebsiella pneumoniae*, Gram-positive *streptococci* and *staphylococci*, as well as *Candida* species are among the most commonly identified microorganisms in the sever biofilms related diseases (Table 2.1) [23]. For instance, the biofilm growth of mucoid, alginate-producing *P. aeruginosa* strains in the lungs of hospitalized patients is the major reason for chronic inflammation and tissue damage, associated with multiple complications, long term morbidity, and a high mortality rate [82]. The alginate in the EPM of this strain is believed to allow for the persistent infection protecting the microcolonies from phagocytosis and antibiotics [83]. *P. aeruginosa* is also frequent pathogen involved in burn wounds, chronic wounds and chronic obstructive pulmonary disorder, where it represents a serious problem (Table 2.1) [82, 84].

Table 2.1 Medical devices and biofilm-related diseases.

Organism	Medical Device	Infection
<i>E. coli</i>	Urinary catheters, orthopaedic devices	Urinary tract infections, biliary tract infections, prostatitis
<i>E. faecalis</i>	Urinary catheters, central vascular catheters	Endocarditis, urinary tract infections
<i>P. aeruginosa</i>	Contact lenses, urinary catheters, central vascular catheters, orthopaedic devices, soft tissue fillers	Cystic fibrosis, burn wounds, chronic wounds
<i>S. aureus</i>	Central and peripheral vascular catheters, arteriovenous shunts, prosthesis, breast implants	Chronic sinusitis, chronic wounds burn wounds, trauma infection,
<i>Staphylococcus epidermidis</i>	Urinary catheters, central and peripheral vascular catheters, prosthesis, soft tissue fillers	Sepsis, endocarditis
<i>Proteus mirabilis</i>	Urinary catheters, orthopaedic devices	Kidney stones, respiratory tract, wound infection, urinary cystitis
<i>K. pneumoniae</i>	Urinary catheters, central vascular catheters	Lower biliary tract, wound infections
<i>S. mutans</i>	Dental implants	Dental plaque, gingivitis, dental caries, periodontitis
<i>Candida albicans</i>	Central venous catheters, urinary catheters	Bloodstream, urinary tract infections

An extremely high percentage of planktonic bacterial cells in the healthcare facilities are difficult to eradicate by most commonly available antibiotics, but when they grow in the structured biofilm communities their eradication is even more challenging [85]. Bacterial biofilms are up to 1000 times more resistant to conventional antibiotic treatments and host defence mechanisms than their free floating counterparts. The increasing incidence of biofilm infections is also considerably related with the progress of the modern medicine and the frequent use of implants and indwelling medical devices (IDMs) [86, 87].

Indwelling medical devices such as urinary catheters are utilised to relieve urinary retention and urinary incontinence. Bacteria readily colonise catheters surface and thereby gain access to human organs or tissues causing severe bloodstream or urinary tract infections (UTIs) [5, 11]. Catheter-associated urinary tract infections (CAUTIs) are the most frequent health care-associated infection worldwide related with the regular and sometimes unnecessary use of indwelling urinary catheters [88, 89]. These infections account for over 40 % all nosocomial infections and form 80 % of all UTIs currently treated in the hospitals [89-91]. CAUTIs are major health concern that delays the patient's recovery and significantly increase healthcare costs, length of antibiotic therapy and risk of resistance development [6, 89].

The most common urinary catheter in use is the Foley indwelling urethral catheter - a soft latex or silicone tube inserted into the human bladder to drain urine [89]. It has inflatable balloon near the catheter tip which serves to hold the device into the bladder over the period of catheterisation (Figure 2.4) [92]. Indwelling catheter systems were originally designed for short-term bladder drainage, but nowadays are common in the long-term care. The systems can be opened - the urine drains into open collection container, and closed - the catheters empties into securely fastened plastic collecting bag. Despite the fact that the closed systems are more resistant to bacterial contamination and UTIs occurrence, it has been reported that 10 to 50 % of patients undergoing short-term catheterisation (0-2 weeks) develop asymptomatic bacteriuria, whereas essentially all patients undergoing long-term catheterisation (more than 6 weeks) will develop symptomatic UTIs [93]. For each day the catheter is in place the risk for acquisition of infection in any part of the urinary system, including urethra, bladder, ureters, and kidney has been estimated to increase by approximately 10 % [94].

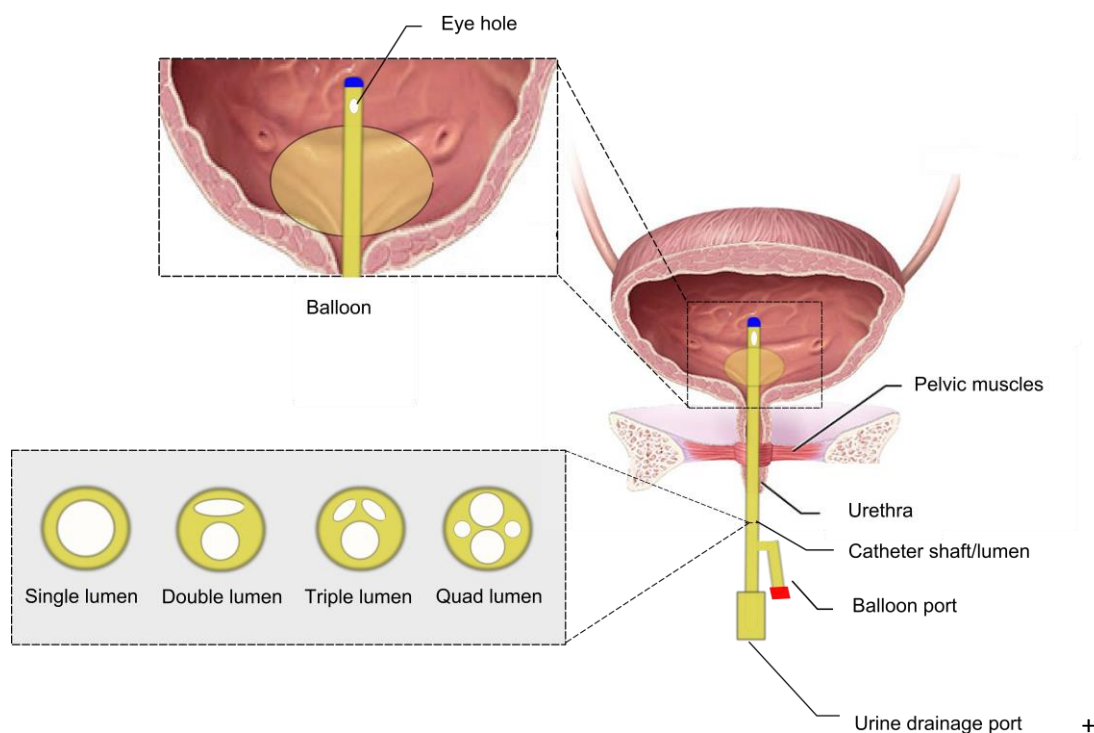


Figure 2.4 Schematic representation of Foley urinary catheter.

There are several routes for bacteria to enter the body and then establish UTIs in the hospitalized patients. At the time of insertion, bacterial microflora from the periurethral area of the patients can colonize the catheter tip and consequently access the bladder [95]. In most cases, however, bacterial entry occurs through the urethral meatus-catheter mucoid film formed on the external surface of already placed catheter [96]. Besides, failure of the drainage system or contamination of the urine in the collection bag will allow bacteria to access the urinary tract [89]. The majority of the identified pathogens are from the patient's own microbial flora, the healthcare personnel or other patients, and other sources available in the hospital environment [16]. Special emphasis should be put when the CAUTIs is caused by species from the hospital settings, that often represent drug-resistant strains complicating significantly the treatment [89].

Soon after the catheters contamination the individual pathogenic cells change phenotypically and initiate biofilm formation [23, 77, 97]. At the beginning these biofilms are composed of single species, but longer time of exposure inevitably results in multispecies biofilm formation with very dynamic microbiology [98]. Up to five different species may be isolated from biofilms of individuals with long-term catheterisation, being the Gram-negative rods (*P. aeruginosa*, *E. coli* and *P. mirabilis*) and enterococci (especially *E. faecalis*) the most frequently identified (Table 2.1) [99, 100]. The specific

interactions and synergism between the distinct species within the polymicrobial biofilms, often results in increased antibiotic resistance and virulence factors production [101]. Multispecies biofilm consortium of Gram-negative *P. aeruginosa*, *Pseudomonas protegens*, and *K. pneumonia* was shown to resist the treatment with tobramycin and sodium dodecyl sulphate, whereas monocultures of these species tolerated the antibacterial action of both compounds in different levels [102]. Depending on the exerted selective pressures, different microorganisms may even evolve to increase the mutual benefit of the consortium and begin to function better together than alone. Despite the significance of the polymicrobial biofilms in many human diseases, the interspecific bacterial interactions are not well characterized and require profound understating in order to develop adequate preventative and treatment strategies.

By far biofilms that contain crystals in their matrix remain the most problematic especially for the patients undergoing long-term catheterisation. There are two main types of crystals: i) struvite, which are rectangular in shape build of magnesium ammonium phosphate, and ii) apatite that represent microcrystalline structures made of a hydroxylated calcium phosphate in which the phosphate groups are replaced by carbonate [103]. The driving force behind their formation is the urease-induced hydrolysis of urea to ammonium hydroxide, which results in elevated pH of the urine followed by precipitation of magnesium and calcium phosphate. The crystals formation and accumulation in the biofilm structures frequently lead to encrustation and blockage of the urinary catheter [104, 105]. As a result the urine is either retained in the bladder or leaks outside the catheter, and if not replaced serious complications, e.g. pyelonephritis, septicaemia and endotoxic shock may occur [106]. Many bacterial species are capable of producing urease including *P. aeruginosa*, *K. pneumoniae*, *Morganella morganii*, some *Providencia* spp, some strains of *Staphylococcus aureus* and coagulase negative staphylococci, but the most abundant bacterium recovered from crystalline biofilms is *P. mirabilis* [89, 95, 107, 108]. Practically, all types of urinary catheters are vulnerable to microbial contamination and biofilm development. The eradication of biofilm-embedded cells is very difficult task and therefore, instead of treating the consequences, the efforts are currently directed towards the development of preventive strategies to reduce the incidence of severe medical device-related infections.

2.5 Current Strategies for Controlling Bacterial Biofilms

To reduce the incidence of biofilm-associated infections various strategies, such as removal of the contaminated medical device, utilisation of novel materials for device construction or surface functionalisation with antibacterial agents, have been suggested [14]. Systematic replacement of contaminated IDMs is only a temporary solution, as the freshly inserted device provides a new surface for bacteria to adhere and establish biofilms [109]. Alternatively, novel silicone materials on which bacteria adhere less, have been used for urinary catheters construction. Silicone-based materials are not the best decision for limiting the spread and occurrence of infections mainly because of the nonspecific protein adsorption on the catheters surface that after some time triggers bacterial attachment [110].

Nowadays, surface functionalisation with broad-spectrum antibacterial agents is a very active field of research for developing of materials with variable efficiency against biofilms [15, 111, 112]. The substantial evolutionary stress that most antimicrobials exert on bacteria ultimately may lead to the emergence of multi-drug resistance species. In consequence significant efforts are being made to design novel antibacterial surfaces able to resist bacterial colonisation without promoting resistance occurrence. Existing antibacterial and antibiofilm materials show different efficiency towards single and multi-species biofilms and can be categorized as:

- i) Engineered nano- and micro-topography surfaces that **inhibit bacterial adhesion** [113, 114]. These anti-adhesive coatings aim to counteract the conditioning layer formation on the surface, i.e. host proteins adherence, and thus repel bacterial cells [13]. Imparting surface characteristics with hydrophilic polymers such as hyaluronic acid, heparin, poly(ethylene glycol) (PEG) and its derivatives, has been received much attention for the development of bacteria repellent surfaces [115-120].
- ii) Surfaces with covalently immobilised antimicrobials that **kill bacteria upon contact** [121]. Cationic macromolecules containing quaternary ammonium and phosphonium moieties have been frequently used for functionalisation of a wide range of contact-killing surfaces [122, 123]. However, the bactericidal effect of these materials can easily be reduced by host biomolecules or residues of dead cells, blocking their direct contact with the cells [124].
- iii) Biocide releasing surfaces. Surfaces leaching antibiotics, metal and metal nanoparticles (NPs) have been designed to provide a local and defined delivery of the killing agents into the affected zones [125-128]. The major

limitation of these antibacterial/antibiofilm leaching materials is their short lifetime [129].

Although some promising results, these approaches suffer from the use of active agents which may be associated with side-effects such as cytotoxicity, hypersensibility, inflammatory responses or progressively increasing antibiotic resistance emergence [130]. Therefore, there is still a need for more efficient and specific control of bacterial biofilms and infection establishment relying on innovative strategies that are superior to the commonly used in the practice methods. Approaches targeting disruption of bacterial QS process and degradation of biofilm matrix components have been successfully applied alternative for the prevention and control of drug resistant biofilms *in vitro* and *in vivo*. In contrast to most commonly used antimicrobials, these anti-infective agents do not directly affect bacterial survival and thus would not lead to selection for resistance. At present the use of nanosized organic particles with high bactericidal activity is also of considerable interest for overcoming bacterial resistance without significant toxicity. The unique properties of nanostructured materials, e.g. small size and large surface area to mass ratio, hold significant promise for improving materials functionality towards bacteria in both planktonic and biofilm forms. Taking into account the complex interplay of factors involved in drug resistance, combination therapies that rely on several antibacterial/antibiofilm agents affecting sequentially or simultaneously several structural component of sessile bacterial communities have been emerged as a new source of inspiration to design antibiofilm materials and coatings.

Various physical or chemical strategies including self-assembled monolayers, graft polymerization, Layer-by-layer (LbL) assembly and covalent attachment have been widely used for the modification of numerous surfaces and medical devices. Among all the techniques, LbL deposition of active agents allows the design of a wide range of sophisticated multifunctional materials and coatings with anti-adhesive and/or bacteria killing properties without the need for chemical modification of the surfaces and the use of crosslinking agents.

2.6 Layer by Layer assembly: A versatile tool for engineering bacteria resistant materials

LbL assembly of polyelectrolytes is an easy, versatile and cost-effective approach for engineering multifunctional antibacterial and antibiofilm coatings on a variety of surfaces with different chemistry and geometrical shape [131]. This technique is based

on the sequential deposition of oppositely charged layers and has been widely used to incorporate a broad range of biomacromolecules [132], enzymes [133], drugs [134], and NPs [135] in coatings, without causing structural changes that could alter their efficacy (Figure 2.5). Several technologies namely immersive, spin, spray, electromagnetic, and fluidic, are available to create tailor-made polyelectrolyte-containing nanocoatings with better characteristics [136]. To date the immersive method, which is performed by dipping a charged substrate into an oppositely charged aqueous solution of the active agent, is the most widely used for the fabrication of multilayer architectures with controllable thickness. In this process, known also as “dip-coating”, the electrostatic interactions between the building blocks are the main driving force, although non-electrostatic interactions such as hydrophobicity, hydrogen bonds, Van der Waals forces, charge transfer halogen interactions could be involved as well [137]. Depending on the interactions between the molecules, their charge density, pH and ionic strength of the solution the multi layering can occur either linearly or exponentially [138].

Linear mode of layers growth is typical for polyelectrolyte pairs such as poly(styrenesulfonate)/poly(allylamine hydrochloride) (PSS/PAH) that are able to interact strongly. The thickness of these coatings increases linearly and the same amount of polyelectrolyte material is added to the growing layers upon each deposition cycle. Such multilayers have a stratified architecture with no diffusion of the polyelectrolytes within the layers. When the interactions between the oppositely charged building blocks are weak, as in the case of hyaluronic acid (HA) and poly(L-lysine) (HA/PLL), the LbL multilayers grow exponentially. The exponentially growing multilayers can adsorb large amount of the polymer, up to hundreds of nanometers per deposition cycle, which opens up opportunities for the design of thick films with reservoir capacities [137-139]. A key feature in this growth pattern is the diffusion of at least one of the two polyelectrolytes “in and out”, leading to the formation of interpenetrated structure with high water content [140]. These highly hydrated coatings are considered a functional platform for the successful immobilisation of proteins or enzymes onto materials and surfaces, without significant loss of their biological activities [138, 141]. The biomolecules can be loaded/entrapped within the polyelectrolyte layers, or might be an integral part of the coating replacing one of the building electrolytes [142]. Moreover, the solutions pH and ionic strength, as well as the type of polymer pairs are fundamental for the successful engineering of stable at use materials [138].

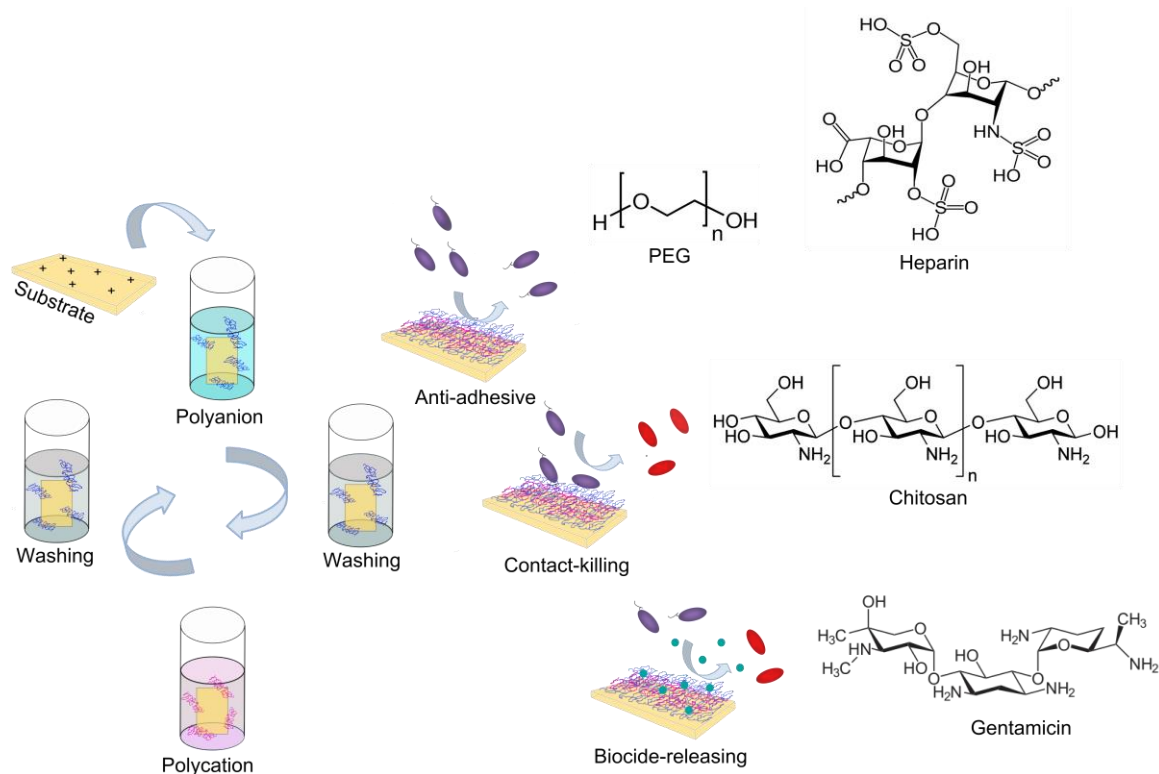


Figure 2.5 A) Schematic representation of the LbL assembling of oppositely charged polyelectrolytes (left). Three major classes of multilayer coatings with antibacterial functionalities have been engineered (right): antiadhesive that inhibits the attachment of pathogens, contact-killing coatings that explore antimicrobial agents on the surface, and biocide-releasing to deliver antibacterials and kill bacteria in the supernatant. PEG-poly(ethylene glycol), purple ellipse (live cells), red ellipse (dead cells).

A wide variety of materials with a potential to repel and kill pathogens, on contact and in close vicinity, could be developed in a LbL fashion (Figure 2.5). The design of bacteria-repelling materials deals mainly with changes in surface wettability, roughness and charge. Hydrophilic polymers such as PEG, poly(L-glutamic acid) (PGA) and poly(acrylic acid) grafted PEG, heparin and hyaluronic acid, are frequently used to increase the surface wettability [138, 143, 144]. The polymers might be introduced into the multilayers or on the top of the coating forming a highly hydrated layer that serves as a physical and energy barrier for bacterial adherence [143, 145, 146]. In particular, the anti-adhesive materials and surfaces possess potential to prevent the first step in biofilm growth, i.e., initial bacterial attachment, but they do not affect the pathogenic bacterial growth in solution, the cells stay alive and may colonise other surfaces. Hence, this antibacterial strategy might be feasible for temporary materials such as sutures, meshes, and drainage tubes, but probably not very practical to control the occurrence of implant associated infections. In addition, the anti-adhesive coatings

indiscriminately may not only suppress the surface bacterial adherence, but also the tissue-cells interaction with the functionalised implants, which would affect the healing process. Approaches attempting to kill bacteria upon surface attachment and/or in the device surrounding have been gaining ground (Figure 2.5).

Up to now a powerful portfolio of functional multilayer assemblies has been created to inhibit the growth of both adhered and adjacent cells. Materials killing the pathogens upon their attachment often explore cationic compounds that interact with the intrinsically anionic bacterial cell wall leading to irreparable membrane damage and bacterial death [147]. Because the bactericidal effect depends on the availability and positive charge densities on the surface most of the assemblies terminate with the active polymer. However, the strong electrostatic interactions with the anionic compound as well as the layers rigidity often result in insufficient charge density and reduced chain mobility to alter bacterial cell membrane. Variation in the pH during and/or after the LbL construction has been proven as very effective to modulate not only the surface roughness, porosity and wettability, but also to fabricate materials and surfaces with high surface charge and mobility. Lichter *et al.* created SPS/PAH multilayers with reversible swelling transition and pH - tuneable antibacterial functionalities. The coating was assembled at high pH, incorporating mainly pockets of hydrophobically associated amine groups, and upon exposure to low pH the amines become protonated turning the adherent, nontoxic surface to highly resistant towards Gram-positive *S. epidermidis* and Gram-negative *E coli* [148].

Chitosan and its derivatives have been widely used in the development of antibacterial and antibiofilm active materials. Chitosan coatings applied on silicon wafer as chitosan/k-carrageenan multilayers, for examples, counteracted the adhesion and biofilm establishment of clinically relevant *E. faecalis* strains. Moreover, chitosan-terminated multilayers imparted higher antibacterial activity than the layers terminating with anionic carrageenan [149]. Assemblies of chitosan and anionic lentinan sulphate onto polyurethane surface also were able to decrease the pathogenic *P. aeruginosa* growth upon contact, without affecting human cells viability [150]. The versatility of LbL technique was further explored for fabricating bacteria resistant multilayer coatings onto natural textiles, e.g. cotton and silk [151, 152]. Functional finishing of cotton fabric via the deposition of the oppositely charged chitosan and sodium tripolyphosphate resulted in the successful elimination of both Gram-positive and Gram-negative species [153]. Nevertheless the innate cationic charge of chitosan the differences in assembly conditions frequently define the amount of the active agent deposited on the surface, the coating thickness and rigidity, and therefore would affect the final antibacterial

performance of the material. To overcome these drawbacks quaternary ammonium salts bearing positive charge independent of the pH have been introduced to design surfaces with better bactericidal properties [138, 154, 155]. Quaternary ammonium salt of chitosan was successfully assembled with poly(acrylic acid) (PAA) on a plasma-treated poly(ethylene terephthalate) to impart high antibacterial activity towards *E. coli* and *S. aureus* [156]. Quaternary ammonium and/or phosphonium salts of pyridoxine, alanine-derived gemini and fatty acids have also been introduced as potent broad spectrum antibiotic alternatives against Gram-positive and Gram-negative bacteria and viruses [157-161].

Apart from the aforementioned compounds, cationic proteins and antimicrobial peptides have also been reported as common building blocks. LbL constructs comprising the lysozyme protein and negatively charged gold NPs, deoxyribonucleic acid (DNA) or pectin demonstrated a promising inhibitory effect towards both Gram-negative and Gram-positive bacteria [162-164]. Positively charged antimicrobial peptide, defensin, was embedded within PLL and PGA multilayers to avoid the peptide's chemical modification grafting and reach effective antibacterial concentrations on the surface. Improved antibacterial activity against *Micrococcus luteus* and *E. coli* was achieved only for the PLL-terminated specimens, indicating that a positive surface charge was necessary for negatively charged bacteria to adhere and then interact with the incorporated antimicrobial peptide within the coating [165]. In another study, the authors designed homopolymer of methacrylamide bearing (oxidized) 3,4-dihydroxyphenylalanine to insure faster layers assembly by covalent coupling with poly(allylamine) (PAH) and subsequent grafting of the peptide. The resulting layers showed durable functionality elimination *B. subtilis* upon the surface [166, 167]. Despite the advantageous of using contact-killing multilayers instead of a simple cationic layer, their action is restricted only to the surface. Moreover, the coatings will inevitably become contaminated by various types of proteins or will be buried under a layer of dead cells, leading to their deactivation [142, 168]. The remaining dead bacteria on the implants surface would trigger inflammation and immune responses. Antimicrobial leaching surfaces appeared the most promising alternative for controlling device related infections acting simultaneously on both sessile and planktonic bacteria [142]. Even so, the continuous release of biocides (e.g. silver ions and antibiotics), whether needed or not, may originate the emergence of resistant bacterial strains and undesirable side effect [169-171]. Various strategies for sustained and controlled-release of the therapeutic agents have recently been developed to address this challenge (Figure 2.5).

Polyelectrolyte multilayer coatings have been widely explored as a platform for delivery of antibacterials on demand upon external stimuli such as pH, electric field and temperature [172-174]. Recently, bacteria and their metabolites have been proposed as polymer hydrolysing organisms, which can be turned into a robust trigger for antibacterial drug release in a self-defence principle [175]. Bacterial species produce acidic substances such as lactic and acetic acid that lead to a pH lowering in surroundings. Taking advantage of this phenomenon Zhuk *et al.* combined positively charged antibiotics gentamicin, tobramycin, and polymyxin B, with an oppositely charged tannic acid, into responsive coating that have a potential to mitigate bacterial infection occurrence. The main driving force for triggering the antibiotics elution from the material, when challenged with bacteria, is the protonation of tannic acid followed by charge imbalance and layers disassembly. Importantly, these self-defence LbL specimens were very stable and did not release the therapeutic cargos under physiological, infection-free conditions for more than one month [175]. In similar manner, gentamicin was assembled with poly(methacrylic acid) (PMMA) and PAA into stable coatings (up to several months) with potential to counteract *S. aureus*, *S. epidermidis* and *E. coli* surface colonisation only when needed [172, 176]. The changes in pH as a result of bacterial growth might also cleave the imine bonds or induce swelling of the coatings that will trigger the release of the incorporated active agents [172, 177].

Bacteria as well produce enzymes hydrolysing the polyelectrolytes within the layers and therefore releasing the incorporated active agents. In contrast to the pH-triggered strategy, which is not species specific, the enzymatic degradation of assemblies would allow the targeting of specific bacteria. To date, only few enzyme triggered release coatings have been reported [142]. Multilayers of hyaluronic acid and chitosan have been shown to release the antimicrobial peptide cateslytin in presence of hyaluronidase, an enzyme secreted by variety of pathogens such as *S. aureus* and *C. albicans* [178]. In contrast to the other bactericide leaching surfaces, stimuli responsive micro and nanocoatings have the advantage to exhibit “on demand” their antibacterial activity and thus extend the useful life time of coatings decreasing the premature depletion of the drug reservoir [142, 179]. However, the elution of bactericides within the therapeutic window and the limitation of the non-triggered background release from the materials are the main issues to be addressed when engineering stimuli-triggered assemblies. Future research efforts should be also dedicated to test the effectiveness against repeated bacterial challenges as well as to generate more triggering pathways. It is worth mentioning that the drug release kinetics and the time scale over which the coating or material should be active are highly application-dependent. A short term,

high dosage release of antibacterial agents is generally preferred to control infection occurrence in early post-operation periods. In contrast, long lasting bacterial resistant properties are required for the implants that have to integrate successfully with the surrounding tissues.

One of the most appealing characteristics of LbL deposition technique is the possibility to combine multiple therapeutic agents, e.g. classical antibiotics and/or novel antimicrobials, into hybrid multilayer coatings with complimentary modes of action. The combination of innovative and conventional antimicrobials, acting as a multiple lines of defences, is being put into practice to improve both the prophylactic and therapeutic efficacy and lower drug dosage, thus reducing toxic side effects [180]. The simultaneous or sequential delivery of each active principle can be achieved at the right time or specific stage of bacterial lifecycle by adjusting the chemistry of building blocks or embedding the active compounds within different levels in the coating [181, 182]. However, the synergism of several compounds is a relatively unexplored field for development of novel release-killing materials and surfaces that are highly effective in controlling both planktonic and sessile bacteria.

Most of the reported multifunctional LbL constructs integrate simultaneously anti-adhesive and bactericidal agents acting as multiple lines of defence against opportunistic pathogens. Sophisticated surface coating comprised of bacteria-repelling PEG as a top layer and releasable silver NPs (AgNPs) beneath has been engineered to simultaneously repulse and kill bacteria at the vicinity [183]. In a similar way, Li *et al.* generated dual-level bactericidal coating which consists of Ag⁺ ions reservoir made of 20 bilayers of PAH and PAA and cationic top region of 10 bilayers of PAH and silica NPs (SiO₂ NPs), previously modified with quaternary ammonium silane. These dual-functional antibacterial coatings bearing both contact-killing and release-killing capacities significantly mitigated *E. coli* and *S. epidermidis* growth. The silver released from the coating reservoir provides a strong initial killing effect during the first few days of bacterial challenge, while the quaternary ammonium cations retained significant contact-killing activity after the depletion of Ag reservoir [184]. However, the release of biocides at high amounts frequently induces selection for resistant bacteria. Current researcher efforts are focused toward the generation of novel bacteria and biofilm resistant coatings using strategies that do not exert selective pressure on bacteria population and minimize the risk of resistance occurrence. Recently, the development of antibiofilm coatings based on molecules interfering with bacterial cell-to-cell communication and biofilm integrity, have been considered a valuable alternatives to prevent infections and tackle bacteria resistance threat.

2.7 Quorum Sensing Inhibitors in Next Generation Antibiofilm Coatings

The development of novel anti-QS drugs that affect bacterial pathogenesis or biofilms, without killing or inhibiting their planktonic growth, has been gaining ground. Inhibition of bacterial cell-to-cell communication process is thought to allow the host defence system to eliminate non-cooperating (and hence less virulent) bacteria or substantially increase the effect of co-administered antibiotics at lower dosage [185]. Various anti-QS strategies towards both Gram-negative and Gram-positive bacteria have been described. These approaches include compounds that may inhibit the signal production, inactivate the AIs in the extracellular environment or block the specific QS receptors. Despite the large number of synthetic compounds reported to act as anti-QS substances, only few of them have been used to design new generation biofilm resistant coatings on medical devices. Since the mechanism of action of these anti-QS based materials is not to kill bacteria, but to influence their ability to induce virulence and form sessile communities, they represent an exciting area of fundamental research that would provide new opportunities to control bacterial infections while minimising the selection for resistance.

Macrocyclic peptides that block the *agr* system in *S. aureus* have been immobilised on glass slides, nonwoven meshes, or within absorbent tampons using the rapidly dissolving polymer carboxymethylcellulose. The peptide-loaded carboxymethylcellulose films released the active agent and inhibited by 95 % the *agr* QS system in reporter *S. aureus* suggesting their application as anti-infective agents able to block the *agr* controlled secretion of virulence factors and toxins, including the toxic shock syndrome toxin-1 (TSST-1) [186]. These coatings might be used further to treat the outer covers of tampons, wound dressings, or other objects to suppress toxin production and mitigate the severity of *staphylococcal* infections in clinical and personal care contexts. Although anti-QS strategies provide new routes for treating bacterial infections, including those caused by resistant strains, many challenges remain in terms of encapsulating, conferring appropriate chemical protection, and controlling the release of the quorum sensing inhibitors (QSIs) in their practical utilisation [187]. Kratochvil *et al.* has reported the generation of superhydrophobic coatings loaded with water-soluble and water-sensitive QSIs interfering with *S. aureus* virulence. The authors used nanoporous, polymer superhydrophobic coatings to host the peptide-based QSIs providing sustained release of the anti-infective agent into the surrounding media for long time periods. The released QSIs efficiently inhibited *agr*-based QS in pathogenic *S. aureus* for more than one month. Moreover, these non-wetting coatings can protect water-labile QSIs from rapid hydrolysis, thereby extending their useful lifetimes.

Importantly, the so formed anti-QS coatings were able to modulate the QS-controlled biofilm formation of *S. aureus in vitro* for prolonged periods without affecting the normal bacterial growth. This approach could prove suitable for the encapsulation, protection, and release of other classes of water-sensitive agents [187].

In addition to the synthetic AI analogues, natural compounds such as furanones are also interesting alternatives to overcome device associated infections of both Gram-negative and Gram-positive bacteria. A few natural products have been shown to inhibit bacterial QS process and biofilm growth. For instance, halogenated furanones (fimbrolides) produced by red macroalga *Delisea pulchra* are among the most intensively studied natural QSIs able to inhibit the swarming motility of *Serratia liquefaciens* and bioluminescence production of *V. fischeri* and *V. harveyi* [188]. The furanone (5Z)-4-bromo-5-(bromomethylene)-3-butyl-2(5H) produced by *D. pulchra* can also attenuate the swarming motility and biofilm formation of *E. coli*. Although natural furanones were shown to affect many QS regulated behaviours, they did not have high activity on pathogenic *P. aeruginosa*. Synthetic derivatives of furanones, however, showed improved survival time of mice infected with a lethal *P. aeruginosa* strain and ability to act on the QS process in other Gram-negative bacteria [65]. Based on these anti-virulence characteristics, the researchers focused their attention on the potential application of furanones as coatings that resist bacterial colonisation and biofilm formation on medical devices. For example, two different methods for covalent immobilisation of the 3-(10-bromohexyl)-5-dibromomethylene-2(5H)-furanone on biomaterials have been reported. Regardless the mode of surface functionalisation used in the study, co-polymerisation with a styrene polymer or grafting on catheter surface previously modified with PAA derivative bearing reactive azide groups, the furanone coatings significantly counteracted the establishment of drug resistant *Staphylococcus epidermidis* biofilm. *In vivo* results suggested that these furanone-coated catheters might control bacterial infections up to 65 days, as demonstrated by the reduced number of living bacteria on the catheters [66]. In another work, furanones have been attached onto silicone oxide surfaces using N-(3-trimethoxysilylpropyl)-4-azido-2,3,5,6-tetrafluorobenzamide (PFPA-silane) as a photoactive cross-linker. This immobilisation approach is considered as very useful, in particular for substrates and molecules that lack reactive functional groups [67]. However, the antibacterial and antibiofilm activities of these materials were not investigated.

Dihydropyrrolones (DHPs) are synthetic analogues of halogenated furanones that interfere with bacterial communication without altering human cells viability. When these QSIs were immobilised on glass surfaces they efficiently inhibited the biofilm

formation of *P. aeruginosa* and *S. aureus* without affecting viability of free floating cells. The authors also demonstrated the potential of DHPs coated surfaces to repress by 72 % the expression of green fluorescent protein, suggesting the existence of a membrane-based pathway for inhibition of the QS phenomenon in *P. aeruginosa* [189]. Furthermore, series of DHPs analogues were covalently attached to various surfaces via a Michael-type addition reaction. The DHPs-treated surfaces significantly decreased the biofilm occurrence by *P. aeruginosa* and *S. aureus*. Among all synthetic analogues - 5-methylene-1-(prop-2-enoyl)-4-phenyl-dihydropyrrol-2-one was identified as the one having broad spectrum activity and consequently was considered as an excellent candidate for the development of anti-infective materials and surfaces.

Another group of natural compounds such as bromoageliferin, 3-indolylacetonitrile, and resveratrol with significant anti-QS activity have been also reported [185, 190-192]. For example, bromoageliferin, a marine natural product, possess antibiofilm activity against Gram-negative bacterium *Rhodospirillum salexigens*. Moreover, its simplified analogues 2-aminoimidazole (2-AI) derivative and 5-amido or 5-imido 2-aminobenzimidazole (2-ABI) may affect the biofilm maturation in both Gram-negative and Gram-positive bacteria [185]. The plant auxin 3-indolylacetonitrile, phytoalexin resveratrol and related stilbene derivatives have been shown to disrupt bacterial QS process and consequently inhibit the biofilm growth of *P. aeruginosa* [191-193]. Frei and co-workers further investigated whether combining structural attributes of the above mentioned compounds into a simple molecular scaffold could result in molecules with improved antibiofilm and/or anti-QS properties. To explore their hypothesis, the authors synthesised a small set of stilbenes containing 2-AI or indole moieties and then assessed their efficiency in inhibiting *P. aeruginosa* biofilms. The results established the 2-ABI containing stilbenes as potent antibiofilm agents for the development of coatings to clear microbial infections and control other important aspects of bacterial behaviour, such as the ability to induce virulence and form drug resistant biofilms [185]. The most promising of all compounds, 5,6-dimethyl-2-aminobenzimidazole, was then encapsulated in thin films of biocompatible poly(lactide-co-glycolide) polymer on glass chips. The released QSI from the films was in sufficient amount to inhibit up to 75–90 % the pathogenic biofilm formation of *P. aeruginosa* on the glass surface [194].

Despite that the synthetic or natural QSIs based coatings were shown to have great potential to act as anti-infective agents and reduce the biofilms of various medically relevant bacterial species, the slow release of the inhibitor, in particular furanones, may limit their further biomedical application. Some furanones have the disadvantage of being extremely reactive and thus may be toxic and mutagenic to human cells. Thus,

the QSI dose and release kinetics should be carefully considered when designing materials for biomedical applications. Furthermore, several clinical strains may resist the action of these inhibitors, and the question arises as to whether the QSIs will meet the same fate as the antibiotics.

2.8 Enzymes in Biofilms Prevention

Enzymes – the ultimate green catalysis have been used to replace harsh chemicals, and improve efficiency of a wide variety of industrial processes, including food processing, textile finishing, biofuel manufacturing and etc. They also have been considered very effective in medical practice for aiding digestion, diagnosis purposes and disinfection in healthcare settings. Antimicrobial enzymes that: i) directly attack microorganisms, ii) interfere with signals and prevent biofilm formation, iii) disperse already mature biofilm structure, and/or iv) eliminate microorganisms through the production of biocides, emerged as promising alternative to create bacteria resistant materials and coatings.

2.8.1 Quorum Quenching Enzymes

Several enzymes have been reported to inactivate the AIs in Gram-negative bacteria and consequently inhibit the QS controlled target genes expression, a phenomenon known as quorum quenching (QQ) [195, 196]. Paraoxonases are enzymes originally found in mammalian cells, which enhance the ability of high-density lipoproteins to oxidize low-density lipoproteins and reduce the risk of atherosclerosis and other heart diseases. However, recent evidences infer their role as QQ agents able to hydrolyse the lactones derivatives of the AHL signals in pathogenic *P. aeruginosa* [197-199]. Acylase and lactonase are other known anti-QS active agents produced by various bacterial species that degrade respectively the amide bond and lactone ring of the AHLs QS signals and consequently act as anti-infective agents able to attenuate the pathogenicity of Gram-negative bacteria (Figure 2.6) [196, 200-202]. Human acylase has been also shown to degrade *in vitro* C4-HSL and C8-HSL AHLs signals and inhibit *P. aeruginosa* surface attachment through the QS interruption [203]. Besides, bacterial species as *R. erythropolis*, *Burkholderia sp. GG4* are able to produce another group of QQ enzymes called oxidoreductases [196, 204]. These enzymes modify the AHLs by oxidising the 3C keto group of the acyl side chain into hydroxyl group [204] (Figure 2.6). Upon this modification, AHL fails to bind with the cognate transcription regulator and then “confuse” bacterial pathogens in their talk for establishing strong sessile community [196].

peptides and enzymes [206]. The enzymatic degradation of the biofilm matrix affects its physical integrity and increases the susceptibility of the encased bacteria to antimicrobials. Hence, polysaccharides, eDNA and proteins, the most important adhesive components of the matrix, appear as attractive targets for controlling bacterial biofilms in clinical settings. Several enzymes including glycosidases, proteases, and deoxyribonucleases are considered as matrix-degrading enzymes capable to inhibit biofilm maturation, detach pre-formed biofilms, and most importantly, increase the susceptibility of pre-formed biofilms to antibiotics and biocides *in vitro* [206].

One of the most studied matrix-degrading enzymes is dispersin B, which is a glycoside hydrolase produced by the periodontal pathogen *Aggregatibacter actinomycetemcomitans*. Dispersin B degrades the matrix poly-*N*-acetylglucosamine polysaccharide that mediates the attachment to abiotic surfaces and the intercellular adhesion of *A. actinomycetemcomitans*, as well as, plays a key role in bacterial resistance to detergents and human phagocytic cells [207]. This matrix-degrading enzyme has been loaded in surface-attached polymer matrices built in a LbL fashion. The LbL matrices were assembled through electrostatic interactions of PAH and PMMA followed by chemical cross-linking with glutaraldehyde and pH-triggered removal of PMMA producing a stable PAH hydrogel matrix used for loading of dispersin B. These enzyme loaded coatings inhibited by 98 % the biofilm development of two clinically relevant *S. epidermidis* strains, without affecting the attachment and growth of cultured human osteoblast cells [208]. Catheters coated simultaneously with dispersin B and triclosan showed synergistic antibiofilm activity inhibiting *in vitro* the surface colonisation by *S. aureus*, *S. epidermidis*, *E. coli* and *C. albicans*. Moreover, these materials demonstrated high *in vivo* efficacy against biofilms of *S. aureus* [209].

Enzymes degrading the biofilm eDNA, such as deoxyribonuclease I, have been also used to develop antibiofilm surfaces. Coatings comprised of deoxyribonuclease I have been formed on polymethylmethacrylate using dopamine as an intermediate. The resulting materials significantly decreased the adhesion of Gram-positive *S. aureus* and Gram-negative *P. aeruginosa* and inhibited the biofilm formation, without affecting mammalian cells adhesion and proliferation. Despite the high effectiveness of the coatings, the enzymes lost significant part of their catalytic activity after 24 h, being applicable only for short-term biomaterial implants and devices [210].

Alginate lyase is another example of antibiofilm enzyme that cleaves β -glycosidic bonds of matrix alginate and possess capacity to control *P. aeruginosa* colonisation on the respiratory tracts in patients with cystic fibrosis [211]. Combination of this enzyme with antibiotic demonstrated higher efficacy in treating *P. aeruginosa* infections,

particularly in the cystic fibrosis airway [212]. Genetically engineered alginate lyase-PEG conjugates removed more than 90 % of the mucoid *P. aeruginosa* biofilm from abiotic surfaces following one hour treatment, whereas the *wild type* enzyme neutralize only 75 % of the biofilm. While biofilms in the human airway have properties distinct from those grown on abiotic surfaces, the fact that lyase-PEG conjugates eradicated the mucoid biofilms, suggested that the matrix-degrading enzymes could yield therapeutic benefits in the treatment of cystic fibrosis [213].

Furthermore, combinations of several matrix degrading enzymes have been shown to achieve better results, compromising the ability of various bacteria to establish antibiotic resistant biofilms. Co-administration of deoxyribonuclease I and alginate lyase, for instance, enhanced the activity of aminoglycoside antibiotics, gentamicin and tobramycin, against *P. aeruginosa*. In addition, during the treatment of biofilms and cystic fibrosis sputum containing *P. aeruginosa*, the conventional and liposomal aminoglycosides were strongly inhibited and their activity was restored when deoxyribonuclease I and alginate lyase were introduced [214]. Mixtures of protein (e.g. serine proteases) and polysaccharide degrading enzymes (e.g. alpha-amylase, β -glucuronidase and dextranase) have also been reported to remove biofilms from numerous surfaces, thus being a valuable alternative to conventional antibiotic therapy [215, 216]. However, their simultaneous incorporation in materials or immobilisation on the surface of medical devices is not much investigated.

2.8.3 Enzymes Targeting Bacterial Cells

Lysostaphin is an example for an antibacterial enzyme capable of cleaving the cross-linking pentaglycine bridges in the cell walls of *Staphylococci*. This antimicrobial enzyme has been covalently attached via polydopamine onto a variety of surfaces and even after immobilisation preserved its endopeptidase activity on the *staphylococcal* cell wall. Lysostaphin-coated surfaces were found to kill hospital strains of *S. aureus* in less than 15 min and prevent biofilm formation [217]. Lysostaphin has been also immobilised on carbon nanotubes. The enzyme-carbon nanotube conjugates have been successfully incorporated in polymer matrices producing composite materials capable to reduce protein adsorption and bacterial adhesion [130, 218]. This antibacterial and antibiofilm active enzyme was also used in formulations for direct intraperitoneal or subcutaneous administrations. Lysostaphin administration cured *S. aureus* infected mice whereas *S. epidermidis* isolates resistant to methicillin were effectively controlled by combination of nafcillin and lysostaphin [215, 219, 220].

Coatings comprised of another well-known antimicrobial enzyme, lysozyme, have been lately investigated. Lysozyme coupled to PEG layer was reported to act against both Gram-negative and Gram-positive bacterial species [221]. Conjugates composed of this enzyme and synthetic triblock copolymer with a central polypropylene oxide block and two terminal polyethylene oxide segments, noted as pluronic F-127, also showed high antibacterial activity towards Gram-positive *Bacillus subtilis*. Further, deposition of the pluronic-lysozyme conjugates on a hydrophobic surface resulted in formation of layers adopting bifunctional brushes with both anti-adhesive and antibacterial properties. The number of colony-forming units present on surfaces was reduced to 30% for the coatings based on pluronic–lysozyme conjugates as compared with coatings of unmodified pluronic, i.e. without lysozyme [222]. Lysozyme was also successfully grafted onto stainless steel surfaces pre-functionalised with an amino-(propyl)-triethoxysilane through a glutaraldehyde cross-linker. However, the enzyme in these coatings showed 20 times lower anti-adhesive activity towards *Micrococcus lysodeikticus* than the one observed in solution, due to the mode of surface grafting impairing the accessibility of the enzymatic active site to bacteria [223]. In the same study, lysozyme was further immobilised on an amino-enriched poly(ethylene imine) pre-activated stainless steel surface through a bifunctional PEG spacer with terminal aldehyde groups. The so-modified surfaces prevented bovine serum albumin (BSA) adsorption and the adhesion of *Listeria ivanovii* and *M. luteus*.

Through these examples, we have highlighted that most enzymes immobilised onto surfaces maintain their antibacterial and antibiofilm activities. Nevertheless, this activity may vary considerably (being generally lower) compared to the one observed for the enzyme in solution. It is possible, however, to increase significantly the activity of a given enzyme towards bacteria by varying the immobilisation conditions, e.g. the nature and the conformation of the spacer between the surface and the enzyme. Although these enzyme-based approaches showed promising results, there are still several limitations. The enzymatic inhibition and eradication of biofilms usually depend on the nature of the matrix constituents, being different among the clinical isolates. *In vitro* and *in vivo* evidences showed that some *Staphylococcus* species may form biofilms without the poly-*N*-acetylglucosamine while in presence of urea *P. aeruginosa*, for example, does not produce alginate containing matrices [109, 224]. In these cases, other matrix components, e.g. proteins or eDNA, substitute the exopolysaccharide in the biofilm matrix. Moreover, the *in vivo* efficacy of such approaches is not well established and treating host with proteins could cause inflammatory and allergic reactions, further affecting their therapeutic potential. The immobilisation methods may

also affect protein conformation resulting in loss of the enzymatic activities [225]. Finally, the still elevated cost of industrial enzymes reduces the feasibility of their large-scale application as antibiofilm agents.

2.8.4 Enzymes Producing Biocides

Besides of targeting the degradation or inactivation of essential biofilm components, enzymes may elicit antimicrobial reactions through the production of hydrogen peroxide, which destroys the invading pathogens. In general, hydrogen peroxide kills bacterial cells through peroxidation and disruption of cell membranes, oxidation of oxygen scavengers and thiol groups, and disruption of protein synthesis [226]. Hydrogen peroxide-producing enzymes such as glucose oxidase and cellobiose dehydrogenase (CDH) can reduce the growth of both Gram-negative and Gram-positive bacteria, therefore they are widely exploited in the food industry, for the development of biosensors, bleaching systems, and continuous antioxidant regenerating systems [227-229]. Despite the extensive use of glucose oxidase as antimicrobial agent, the requirement for glucose as a substrate is an important drawback, because glucose is also a growth substrate for most microorganisms. In contrast, CDH can oxidize cello-oligosaccharides (including cellobiose) that are not considered essential compounds for the pathogenic bacterial growth. A novel in situ antimicrobial and antibiofilm approach based on CDH was able to generate H₂O₂ in the presence of cellobiose or other biofilm exopolysaccharides, thereby preventing the microbial colonisation on silicone urinary catheters. Recombinant CDH produced by *Myriococcus thermophilum* was shown to inhibit the growth of many common microorganisms colonizing the urinary catheter surfaces such as multidrug-resistant *E. coli*, *S. aureus*, *S. epidermidis*, *P. mirabilis*, *Stenotrophomonas maltophilia*, *Acinetobacter baumannii* and *P. aeruginosa* in presence of cellobiose as a substrate. Interestingly, CDH was also able to produce H₂O₂ during the oxidation of extracellular polysaccharides formed by bacteria in absence of cellobiose. Further combination with glycoside hydrolases enhanced CDH antimicrobial and antibiofilm activity by the larger amount of H₂O₂ produced. Moreover, CDH incorporated in catheter lubricants killed bacteria in biofilms already established on silicone catheters [230]. In another study, CDH was grafted onto plasma-activated silicone catheters reducing the amount of viable *S. aureus* cells and biofilm formation under both static and dynamic conditions by 60 and 70 %, respectively. The CDH coated surfaces did not affect the growth and physiology of mammalian cell lines (HEK-293 and RAW 261.7) suggesting their application to control the CAUTIs [231]. The enzyme was also embedded into multilayer assemblies comprised of PSS and synthetic antifouling copolymer bearing

zwitterionic and quaternised groups. The production of antibacterial and antibiofilm effective H_2O_2 by the CDH coated catheters depended on the enzyme location within the structure and the percentage of the zwitterionic fraction [232]. CDH-NPs of varying sizes (from 50 to 100 nm) have been generated in situ and subsequently deposited onto the silicone surface using ultrasonic waves. The immobilised CDH-NPs effectively produced in situ H_2O_2 able to reduce the amount of viable *S. aureus* cells as well as the total amount of biomass deposited on the urinary catheter [233].

Haloperoxidases (e.g. myeloperoxidase, lactoperoxidase and haloperoxidase) are another type of antibacterial enzymes, found in many plants, animals and humans. They use H_2O_2 as a substrate to oxidize halide/pseudohalide to more potent antimicrobials towards many bacterial species in both planktonic and sessile forms [234]. Horseradish peroxidase and glucose oxidase were incorporated in polyurethane electrospun fibers and significantly affected the growth of both *E. coli* and *S. aureus* [235].

An important feature that should be mentioned is the fact that enzymes generating biocides must be submitted to the appropriate legislation before being implemented. Moreover, the enzymes may also contribute to the unwanted degradation of biological compounds present in the surrounding of the material.

2.9 Nanomaterials for Controlling Bacterial Biofilms

Nanomaterials have emerged as a potential platform that may solve limitations of traditional therapies such as low specificity and therapeutic efficacy. They exhibit unique physical and chemical properties at nanometre scale which frequently differ from their bulk counterparts [236]. The utility of nanotechnology as a tool to enhance clinical effectiveness of drugs and fight antibiotic resistance mostly rely on liposomes, nano/microcapsules and nano/microparticles as drug carriers for delivering the antibacterial agents at the site of infection [237]. The transformation of the active agents themselves into nanosize therapeutic entities with improved antibacterial and antibiofilm features has been only sparsely reported [238]. We have reported that antibacterial NPs of cationic biopolymer derivatives such as thiolated chitosan or aminocellulose were more effective than the biopolymer itself killing planktonic bacteria via the disturbance of the cell membrane [147]. However, preventing biofilm infections or treating the pre-existing biofilm is much more challenging. Numerous metals, metal oxides, hybrid polymer-metal and biopolymer nanomaterials have been suggested as next generation materials with high capacity against biofilm resistant bacterial

phenotypes. Their high effectiveness is mainly because of the NPs ability to penetrate into the EPM and act on bacterial cells within the biofilm depths [239].

Besides acting as therapeutics able to eradicate already developed biofilms, NPs may be also used for prevention of bacterial infections. Their deposition onto surfaces prone to bacterial colonisation and biofilm formation is thought to significantly reduce the growth rate or inhibit the formation of drug resistant cells communities. Methods as ultrasound sonochemistry, ultraviolet (UV) irradiation and LbL assembly have been used to generate NPs and/or incorporate them into functional materials or coatings [240, 241].

2.9.1 Sonochemistry for Synthesis of Nanoparticles

Varieties of methods have been described for the preparation of nanostructures with desired size, size distribution and morphology/shape. Some of the most common techniques used to prepare stable colloidal NSs and nanocapsules (NCs) include coacervation and phase separation, emulsification diffusion, solvent displacement and solvent evaporation, sol-gel encapsulation, supercritical fluid technology, spray drying and spray congealing [242]. Synthesis of polymeric nanoscale materials by ultrasound emulsification is an area of considerable interest to obtain biopolymer and protein based nano/microcapsules with altered physical properties and novel biological modes of action [243-245].

The use of sonochemical technology for generation of nanostructures is justified by its simplicity (one-step process), fastness and absence of aggressive organic solvents [246]. The ultrasound emulsification involves high intensity mixing of aqueous and organic solutions comprising either hydrophilic compounds for accumulation in the shell or hydrophobic actives for encapsulation in the NCs core. Indeed, the ultrasound assisted NPs generation is a combination of two acoustic phenomena, emulsification (a physical effect) and cavitation (the subsequent chemical effects). Sonication creates an emulsion with polymers in the oil/water interface [245]. However, emulsification alone is not sufficient to prepare stable colloidal particles. The ultrasonic irradiation of liquids produces acoustic cavitation comprised of formation, growth, and implosive collapse of bubbles. The collapse of these bubbles forms hot spots with very high temperature and induces water sonolysis that leads to free radicals production (e.g. HO₂). In protein NPs synthesis these radicals provoke disulphide bonds formation between cysteine thiol groups and stabilise the resulting core/shell system [245, 246]. Besides hydrogen bonding, van der Waals, hydrophobic, and electrostatic interactions have been also involved in the successful synthesis of polysaccharides, antibiotic and protein-based

NPs, without cysteine amino acids in their structure. Ultrasonic irradiation is very attractive technique for generation of variety of materials including NP coatings on medical devices and textiles for infection prophylaxis and formulations for complete bacterial/biofilm elimination.

2.9.2 Nanoparticles Interaction with Bacteria and Biofilms

Entire biofilm elimination requires efficient penetration and accumulation of the particles into the biofilm structure [236]. The NP-biofilm interactions are complex and can vary during the time of the treatment. Upon attachment NPs, smaller than 10 nm, easily diffuse through pores sizes in the biofilm structure and access the cells. Then the particles may affect the membrane integrity, inactivate the surface proteins or develop spatiotemporal aggregation patterns on Gram-positive and Gram-negative bacteria causing cells lysis and death (Figure 2.7) [247]. NPs deposition within the biofilms and consequently the interaction with the building blocks depends on the electrostatic interactions and heterogeneity of the charges across the entire biofilm structure [236, 248]. For instance, cationic quantum dots functionalized with hydrophilic moieties were able to pass the matrix barrier and accumulate inside bacteria, whereas hydrophilic groups leded mainly to their distribution in the EPM surrounding the cells [249]. The electrostatic interactions are more relevant for metal NPs, whereas surface properties such as steric effect manifests in the interplay between the matrix components and polymeric or lipid NPs [250-252].

The diffusion of NPs into the biofilms matrix could be significantly hindered by the: i) size of the EPM pores, ii) presence of high repulsive forces between oppositely charged NPs and biofilm matrix components, iii) different hydrophobicity of the surrounding environment, and iv) existence of chemical gradients within the EPM [239, 253, 254]. Capping the NPs surface with small ligands or polymers such as polysaccharides, PEG and glycolipids except to increase the suspensions stability, might also tune NPs surface functionality and alleviate their cellular/biofilm internalisation and biocompatibility. Amino-decorated SiO₂ NPs were engineered to penetrate and eradicate pathogenic *P. aeruginosa* and *E. coli* biofilms through the rapid release of the bactericidal payload [255]. In another study, biodegradable lignin NPs infused with silver ions were coated with a cationic poly(diallyldimethylammonium) chloride to develop green alternative to AgNPs that killed a broad spectrum of bacteria, including quaternary amine-resistant strains [256]. Triblock copolymer structure consisting of poly(D,L-lactic-co-glycolic acid)-b-poly(L-histidine)-b-poly(ethylene glycol) was transformed into pH-responsive NPs that released antibiotic vancomycin only in presence of *S. aureus* at antibacterial effective concentrations [257]. Similarly, pH-

responsive polymer-based NPs have been reported as novel carriers of hydrophobic drugs for treatment of antibiotic resistant bacterial communities. These NPs have a cationic outer shell to stick with the biofilm polysaccharides and a pH-responsive hydrophobic inner shell to release encapsulated antibacterial farnesol on demand [258]. The simultaneous application of matrix degrading enzymes and NPs could have been also proposed as an alternative method facilitating the NPs diffusion and the cells removal from tissues or materials [259].

The biocompatibility of nanomaterials, however, is an essential characteristic for their therapeutic application. In principle, cationic particles or particles with a high surface reactivity and smaller size are toxic, while large and hydrophobic NPs are less harmful to the human cells [253]. The undesirable absorption of organic molecules (e.g. proteins form the matrix or host) and the possible reduction of the antibacterial and antibiofilm properties of the NPs should be taken into consideration [260].

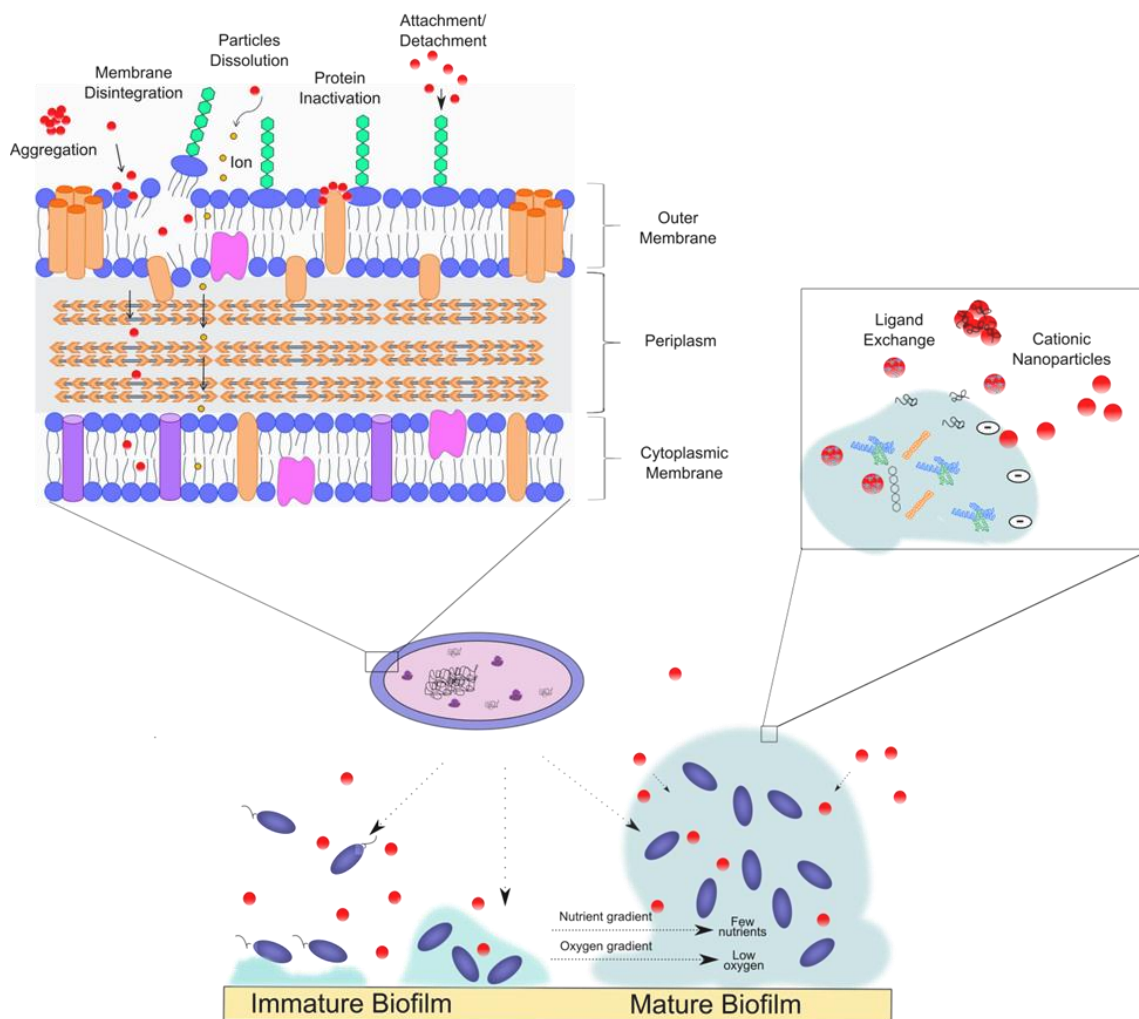


Figure 2.7 Schematic representation of the mechanisms involved in the NPs (red circles) interaction with free floating and sessile bacterial cells. In mature biofilms the NPs efficiency is altered by the exchange with matrix compounds resulting in NPs aggregation or interfacial interaction with biofilm cells (adapted from [247]).

2.9.3 Metal and Metal Oxide Nanoparticles

Metal and metal oxide NPs are widely used for controlling bacterial biofilms. The underlying mechanism of killing, when bacteria exist in the form of biofilm, differs from the antibacterial action of metallic NPs on the free floating cells. The unique surface moieties, shape, size, and aggregation propensity of the particles together with the biofilm tolerance to most antibacterials add significant complication in understanding NP-biofilm interactions. For example, while AgNPs and starch-stabilised AgNPs could eradicate individual *E. coli* cells, their effect on the sessile bacterial communities was significantly reduced. The authors suggested that the biofilm resistance is a result of

lower stability and particles aggregation within biofilms, which is attributed to the differences in ionic strength [247, 261, 262]. In another study, however, colloidal suspension of AgNPs prevented bacterial attachment and biofilm growth on model surface and even after incorporation into plasma-deposited layers of allylamine or hydrocarbon matrices the effect was not decrease [263, 264]. Implants coated with AgNPs also resisted the biofilm growth without silver accumulation in host tissues of rabbits, suggesting the great potential of the particles in preventing bacterial infections. [265].

Once inside the cells, metallic NPs, either by themselves or by the released ions, may interact with proteins, DNA or RNA molecules, inhibiting essential cellular functions [266]. The NPs have preferential binding sites in sulfur and phosphorous-containing proteins and enzymes, modifying their activity and leading to cell death [267]. They may generate reactive oxygen species (ROS) and induce cell damage and death. Some nanostructured materials possess multiple antimicrobial mechanism of action which significantly reduce the risk of drug resistance development [268]. Despite the promising results metal and metal oxide NPs can be toxic for human cells [269].

The formation of hybrid polymer-metal NPs was shown to increase significantly the NPs stability, biocompatibility and antibacterial activity [270]. Polymer-Ag bromide NPs and hydrogels containing AgNPs have been prepared showing strong inhibitory activity on both planktonic and biofilm forms [271, 272]. Permanent immobilisation of these hybrid polymer-metal NPs onto different surfaces is of great interest for durable antibiofilm effect [273]. In our group, hybrid Ag/chitosan system has been generated and then enzymatically grafted on the surface of cork. These particles synergistically inhibited of *S. aureus* and *E. coli* bacterial growth [273]. On the other hand, Li *et al.* constructed Ag containing polymer coatings with dual-function: chemical-releasing bacteria-killing capacity and contact bacteria-killing [184].

Copper oxide and zinc oxide (ZnO) NPs with excellent bactericidal effect against the common pathogens *E. coli* and *S. aureus* have been also reported. They were able to inhibit the biofilm growth most probably due to the generation of ROS or damage of the proteins involved in biofilms adhesion and formation [240]. The antimicrobial properties of copper have been observed also in other studies.

The antimicrobial activity and cytotoxicity of ZnO NPs have been also widely investigated in the last years. Nair *et al.* prepared polyethylene glycol-capped ZnO NPs that showed even higher antimicrobial efficacy when the particle size was reduced [274]. In other *in vitro* studies on the antibacterial action of ZnO NPs alone and in combination with a biopolymer, the great potential of these materials to prevent drug resistant biofilm occurrence was also demonstrated [275]. ZnO NPs-coated fabrics, for

instance, showed a differential antimicrobial activity against medically relevant *S. aureus* and *E. coli* inhibiting their growth by 67 % and 100 %, respectively [276]. Furthermore, the functionalisation of textiles with hybrid ZnO-chitosan NPs resulted in enhanced antibacterial efficiency against *S. aureus* and *E. coli* even at low ZnO concentration, compared to the individual ZnO and chitosan coatings. The presence of biocompatible polymer in the hybrid chitosan-ZnO NP reduced the cytotoxic effect of Zn, avoiding the risk of adverse effects on human health [277]. Recently, combinations of antibacterial metal NPs - ZnO and MgF₂ NPs, were used to synergistically inhibit the *S. pneumoniae* and *S. aureus* biofilms on cochlear implants [278]. Biocompatibility studies demonstrate that the antibiofilm active metal NPs coating do not exert toxicity toward primary human fibroblasts from the auditory canal. These findings underscore the potential of using NP combinations to efficiently inhibit bacterial colonisation and growth on medical devices.

2.9.4 Nanoantibiotics

Despite some promising results, most of the above discussed antibacterial agents may induce cytotoxicity and inflammatory responses limiting their clinical applications. Nanoantibiotics (NPs of antibiotics) are new antibacterial agents able to solve these drawbacks and improved the efficiency of antibiotics against drug resistant bacteria [279]. For example, penicillin, discovered in 1928, is still in use despite of its limited bactericidal effect towards antibiotic resistant bacterial strains. In order to renew the interest in this antibiotic, Yariv *et al.* synthesised penicillin NPs that showed higher bactericidal effect on *S. aureus* compared to the bulk form [280]. Nystatin is an example of nanoencapsulated antibiotic showing superior *in vitro* growth inhibition toward *C. albicans* compared with conventional nystatin in solution [281]. Tetracycline (TET) is a broad-spectrum antibiotic that increased its bactericidal effect against both TET sensitive and TET resistant bacterial strains after sonochemically induced transformation into NPs (TETNPs) [238]. TETNPs have been also deposited on graphene oxide sheets by a facile one-step sonochemical technique. Sonochemically synthesised graphene oxide/TET composite showed an enhanced activity against both sensitive and resistant *S. aureus* compared to the same concentration of non-transformed TET [279]. Sonochemistry was also used to simultaneously generate and deposit TETNPs onto parylene-C coated glass slides with potential to counteract pathogenic bacterial growth. In another study, TET has been loaded in microspheres of BSA [282]. TETNPs and TET-BSA microspheres showed high bactericidal effect against *E. coli* and *S. aureus*. Liposomes have also been used as carriers with

elevated effectiveness and safety of several antibiotics, such as amikacin [283], ciprofloxacin, meropenem, and gentamicin [284].

Nano-size transformation of clinically relevant antibiotics can be a facile method to improve the infection treatment, as an alternative to the rather time- and resource-consuming screening for new drugs. Moreover, the most common strategies rely on chemical modification of the obsolete antibiotics that does not change their interaction with the bacterial targets. Therefore, the underlying resistance mechanisms are still present. The produced nanoantibiotics are meant as novel antimicrobial agents with a broad-spectrum of activity, relying on a mechanism of action that comprises bacterial membrane disturbance and easy penetration into the biofilm structure. Further combination with other antibiofilm agents including QSI, enzymes, and AMPs might allow the development of hybrid antimicrobials able to address both the “evolutionary” and “cooperatively” acquired antimicrobial resistance.

3 Objectives of the Thesis

The overall objective of this thesis **is to develop materials and coatings for prevention or eradication of biofilm-related bacterial infections**. Novel strategies for counteracting bacterial growth and biofilm establishment will be adopted based on the mode of their action either on the biofilm matrix and signalling molecules or bacterial cells membrane. These approaches have advantages over the known methods because effectively reduce bacterial spread on the surface of interest without the use of antibiotics, thereby having a great potential to minimise the selection for resistant emergence.

To achieve the main goal of the thesis, the following **specific objectives** have been set up:

- i) To develop stable at use multilayer coatings comprising the QS disrupting enzyme acylase on silicone urinary catheters using LbL technique. The main advantage of this approach is that it might **attenuate bacterial virulence exerting less selective pressure on bacteria and reducing the risk of resistance development**. The pathogen may fail to establish infection and could be eliminated by the host immune system without the need of harsh antibiotic treatment.
- ii) To design novel integrated strategies to coat indwelling medical devices in order to impart specific surface activity toward bacterial biofilms. The approach relies on multilayer assembling of QQ enzyme, able to interrupt the communication among bacteria and matrix-degrading enzyme targeting the extracellular matrix polysaccharide. **Considering the key stages of the biofilm formation, the combination of both enzymes into hybrid nanocoatings is expected to enhance their antibiofilm activity against medically relevant bacteria in vitro and in vivo.**
- iii) **To engineer self-defensive surface coatings that release on demand bactericidal biopolymer NSs.** Polycationic AC will be sonochemically processed into polymer NSs with improved antibacterial and antibiofilm potential against common Gram-negative pathogens found in catheter related infections. The processed NS will be then assembled into multilayer coatings on silicone catheters and their ability to eradicate bacteria and prevent the biofilm formation in an *in vitro* model of catheterised human bladder will be assessed.

- iv) **To permanently embed antimicrobial polycationic NSs on silicone through epoxy/amine grafting.** The NSs decorated materials will counteract bacterial attachment and biofilm growth and therefore might have potential as a platform for prevention of biofilm infections on silicone based materials and implants.
- v) **To transform sonochemically into nano-form a clinically relevant antibiotic as a facile method to create broad-spectrum bactericidal drugs.** The nano-size antibiotic is expected to physically interact with the bacterial cell wall and demonstrate higher antibacterial and antibiofilm activities against Gram-negative bacteria.

4 Materials and Methods

4.1 Materials and Reagents

Acylase from *Aspergillus melleus* (4.5 % (w/w) protein content and 0.05 U/mg specific activity) and α -amylase from *Bacillus amyloliquefaciens* (32 mg/mL protein content and 20 U/mg specific activity), both purchased from Sigma-Aldrich (Spain), were used as QQ and matrix degrading enzymes, respectively. QS signalling compounds of Gram-negative bacteria including N-Butyryl-DL-homoserine lactone (C4-DL-HL), N-Hexanoyl-DL-homoserine lactone (C6-DL-HL), N-(3-Oxodecanoyl)-L-homoserine lactone (3-oxo-C10-L-HL) and N-(3-Oxododecanoyl)-L-homoserine (3-oxo-C12-L-HL) were also obtained from Sigma-Aldrich (Spain). AlamarBlue[®] Cell Viability Reagent and Live/Dead[®] BacLight[™] kit (L7012) were purchased from Invitrogen, Life Technologies Corporation (Spain).

Medical grade chitosan (15 kDa) was obtained from Kytzyme (Belgium). Cationic derivative of cellulose, 6-deoxy-6-(ω -aminoethyl) aminocellulose (AC, ~15 kDa), was synthesised from microcrystalline cellulose (Fluka, Avicel PH-101) via a tosyl cellulose intermediate, using a previously described procedure [273, 285]. Negatively charged hyaluronic acid (HA) with average Mw~750 kDa was obtained from Lifecore Biomedical (USA) in the form of its sodium salt, whereas a 25 kDa linear polyethyleneimine (PEI) bearing a positive charge was purchased from Polysciences, Inc., (Spain).

Polydimethyl/vinylmethyl siloxane (PDMS) urinary (Foley) catheters and strips from the same material, defined by the ASTM D 1418 standard, were provided by Degania Silicone Ltd. (Israel). All other chemical and microbiological reagents were purchased from Sigma–Aldrich unless otherwise specified.

4.2 Bacterial and Human cells

Proficient in biofilm formation bacteria *P. aeruginosa* (ATCC[®] 10145[™]), *E. coli* (ATCC[®] 25922[™]), and *S. aureus* (ATCC[®] 25923[™]), and human foreskin fibroblast cells (ATCC[®] CRL-4001[™], BJ-5ta) were obtained from American Type Culture Collection (ATCC, LGC Standards S.L.U, Spain). *C. violaceum* (CECT 5999), a mini-Tn5 mutant of *C. violaceum* (ATCC[®] 31532[™]) which cannot produce violacein without exogenous addition of AHLs, was purchased from Spanish Type Culture Collection (CECT, Spain).

4.3 Experimental Methods

4.3.1 Enzymatic Degradation of Biofilm Components

4.3.1.1 Acylase Assisted Degradation of Bacterial Quorum Sensing Signals

The degradation of several QS signals of Gram-negative bacteria as C4-DL-HL, N- C6-DL-HL, 3-oxo-C10-L-HL and 3-oxo-C12-L-HL by acylase was carried out as follows: 30 µg/mL of each AHL compound and 2.16 U/mL of the enzyme were incubated in 100 mM tricine buffer pH 8 for 15 min at 37 °C in a thermo-shaker bath. The resulting degradation products were analysed by a fluorescamine fluorimetric assay and *C. violaceum* CECT 5999 bioassay. In the fluorimetric quantification assay, 150 µL of the reaction mixture containing HL was added to 50 µL of fluorescamine reagent (3 mg/mL in dimethyl sulfoxide, DMSO) and after incubation at room temperature (RT) for 3 min the fluorescence at 390/470 nm was measured. The amount of HL released in the enzymatic reaction was calculated from the calibration curve built with α -amino- γ -butyrolactone hydrobromide as a standard.

In the *C. violaceum* bioassay only the degradation of C6-DL-HL by acylase was tested. *C. violaceum* is a mutant that produces a purple pigment, called violacein, only in the presence of AHLs. The most easily detectable AHL is C6-DL-HL, whereas the sensitivity to the other model compounds is different depending on their structure [286]. Before performing the bioassay, the products from the reaction mixture were extracted three times with ethyl acetate as previously described [287]. The organic phase was then evaporated to dryness and the sample reconstituted in 300 µL methanol. Thereafter, 60 µL of the reconstructed sample were tested for the presence of AHLs by *C. violaceum* bioassay. The sample solutions were pipetted into wells ($\emptyset = 7$ mm) punched in the LB agar (supplemented with 25 µg/mL kanamycin) and the plates were incubated at 26 °C for 48 h. Then, the degradation of C6-DL-HL signal by acylase was confirmed by the decrease of the purple zones surrounding the wells. C6-DL-HL extracts without acylase served as a control.

4.3.1.2 Amylase-Induced Degradation of Model Biofilm Exopolysaccharides

Chitosan, hyaluronic acid from *Streptococcus equi*, polygalacturonic acid and sodium alginate were used as model exopolysaccharide (EPS) components to evaluate the biofilm matrix degrading activity of α -amylase. The reaction between 700 µL of 5 mg/mL polysaccharide solutions in 20 mM sodium phosphate buffer pH 6.9 (NaPB) with 6.7 mM sodium chloride (NaCl) and 300 µL α -amylase (100 U/mL) was carried out

for 15 min at 37 °C in a thermo-shaker bath. The same solution without the polysaccharides served as a control. After the incubation period, the samples were subjected to 3,5-dinitrosalicylic acid (DNSA) assay for determination of the reducing sugars released upon polysaccharides degradation [288]. Briefly, 100 µL of tested samples were mixed with 100 µL DNSA solution and the samples incubated at 100 °C for 15 min. Then, the samples were cooled down on ice and diluted (ratio 1:3) with distilled H₂O. The absorbance was measured at 540 nm using TECAN Infinite M200 (Austria). All experiments were performed in triplicate. The amount of the glucose-equivalent reducing sugars in the reaction mixture was determined from the standard curve prepared by plotting absorbance versus glucose concentration.

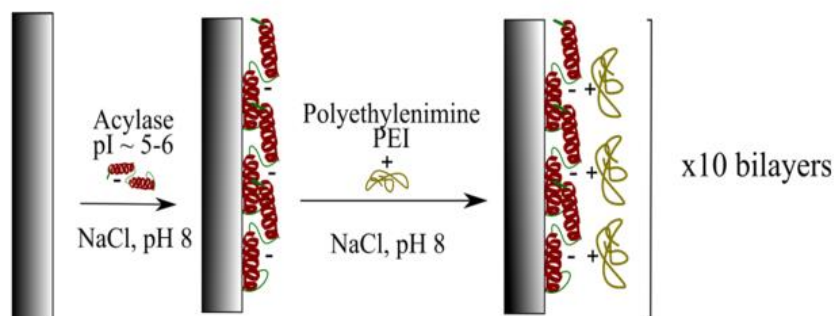
4.3.2 Enzyme Multilayer Coatings for Prevention of Bacterial Biofilm Formation on Silicone Foley Catheters

4.3.2.1 Silicone Surface Pre-treatment

Prior to coating, silicone catheter samples (3.5 × 9 cm²) were washed for 30 min with 0.5% (w/v) sodium dodecyl sulfate (SDS), distilled H₂O and 96% ethanol (EtOH, Scharlau, Spain). The silicone stripes and catheters were pretreated using 5% (v/v) (3-aminopropyl)triethoxysilane (APTES) in 96 % EtOH for 24 h at RT. After the incubation, the samples were washed with EtOH to remove the unbound APTES molecules and dried under nitrogen. The amination of the silicone was confirmed by attenuated total reflection-Fourier transform infrared (ATR-FTIR) analysis and ninhydrin test [289].

4.3.2.2 Assembling of Acylase Multilayer Coatings

The APTES treated silicone stripes were coated in a layer-by-layer (LbL) fashion (Scheme 4.1). Acylase, having isoelectric point between pH 5 and 6 (negatively charged at a pH higher than 6) was used as polyanion, whereas linear PEI (M_w = 25 kDa) was used as a polycation. A bilayer of oppositely charge polymers was constructed by dipping the silicone stripes for 10 min in 1 mg/mL acylase solution in 100 mM tricine buffer pH 8, followed by dipping in 1 mg/mL PEI solution, pH 8. After each polyelectrolyte deposition, a 10 min rinsing step in 0.15 M NaCl, pH 8 was performed. This procedure was repeated for ten times, and the coated silicone samples were finally dried with a continuous flow of nitrogen. LbL coating with a bilayer architecture of (Acy/PEI)₁₀/Acy was built, with the outermost layer being acylase (LbL Acylase) (Scheme 4.1). The same procedure was performed to coat silicone Foley urinary catheters.



Scheme 4.1 LbL assembly of acylase on the silicone catheters.

4.3.2.3 Assembling of Hybrid Multilayer Coatings Comprising Quorum Quenching Acylase and Matrix-Degrading Amylase

Amino-preactivated silicone stripes were coated with the QQ and/or matrix-degrading enzymes by LbL deposition technique as described above with some modifications. For each polyelectrolyte deposition step, silicone pieces were first immersed for 10 min into anionic enzyme solution (1.5 mg/mL of acylase in 100 mM tricine buffer, pH 8, or 1.5 mg/mL of α -amylase in 20 mM NaPB buffer with 6.7 mM NaCl, pH 6.9) and then in 1.5 mg/mL solution of positively charged branched PEI ($M_w = 75$ kDa) in tricine buffer for acylase or NaPB for α -amylase. Each deposition step was followed by 10 min of washing in 0.15 M NaCl solution, pH 8. LbL coatings with the following architectures ((Acy/PEI)₁₀/Acy, (Amy/PEI)₁₀/Amy, (Acy/PEI/Amy/PEI)₅/Amy, and (Acy/PEI/Amy/PEI)₅/Acy (hybrid coatings)) were formed, with the uppermost layer being acylase for the LbL Acy and the LbL Hyb-Acy and α -amylase for the LbL Amy and LbL Hyb-Amy coatings.

4.3.2.4 Coatings Formation with Non-Antibiofilm Active Protein

Considering the antibacterial properties of PEI its role in inhibiting bacterial biofilms on catheter surface after the LbL assembling was further investigated. Cationic PEI ($M_w=75$ kDa) and a nonactive protein (e.g., bovine serum albumin (BSA)) bearing negative charge were sequentially deposited in a LbL fashion on silicone material as already described. The resulting PEI/BSA coatings always had the non antibiofilm active protein as an outermost layer.

4.3.2.5 Characterisation of Enzyme Multilayers

Attenuated Total Reflection Fourier Transform Infrared Spectroscopy Analysis. The deposition of enzyme proteins on the silicone surface was analysed by FTIR-ATR using a Spectrum 100 FT-IR spectrometer (Perkin Elmer, USA). The FTIR-ATR spectra of non-treated silicone and LbL samples were collected in the range over 4000 to 625 cm^{-1} . All the spectra were obtained after 64 scans at 4 cm^{-1} resolution and the data were analysed using essential eFTIR - 3.00.019 software.

Atomic Force Microscopy. The morphology of the different surfaces was studied by atomic force microscopy (AFM) using a Dimension 3100 AFM from Veeco. The AFM images were analysed and post-processed using the Nanotec WSxM software [290].

Water Contact Angle Measurements. The hydrophilicity of the coatings comprised only of QQ acylase was assessed measuring the static contact angle (sessile drop method) of 5 μL ultra-pure water droplet on the material, using drop shape analysis system DSA 100 (Krüss, Hamburg, Germany), equipped with $\frac{1}{2}$ CCD camera. Three independent measurements were performed and analysed using Krüss DSA3 v1.0.1.3-02 software for each sample.

Stability of Enzyme Multilayers. The stability of enzyme-based multilayers was assessed by monitoring the fluorescein isothiocyanate (FITC)-labelled amylase or acylase released from the silicone surface in artificial urine. For enzyme labelling, acylase and amylase (2 mg/mL) were dissolved in 0.1 M sodium carbonate buffer, pH 9. Then, 1 mg/mL FITC solution was prepared in anhydrous DMSO and mixed with protein solutions (for each 1 mL of protein solution 50 μL of FITC solution were added). The reaction mixture was incubated in the dark for 12 h at 4 °C. Thereafter, the unreacted FITC was separated from the FITC-enzyme conjugates using PD-10 desalting columns (GE healthcare), and the LbL assembly with the labelled proteins was performed as already described.

The treated silicone strips were cut into small pieces ($1 \times 1 \text{ cm}^2$) and incubated in 5 mL of artificial urine at 37 °C under slow shaking (20 rpm) for 7 days. At desired time intervals, 0.2 mL of urine sample was collected and replaced with 0.2 mL of pre-warmed urine (37 °C). The fluorescence intensity of the urine samples was measured at Ex/Em (490/525) using TECAN Infinite M 200. Then, the cumulative fluorescence intensity divided by the total fluorescence intensity of FITC-labelled enzymes in the multilayers, I/I_{total} , was used to determine the amount of labelled enzyme released from the coatings as a function of the incubation time.

The stability of the FITC-labeled coatings was further studied through the changes of coatings intensity before and after incubation in artificial urine by fluorescence microscopy. The same gain and offset settings were used to acquire all images.

Total Amylase and Acylase Fluorescence Intensity in the Multilayer Coatings. The total fluorescence intensity of the proteins, amylase or acylase, in the multilayer coatings was determined after the detachment of the fluorescently labelled coatings from the surface using a surgical blade. The pieces ($1 \times 1 \text{ cm}^2$) and the corresponding blades were placed in 2 mL 5% (w/v) SDS solution and vortexed for 1 min. Afterward, 200 μL of the FITC-labelled protein solutions were transferred in 96-black well plates and the fluorescence intensity of each test sample was measured at Ex/Em (490/525). The relative amount of protein immobilised per square centimetre of silicone was calculated using calibration curves plotted between fluorescence intensity of the FITC-labelled acylase or amylase and their protein content.

4.3.2.6 Enzymatic Activities in Multilayer Coatings

Acylase Activity in the Assemblies. The activity of acylase, in both free and immobilised forms, was initially evaluated by a colorimetric assay using N-acetyl-L-methionine (NAMET) as a substrate. Briefly, 2 mL of 100 mM tricine buffer, pH 8.0 and 1 mL of 0.5 mM cobalt chloride solution were added to the samples and equilibrated at 37 °C. Then, 1 mL of 100 mM NAMET in tricine buffer was added and the test tubes were incubated for 30 min. The reaction was stopped by rising the temperature to 100 °C for 4 min. The product of the enzymatic reaction was determined using the colorimetric ninhydrin assay as follows: 1 mL of the sample was mixed with 2 mL of 2% (w/v) ninhydrin solution (prepared in 200 mM citrate buffer pH 5 and ethylene glycol monomethyl ether (1:1)) and 0.1 mL 1.6% (w/v) stannous chloride solution. The samples were incubated for 20 min at 100 °C and cooled down before measuring their absorbance at 570 nm. Non-treated silicone material was used as a control in all experiments. The immobilisation efficiency of acylase on silicone material was evaluated as a percentage of the enzyme specific activity retained after immobilisation on the surface.

In addition, the potential of the acylase coatings to degrade the AHLs molecules in bacterial surroundings and consequently quench the QS process was assessed in a reporter bacterial strain *C. violaceum*. Untreated silicone sample (negative control) and acylase-coated silicone stripes were cut into $2 \times 2 \text{ cm}^2$ pieces and placed in sterile test tubes. The silicone pieces were inoculated with 5 mL overnight bacterial culture of *C. violaceum* (grown at 26 °C) diluted to $\text{OD}_{660} = 0.002$ in Luria-Bertani Broth (LB), supplemented with 25 $\mu\text{g}/\text{mL}$ kanamycin and 5 μM C6-HSL. Thereafter, the tubes were

incubated at 26 °C with shaking (230 rpm) for 18 h. After the incubation period 200 µL of the cell suspension were transferred into Eppendorf tubes and mixed with 200 µL 10% SDS (w/v) [291]. The samples were mixed, vortexed for 5 s and the violacein extraction was performed by addition of 500 µL 1-butanol followed by centrifugation for 5 min at 13 000 rpm. After phase separation, the butanol (upper phase) was collected and the absorbance measured at 584 nm. Non-immobilised acylase was used to compare the QQ efficiency of the enzyme in the coatings.

Amylase Activity Using Bacterial Extracellular Polymeric Matrix as Substrate. The EPS-degrading activity of amylase in the hybrid multilayers was evaluated using *P. aeruginosa* biofilm matrix as a substrate. A culture of *P. aeruginosa* grown overnight in tryptic soy broth (TSB) was poured on tryptic soy agar plates. Afterward, the plates were incubated at 37 °C for 24 h to allow biofilm development. The biofilms were harvested using a sterile spatula and washed with sterile distilled H₂O. The cell suspension was then immediately subjected to EPM extraction with high-speed centrifugation at 20 000 rpm and 4 °C for 20 min. The supernatants were filtered through a 0.22 µm membrane, and the filtrates were used as the EPM sample containing EPS constituents [292]. Afterward, 7 mL of *P. aeruginosa* EPM extracts were incubated with silicone samples (2 × 2 cm²) at 37 °C with shaking for 24 h. After the incubation period, samples were analysed for reducing sugar content using DNSA assay as described. Pristine silicone and EPS-containing extracts served as controls. The amount of reducing sugars present in the extracts was subtracted from the values obtained for all amylase-containing samples. Free amylase was used to compare the activity of the enzyme multilayer coatings toward the biofilm EPS.

4.3.2.7 Functional Characterisation of Catheters Coated With Antibiofilm Enzymes

Initial Bacterial Adhesion. Initial bacterial adhesion was studied on acylase-coated and non-treated silicone sheets. The samples were cut into 1 x 1 cm² pieces and placed in a cell-culture 24-well plate. Then, the samples were inoculated with 1 mL of bacterial culture of *P. aeruginosa* in TSB in which the concentration of glucose was 0.25% (w/v). The bacterial inoculum was prepared from overnight culture grown in TSB and diluted to OD₆₀₀ = 0.01. The culture plate was incubated for 3 h at 37 °C to allow bacterial adhesion. Thereafter, the samples were washed three times with sterile phosphate buffered saline (PBS) and left in 4% (v/v) formaldehyde at 4 °C overnight to allow fixation of the bacteria. Then, the samples were washed with sterile PBS and 25, 50, 75 and 96 % ethanol for 10 min. The initial bacterial attachment was studied in a bright field mode using Eclipse Ti-S microscope (Nikon Instruments Inc., The Netherlands).

Single Species Biofilm Inhibition. Crystal violet (CV) assay was used to quantify the biofilm inhibition activity (i.e. total biomass reduction) of enzyme-coated catheter materials in both static and dynamic conditions, against Gram-positive *P. aeruginosa* or Gram-positive *S. aureus*. Briefly, inoculum of each bacterium was prepared from overnight grown culture in TSB diluted to $OD_{600} = 0.01$. The enzyme-coated samples were cut into $1 \times 1 \text{ cm}^2$ pieces and placed in a cell-culture 24-well plate. Thereafter, 1 mL of bacteria was inoculated in each well and the plate was incubated for 24 h at 37 °C. The liquid media was removed and the biofilm washed with distilled H_2O three times to eliminate non-adhered bacteria. The biofilms were further fixed by heat (60 °C for 60 min) and the biofilm mass quantified using CV. Briefly, 700 μL of 0.1% (w/v) crystal violet were added to each well and incubated for 10 min at RT. Then, CV was discarded and samples washed with sterile distilled H_2O three times. The remaining stain was eluted with 1 mL 30% (v/v) acetic acid and the total biomass was determined as the amount of CV bound to each sample by measuring the absorbance at 595 nm. Untreated silicone samples served as negative control (no biofilm inhibition) in all experiments.

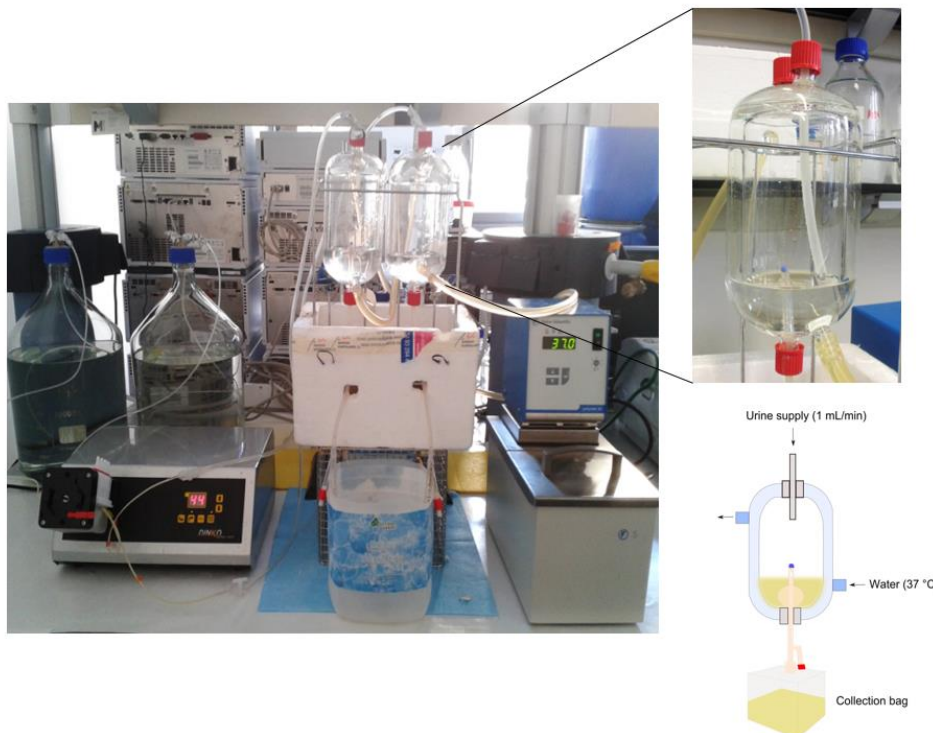
Mixed Species Biofilm Inhibition. Following the combination of the two enzymes, acylase and amylase, into a hybrid multifunctional coating, the biofilm inhibition potential was evaluated against mixed-species biofilms of Gram-negative bacteria. The silicone samples were incubated with 1 mL of bacterial suspension containing mixture of *P. aeruginosa* and *E. coli* ($OD_{600} = 0.01$, final concentration of each bacterium) pathogens frequently found in urinary catheter biofilms. Then, the biofilms were allowed to grow statically and the total biofilm mass was measured with the CV assay as described.

Bacterial Viability in the Biofilms. Single- and dual-species biofilms were grown on acylase on hybrid silicone samples and then subjected to analysis with Live/Dead[®] BacLight™ kit. Following 24 h of incubation, the non-adherent bacteria were rinsed with 1 mL of sterile 0.9% NaCl, pH 6.5, and the biofilms were stained using a mixture of two dyes: green fluorescent Syto 9 and red fluorescent propidium iodide (1:1). Then, the biofilms were analysed by fluorescence microscopy at Ex/Em (480/500) for Syto[®] 9 labelling the nucleic acid of all bacteria, with intact and damaged membranes in green and at Ex/Em (490/635) for propidium iodide quenching the green fluorescence of Syto[®] 9 dye after penetration into the damaged cells, consequently staining dead bacteria in red.

Effect of Enzyme Multilayer Coatings on Bacterial Growth. The effect of enzyme coated silicone materials on planktonic bacterial growth was also evaluated. Overnight culture of bacteria in TSB was diluted to $OD_{600} = 0.01$ (final concentration) and then 1 mL of freshly prepared single or mixed bacterial inocula was cultured with treated and non-treated silicone for 24 h at 37 °C. After incubation, single- or dual-species bacterial growth was determined spectrophotometrically by measuring the OD at 600 nm.

Functional Stability of the Coatings. The stability of acylase-comprising coatings was studied after incubation in artificial urine containing 25 g/L urea, 9 g/L sodium chloride, 2.5 g/L disodium hydrogen orthophosphate, 3 g/L ammonium chloride, 2.5 g/L potassium dihydrogen orthophosphate, 2 g/L creatinine, and 3 g/L sodium sulfite, pH 6.8. The samples were cut, placed in a test tube containing 2 mL artificial urine and incubated for 1 and 7 days at 37 °C with 20 rpm shaking. Afterwards, the silicone pieces were washed with distilled H₂O and the antibiofilm activity was determined in static conditions against *P. aeruginosa*, as already described.

Dynamic Biofilm Inhibition Tests. LbL assemblies on Foley urinary catheter were analysed for their stability under dynamic conditions using a previously described physical model of catheterized human bladder [293]. This model consists of a glass bladder model maintained at 37 °C by a water jacket (Scheme 4.2). After the insertion of non-treated and treated Foley catheters, the model was filled up to the catheter's eye with sterile artificial urine, pH 6.8 (supplemented with 1 mg/mL TSB), containing only Gram-negative *P. aeruginosa*, Gram-positive *S. aureus* or both *P. aeruginosa* and *E. coli* bacterial species (final $OD_{600} = 0.01$ for each bacterium). During the 7 days of catheterisation, the model was maintained at 37 °C and supplied with sterile artificial urine at a flow rate of 1 mL/min. Then, the catheter was removed, and the biofilm formation on the catheter-balloon (1×1 cm) and catheter shaft (also referred to as urethra) surface were subjected to analysis for biofilm formation using CV and Live/Dead kit as described. The same parts of pristine silicone Foley catheter were used as controls for biofilm formation (no antibiofilm effect).



Scheme 4.2 Physical glass model of catheterised bladder used in dynamic biofilm inhibition tests.

Biocompatibility Tests. The biocompatibility of the silicone samples ($1 \times 1 \text{ cm}^2$) coated with acylase, amylase, and both enzymes (hybrid coatings) was studied using human foreskin fibroblasts. The cells were maintained in 4 parts Dulbecco's Modified Eagle's Medium (DMEM) containing 4 mM L-glutamine, 4500 mg/L glucose, 1500 mg/L sodium bicarbonate, 1 mM sodium pyruvate and 1 part of Medium 199, supplemented with 10% (v/v) of foetal bovine serum, and 10 g/L hygromycin B at 37 °C, in a humidified atmosphere with 5 % CO₂. At pre-confluence, the cells were harvested using trypsin-EDTA (0.25 % (w/v) trypsin/0.53 mM EDTA solution in Hank's BSS without calcium or magnesium) and seeded on 24-well tissue culture-treated polystyrene plate (Nunc) at a density of 4.5×10^4 cells/well. After 24 h of culturing, silicone samples were placed in a contact with the cells for 1 and/or 7 days. Thereafter, the cell viability was determined using alamarBlue[®] assay.

Resazurin, the active blue ingredient of the alamarBlue[®], is a nontoxic, cell-permeable compound that, once in a viable cell, is reduced to red-coloured resorufin. AlamarBlue[®] reagent was diluted in culture medium (1:10) and added to each well after aspirating the culture medium containing the samples in contact with cells. After 4 h of incubation at 37 °C, the absorbance at 570 nm was measured in a microplate reader, using 600 nm as a reference wavelength. The quantity of resorufin formed is directly proportional to the number of viable cells. The cell viability (%) was assessed for each

silicone sample (treated and non-treated) and compared to that of a control sample of culture medium, corresponding to 100 % cell viability. The error bars represent the standard deviation of three independent measurements.

In Vivo Biofilm Tests. The antibiofilm potential of hybrid coatings containing acylase as outermost layer was also assessed using an *in vivo* rabbit model. All the experiments with rabbits were performed after the acceptance by the appropriate ethical approval committee. New Zealand white male rabbits (3–4 kg body weight) were catheterized with treated (n = 3) and non-treated (n = 3) silicone Foley catheters for 7 days. During the catheterisation, the weight and temperature of the animals were recorded. To minimise pain and distress, the rabbits were treated with buprenorphine according to the requirements of the ethical committee. The rabbits received physical examinations, and only these that met the health and weight criteria were used in the study. Prior to catheterisation, the animals were anaesthetised, and the penis was cleaned and swabbed. Throughout the experiment, anaesthesia was maintained with isoflurane/oxygen, and the body temperature and vital signs were monitored. The urethra was filled with lubricant, and the catheter was then threaded into the penis meatus. After insertion into the bladder, the catheter balloon was inflated with 4 mL of sterile 0.9 % NaCl, pH 6.5. The ports that connect the catheters with the drainage bag were removed, so that the animal did not need to be restrained. To maintain the catheter into the animal's body, the entrance was blocked and held by suture. Although the catheter's opening could distress the animals, the trauma would be less than that of movement restriction and attachment to a drainage bag.

The procedure for rabbit catheterisation allowed spontaneous bacterial contamination, mimicking the occurrence of catheter-associated infections. The continuous urine flow through the catheter shaft and the wet zone exposed to nonsterile conditions in the housing cage contribute to the catheter's contamination after insertion.

Bacterial growth in the urine collected from the rabbits was monitored every day during the catheterisation. Briefly, the urine was serially diluted in sterile 0.9% NaCl, pH 6.5, and then plated on LB agar. The plates were incubated at 37 °C for 24 h, and the number of live bacteria was determined. After 7 days of incubation, the control and enzyme-coated catheters were removed and examined for the presence of biofilm.

4.3.2.8 Statistical Analysis

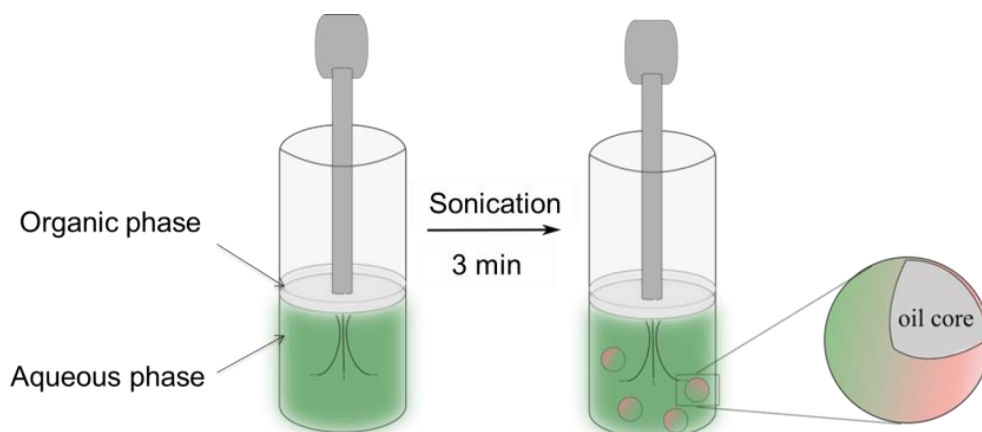
All data are presented as mean \pm standard deviation. For multiple comparisons, statistical analysis by a one-way analysis of variance (ANOVA) followed by posthoc

Tukey test was carried out using Graph Pad Prism Software 5.04 for windows (USA). P values less than 0.05 were considered statistically significant.

4.3.3 Nanomaterials for Controlling Planktonic Bacterial Growth and Biofilm Occurrence: Polycationic Aminocellulose Nanospheres

4.3.3.1 Preparation of Polycationic Aminocellulose Nanospheres

Highly cationic ACNSs with sunflower oil as a lipid core were prepared by an adapted sonochemical method of Suslick, reported elsewhere for different kinds of biopolymers and their derivatives (Scheme 4.3) [294, 295]. Briefly, the pH of the AC aqueous solution (1 mg/mL) was adjusted to 5.5 using 0.1 M hydrochloric acid (HCl). Then, a mixture of 70 % AC and 30 % commercial sunflower oil was prepared in a thermostated (4 ± 0.5 °C) sonochemical cell. The NSs were generated using a Ti horn of a high-intensity Vibra-Cell VCX 750 ultrasonic processor (Sonics and Materials, Inc., USA), employing 20 kHz at 35 % amplitude. The Ti horn was positioned at the aqueous-organic interface. An acoustic power of ~ 0.5 W/cm³ was applied for 3 min and the resulted suspension was cleaned from non-encapsulated oil by three consecutive centrifugations at 1500 rpm for 15 min.

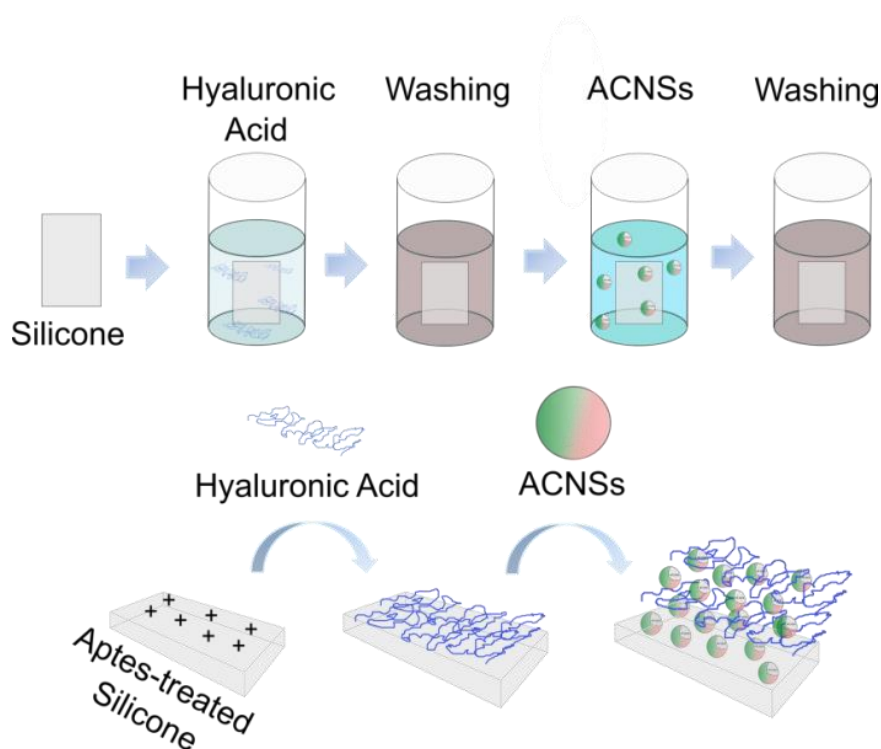


Scheme 4.3 Nanospheres formation via one-step sonochemical process.

4.3.3.2 Nanospheres Deposition onto Silicone Material

Multilayer coatings of ACNSs were assembled on APTES functionalised silicone supports (Section 4.3.2.1 Silicone surface pre-treatment) to facilitate the deposition of the first negatively charged HA layer. A solution of HA polyanion and a dispersion of ACNSs polycation were prepared with 0.15 M NaCl to reach final concentrations of 0.5 mg/mL. The pH was adjusted to 5.5 with 1 M HCl or 1 M sodium hydroxide aqueous

solutions. The polyelectrolytes were alternately deposited using a multi-vessel automated dip coater system (KSV NIMA, Finland) on silicone starting with HA and finishing with ACNSs to form 5, 10 and 100 bilayers. Each deposition lasted for 10 min and was followed by a 10 min rinsing step with 0.15 M NaCl, pH 5.5 (Scheme 4.4). The obtained multilayer coatings were named after the number of bilayers employed for their assembling: (HA/ACNSs)₅, (HA/ACNSs)₁₀ and (HA/ACNSs)₁₀₀. Non-processed AC in solution and the same procedure for 5 and 10 bilayers were used to prepare the corresponding controls designated as (HA/ACsol)₅ and (HA/ACsol)₁₀.



Scheme 4.4 LbL assembly of aminocellulose nanospheres (ACNSs) on the catheters surface.

The LbL build up was followed by a quartz crystal microbalance with dissipation (QCM-D, E4 system from Q-Sense, Sweden). The deposition was carried out on gold-coated AT-cut quartz crystals (QSX301, Q-Sense, Sweden) previously cleaned with 5:1:1 solution of H₂O:NH₃:H₂O₂ at 80 °C for 10 min, and amino functionalised with 11-amino-1-undecanethiol hydrochloride (HS(CH₂)₁₁NH₂) as described elsewhere [296]. Briefly, the crystals were immersed into 20 µM ethanol solution of HS(CH₂)₁₁NH₂ for 48 h to ensure well-ordered amino ended self-assembled monolayers. After this treatment, the sensors were washed several times with ethanol, dried under N₂ and placed in the QCM-D flow chambers. A stable baseline was acquired in 0.15 M NaCl solution at 25 °C. The polyelectrolytes (0.5 mg/mL) deposition was carried out at a constant flow rate

(50 $\mu\text{L}/\text{min}$). Each polyelectrolyte solution was injected into the measurement chamber for 10 min followed by a rinsing step with 0.15 M NaCl pH 5.5 to remove loosely bound material. The measurements (changes in the frequency ΔF and dissipation ΔD) were performed at several harmonics ($n = 3, 5, 7, 9, 11$ and 13). $\Delta F/n$ and ΔD were fitted for the seventh and ninth overtone using the Q-Tools software (v 3.0.6.213). Voigt element-based model was used to obtain the thickness of the produced multilayers.

4.3.3.3 Characterisation of Aminocellulose-based Coatings

The multilayer coatings with 5 and 10 bilayers of HA/ACsol and HA/ACNSs were characterised by ATR-FTIR (Section 4.3.2.5-Characterisation of enzyme multilayers). Prior to analysis, the coated silicone stripes were thoroughly washed in distilled water at 100 rpm for 24 h and then dried under N_2 . The morphology of the LbL coatings was investigated by SEM (JSM 5610, JEOL Ltd, Japan) and AFM. Changes in the surface hydrophilicity of the material as a result of the polyelectrolytes deposition were followed by static water contact angle measurements (OCA 15+, DataPhysics Instruments, Germany) using the sessile drop method (drop of 1 μL in high-performance liquid chromatography (HPLC) grade water). At least six measurements per sample were performed and averaged.

4.3.3.4 Antimicrobial activity

The antibacterial activity of the coated silicone towards the *P. aeruginosa* planktonic growth was evaluated using shake flask method. Briefly, a single colony from the *P. aeruginosa* stock bacterial culture was grown overnight in nutrient broth (NB, Sharlab, Spain). Then, the bacterial cells were harvested by centrifugation and diluted in sterile 0.9% NaCl solution, pH 6.5, until reaching solution absorbance of 0.28 ± 0.1 at 600 nm, which corresponds to $1.5 - 3.0 \times 10^8$ colony-forming unit (CFU)/mL. The silicone samples ($1 \times 1 \text{ cm}^2$) were incubated with 2 mL cells suspension at 100 rpm and 37°C for 2 h. These suspensions were serially diluted in the same NaCl solution, then plated on a cetrimide agar and incubated at 37°C for 24 h to determine the number of viable bacteria. Three independent measurements were performed per sample and the results are expressed as a reduction percentage of the survived bacterial colonies (CFU) after incubation with the specimens (B) compared to the CFU survived from the suspension in contact with pristine silicone (A), calculated as follows:

$$\text{Reduction (\%)} = (A-B)/A \times 100.$$

4.3.3.5 Degradation of the Coatings in Presence of Bacteria

The degradation of the multilayer coatings in the presence of *P. aeruginosa* was assessed using FITC-labelled AC component (Section 4.3.2.5 Characterisation of enzyme multilayers, *Stability of enzyme multilayers*). Prior to immobilisation, AC (6 mg/mL) was dissolved in 0.1 M sodium carbonate buffer, pH 9. Then, 1 mg/mL FITC solution was prepared in anhydrous DMSO and mixed with AC in buffer (for each 1 mL of AC 50 μ L of FITC were added). The reaction mixture was incubated in the dark at 4 °C for 12 h. The unreacted FITC was separated from the AC-FITC conjugate and the LbL assembly between HA and AC-FITC was performed on silicone stripes as described. The coated silicone samples were further cut in equal pieces and incubated in distilled H₂O and TSB (both as control samples) and TSB containing *P. aeruginosa* (OD₆₀₀ = 0.01) at 37 °C for 6 and 24 h. At the end of these time intervals, the samples were withdrawn and washed with distilled H₂O prior to analysis by fluorescence microscopy. The same microscope gain and offset settings were used to acquire all images. The stability of the coatings was further assessed by their fluorescence intensity in absence and presence of *P. aeruginosa*.

4.3.3.6 Biofilm Inhibition Tests

The ability of the ACNSs coated silicone materials to control *P. aeruginosa* biofilms in both static and dynamic conditions was studied using Live/Dead[®] BacLight[™] bacterial viability kit as described in the section 4.3.2.7 Functional characterisation of catheters coated with antibiofilm enzymes, *Bacterial Viability in the Biofilms*.

4.3.3.7 Statistical Analysis

The results for the samples hydrophilicity and antibacterial activity are presented as mean values \pm standard deviation (SD). Statistical analysis was carried out by Graph Pad Prism 6 Software (USA) by performing ANOVA followed by post-hoc Tukey test to determine the statistical significance of the observed differences among the samples. The differences were considered significant only if $p < 0.01$.

4.3.4 Covalent Grafting Of Aminocellulose Nanospheres onto Silicone Material for Escherichia Coli Biofilm Prevention

4.3.4.1 Silicone Material Functionalisation with Aminocellulose Nanospheres

PDMS stripes (9 x 3.2 cm²) were washed and then functionalised with 5 % (v/v) 3-(glycidoxypropyl) trimethoxysilane (GOPTS) solution in 96 % EtOH for 12 h at room temperature. The samples were washed with EtOH, dried at 85 °C for 2 h and stored in the dark for at least 2 days prior to functionalisation with ACNSs. The presence of

epoxy groups on the surface was confirmed by development of characteristic pink colour in a 4-(para-nitrobenzyl) pyridine (p-NBP) test. Briefly, treated and non-treated silicone samples were incubated in 5 mL of 200 mM p-NBP solution in methoxyethanol for 30 min at 80 °C.

ACNSs were prepared as previously described ACNSs (Section 4.3.3.1 Preparation of Polycationic Aminocellulose Nanospheres). For epoxy/amine curing reaction, the pre-activated silicone strips were cut and placed in 15 mL test tubes containing 5 mL of 0.1 mg/mL and conditioned at pH 3 and 6. Then, the tubes were transferred in a water bath at 60 °C and kept overnight with shaking. Afterwards the silicone stripes were washed three times with distilled H₂O, until no spheres were released into the washing solution, verified by optical microscopy and dynamic light scattering (DLS) and stored at 4 °C for further analysis.

The deposition of ACNSs on the silicone material was assessed by ATR-FTIR using a Spectrum 100 FT-IR spectrometer (Perkin Elmer, USA) as describes. The shape and morphology of immobilised NSs onto silicone was assessed with SEM using a cross-beam workstation (Zeiss Neon 40) with Focused Ion Beam FIB/SEM beams for observation. Prior to imaging the silicone samples (1x1 cm²) were coated with carbon under vacuum.

4.3.4.2 Inhibition of *E. coli* Biofilms

Prior to immobilisation of the spheres on silicone samples, the biofilm inhibition activity of the ACNSs was evaluated and compared to non-processed AC in solution. For optimal biofilm growth, fresh single *E. coli* colony was inoculated in 5 mL TSB and cultured overnight at 37 °C with shaking (230 rpm). 100 µL of *E. coli* cells were mixed with 100 µL ACNSs or ACsol at 0.5 mg/mL in a 96-well plate (polystyrene, surface-treated) and then cultured for 24 h at 37 °C. After incubation, the mixtures were withdrawn from the wells and the surfaces further washed with sterile distilled H₂O, fixed by heat (60 °C for 60 min) and the total biofilm mass was measured with 0.01 % (w/v) crystal violet solution. Total biomass assessment and cells viability was also performed for the ACNSs decorated silicones as described.

4.3.5 Nano-sized Penicillin G for Overcoming Gram-Negative Bacterial Resistance

4.3.5.1 Sonochemical Preparation of Penicillin G Nanospheres

Penicillin and control nanospheres (NSs) were prepared using ultrasound. Two-phase solution containing 70 % of 0.250 g/L antibiotic aqueous solution containing 0.1 % (w/v)

of Poloxamer 407 surfactant (the antibiotic is omitted in the control NSs) and 30 % commercial sun-flower oil (organic phase) was prepared and placed into a thermostated sonicator cell (Section 4.3.3.1 Preparation of Aminocellulose Nanospheres). The resulted NSs dispersion was purified by three consecutive centrifugations at 1500 rpm for 15 min to remove the organic phase.

4.3.5.2 Nanospheres Characterisation

Dynamic light scattering (DLS) was used to measure the size of NSs (DL135 Particle Size Analyzer, Cordouan Technologies, France). The data were analysed using NanoQ 1.2.1.1 software to calculate the mean particle diameter. The determination of zeta potential was carried out using a Zetasizer Nano Series (Malvern Instruments Inc., Worcester, UK) after appropriate dilution of NSs using ultrapure-grade water at pH 6. The shape and morphology of NSs was visualised with SEM using a cross-beam workstation (Zeiss Neon 40) with Focused Ion Beam FIB/SEM beams for sample observation. SEM samples were prepared by applying a small drop of NSs suspension on a glass slide and dried at RT before gold-palladium sputtering.

4.3.5.3 Interaction with Cell Membrane Models

The interaction of penicillin and nanopenicillin with cell membrane models was assessed using a Langmuir monolayer technique by measuring the effect of the antimicrobial agents in contact with L- α -Phosphatidylethanolamine (PE) phospholipid extracted from *E. coli* [297, 298].

The interaction was evaluated by the Langmuir monolayer compression technique and by measuring the kinetics of insertion of the both agents into the monolayer performed in a Langmuir trough (KSV NIMA model KN2002, Finland) with a total area of 273 cm² mounted on an antivibration table and housed in an insulation box at a temperature of 22 \pm 2 °C.

Langmuir Monolayer Compression Measurements. Penicillin solutions, nanopenicillin and control NSs suspensions at 0.250 mg/mL were used. The samples were then diluted 500 times with MilliQ water (18 M Ω cm) to a concentration of 0.5 μ g/mL and studied in the subphase for their interaction with an *E. coli* PE monolayer. The Langmuir trough was filled with a subphase solution that was either MilliQ water (control) or the nanopenicillin, penicillin diluted solutions or control NSs suspension, and 10 μ L of 0.5 mg/mL PE solution in chloroform was carefully spread onto the subphase with a gas-tight syringe. After chloroform evaporation (10 min), the floating film was continuously compressed at the air-water interface at a linear speed of 25 mm/min. The surface pressure (π) was recorded against the area (A), measured with a

Wilhelmy balance plate (Pt) connected to an electrobalance. The isotherms provide information about the film states, phases and phase transitions, where π is the difference between the surface tension of pure water (γ_0) and that of the film (γ), i.e. $\pi = \gamma_0 - \gamma$. The compression modulus (in-plane elasticity) C_s^{-1} was calculated from the slope of the π vs A isotherm in order to elucidate the phase transitions that occur in the monolayer [299]:

$$C_s^{-1} = -A \left(\frac{d\pi}{dA} \right)_T \quad (1)$$

Whereas the minimum value in the plot of C_s^{-1} vs π indicates a phase transition, the maximum allows the classification of these transitions as liquid-expanded ($12.5 < C_s^{-1} < 100$ mN/m), liquid-condensed ($100 < C_s^{-1} < 250$ mN/m) and condensed ($C_s^{-1} > 250$ mN/m).

Insertion into Phospholipid Monolayer. The kinetics of insertion of penicillin, nanopenicillin and control NSs into monolayers was measured using the phospholipid monolayer built at surface pressure of 30 mN/m that corresponds to the lateral pressure of bacterial cell membrane [300]. 40 μ L of 0.5 mg/mL PE phospholipid solution in chloroform was carefully spread onto the subphase with a gas-tight syringe. The monolayer was then compressed until a surface pressure of 30 mN/m was obtained at a velocity of 5 mm/min. The monolayer was allowed to reach equilibrium (20 - 30 min) and once stabilised 10 mL of 25 μ g/mL penicillin and nanopenicillin were injected in the subphase. The surface pressure was monitored over time until it reached a constant value.

4.3.5.4 Antibacterial and Antibiofilm Activities

Bacterial Susceptibility to Penicillin G. Serial twofold dilutions of Penicillin G was prepared in test tubes containing 1 mL of NB medium. The inoculum density of *P. aeruginosa*, *E. coli* and *S. aureus* had a final concentration of $\approx 5 \times 10^5$ CFU/mL. 10 μ L of bacterial suspension was added to the 96-well plate previously filled with 190 μ L of different concentrations of penicillin G and incubated at 37 °C overnight. The OD=600 nm was recorded and the susceptibility of the bacterial strains evaluated.

Antibacterial Activity of Nano-sized Penicillin. *P. aeruginosa* and *E. coli* growth inhibition assay was performed in presence of the nanopenicillin and penicillin (as a control). The absorbance of the inoculated bacterial culture was adjusted to 0.01 at 600 nm in NB medium. Thereafter, 200 μ L of antimicrobial agent at 250 μ g/mL was incubated with 200 μ L of diluted bacterial suspension. This was further incubated at 37 °C and 230 rpm for 24 h. After 24 h the suspensions were serially diluted in sterile

buffer solution, plated on appropriate plate count agar and further incubated at 37 °C for 24 h to determine the number of surviving bacteria colonies. The bacterial reduction (Log₁₀ reduction) was calculated using the following formula:

$$\text{Bacterial log}_{10} \text{ reduction} = \log_{10} (\text{CFU/ml control sample}) - \log_{10} (\text{remaining CFU/ml after exposure with antimicrobial agent})$$

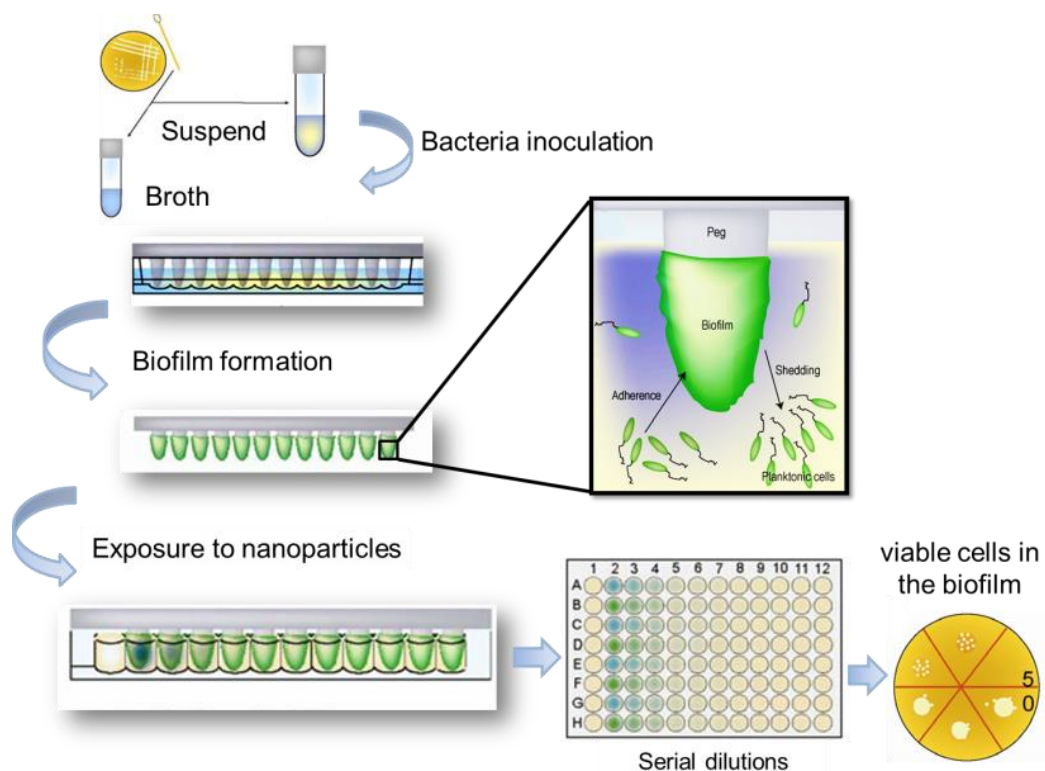
All antibacterial data represent mean values ± SD (n=3).

Bacterial Viability in Biofilm. The viability of *P. aeruginosa* and *E. coli* bacteria within biofilms after treatment with penicillin, nanopenicillin and control NSs was assessed by fluorescence microscopy using Live/Dead® BacLight™ cell viability kit and by Calgary Biofilm Device using a Minimum Biofilm Eradication Concentration (MBEC™) High-throughput (HTP) assay (Biofilm Technologies, Calgary, Alberta).

Live/dead cells viability assay: *P. aeruginosa* and *E. coli* biofilm was grown on tissue culture-treated polystyrene 24-well plates for 24 h at 37 °C as previously described (Section 4.3.2.7 Functional Characterisation of Catheters Coated with Antibiofilm Enzymes, *Biofilm Inhibition Tests*). Then, the biofilm was washed with TSB under aseptic conditions to eliminate non-adhered bacteria and 1 mL of the samples diluted in TSB at a concentration of 125 µg/mL was added to each well. After exposure to penicillin, nanopenicillin and control NSs for 24 h at 37 °C the solutions were discarded and biofilm washed with 0.9 % NaCl, pH 6.5. The biofilm eradication was analysed using Live/Dead BacLight kit (Section 4.3.2.7 Functional Characterisation of Catheters Coated with Antibiofilm Enzymes, *Bacterial Viability in the Biofilms*). Non-treated with antibiotic biofilm was used as a negative control (lack of biofilm eradication).

MBEC™ HTP Assay on Calgary Biofilm Device: Biofilms of *P. aeruginosa* and *E. coli* were grown on a device comprised of a microtiter plate lid with 96 pegs, which provide the surface for cells to adhere, colonize and form a uniform biofilm (**Error! Reference source not found.**). The pegs fit precisely into the wells of a standard 96-well microtiter plate. The lid was used in conjunction with special troughs for growing of bacteria, washing, and incubating. The trough was inoculated with bacteria and placed in contact with the pegged lid and further incubated in a Plate Shaker-Thermostat for 24 h at 37 °C, 100 rpm. Afterwards, the pegs with the developed biofilm were washed twice with 0.9 % NaCl with pH 6.5 and then placed in contact with the 96-well plate containing different concentrations of the test compounds including penicillin solution, and penicillin and control NSs at 37 °C for 24 h. The pegged lids were then transferred in 96-well plate containing 200 µl recovery medium (Mueller Hinton Broth,

supplemented with 20 g/L saponin, 10 g/L Tween-80 and 2.5 % (v/v) neutralizing agent containing L-histidine (50 g/L), L-cysteine (50 g/L) and reduced glutathione (100 g/L) and placed in a ultrasonic bath for 10 min. The viable bacterial cells after treatment with antibacterial agents were count after appropriated dilution in sterile buffer and plating on specific agar (Scheme 4.5).



Scheme 4.5 Inoculation of Minimum Biofilm Eradication Concentration (MBEC™) High-throughput (HTP) assay assay kit. A fresh sub-culture of *P. aeruginosa* or *E. coli* was used to create an inoculum with $OD_{600} = 0.28$. The bacterial suspension was diluted with TSB (1:30) and 22 ml of dilution were added to the trough of the MBEC™-HTP device. The device was placed at 37 °C with shaking to assist the formation of biofilms on the polystyrene pegs. After washing with 0.9 % NaCl, pH 6.5, the lid with the developed biofilm was transferred to another plate containing different concentrations of penicillin G solution and nanospheres.

4.3.5.5 Cytotoxicity Evaluation

The potential toxicity of the NSs towards human foreskin fibroblast was also evaluated. Different concentrations of NSs were placed in contact with previously seeded cells and after 24 h the number of viable cells was quantified using alamarBlue® (section 4.3.2.7 Functional Characterisation of Catheters Coated With Antibiofilm Enzymes, *Biocompatibility Tests*). Cells were seeded at a density of 4.5×10^4 cells/well on a 96-well tissue culture-treated polystyrene plate (Nunc) the day before experiments and then exposed to different concentrations of NSs (1000, 100 and 1 µg/mL diluted in

DMEM) at final volume of 150 μ L and incubated at 37 °C in a humidified atmosphere with 5 % CO₂. After 24 h contact with cells, the NSs were removed, the cells washed twice with PBS and stained with 100 μ L of 10 % (v/v) AlamarBlue[®] Cell Viability reagent in DMEM. BJ5ta cells relative viability (%) was determined for each concentration of NSs and compared with that of cells incubated only with cell culture medium. H₂O₂ 500 μ M was used as a positive control of cell death. Data are expressed as the mean of three measurements with a standard deviation as a source of error.

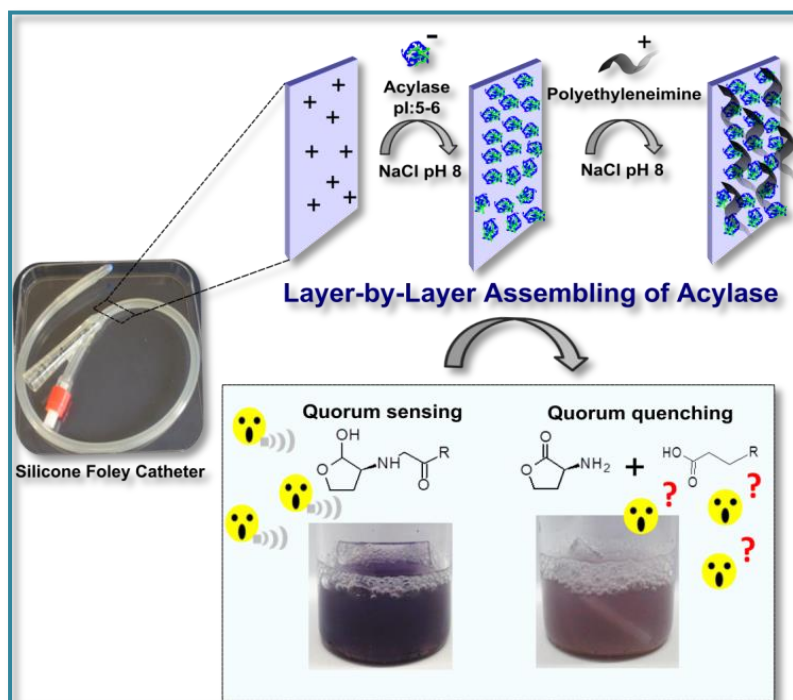
4.3.5.6 Data analysis

Results were analysed using Graph Pad Prism 5.04 (Graph Pad Software, San Diego, CA). Statistical significances were determined using ANOVA, followed by the Dunnett post-hoc test or, alternatively, by the unpaired two-tailed Student's t-test. P values < 0.05 were considered to be statistically significant (expressed in the figures with asterisks [*]: *p < 0.05, significant; **p < 0.01, very significant; ***p < 0.001, extremely significant).

5 Results and Discussion

**Enzyme Multilayer Coatings for Inhibition of
Bacterial Biofilm Formation on Silicone Foley
Catheters**

5.1 Quorum Quenching Acylase in Multilayer Coatings



Despite the advances in QQ enzymes for anti-virulence purposes, these have never been applied to prevent the QS regulated biofilm formation on indwelling medical devices. The goal of the present study is to develop multilayer acylase coatings on silicone urinary catheters able to interfere with bacterial QS phenomenon in the

extracellular space and thereby inhibit the growth of drug resistant biofilms. Taking into account the advantages of the nanostructured polymeric systems to preserve proteins folding and bioactivity, the LbL deposition technique is used to incorporate the enzyme acylase into biologically stable multilayer coating on the silicone material. The disruption of QS process in Gram-negative bacteria, through the enzymatic degradation of the signals by the LbL construct is studied with reporter strain *C. violaceum*. Then, the ability of the resulting coating to prevent *P. aeruginosa* biofilm formation on urinary catheters is assessed in both static and dynamic conditions using an *in vitro* model of a catheterised human bladder.

This section is based on the following publication:

Ivanova K, Fernandes MM, Mendoza E, Tzanov T, "Enzyme multilayer coatings inhibit *Pseudomonas aeruginosa* biofilm formation on urinary catheters", *Applied Microbiology and Biotechnology*, 2015, 99(10):4373-85. doi: 10.1007/s00253-015-6378-7.

5.1.1 Acylase Induced Degradation of QS Signals

The increased antibiotic resistance of bacteria within biofilms is a common reason for difficult-to-treat infections caused by foreign bodies. This is a medical and public health issue that requires the application of novel approaches to counteract the biofilm growth on indwelling catheters. Strategies that target the bacterial molecular mechanisms involved in biofilm occurrence such as QS are reported to exert less evolutionary pressure on the bacterial population and thus could decrease the possibility of resistance development. Previous studies have demonstrated the key role of QS in biofilm differentiation of pathogenic *P. aeruginosa* into complex multicellular structures. *P. aeruginosa* uses *las*, *rhl* and *pqs* QS systems to regulate a number of factors important for biofilm development on various surfaces [301]. Therefore if any of these QS systems is blocked by mutation or by QSIs, the individual bacterial cells could lose ability to communicate with the others and form well defined surface-attached biofilms structures [302]. Davies *et al.*, for example, showed that mutants lacking the *las* QS system are incapable of producing the 3-oxo-C12-HSL signal molecules and form frail and unstructured biofilms which are sensitive to detergents [303]. The *las* QS system is involved in the expression of numerous genes; hence it is believed that the biofilm-defective phenotype is multifactorial including defects in swarming, DNA release, and defects in the production of other structural components of the biofilm matrix [304].

The ability of acylase to act upon different model AHLs was first evaluated in order to confirm the QS inhibiting concept of this study. Acylase was able to degrade several AHL model compounds, including C4-DL-HL, C6-DL-HL, 3-oxo-C10-L-HL, and 3-oxo-C12-L-HL (Figure 5.1A), through amide bond cleavage, producing HL and the corresponding fatty acid. Among them, the acylase-induced degradation of 3-oxo-C12-L-HL was of main importance as this signal was found to play a key role in *P. aeruginosa* biofilm formation [109, 303]. The enzyme showed higher activity on 3-oxo-C10-L-HL and 3-oxo-C12-L-HL (more than 50 and 40 % conversion, respectively) when compared to C4-DL-HL and C6-DL-HL (up to 10 and 15 % conversion, respectively) (Figure 5.1A). Acylase I from *A. melleus* is highly enantioselective in its interaction with the substrate mainly promoting the degradation of the L-configuration of amide bond, which suggests that the lower conversion of C4-DL-HL and C6-DL-HL was due to the presence of both D- and L-configurations in the substrates [305]. This factor may play a significant role in quenching the QS, as bacteria recognize and respond to these configurations [306].

The bioassay using *C. violaceum* also revealed the decreasing concentration of the QS molecule C6-DL-HL upon contact with acylase (smaller purple area in presence of

acylase) accounting for the QQ activity of this enzyme (Figure 5.1B) [287]. Based on the observed *in vitro* enzymatic inactivation of the QS molecules, we assumed that acylase from *A. melleus* could inactivate the AHLs of Gram-negative bacteria such as *P. aeruginosa* and thereby inhibit the signal accumulation in the extracellular environment and subsequent biofilm formation. Xu *et al.* reported similar findings about acylase isolated from kidney, which efficiently degraded *in vitro* several model QS signals, C4-HSL and C8-HSL, and inhibited *P. aeruginosa* biofilm formation on polystyrene surface [203]. Therefore, the ability of acylase to interrupt the cell-to-cell communication process that the Gram-negative *P. aeruginosa* uses to coordinate and establish resistant biofilm lifestyle, suggested the enzyme application as antibiofilm coating on indwelling medical devices.

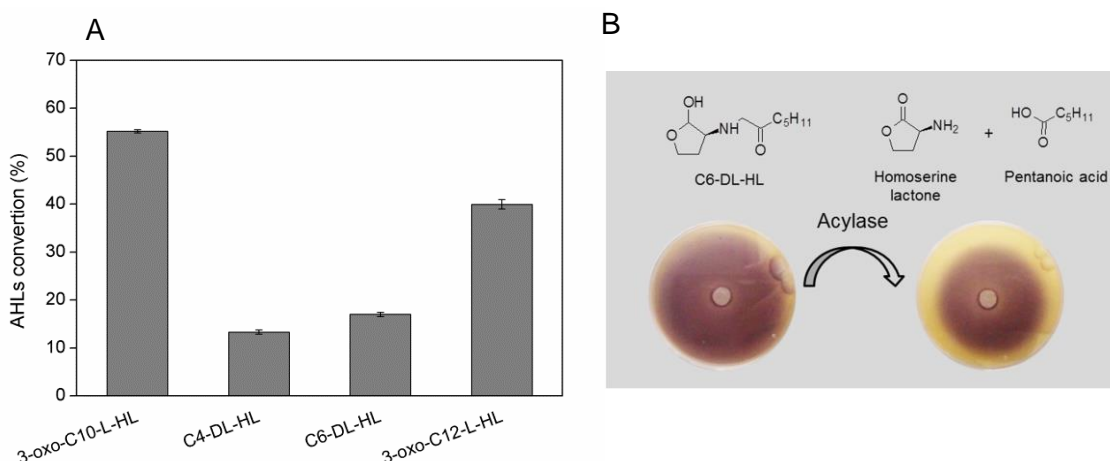


Figure 5.1 A) AHL degradation by acylase assessed with fluorescamine method and B) C6-DL-HL degradation study using the *C. violaceum* CECT 5999

5.1.2 Acylase Multilayer Coatings Build-Up onto Silicone and its Characterisation

In order to obtain a coating with QQ activity, acylase was immobilised in an LbL fashion onto silicone sheets and urinary catheters. A pre-amination of the silicone surface with APTES was performed in order to provide amine groups for better deposition of the first enzyme layer. This chemisorption procedure has been described by some authors as likely to take place with a thin water layer on the substrate and not only with hydroxyl groups scarcely present on the surface of the material [307]. The successful amination of silicone with APTES was confirmed by the formation of Ruhemann's purple in 2 % ninhydrin solution (Figure 5.2A). This was further supported by the presence of two dominating vibrational modes found around 1575 and 1485 cm^{-1} and the shoulder at

1330 cm^{-1} in the FTIR spectra of the APTES treated silicone. The oxidation upon air exposure of such salts gives rise to the formation of imine groups responsible for the absorption peak at around 1650 cm^{-1} (Figure 5.2B) [289, 308].

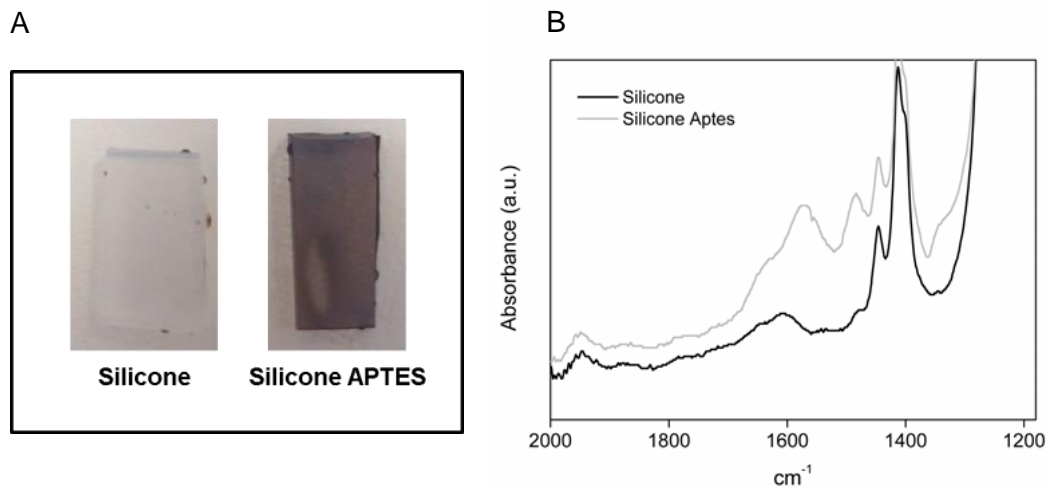


Figure 5.2 A) Non-treated and APTES-treated silicone sheets after incubation in 1mL of 2 % ninhydrin solution. The formation of characteristic Ruhemann's purple demonstrated the presence of amino groups on the surface. B) ATR-FTIR spectra of non-treated and APTES-treated silicone. Two dominating vibrational modes around 1575 and 1485 cm^{-1} appeared in the FTIR spectra of the APTES-treated samples.

After ten consecutive immersions of the silicone material into anionic enzyme solution and oppositely charged linear PEI (Mw=25 kDa) typical protein bands, that were not observed on the untreated silicone control, appeared in the FTIR spectra of the acylase coated samples (Figure 5.3). The band with a maximum around 3300 cm^{-1} was assigned to N-H stretching vibrations, whereas the band at 1650 cm^{-1} and the broad region between 1490 and 1590 cm^{-1} were ascribed to amide I (C=O stretching) and amide II (mainly N-H bending) vibrations. The FTIR analysis demonstrated the development of the enzyme multilayer assemblies onto the catheter surface [309].

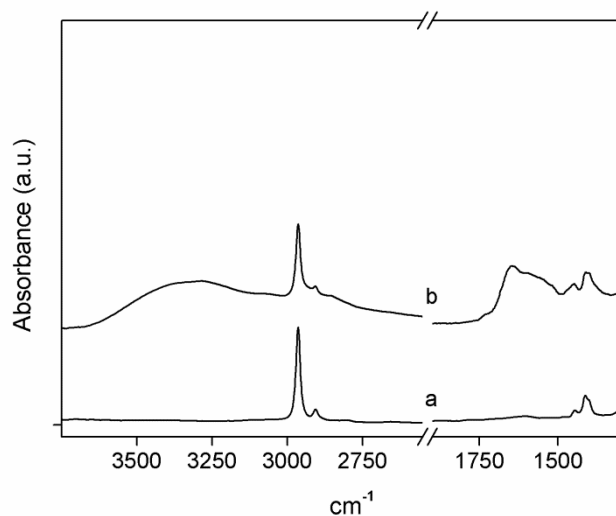


Figure 5.3 Representative FTIR-ATR spectra of (a) untreated silicone and (b) acylase multilayer coatings.

The surface morphology and roughness of the acylase/PEI multilayer coatings were also studied by AFM. AFM two-dimensional and three-dimensional analysis demonstrated nanostructural changes in the silicone surface topography after the multilayer coating assembly (Figure 5.4). After deposition of ten bilayers, the silicone surface was coated with relatively large clusters (Figure 5.4, right image). The 2D AFM topographic profiles, analysed using Nanotec WSxM software, showed that the surface roughness of acylase-coated silicone increased when compared to non-treated silicone, with a peak height maximum about 35 nm (Figure 5.4). According to the generally accepted polyelectrolyte multilayer build-up mechanism, the oppositely charged polyelectrolytes form small islets on hydrophobic surfaces, such as those of PDMS, at early deposition stages [310]. As the number of deposited layers increases, the islets coalesce and become larger until a continuous coating is formed. However, in this study, the deposition of ten enzyme-PEI bilayers was not sufficient for a continuous and homogeneous coating formation. The number of bilayers required to completely cover a substrate surface would be lower when (i) the electrostatic interactions between the components of the coating are stronger and (ii) the conformations of the adsorbed components are adequate to favour the deposition [311].

The differences in the surface coverage of the catheter material could be also observed in terms of wettability (Figure 5.4). From AFM and water contact angle images, it is apparent that the wettability is directly proportional to the extent of silicone surface coverage with enzyme protein. The water contact angle of the untreated

silicone specimen ($136^{\circ}\pm 10^{\circ}$) decreased significantly after depositing the acylase multilayer coating ($94^{\circ}\pm 9^{\circ}$) due to its hydrophilic character (Figure 5.4).

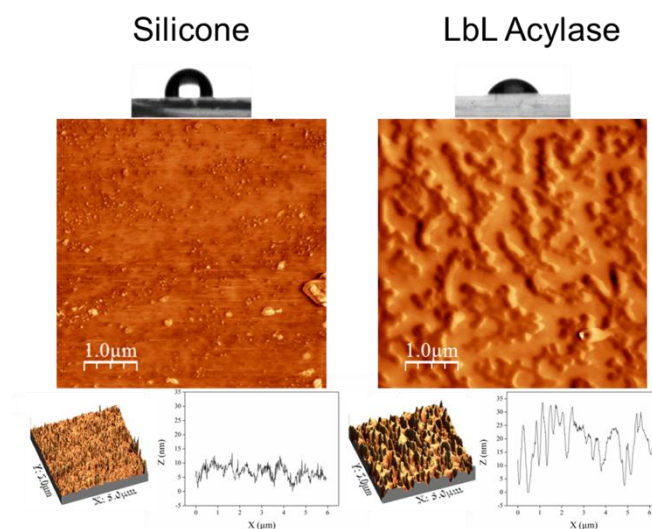


Figure 5.4 AFM (2D and 3D topographic) and water contact angle images of untreated silicone before APTES functionalisation and acylase multilayer coatings.

5.1.3 Acylase Activity in The Multilayers

The activity of the enzyme in the multilayer coating was evaluated through the degradation of N-acetyl-methionine using a standard colorimetric method. Despite acylase in the free form efficiently degraded the QS signals and inhibited the *P. aeruginosa* biofilm formation, after immobilisation this efficacy could be impaired due to the lower amounts of active protein attached onto silicone surface and loss of enzymatic activity [203]. Acylase retained 80 % of its specific activity, when compared to the relative amount of protein immobilised on the silicone surface determined by measuring the fluorescence of FITC-labelled acylase multilayer coatings. In fact, the LbL technique used to construct these enzyme multilayer coatings is considered as a method that uses mild conditions (e.g., aqueous solutions) and could preserve the protein folding and activity. Most probably, the entrained water presented in between the polyelectrolyte layers is the reason why the proteins remained active on the surface [141]. Previous studies have shown that enzymes immobilised on different surface using LbL approach retained high percentage of their catalytic activity and also were more stable than their free counterparts [312-314].

The activity of acylase in the multilayered coatings and in solution was further determined at physiological conditions by measuring the QS-regulated violacein production in reporter bacterial strain *C. violaceum* [315]. The degradation of C6-DL-HSL QS molecule by acylase was indicated by the decrease of violacein pigment production in the AHL containing liquid broth. Clear difference was observed between the positive control (non-treated silicone in the presence of QS molecules) and the samples containing immobilised/non-immobilised acylase together with the same concentration of QS molecule, where less violacein was synthesized (Figure 5.5A). Therefore, acylase multilayer coatings show the ability to act upon the QS signals produced by Gram-negative bacteria involved in UTIs, e.g. *P. aeruginosa*.

The degradation of C6-DL-HSL in the liquid broth was also quantified spectrophotometrically after the extraction of violacein from the *C. violaceum* cultures with butanol [291]. The C6-DL-HSL-inducible violacein production was inhibited by acylase up to 40 % in both free and immobilised forms of the enzyme (Figure 5.5B). The reduced QS-regulated response of *C. violaceum* by acylase-coated silicone catheters showed their potential for inhibition of QS-controlled biofilm formation.

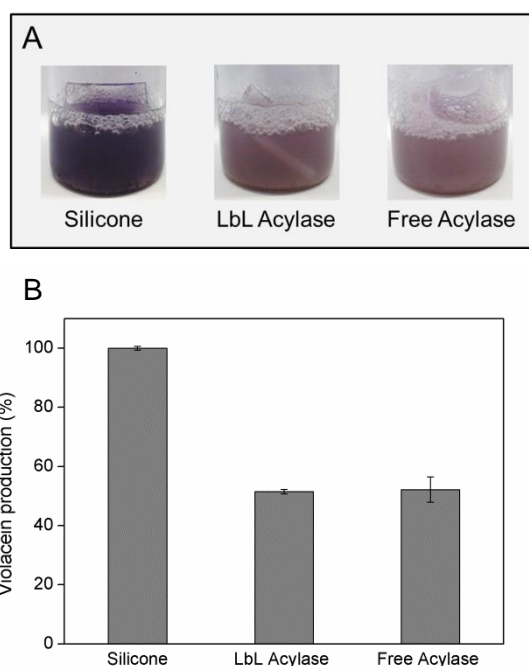


Figure 5.5 Violacein production by *C. violaceum* CECT 5999 in presence of free acylase solution and acylase multilayer coatings on silicone. The control - untreated silicone was set as 100% violacein production.

5.1.4 Functional Properties of the Acylase Multilayer Coatings

After proving the functionalisation of silicone catheters with acylase using LbL technique as well as the activity of these multilayered coatings toward the *P. aeruginosa* QS signals, their functionality in terms of antibiofilm activity was also assessed. Since the initial bacterial adhesion is thought as a part of the biofilm development process on the surface, we studied whether the cell adherence would be delayed by the protein multilayer coatings. The initial attachment of *P. aeruginosa* (after 3 h of contact) was reduced by the acylase multilayer coating when compared to the untreated silicone material (Figure 5.6A). Microscope images showed that *P. aeruginosa* formed bacterial clusters on untreated silicone as a first indicator for the initiation of biofilm growth, while the cells present on the acylase coatings were spread, and the clusters formed on the surface were considerably smaller (Figure 5.6A). Hydrophobic interactions have been suggested as one of the important factors promoting bacterial cell adherence on surfaces [316]. The hydrophobic character of the silicone surface is believed to govern the primary adhesion of *P. aeruginosa*, which possesses a thin layer of glycoprotein covered by a thick layer of lipoproteins and lipids facilitating the interaction of bacterial cells with various hydrophobic surfaces [145]. The decrease of *P. aeruginosa* initial adhesion on the acylase-coated silicone surface could have been favoured by the increased hydrophilicity of the enzyme-modified surface. These qualitative observations suggested that the process of mature biofilm formation could be delayed when silicone is coated with QQ enzyme, e.g. acylase, corroborating the results obtained on the ability of acylase coatings to affect the QS process in the reporter strain *C. violaceum* (Figure 5.5).

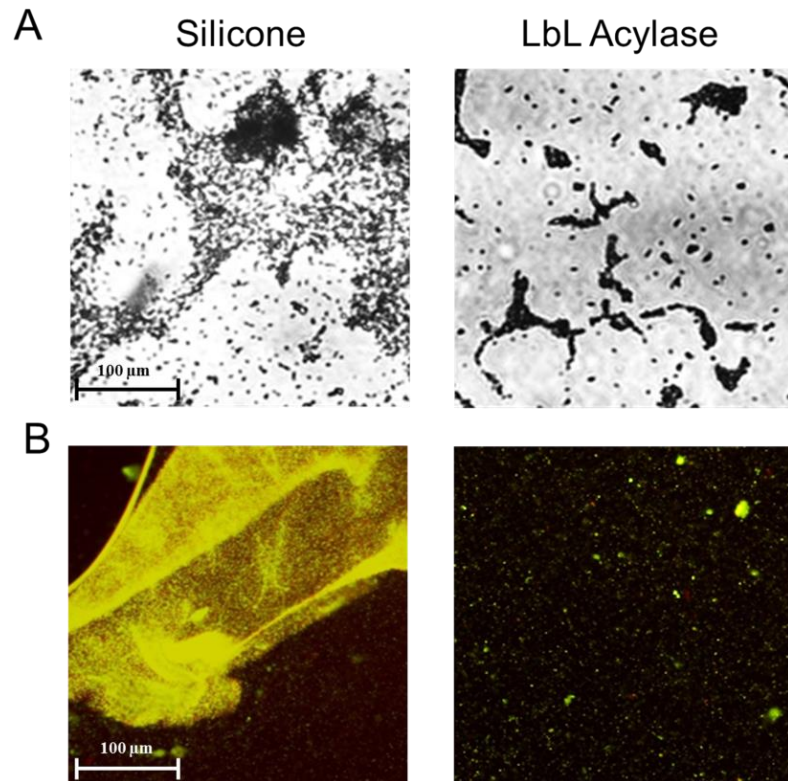


Figure 5.6 A) Initial adhesion of *P. aeruginosa* on untreated silicone and acylase multilayer coatings after 3-h contact ($\times 40$ magnification). B) Fluorescence microscopy images of 24 h-old *P. aeruginosa* biofilms (formed in static conditions) on untreated silicone and acylase multilayer coatings analyzed after Live/Dead staining ($\times 20$ magnification).

Besides increasing the wettability of silicone surface, the specific enzyme function in the coating is believed to have a major contribution to the inhibition of biofilm maturation on the catheter material. To prove this assumption, the formation of *P. aeruginosa* biofilms after 24 h contact with pristine and coated silicone samples was studied in static conditions using CV for total biomass assessment and Live/Dead[®] cell viability kit for structural characterisation of the developed biofilm. Fluorescence microscopy images after Live/Dead staining showed that the biofilm is well established on the untreated silicone material, with characteristic microcolonies of bacterial cells, while on the acylase coated silicone, the biofilm was significantly reduced (Figure 5.6B). A characteristic 3D structure was observed on the control with both viable (stained in green) and non-viable (stained in red) cells due to the repeatable pattern of death and lysis in biofilms, which corresponds to the normal course of biofilm development of *P. aeruginosa* [317]. In contrast, only few bacteria spread individually on the silicone surface without the presence of typical bacterial clusters were observed for the acylase multilayer coatings (Figure 5.6B). The total biomass assessment of the

biofilms supported these results showing about 50 ± 0.2 % inhibition of biofilm formation on silicone coated with QQ enzyme, when compared to the untreated sample (Figure 5.9).

With the emergence of antibiotic-resistant bacteria, alternative approaches targeting different processes than bacteria killing mechanisms to control pathogenic biofilm formation on medical devices have been sought. While conventional antibiotics kill or inhibit bacteria by targeting their survival processes, interrupting the QS pathways through signal degradation efficiently quenched the QS process and inhibited *P. aeruginosa* biofilm formation in static conditions without affecting planktonic bacterial growth after 24 h contact (Figure 5.7). Consequently, these multilayer coatings might prevent biofilm-associated urinary tract infections exerting less selective pressure on the target bacteria and reducing the risk of resistance development.

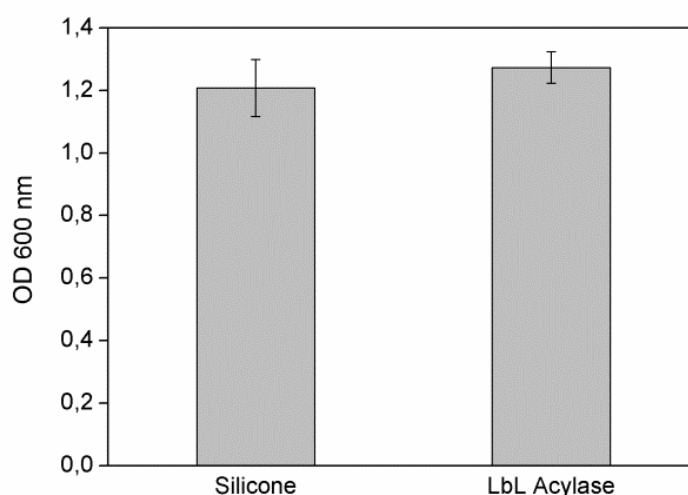


Figure 5.7 Inhibition of *P. aeruginosa* planktonic growth in the presence of untreated silicone and acylase multilayer coatings.

Aiming at developing enzymatic coatings for urinary catheters, the stability of the developed materials in artificial urine is a prerequisite due to the possible influence of the various compounds present in the human fluids on the enzyme activity. Hence, we evaluated the biofilm inhibiting activity of acylase coated silicone samples ($1 \times 1 \text{ cm}^2$) after 1 and 7 days incubation in artificial urine. No significant difference in the biofilm inhibiting capacity of acylase based coatings and the freshly prepared ones was observed (Figure 5.9).

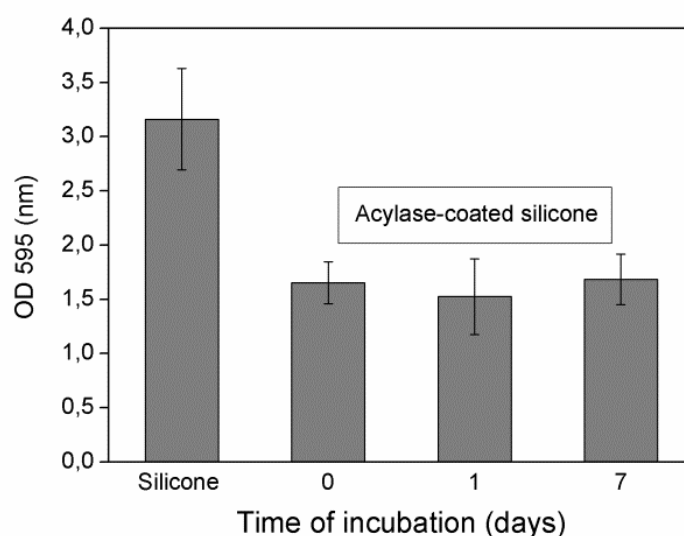


Figure 5.8 Crystal violet assessment of biofilm formation of *P. aeruginosa* on untreated silicone and acylase multilayer coatings after incubation in artificial urine for 1 and 7 days.

5.1.5 Antibiofilm Efficacy of Acylase Multilayer Coatings in an *In Vitro* Model of Catheterised Human Bladder

Biofilm formation on pristine and acylase-coated urinary catheters was also evaluated in dynamic conditions using a catheterised bladder model, where the shear stress and flow rate vary similarly to the situation in the human bladder during catheterisation. Biofilms were allowed to grow on the catheters for 7 days, and the biofilm inhibition by the acylase-based coating was analysed (Figure 5.9). The fluorescence images after staining of live and dead bacteria attached to the balloon and urethra demonstrated decreased biofilm formation, when compared to pristine Foley catheters after 7-day of catheterisation (Figure 5.9A). The bacterial biofilm formation was inhibited by 80 % in the balloon part, which was immersed over 7 days in the bladder model infected with *P. aeruginosa*. The acylase-coated urethra part inserted into the model bladder was also able to inhibit the biofilm formation by 45 % compared to the untreated silicone Foley catheter (Figure 5.9B). The results obtained with the dynamic system showed the same tendency in inhibiting biofilm formation as in static conditions. Therefore, the acylase-coated Foley catheters would have potential in preventing biofilm-associated UTIs.

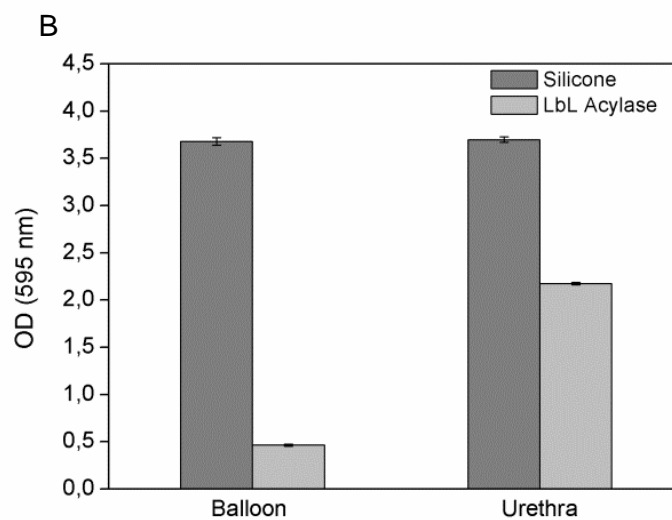
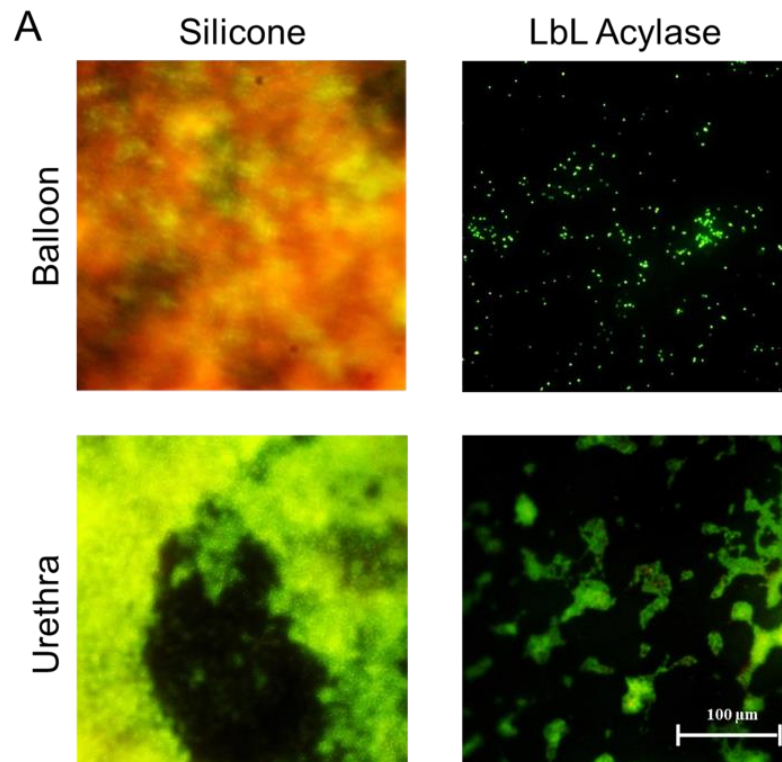


Figure 5.9 A) Microscopic images of untreated and acylase coated Foley catheters after 7 days incubation in dynamic bladder model system (40x magnification); B) Crystal violet assessment of total biomass formed on urinary catheters: untreated and acylase multilayer coatings on silicone Foley catheter.

5.1.6 Biocompatibility Evaluation

Prior to the utilisation of these enzyme multilayer coatings on urinary catheters in vivo their potential cytotoxicity to human cells is an essential parameter that should be taken into account. Despite the presence of PEI, regarded as toxic, the acylase coated

silicone material did not cause any adverse effect upon interaction with human cells compared to the pristine silicone (Figure 5.10) [318]. Neither 24 h nor 7 days of contact affected cells viability, suggesting that the PEI in the coatings is in a rather low concentration to affect the human cells viability [318]. Moreover, the combination with negatively charged enzymes during the LbL assembly may reduce the availability of positively charged PEI amino groups thought to induce human cells cytotoxicity [319]. Previous studies have shown that the toxicity of amine-terminated polymers is solely related to their positive charges. In particular, the acylation of the amine groups of PEI to form neutralized and negatively charged materials has been shown to provide biocompatibility with mammalian cells [320]. Based on the results about the cytotoxicity and antibiofilm activity (Figure 5.10 and Figure 5.9, respectively), we assumed that the prolonged usage (over 7 days) of enzyme-modified catheters in vivo would not imply any concern for consumer's safety. Thus, the QQ active coatings could be a promising alternative to control biofilm-associated urinary tract infections.

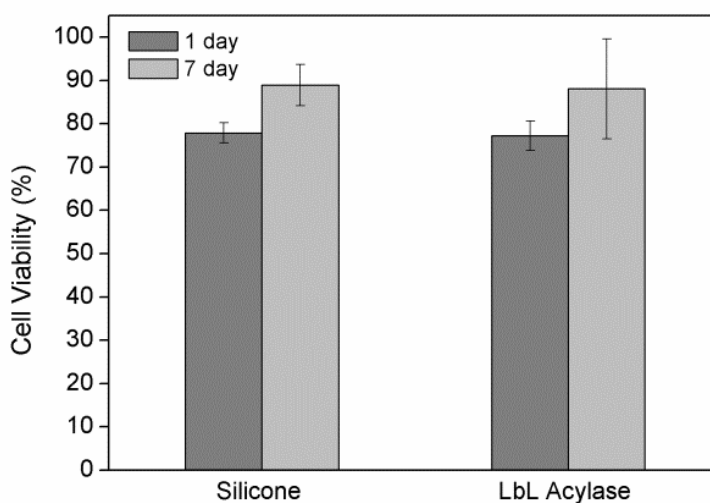


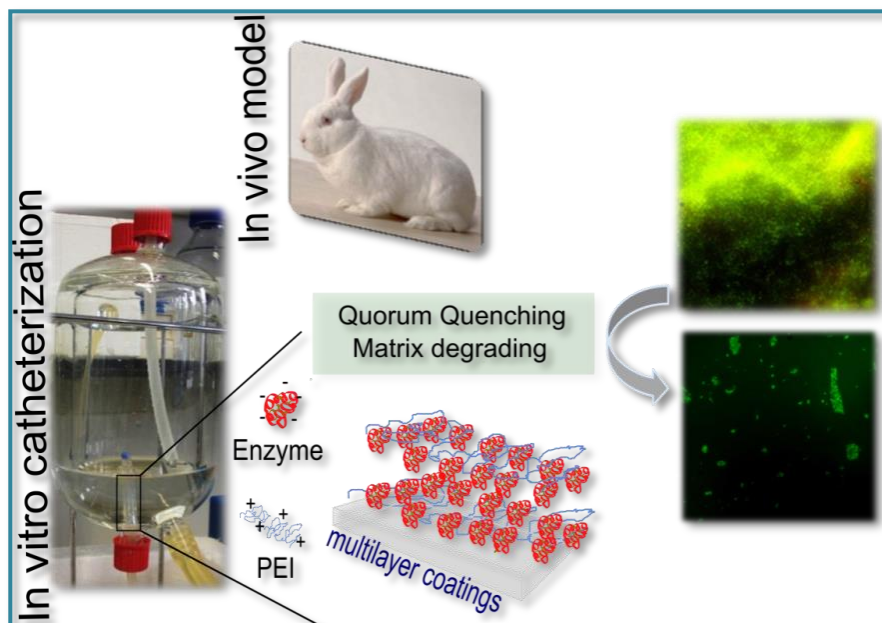
Figure 5.10 Viability of fibroblasts (BJ5ta) after being in contact with untreated silicone and acylase multilayer coatings: 1 day and 7 days.

5.1.7 Conclusions

The strategy used in this work to induce antibiofilm activity on indwelling medical devices is considered beyond the state of the art because it targets the inactivation of bacterial QS process, instead of simple killing of bacteria and related antibiotic resistance issue. While conventional antibiotics kill or inhibit bacteria by targeting their structure or survival processes, interfering with QS pathways is thought to exert less selective pressure on bacterial population and could reduce the threat of resistance emergence. In fact, inactivation of AHL signals in the extracellular environment is a way of breaking down the bacterial communication before it starts. As a consequence, bacteria will not realise that the threshold population density was achieved necessary to establish mature biofilm on silicone material.

In summary, we have developed coating on silicone catheter surface that significantly reduced the formation of *P. aeruginosa* biofilm due to the acylase-induced degradation of QS signals involved in bacterial cell-to-cell communication process. These findings suggested that the acylase coated catheters could be a viable alternative to prevent QS-regulated biofilm occurrence on urinary catheters.

5.2 Quorum Quenching and Matrix Degrading Enzymes in Hybrid Multilayer Coatings



Herein we attempt to integrate for the first time two enzymatic inhibition approaches into a unique and efficient antibiofilm strategy. The enzymes acylase and α -amylase were used to interfere simultaneously with bacterial QS

phenomenon and biofilm stability of Gram-negative species, respectively. To achieve this, we deposit acylase and/or α -amylase in a LbL fashion to build multilayer coatings on silicone catheters able to prevent drug-resistant biofilm formation. The ability of these enzymes to interfere with the bacterial QS process and to degrade the polysaccharides of *P. aeruginosa* biofilm matrix is assessed. The activity of the coatings comprising both enzymes against Gram-negative *P. aeruginosa*, Gram-positive *S. aureus*, and dual-species (*P. aeruginosa* and *E. coli*) biofilms is further investigated under static and dynamic conditions using a physical model of catheterised bladder. Finally, the *in vivo* rabbit model is used to assess the potential of the developed materials to control bacterial biofilm formation on indwelling medical devices in a clinical setting.

This section is based on the following publication:

Ivanova K, Fernandes MM, Francesko A, Mendoza E, Guezguez J, Burnet M, Tzanov T "Quorum-quenching and matrix-degrading enzymes in multilayer coatings synergistically prevent bacterial biofilm formation on urinary catheters", *ACS Applied Materials & Interfaces*, 2015, 7(49):27066-77. doi: 10.1021/acsami.5b09489.

5.2.1 Enzymatic Degradation of Biofilm Matrix Components

The efficacy of acylase in inhibiting QS-regulated biofilm formation through the *in vitro* degradation of several model AHL signals was already demonstrated in the previous section (Figure 5.1). Therefore, prior to catheter coating, only the ability of α -amylase to degrade the EPS biofilm components *in vitro* was assayed in order to evaluate the potential of the entire concept.

Exopolysaccharides are one of the major fractions of EPM that play an important adhesive and structural role in biofilms. Depolymerisation of EPS is expected to prevent irreversible bacterial adhesion and further biofilm formation [25]. Taking into account the wide heterogeneity of EPS between bacterial species, we investigated *in vitro* the ability of α -amylase to degrade several model EPS including alginate, hyaluronic acid, polygalacturonic acid, and chitosan (Figure 5.11). Alginate is the main capsular EPS produced by mucoid bacterial strains such as pathogenic *P. aeruginosa*, and it aids surface colonisation and biofilm persistence [321]. Hyaluronic acid was shown to support *Streptococcus pneumoniae* growth within biofilms *in vitro* [322]. The other exopolysaccharides herein examined (polygalacturonic acid and chitosan) are model EPS components and potential α -amylase substrates. The enzyme efficiently hydrolysed chitosan and hyaluronic acid glycosidic bonds, yielding 10 and 4 $\mu\text{g}/\text{U}$ reducing sugars (in glucose equivalents), respectively, in good agreement with literature (Figure 2.1) [323]. In contrast, polygalacturonic acid and alginate were degraded to a lower extent, releasing 2.6 and 2.5 $\mu\text{g}/\text{U}$ reducing sugars, respectively. α -Amylase normally catalyses the endohydrolysis of 1,4- α -glycosidic bonds in polysaccharides, but other factors such as the specific tertiary and quaternary structural domains, i.e., crystalline and amorphous regions, can also affect the breakdown process [324]. Relying on the successful *in vitro* degradation of the model EPSs, α -amylase was further evaluated in the form of multilayer coatings for preventing biofilm formation.

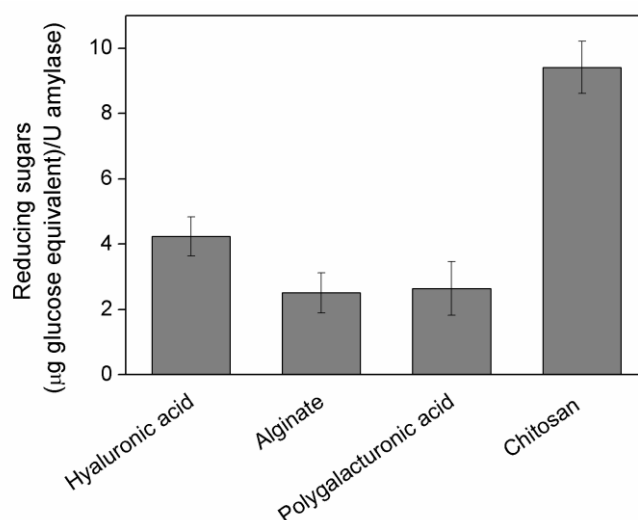


Figure 5.11 *In vitro* degradation of model exopolysaccharide components of bacterial biofilm matrix by α -amylase.

5.2.2 Characterisation of the Multilayer Enzyme Coatings

To obtain active antibiofilm coatings, amylase and/or acylase were further deposited in a LbL manner on APTES pre-treated silicone stripes and Foley catheters (Figure 5.2). The aminated silicone/catheter was subjected to 10 sequential immersions into negatively charged acylase or amylase solution and cationic PEI. Three typical protein bands were observed in the FTIR spectra of all enzyme-coated surfaces (Figure 5.12A: b–e). The absorption band around 3300 cm^{-1} was assigned to the N–H stretching vibrations, whereas the vibration modes found at 1650 cm^{-1} and the region between 1490 and 1590 cm^{-1} correspond to amides I and II. These signals did not decrease even after 7 days of incubation in artificial urine, pH 6.8, at $37\text{ }^{\circ}\text{C}$ with shaking (20 rpm), demonstrating the formation of stable enzyme-based multilayer assemblies. For simplicity, only the LbL Amy spectra are shown here (Figure 5.12B).

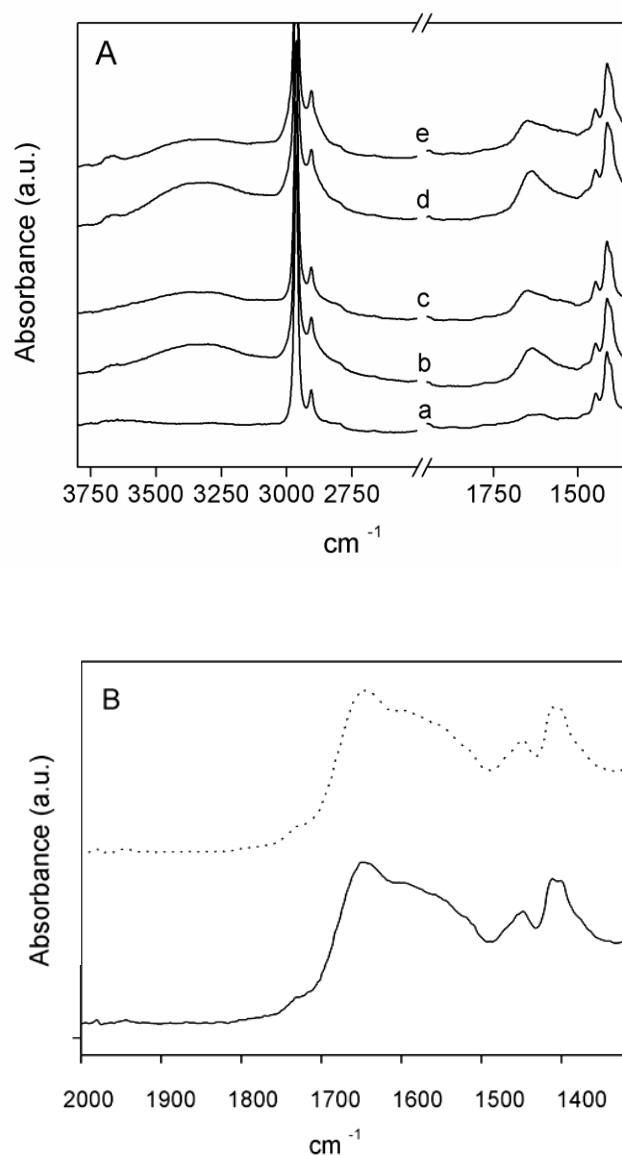


Figure 5.12 A) ATR-FTIR spectra of a) pristine silicone, and multilayer assemblies: b) LbL Acy, c) LbL Amy, d) LbL Hyb-Acy and e) LbL Hyb-Amy; and B) normalised LbL Amy spectra: non-washed (dot line), washed (solid line).

The morphology of the obtained coatings was further studied using AFM. The 2D and 3D AFM images clearly demonstrated the changes in the surface topography after the enzymes deposition onto silicone (Figure 5.13). The 2D topographic profiles were further analysed along the drawn lines to determine the surface roughness (Figure 5.13, inset images). For comparison, the unmodified silicone surface was also examined and was found to display a roughness with a 60 nm peak height maximum (Figure 5.13A). The AFM images show uneven build-up of protein multilayer coatings after 10 sequential depositions of enzyme and PEI (Figure 5.13 B-E). Nevertheless,

considering that the coatings are made of enzymes the observed nonhomogeneous surface could even be an advantage. Deposition of enzymes in continuous coatings may hinder the substrates' diffusion and consequently decrease the specific activity of the amylase and acylase per layer [318, 325].

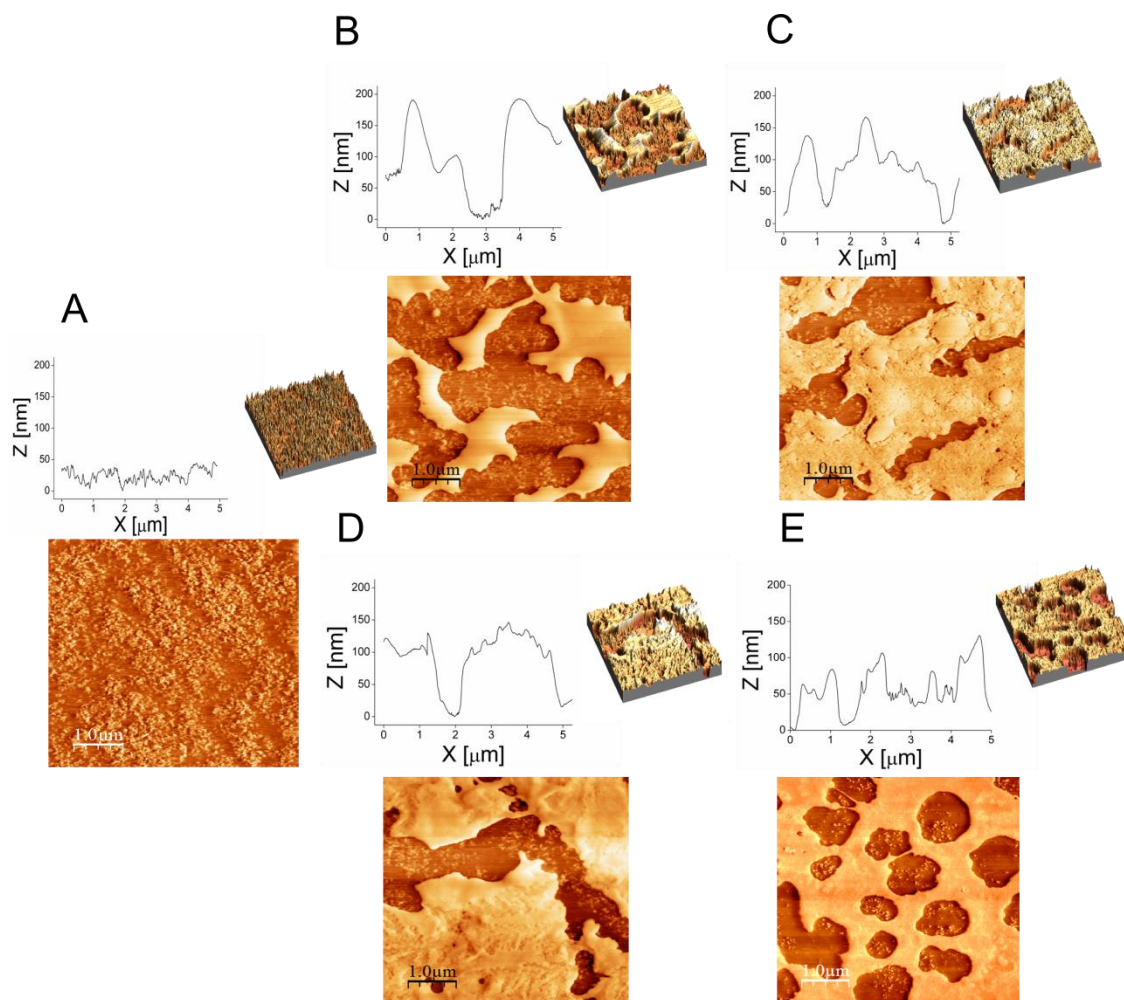


Figure 5.13 AFM images of A) pristine silicone surface and enzyme-coated silicone: B) LbL Amy, C) LbL Acy, D) LbL Hyb-Acy and E) LbL Hyb-Amy

The interactions between polyelectrolytes govern the build-up process of the polyelectrolyte multilayer coatings, distinguishing between linear and exponential mode of growth [326]. The exponential mode, a faster mode of growth, implies an effective diffusion of the polyelectrolytes “in and out” of the coating during the build-up process [326]. On these particular AFM images, acylase-containing coatings (LbL Acy and LbL Hybrid with either acylase or amylase as outermost layer) displayed larger islets compared to the amylase-based multilayers (LbL Amy) and, consequently, greater silicone surface coverage (Figure 5.13). In fact, more enzyme protein was deposited on

the silicone material when both enzymes (amylase and acylase) were used for the LbL build-up process (Table 5.1).

Table 5.1 Protein content on silicone surface.

Sample	Protein content (ng/cm²)
LbL Amy	77,72 ± 3,65
LbL Acy	81,33 ± 1,32
LbL Hyb-Acy	301,65 ± 9,24
LbL Hyb-Amy	322,15 ± 2,53

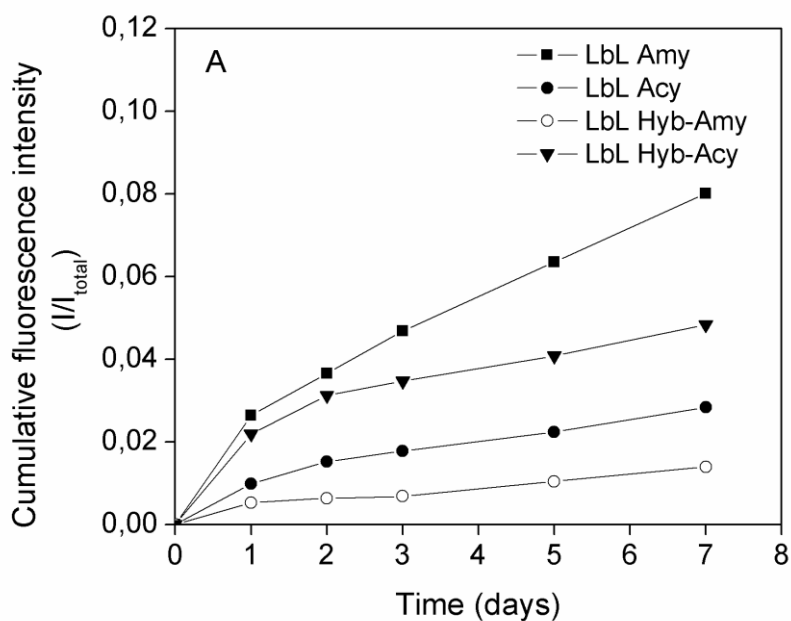
This probably means that the mode of growth is different when acylase versus α -amylase is used as a polyanion (exponential vs linear, respectively). The former hypothesis is corroborated by the surface morphology of the obtained multilayers. The uneven surfaces of the acylase-containing assemblies indicate heterogeneity in their outermost layers in agreement with the polyelectrolyte diffusion in and out of the coating during the exponential growth. In contrast, the smoothness of the amylase assembly indicates homogeneity of the outermost surface with no diffusion of the polyelectrolytes, corresponding to a linear coating growth.

The non-continuous nature of the enzymatic assemblies further allowed for a direct measurement of their thicknesses (without scratching the coating with the tip of the cantilever; Figure 5.13, graph insets). It is worth mentioning that the size of the islets was not related to the coating thickness, with the LbL Amy multilayer being the thickest among all experimental groups.

The protein release from the surface as a function of incubation time was further analysed using fluorescence spectroscopy to assess the physical stability of the coatings in urine. The relative cumulative release of FITC-labelled enzymes, amylase or acylase, in artificial urine, pH 6.8, was monitored over 7 days, corresponding to the extended useful life of the enzyme-treated urinary catheters in this study (Figure 5.14). The increase in the fluorescence intensity with time was sharp during the whole 7 day period for the LbL Amy assembly. In contrast, when acylase was used individually or in a combination with amylase, a different release pattern was observed (Figure 5.14A). The cumulative release of LbL Acy, LbL Hyb-Acy, and LbL Hyb-Amy assemblies within the time of incubation demonstrate an exponential tendency with negligible burst release at the beginning (after 1 day of incubation; Figure 5.14A). Such outcome might

be related to the presence of branched PEI in the multilayer coatings that increases their stability similar to previous works demonstrating prolonged stability of PAA/DNA multilayers due to PEI insertion [314].

Additionally, fluorescence microscopy was used to qualitatively assess the stability of the coatings in the presence of artificial urine after 7 days of incubation. The fluorescence intensity images of silicone surface did not show detectable differences in the intensity and surface homogeneity before (0 days) and after (7 days) incubation, which indicated the formation of stable enzyme coatings. For simplicity, only the LbL Hyb-Amy images are shown here (Figure 5.14B).



B

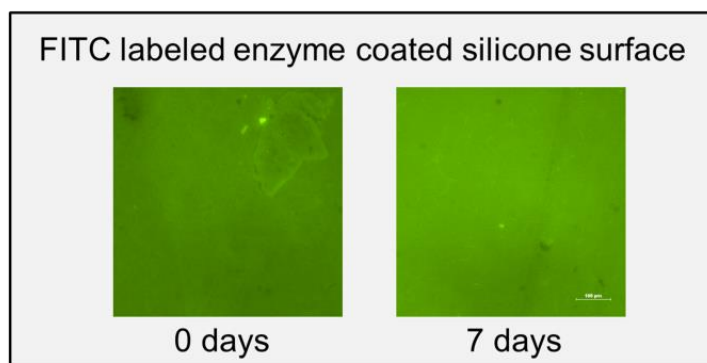


Figure 5.14 A) Cumulative fluorescence intensity vs. time of incubation for: LbL Amy (■), LbL Acy (●), LbL Hyb-Amy (○) and LbL Hyb-Acy (▼). B) Microscopic images of FITC labelled LbL Hyb-Amy coatings before (0 days) and after (7 days) incubation in artificial urine.

5.2.3 Enzymes Activities in the Multilayers

The activity of the enzymes, in both immobilised and free forms, on biofilm components was further evaluated. The ability of acylase to interfere with bacterial QS process through AHL inactivation in bacterial surroundings (i.e., acylase QQ activity) was assessed at physiological conditions by *C. violaceum*. The antibiofilm potential of amylase was determined by the amount of the released reducing sugars upon the degradation of EPS-based biofilm matrix extracted from *P. aeruginosa*.

All acylase-containing coatings (LbL Acy, LbL Hyb-Amy, and LbL Hyb-Acy) inactivated the C6-HSL signal in the extracellular environment of *C. violaceum* and inhibited QS-regulated violacein production up to 40 % compared to 100 % violacein production in the control (untreated silicone, Figure 5.15A). In addition, no significant difference in QQ activity was observed between acylase in free and immobilised forms. Therefore, the LbL approach used to deposit acylase on silicone material favours the preservation of the enzyme QQ activity. The enzyme treated surfaces did not affect *C. violaceum* growth after 24 h (turbidity was observed with naked eye), suggesting their potential to inhibit bacterial biofilm formation by interfering only with the QS process. Therefore, the enzyme based approach used in this study would not induce selective pressure on bacteria to become resistant [302].

After 10 sequential deposition steps on the silicone surface, individually or together with the QQ acylase, α -amylase was still able to degrade *P. aeruginosa* biofilm EPS, confirmed by the amount of released reducing sugars (Figure 5.15B). Lower values of reducing sugars were obtained for the LbL Amy assembly when compared to those obtained with the hybrid coatings that demonstrated higher EPS-degrading activity, especially when amylase was the outermost layer (Figure 5.15B). In fact, the EPS components of *P. aeruginosa* EPM are high-molecular-weight biomolecules that diffuse slowly in the multilayers; consequently, the contact with the enzymes could be limited and the specific activity decreased [321]. In contrast, less enzyme protein was deposited in the LbL Amy assemblies, suggesting that these amounts do not possess sufficient activity to act on the EPS of *P. aeruginosa* biofilm matrix (Table 5.1). Despite the lower α -amylase activity on EPM extracted from previously formed *P. aeruginosa* biofilms, we believe that at physiological conditions, i.e. during the biofilm formation, α -amylase would affect the EPS once bacteria are attached and biofilm matrix is produced. Therefore, the potential of the hybrid coatings to inhibit *P. aeruginosa* biofilm formation was further investigated and compared to that of the coatings of amylase and acylase applied individually on the silicone material.

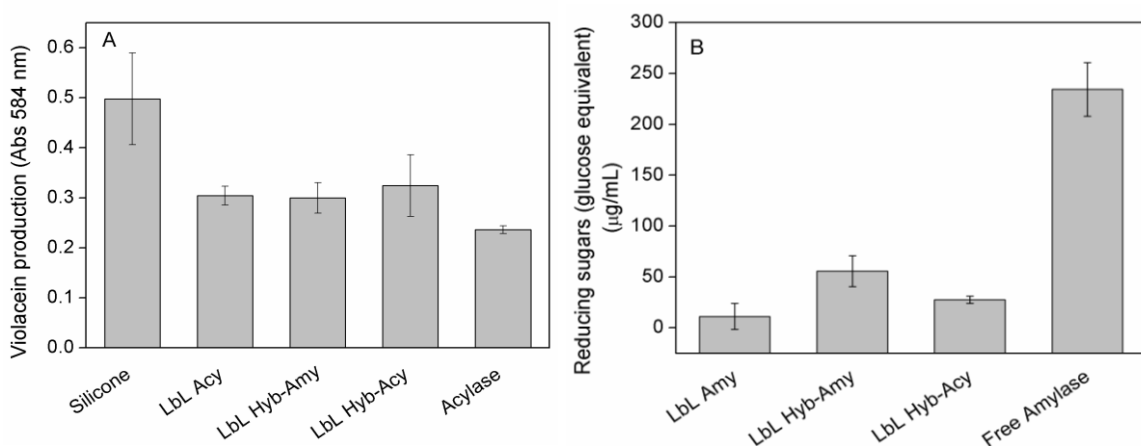


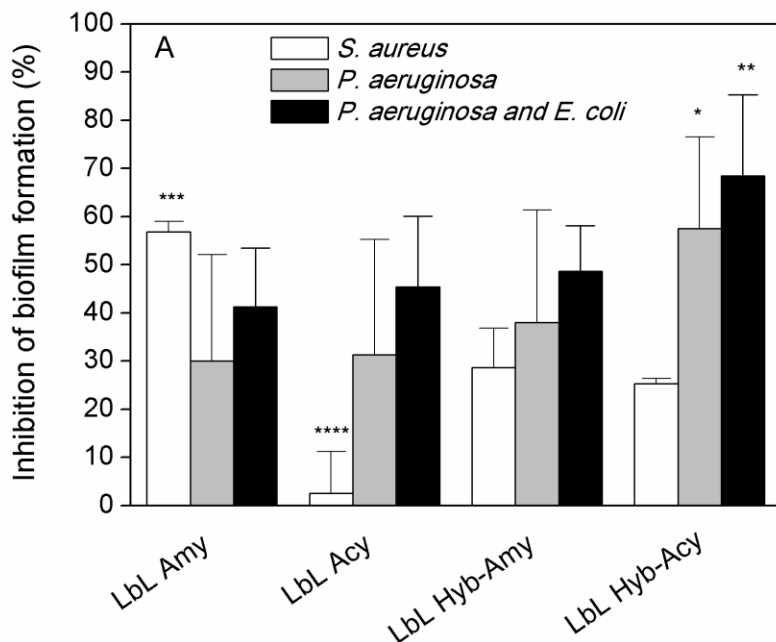
Figure 5.15 A) Quantification of violacein production in presence of acylase and acylase/amylase comprising coatings. B) EPS-induced degradation by α -amylase comprising silicone samples.

5.2.4 Antibiofilm Activity of Enzyme Multilayers in Static Conditions

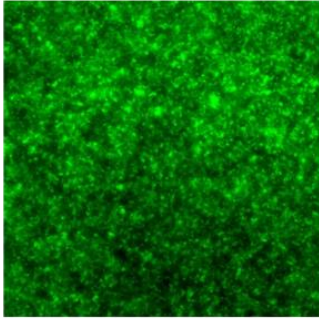
The biofilm occurrence by *P. aeruginosa* was assessed on treated and untreated silicone catheters under static conditions using CV assay. After 24 h of incubation with *P. aeruginosa*, the total biofilm mass formed on enzyme multilayers was reduced when compared to that on pristine silicone (100 % biofilm formation, Figure 5.16). Individually immobilised acylase or amylase inhibited the biofilm growth by 30 %, whereas the hybrid coatings demonstrated an enhanced antibiofilm efficiency, decreasing the total biomass by 38 and 60 % for LbL Hyb-Amy and LbL Hyb-Acy, respectively (Figure 5.16A). The QQ enzyme of the hybrid's outermost layer played a key role in the biofilm inhibition, increasing significantly its antibiofilm activity by more than 20 % of that of the other LbL Amy, LbL Acy, and LbL Hyb-Amy assemblies (Figure 5.16A). Such outcomes could be related with the natural sequence of *P. aeruginosa* biofilm development—from bacterial communication to surface attachment and EPS based matrix production. The deposition of acylase as the top layer (closest to the solution) reduces the diffusion time and path for the QS signals increasing the overall biofilm inhibiting effect of the hybrid coatings [327].

Amylase in the multilayer coatings may insert its activity upon the biofilm matrix of both Gram-negative and -positive bacterial species; thus, the potential of these assemblies to counteract biofilm formation of *S. aureus* was also evaluated [328, 329]. As expected, acylase-coated silicone samples were able to quench only the AHL-based QS of Gram-negative bacteria and did not affect the biofilm occurrence of Gram-

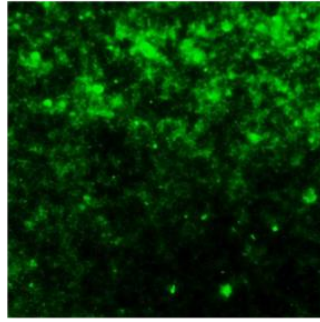
positive *S. aureus*, a bacterium that uses other QS signals to induce virulence and form biofilms [38]. In contrast, all amylase coatings demonstrated different tendencies in inhibiting *S. aureus* biofilms (Figure 5.16A), with LbL Amy being the most efficient. Following the combination of both enzymes in the hybrid assemblies, the antibiofilm activity decreased. Although both enzymes acylase and amylase in these coatings act sequentially on two key components (QS and EPS) of *P. aeruginosa* biofilm growth, in the case of *S. aureus*, amylase may exert its activity only on the biofilm matrix. Therefore, the overall synergistic efficiency of the hybrids toward this Gram-positive bacterium will be reduced. On the basis of these observations, we assume that the developed materials possess greater potential against Gram-negative bacteria (Figure 5.16A). Fluorescence microscopy images of live (green) and dead (red) bacteria in the biofilm corroborated these results: A well-established *S. aureus* biofilm was observed on pristine silicone and acylase multilayers, whereas fewer bacterial clusters were attached on LbL Amy, LbL Hyb-Amy, and LbL Hyb-Acy (Figure 5.16C). Moreover, the bacterial clusters depicted in the images were smaller on LbL Hyb-Amy than on LbL Hyb-Acy, suggesting that the antibiofilm activity of these coatings is a function of the QQ or EPS-degrading enzymes position in the layers.



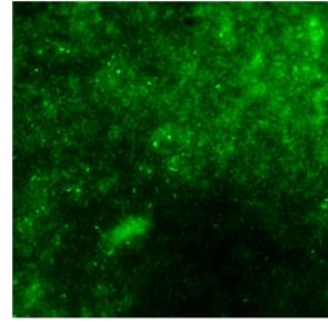
B



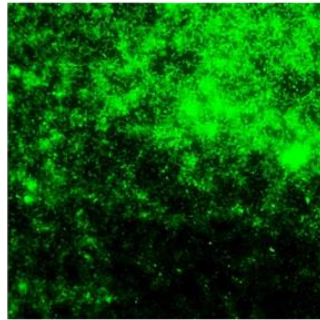
Silicone



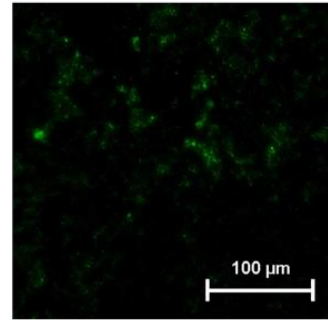
LbL Amy



LbL Hyb Amy

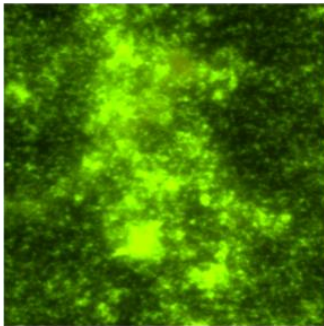


LbL Acy

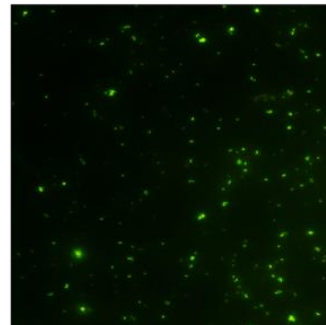


LbL Hyb Acy

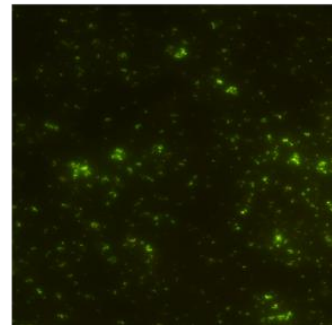
C



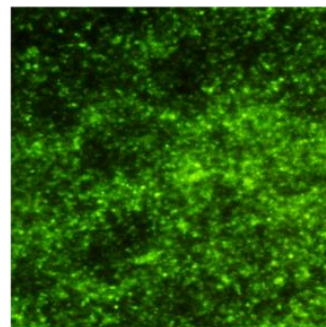
Silicone



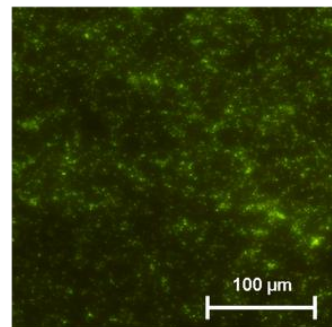
LbL Amy



LbL Hyb Amy



LbL Acy



LbL Hyb Acy

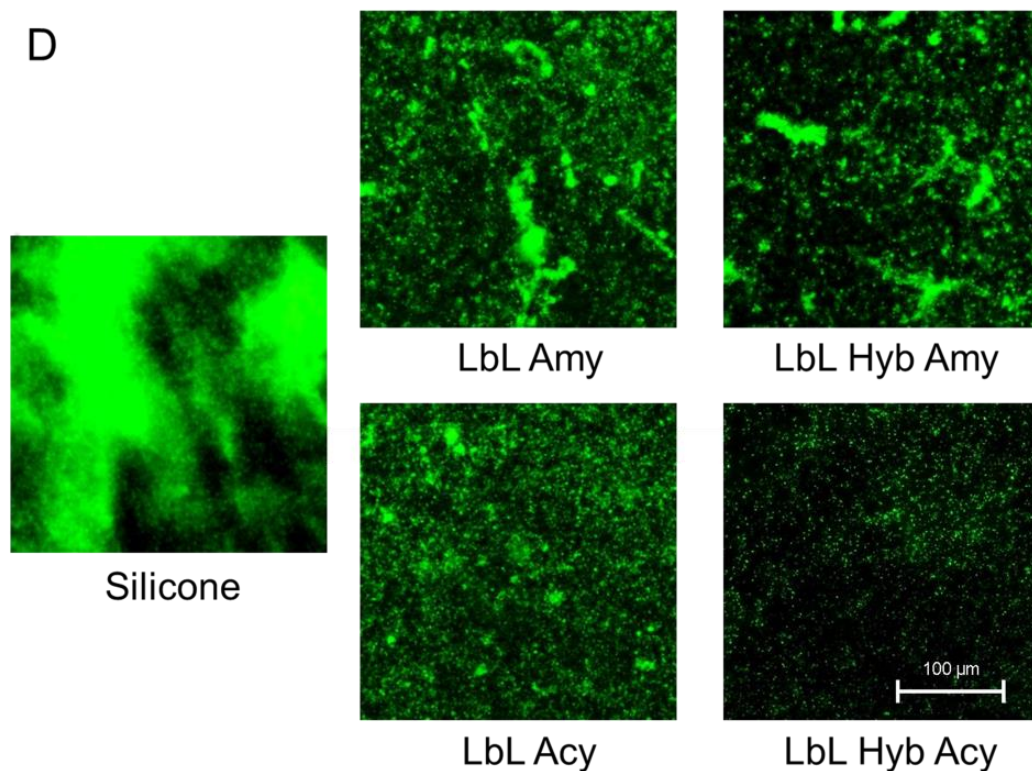


Figure 5.16 (A) Inhibition (%) of single-species (*P. aeruginosa* and *S. aureus*) and dual-species (*P. aeruginosa* and *E. coli*) biofilm formation on enzyme coated silicone catheters. Stars represent the statistical differences between the different groups of samples; $p < 0.05$. (B) Fluorescence microscopy images of *P. aeruginosa* biofilms grown for 24 h on pristine and enzyme-coated silicone materials analysed after Live/Dead staining. (C) Fluorescence microscopy images of *S. aureus* biofilms grown for 24 h. (D) Fluorescence microscopy images of mixed *P. aeruginosa* and *E. coli* biofilms. The green and red fluorescence images are overlaid in one picture for better comparison of live and dead cells, respectively.

Most biofilms that colonise catheter surfaces are mixed bacterial communities with enhanced resistance and virulence. Therefore, the occurrence of dual-species biofilm with two Gram-negative bacterial species, *P. aeruginosa* and *E. coli*, was also studied. CV assessments of total biomass grown on treated and untreated silicone material revealed the same tendency as single *P. aeruginosa* biofilms (Figure 5.16A). Significant biofilm reduction was observed for LbL Hyb-Acy assemblies with acylase initially acting on the AHLs produced by *P. aeruginosa* and α -amylase exerting its activity on the EPS produced by both *P. aeruginosa* and *E. coli* (Figure 5.16A). The single- and dual-species biofilms were well-established on pristine silicone material, fully covering its surface, whereas on the enzyme based multilayer coatings, the biomass was decreased (Figure 5.16B and D). Although no significant difference was observed for the coatings individually comprising amylase or acylase, less viable

bacteria (stained in green) were visualized on the LbL Hyb-Acy assemblies on silicone (Figure 5.16B and D). The overlapped images of green and red fluorescence showed the presence of live bacteria on the enzyme-coated catheters, which suggested that these active agents do not possess antibacterial activity, i.e., do not kill bacteria. The lower quantity of biomass observed on these images indicated the prevention capacity of the multilayered coatings on the silicone surface, due to the ability of the enzymes to exert QQ and/or EPS-degradation activities against biofilm-forming Gram-negative bacteria.

Further studies have shown that the hybrid coatings could control the single- and dual-species biofilm formation without affecting planktonic bacterial growth (Figure 5.17), an important outcome that is believed to decrease the risk of emergence of multidrug resistance. Consequently, interfering simultaneously with the QS process and EPM constituents that are essential for pathogenic biofilm growth could be a viable alternative for controlling biofilm establishment on urinary catheters.

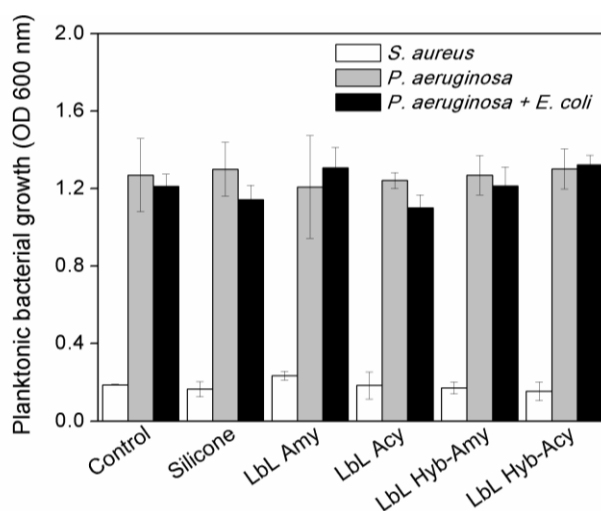


Figure 5.17 Planktonic growth of Gram-negative *P. aeruginosa*, Gram-positive *S. aureus*, and mixed inoculum of *P. aeruginosa* and *E. coli* in the presence of pristine silicone and multilayer enzyme coatings.

Considering the previously reported antibiofilm activity of PEI, it was also reasonable to assess its biofilm inhibition potential in the multilayers [330]. Thereby, PEI and an inactive protein (e.g. BSA) were sequentially deposited in a LbL fashion on silicone material. The developed coatings did not reduce the total *P. aeruginosa* biomass, confirming that the above demonstrated antibiofilm activity towards Gram-negative bacteria is a result of acylase and amylase activity upon the target biofilm components (Figure 5.18). Likewise, the electrostatic interactions with the enzymes in the

multilayers might decrease the amount of PEI amino groups required to interact with negatively charged membrane and disrupt bacterial cells [331].

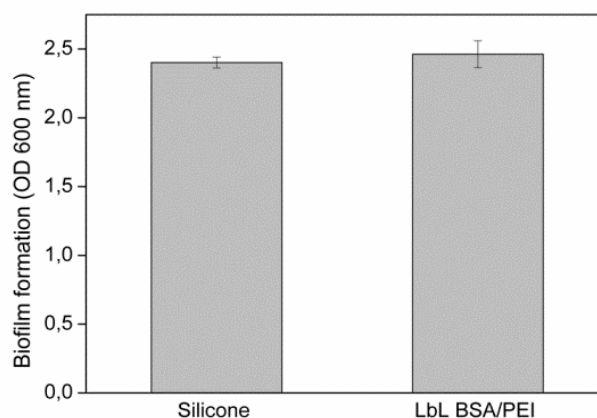


Figure 5.18 *P. aeruginosa* biofilm growth on pristine silicone and polyethyleneimine/bovine serum albumin (PEI/BSA) multilayer coatings

5.2.5 Dynamic Biofilm Inhibition Tests

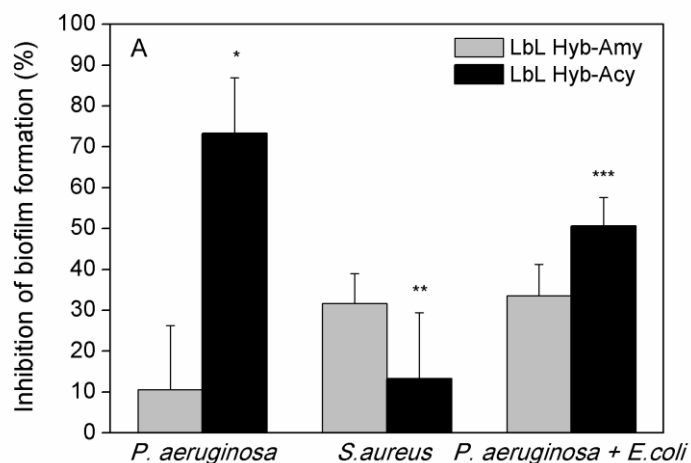
The hybrid coatings, which demonstrated high efficiency in controlling single- and dual-species biofilm formation of Gram-negative bacteria, were further subjected to dynamic biofilm inhibition tests in a physical model of the human bladder. After 7 days of catheter incubation in the bladder model, the biofilms formed on urinary catheters surface were studied using CV and live/dead cell viability assays. Although different growth conditions are present in the dynamic system, the observed biofilm inhibition by the enzyme-treated silicone catheters was comparable to that obtained under static conditions. The total biofilm mass of Gram-negative bacteria on the catheter shaft was significantly reduced for the LbL Hyb-Acy catheters (Figure 5.19). However, when the bladder was infected with Gram-positive bacteria, the hybrid assemblies with amylase as outermost layer were more active, similar to what was observed in the static environment. Single-species *P. aeruginosa* biofilm formation was inhibited up to 70 % by the acylase-terminated hybrid LbL coatings, whereas only 10 % of biofilm was reduced for the hybrid assemblies with EPS-degrading amylase as the outermost layer (Figure 5.19A). Recently, Cole *et al.* demonstrated that urea might induce the production of an EPS-independent biofilm matrix in some *P. aeruginosa* strains [109]. Under dynamic conditions, simulated urine may affect the EPS production by this bacterium, hindering the matrix-degrading potential of amylase in the coatings. Hence, to establish biofilm on the catheter surface, *P. aeruginosa* switches its genetic program

and produces extracellular DNA-based matrix, under the control of the QS process [332]. Under these conditions, QQ acylase on the top of the layers play a key role in inhibiting the QS-regulated *P. aeruginosa*, as confirmed by fluorescence microscopy. Thinner biofilms lacking the characteristic mushroom formations on the urethra surface were observed after microscopic visualization of live and dead bacteria on the LbL Hyb-Acy surface (Figure 5.19B). We hypothesise that the efficiency of the hybrid coatings is a function of the position of the active agent in the layers, which was further confirmed through the biofilm inhibition tests toward *S. aureus*. Although no significant difference was obtained in between the hybrids in static conditions, dynamic experiments *in vitro* revealed improved functional characteristics when amylase was assembled as a top layer (Figure 5.19).

Under dynamic conditions, *S. aureus* showed a lower degree of biofilm formation on pristine silicone catheter shaft (Figure 5.19B) than when grow in static conditions (Figure 5.16C). Because of the low urine flow, the catheter shaft presents a liquid–air interface, and in contrast to *P. aeruginosa* and *E. coli*, under these conditions the facultative anaerobic *S. aureus* hardly builds biofilms [289, 333]. Because most of the biofilms colonising catheter surfaces contain more than one species, we assumed that the presence of α -amylase in the multilayers could interfere with EPS dependent biofilms of other Gram-negative species that do not rely only on the AHLs based signalling to establish biofilms. Herein, we demonstrated that the biomass formed simultaneously by *P. aeruginosa* and *E. coli* was decreased when the silicone surface was functionalized with both acylase and amylase. Despite the fact that LbL Hyb-Amy catheters did not exert significant antibiofilm activity toward single *P. aeruginosa* species, the dual species biofilm occurrence was inhibited by more than 20 % (Figure 5.19A). Considering the previously described mode of growth in artificial urine of mixed *P. aeruginosa* and *E. coli* biofilms, we suggested that the EPS-degrading enzyme in the hybrid coatings could affect the initial *E. coli* colonisation on the catheters and prevent the total dual-species biofilm growth [334]. Previous studies demonstrated the importance of EPS such as cellulose, colanic acid, and poly-L-1,6-N-acetyl-D-glucosamine for *E. coli* biofilm occurrence; therefore, their degradation by amylase might reduce the total biomass attached to the silicone materials [334]. LbL Hyb-Acy samples however showed enhanced antibiofilm activity by up to 15 % when compared to that of LbL Hyb-Amy (Figure 5.19A), which could be associated with the acylase QQ activity against *P. aeruginosa* because *E. coli* cannot produce AHLs. The inhibition of single- and dual-species biofilm formation up to 50 % demonstrated the potential of these enzyme-decorated silicone surfaces to control bacterial biofilms of one or more

species targeting simultaneously AHL based QS systems and EPS adhesives of the most frequently found Gram-negative pathogens in CAUTIs [95].

The fluorescence images of LbL Hyb-Acy catheters also confirmed their capacity to delay the single- and dual-species mature biofilm formation over 7 days in the *in vitro* catheterized human bladder (Figure 5.19B). Although characteristic bacterial clusters were visualized on pristine silicone surface, fewer live *P. aeruginosa* bacterial cells (stained only in green) were observed on LbL Hyb-Acy catheter shaft in the single-species experiments (Figure 5.19B), whereas the presence of small cells clusters in the mixed biofilm tests on the treated coatings in the CV quantification assay showed reduction of the biofilm growth by 50 % (Figure 5.19A), suggesting their potential to control dual-species biofilm development on medical devices.



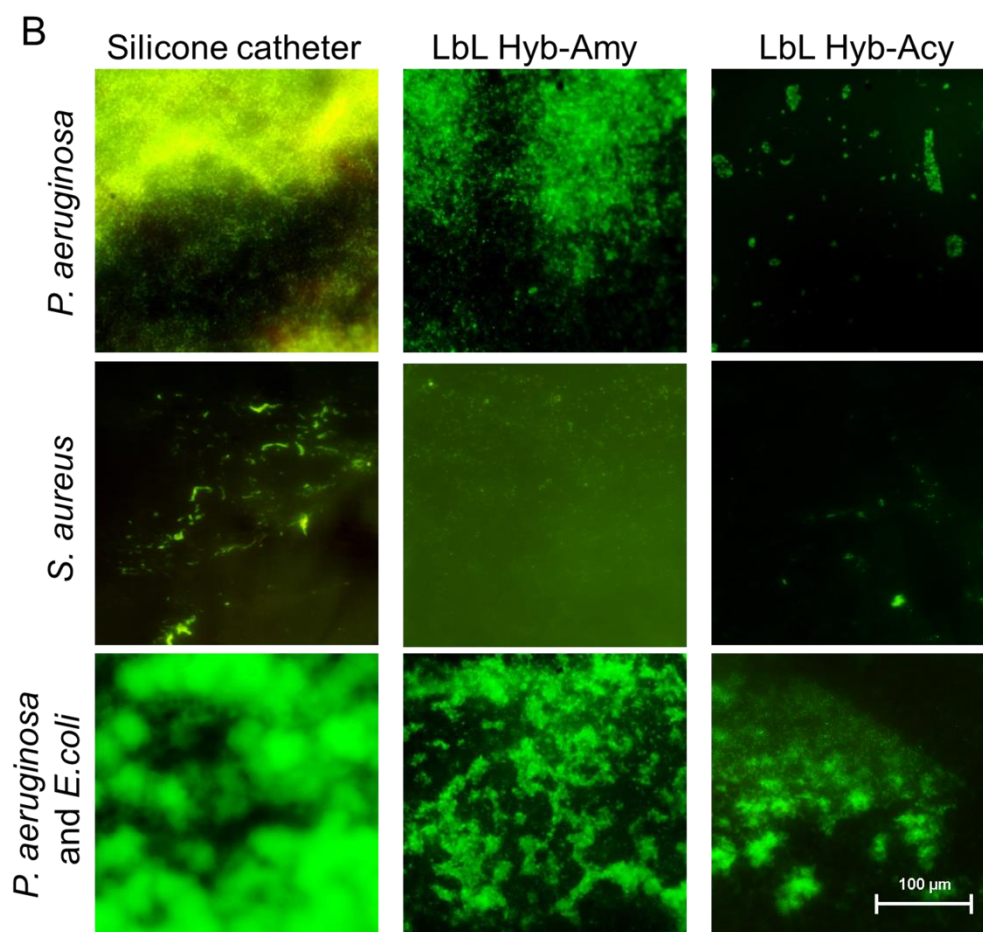


Figure 5.19 Biofilm inhibition tests of *in vitro* catheterized bladder model system. (A) Inhibition of *P. aeruginosa*, *S. aureus*, and mixed species (*P. aeruginosa* and *E. coli*) biofilm formation on enzyme-coated silicone urinary catheters assessed with CV. Stars represent the statistical differences between the different groups of samples; $p < 0.05$. (B) Fluorescence microscopy images of live (green) and dead (red) bacteria in biofilms grown for 7 days on pristine and enzyme-coated silicone Foley catheter shaft. The green and red fluorescence images are overlaid in one picture for better comparison.

5.2.6 Biocompatibility Tests

Because the PEI used in the assembly of the hybrid multilayers is regarded as a toxic compound, it was important to evaluate the effect of the developed materials on human cells for further biomedical application [335]. To assess the cytotoxicity of the materials independent from the influence of their mechanical properties, the coated silicone samples were placed in contact with previously cultured cells. This method would allow study of the potential effect of the released PEI from the surface on the skin fibroblasts during the time of incubation [336]. The results obtained after 1 week of contact with human cells demonstrated no significant difference between enzyme-coated materials and control-pristine silicone (nontoxic material; Table 5.2). The human cells viability

was not affected, and more than 90 % of the cells were viable, suggesting that the PEI is in amounts insufficient to cause toxicity and/or is not released to the medium [335]. The interaction of positively charged PEI with negatively charged amylase or acylase could also lead to the neutralization of PEI amino groups and subsequent reduction of its cytotoxicity. In principle, polymers containing amino groups damage human cells because of their strong positive charges [320, 337]. Modifications of polymeric backbone in order to decrease the positive charge of PEI including the acylation of the amine groups were shown to possess very good biocompatibility with mammalian cells [338].

Table 5.2 Viable human fibroblasts (BJ5ta) after 7 days of contact with silicone samples

Sample	Silicone	LbL Acy	LbL Amy	LbL Hyb-Acy	LbL Hyb-Acy
Fibroblasts viability (%)	88.3 ± 6.7	88.9 ± 7.1	87.7 ± 3.6	91.4 ± 4.2	88.8 ± 4.6

5.2.7 *In Vivo* Biofilm Inhibition Tests

The antibiofilm activity of the hybrid multilayer coatings in which the outermost layer was the QQ enzyme acylase was further studied *in vivo* using a rabbit model. After 7 days of catheterisation, the catheters were removed and analysed for biofilm formation. Because the enzymes used in this work do not affect planktonic bacterial growth but rather the mechanism of biofilm formation, only the reduction of bacterial biofilm growth inside and outside the catheters surface was examined.

Photographs of the collected catheters demonstrate that LbL Hyb-Acy coatings inhibit to a certain extent biofilm formation on silicone catheters. Nevertheless, the antibiofilm activity of the enzyme based coatings varied depending on the catheter segments and their location, inside or outside the animal body (Figure 5.20).

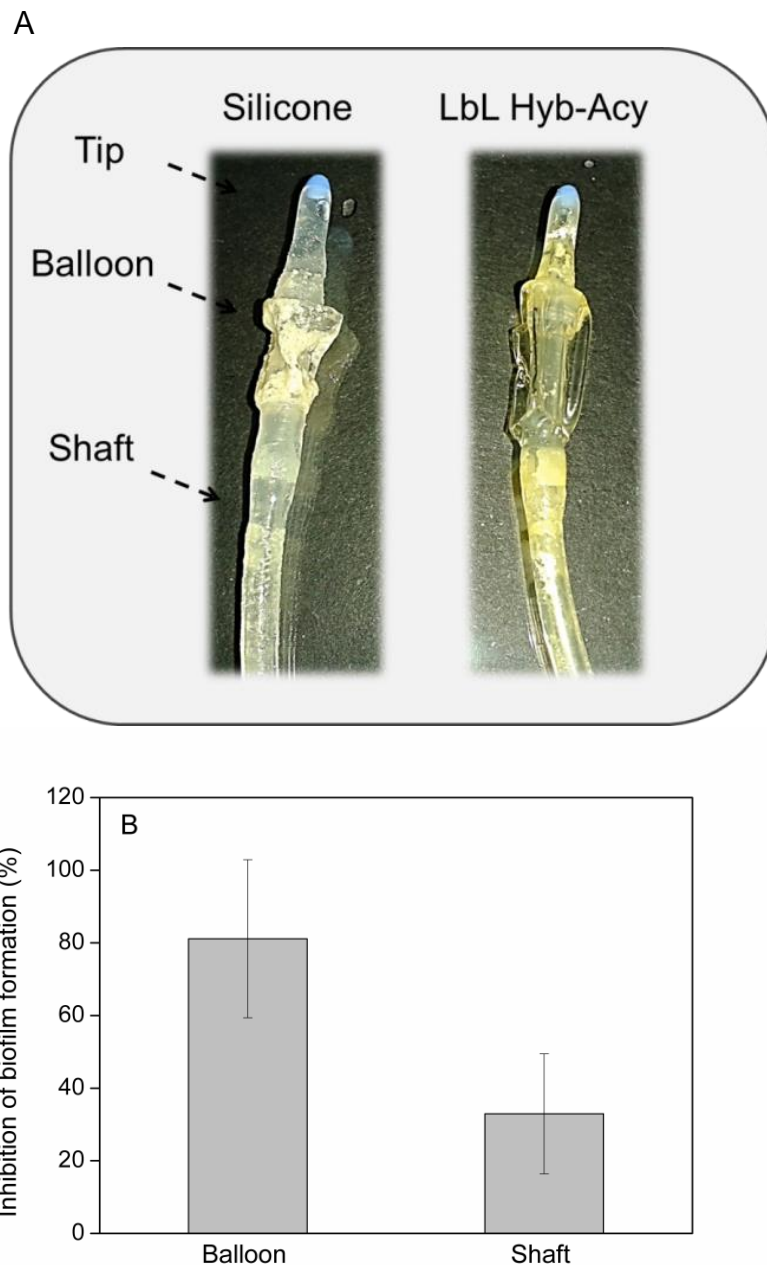


Figure 5.20 Biofilm formation in *in vivo* rabbit model. A) Representative images of the control catheter and enzymes coated silicone urinary catheters and B) Total biomass formation after 7 days of catheterisation.

Quantification of the total biofilm growth on the catheters surface further revealed the potential of acylase and amylase in the multilayer coatings to synergistically reduce biofilm formation up to 70 % on the balloon part (Figure 5.20, right side photo). The biofilms on catheter balloon are frequently associated with bacterial colonisation of bladder epithelia; thus, the significant biofilm reduction observed in this part of the catheter is thought to decrease the trauma to the bladder and consequently delay UTI occurrence [339]. The main complication during catheterisation, however, is the

blockage of the urine flow through the catheter as a result of mature biofilm formation on the luminal surfaces/catheter shaft. A common way for bacteria to access the bladder and colonise the device surface is through the catheter tip during the insertion into the body. Once attached, bacteria move with the urine flow along the catheters segments and establish biofilms [339]. Despite the biofilm growth on the catheter tip, the enzymes delayed biofilm spread along the inner side of the catheter shaft by more than 30 % when compared to the spread along the control silicone catheter. Consequently, we believe that amylase and acylase multilayers are able to delay the biofilm growth of medically relevant bacterial species such as *P. aeruginosa* and *E. coli* that prefer to grow on the air-liquid interface constantly present on the catheter shaft, which is the most attractive site for bacterial growth. Similarly, enhanced antibiofilm activity of the balloon immersed in the urine during the time of incubation versus the lower effect on the tip and catheter shaft was obtained previously in the *in vitro* model of human catheterized bladder infected with Gram-negative *P. aeruginosa* [289]. Although our initial findings are in good agreement with the results obtained *in vitro*, the *in vivo* study has revealed several limitations. A small number of rabbits were tested in each group, and the enzymes in the coatings prevented biofilm occurrence on catheter segments depending on the location in the animals' body. Considering the resistance mechanisms of bacterial biofilms, it can be hypothesized that delaying the biofilm growth would further increase the bacteria susceptibility to antimicrobials at subinhibitory concentrations.

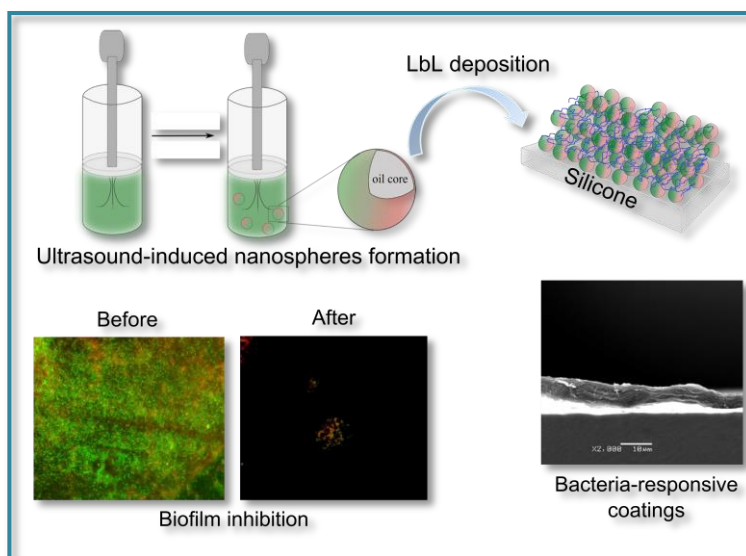
5.2.8 Conclusions

Emerging resistance of bacteria and their biofilms to conventional antibiotic treatments requires the development of novel approaches to counteract the biofilms and device-associated infections in clinical settings. Targeting the extracellular components of biofilms is thought to decrease the possibility of resistance development because of reduced selective pressure on bacterial population and is emerging as a potential alternative for antibiofilm strategies. The ability of acylase and α -amylase to degrade QS signalling molecules and polysaccharide components of the biofilm matrix makes them potentially applicable as antibiofilm active agents. This study combined these two negatively charged enzymes with positively charged branched PEI in a sequential multilayer fashion to build stable and biocompatible multilayer coatings on silicone catheter material. Both individual enzyme coatings inhibited the aggregation of medically relevant Gram-negative *P. aeruginosa* and Gram-positive *S. aureus* on silicone catheter under static conditions. However, combining the two antibiofilm enzymes into a hybrid multifunctional surface coating resulted in enhanced antibiofilm activity against only *P. aeruginosa* and mixed-species (*P. aeruginosa* and *E. coli*) biofilms because of their simultaneous action on biofilm components, i.e., QS signals and EPS adhesives. Moreover, the obtained preliminary results in the in vivo rabbit model suggested the potential of this alternative enzyme-integrated strategy to delay pathogenic biofilm formation on urinary catheters.

Nanomaterials for controlling bacterial growth and biofilm occurrence

5.3 Bacteria-Responsive Multilayer Coatings Comprising Polycationic Nanospheres

In the current study, sonochemically-processed NSs from cationic AC conjugate are combined with biodegradable HA to engineer “smart” bacteria/biofilm resistant coating. The rationale of this work comes from previous findings in our group that planktonic bacteria are more



susceptible to nano-sized cationic biopolymers than to their free counterparts [147]. The bactericidal efficacy is result of massive membrane surface defects caused by ACNSs and consequent disruption of bacterial cell wall. The efficiency of the developed multilayer coatings incorporating ACNSs to eradicate bacteria and prevent biofilm occurrence on demand, i.e. only in presence of pathogenic bacteria, is demonstrated in both static and dynamic conditions, mimicking the real situation during catheterisation.

This section is based on the following publication:

Francesco A, Fernandes MM, **Ivanova K**, Amorim S, Reis RL, Pashkuleva I, Mendoza E, Pfeifer A, Heinze T, Tzanov T “Bacteria-responsive multilayer coatings comprising polycationic nanospheres for bacteria biofilm prevention on urinary catheters”, *Acta Biomaterialia*, 2016, 33: 203-12. 10.1016/j.actbio.2016.01.020.

5.3.1 Assembling Of the Multilayer Coatings

The successful build-up of the LbL assemblies was confirmed by QCM-D. The obtained results suggested an exponential growth of the coatings with each deposition (Figure 5.22). Typical stepwise decrease in frequency (ΔF) was measured for both coatings, i.e. for (HA/ACsol)₅ and (HA/ACNSs)₅, showing the overall increased mass adsorption (ΔF in Figure 5.21, A1 vs. B1, black lines) bigger in the case of the coating obtained with ACsol as polycation. Since ΔF accounts for both polycation and water deposition on the QCM crystal, the bigger mass adsorption obtained for ACsol specimen may indicate less adsorbed polycation in the case of ACNSs or more hydrated LbL constructs when ACsol is used. The dissipation curves supported the former statement as true. In contrast, more dissipative layers were measured for (HA/ACNSs)₅ (Figure 5.21, A1 vs. B1, blue lines). The formation of the first layer, HA on APTES treated silicone is characterized with a strongly attached (very small ΔD) ad-layer formed (the first green arrows on Figure 5.21, A1 and B1), followed by the attachment of a loosely bound polycation in both cases (Figure 5.21, A3 and B3), seen via higher dissipation shifts from the second layers (the first red arrows on Figure 5.21, A1 and B1). The formation of the first layer is the same for both constructs and it is merely electrostatically driven, as the negatively charged carboxyl groups from HA interact with the positively charged amino groups (from APTES) available on the silicone surface. Because of the charge compensation between the surface and the first layer, the second layer is not fixed by strong electrostatic interactions. Weakly bound polycations (from the second layer) allow for larger amount of trapped water that contributes to the higher dissipation shifts [340]. However, the absolute values for ΔD , as well as the shape of the dissipation signal for the second layer are different for ACsol and ACNSs. Upon the injection of ACsol in the QCM chamber, a burst increase of ΔD is observed, followed by a common stabilization of the dissipation signal (marked by the first blue arrow on Figure 5.21, A1). When ACNSs is used as a polycation, a steady increase of ΔD is detected instead. We have also plotted ΔD vs ΔF (Figure 5.21, A2 and B2) to relate the dissipation caused by a unit frequency (mass) change. A comparison between these two plots demonstrate clearly that in the case of (HA/ACNSs)₅ there is less adsorbed material that is more dissipative in comparison with the (HA/ACsol)₅. Finally, the thicknesses of the constructs were calculated by a viscoelastic model based on a Voigt element. We obtained 82.33 nm for the (HA/ACsol)₅ and 141.5 nm for the (HA/ACNSs)₅ constructs.

The shape of the shifts for the second layer are different for ACsol and ACNSs, because of the different structure of the employed polycations: ACsol is a linear

polymer deposited in a single step, while ACNSs has a spherical shape that needs reorganization and hydration upon the deposition. The greater dissipation measured for ACNSs can be related with both the shape of the NSs and the hydration state of the layers. Moreover, the difference in the adsorbed material reflected in the $\Delta D/\Delta F$ plot is expected, since ACNSs cannot be closely packed in a layer because of the repulsion forces between the NSs due to their high positive charge (the main reason for the stability of ACNSs dispersion). The free space between the spheres is hydrated and as a result the obtained layer is much more dissipative. The differences in the structure of the used polycations and the mechanism of their deposition were also reflected in the thickness of the final constructs. The main observation from QCM-D findings is that the thickness is not fully a function of the adsorbed material, but also depends on the structure and shape of the used polyions.

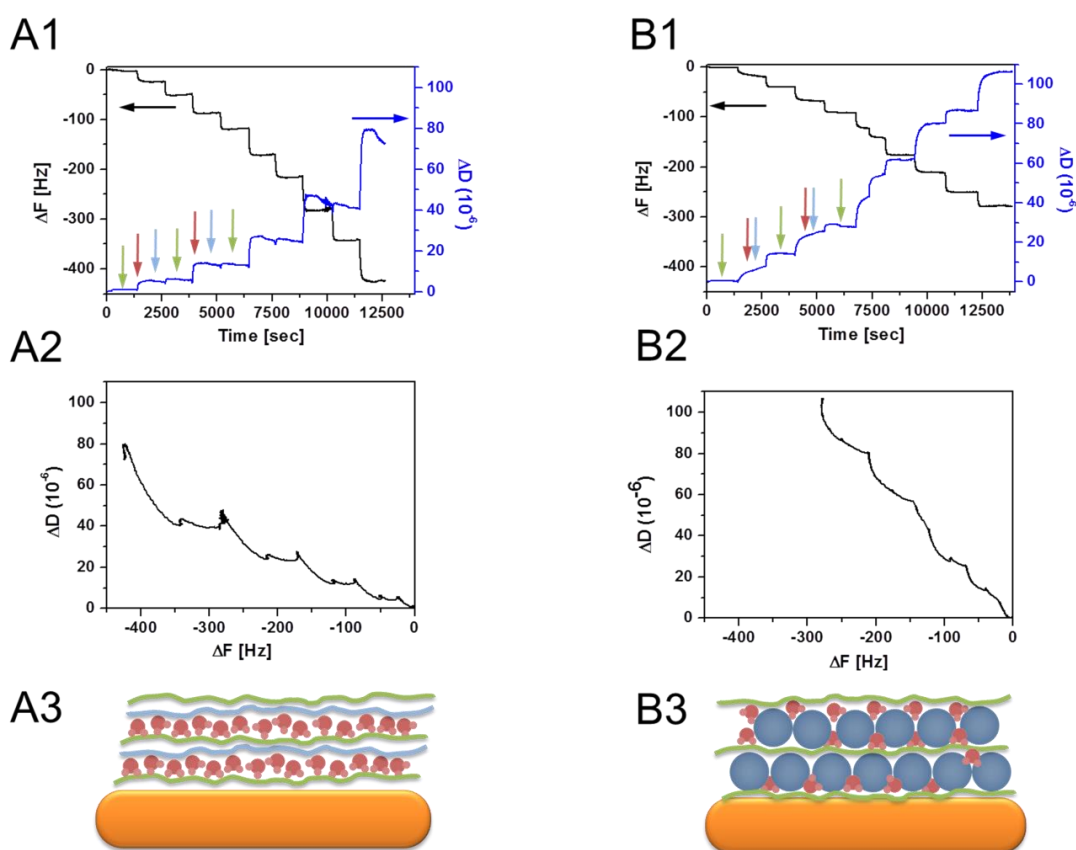


Figure 5.21 Representative frequency and dissipation changes obtained for the LbL build-up onto amino-functionalised gold surfaces using ACsol (A1) or ACNSs (B1) as polycations and the respective $\Delta D/\Delta F$ plots for the same experiments (A2 and B2). Schematic presentation of these build ups (A3 and B3) based on the obtained data – HA in green, water in red and ACsol/ACNSs in blue. The presented data are for the 7th overtone.

5.3.2 Characterisation of the Coated Silicone Materials

FTIR spectra confirmed the presence of the multilayer assemblies on the surface of silicone (Figure 5.22A). Three new bands appeared in spectra of all coated stripes: the signal at around 3300 cm^{-1} was assigned to stretching vibrations of N-H and O-H in AC, and O-H in HA, whereas the broad band between 1500 cm^{-1} and 1700 cm^{-1} was associated with the amines of AC. In general, all the bands were more pronounced after the deposition of 10 bilayers revealing that the coating thickness is directly proportional to the number of the deposited layers. The typical AC and HA bands found in the spectra of the coatings were more intense when ACsol was used for multilayer build-up (dotted lines), again suggesting more deposited material when compared to HA/ACNSs. Moreover, several new peaks that could be associated with triglycerides [341] and fatty acids [342] appeared in the spectra of HA/ACNSs specimens (containing sunflower oil), particularly pronounced in $(\text{HA/ACNSs})_{10}$ spectra (marked with arrows). The peaks at around 2930 cm^{-1} and 2850 cm^{-1} could be associated to C-H stretching vibrations in methylene ($-\text{CH}_2-$) and methyl groups ($-\text{CH}_3$), respectively, whereas the large peak around 1740 cm^{-1} is due to C=O double bond stretching vibration.

The coating deposition was also suggested by changes in the wettability of the treated silicone (Figure 5.22B). The untreated silicone is a hydrophobic surface ($112.7 \pm 0.4^\circ$). Upon coating, the water contact angle decreased significantly ($p < 0.01$) only for $(\text{HA/ACsol})_{10}$ ($83.4 \pm 1.7^\circ$), whereas the values measured for the silicone functionalized with $(\text{HA/ACsol})_5$, $(\text{HA/ACNSs})_5$ and $(\text{HA/ACNSs})_{10}$ were $105.9 \pm 0.6^\circ$, $111.0 \pm 0.5^\circ$ and $106.4 \pm 2.6^\circ$ respectively (Figure 5.22B, inset images). The contact angle measurements demonstrated that 5 sequential depositions are not sufficient to alter significantly the silicone wettability, regardless of the used AC. On the other hand, despite of the lower degree of polyion deposition, the higher hydrophobicity of both HA/ACNSs specimens is explained by the presence of oil in the NSs core which additionally repels water from the silicone surface.

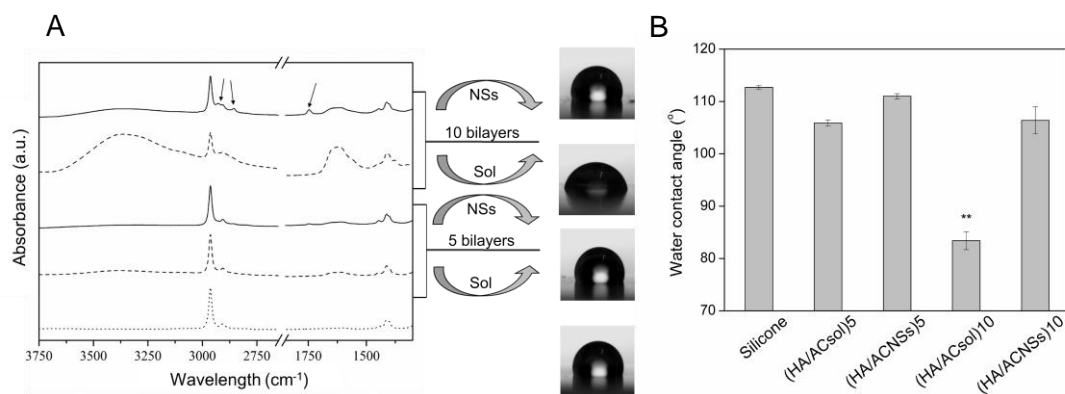


Figure 5.22 A) Representative FTIR spectra of silicone control (silicone-APTES) with dotted line and multilayer assemblies on silicone: HA-ACsol specimens with dashed lines and HA-ACNSs specimens with full lines. B) Water contact angles of HA/AC coatings deposited onto silicone. Statistical difference in the case of (HA/AC_{sol})₁₀ is related to the pristine silicone and represented as ** $p < 0.01$. Images of water contact angle measurements are given for each specimen.

The surface topography and morphology of the 10-bilayered coatings were visualised using AFM and SEM. Both (HA/ACsol)₁₀ and (HA/ACNSs)₁₀ coatings exhibited rough and irregular surfaces typical for LbL coatings (Figure 5.23A). The mean squared roughness (R) values were 7.7 nm and 3.0 nm, whereas the average heights (H) were 2.6 nm and 1 nm for ACsol and ACNSs, respectively. Unexpectedly, the profile of the ACNSs coating was smoother compared to the one built with ACsol [343]. Increased roughness of the ACsol-containing compared to relatively smooth surface of the structure with NSs is owed to the higher mobility of the free biopolymer, which after deposition takes the shape of the previous layer. Taking into account that the build-up of multilayers starts with the formation of isolated islets that grow and coalesce into continuous coatings only in the second stage of the build-up process (usually above 10 bilayers), the obtained AFM profile for (HA/ACsol)₁₀ is expected. In contrast, ACNSs solely dictates the morphology of the multilayer constructs independently of the shape of the below layers [310]. Due to both spherical shape and lower mobility of the NSs the related coating displayed a smoother surface [175].

Important for proving the hypothesis that nanostructures are more efficient than their molecular counterparts even after immobilisation onto solid surfaces, the incorporation of the intact soft NSs in our multilayer structures (SEM images in Figure 5.23) made relevant the further investigation. The SEM images taken at the cross-section of the coatings confirmed an irregular surface structure after 10 depositions, but also revealed a complete surface coverage by either (HA/ACsol)₁₀ or (HA/ACNSs)₁₀ (Figure 5.23B). The dry thicknesses of ~3 μm for (HA/ACsol)₁₀ and ~7 μm for (HA/ACNSs)₁₀ confirmed

the same tendency as calculated from the QCM-D data - ACNSs coating is thicker. Since the outermost layer of the coatings was made from the polycations, the top view on the surface revealed additional details about the coating structures (Figure 5.23C). The key difference was the presence of spheres on top of (HA/ACNSs)₁₀, which appear intact (black arrows in Figure 5.23C). Besides the NSs, some bigger than 1 μm formations (marked with red arrows on Figure 5.23C) also visible are oil bubbles which were not completely removed by the centrifugation steps. Previously we have observed the same artefacts in ACNSs dispersions [147]. This finding was also confirmed by the presence of the residual sunflower oil, identified with FTIR (Figure 5.22). Overall, the assembling of multilayers using intact core/shell NSs with a soft core as in our case is considered advantageous, since the added value of processing polymers into nanostructures could be transferred to the functionalised materials/surfaces.

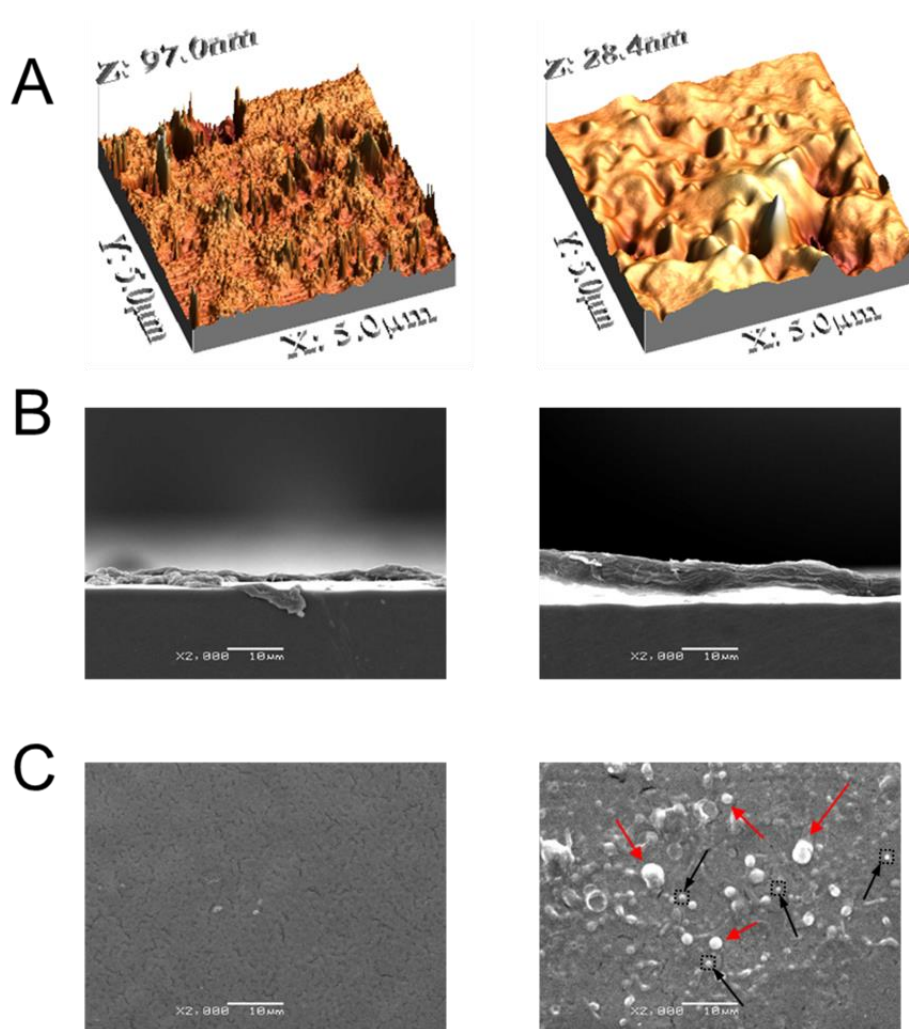


Figure 5.23 (A) AFM images ($5 \times 5 \mu\text{m}^2$) of (HA/ACsol)₁₀ and (HA/ACNSs)₁₀ deposited onto silicone strips. (B) Cross-section and (C) top view of the same samples taken with SEM.

The feasibility for deposition of 100 bilayers onto silicone surface was directed to demonstrate versatility of the LbL technique to fabricate macroscopic materials comprising ACNSs. Since such materials are not suitable to be employed as urinary catheter coatings, the deposition of 100 bilayers was performed only on silicone stripes. Moreover, these materials allowed to verify the presence of unbroken NSs in the HA/ACNSs multilayers due to the ease of sample handling, i.e. to make a suitable transversal cut. Figure 5.24A shows a side view SEM image of the membrane comprising 100 sequential HA/ACNSs depositions with an approximate thickness of 85 μm . The image was taken after 3 weeks storage of silicone in water (at 4 $^{\circ}\text{C}$), revealing high stability of the material in aqueous solutions. The top view of the 100-bilayer material is similar to the 10-bilayer coating with NSs dispersed over the last layer (Figure 5.24B). As mentioned above, the membrane was further intentionally damaged with a small cut in order to investigate the state of ACNSs inside the material. Once again, the NSs embedded in multilayers were intact (Figure 5.24C and D), demonstrating the suitability of the LbL technique for such application. At the same time, these findings also confirm the feasibility of the technique for production of free-standing membranes with embedded soft nanoarchitectures.

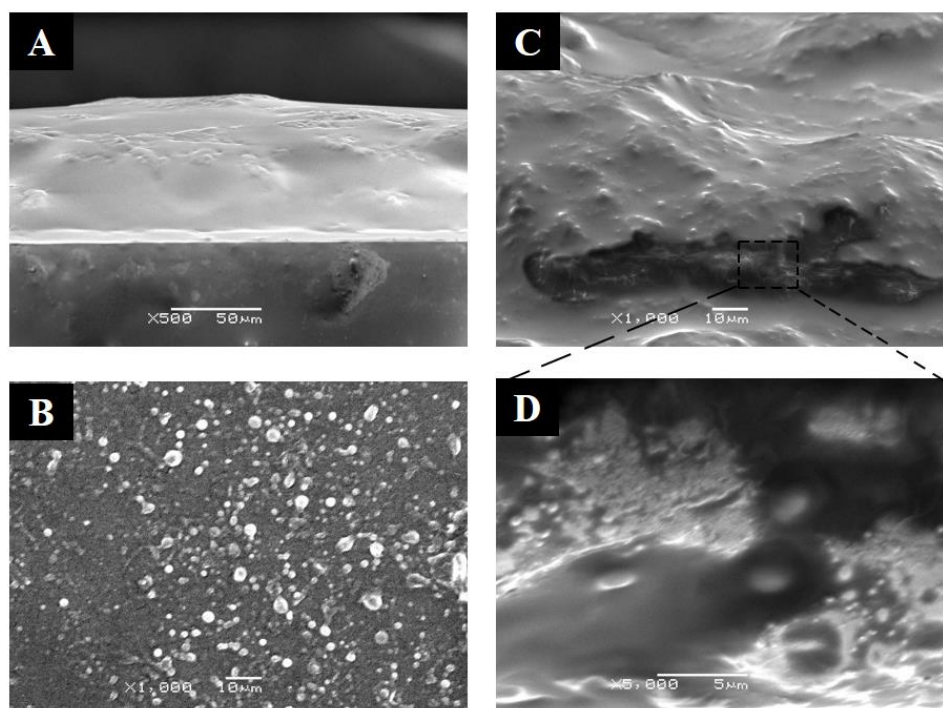


Figure 5.24 SEM images of (HA/ACNSs)₁₀₀ deposited onto silicone: (A) side view, (B) top view, (C) view at 60° with a cut, and (D) magnified zone of the cut.

5.3.3 Antimicrobial Action upon Bacteria-Induced Degradation of Coatings

AC is well known antibacterial agent owing to its positive charge and related perturbation of the bacterial membrane [344]. AC processed into NSs displays even higher disturbing capacity on bacterial membrane and bactericidal effect on planktonic bacteria [147]. Such bactericidal mechanism induces less selective pressure on bacterial population and consequently reduces the risk of resistance development. After proving their effectiveness in solution, the next step is incorporation of these antibacterial NSs into biomedical devices to effectively control nosocomial infections. In this aspect, building the multilayer polyelectrolyte coatings are regarded as a simple, but efficient approach for immobilisation of bioentities with preserved bioactivity [345].

Antibacterial and antibiofilm activities of the developed coatings were assessed against *P. aeruginosa*. A significant improvement ($p < 0.001$) in inhibition of the *P. aeruginosa* growth was observed already after 2 h incubation with most of the specimens, compared to the control (non-coated silicone). The ACNSs in the multilayer coatings (5 and 10 sequential depositions) reduced planktonic bacterial growth similarly (around 70 %), whereas the ACsol-based coatings affected up to 42 % the bacterial cells (Figure 5.25, Table 5.3). Interestingly, in the case of (HA/ACsol), the 5-bilayer coating was more efficient compared to the 10-bilayer one, which reduced the bacterial growth only 9 %. We relate this effect to the motility of the layers and their availability to interact with bacterial cells. An increased motility of the layers in thicker coatings usually favours bioactivity, e.g. antimicrobial effect, due to improved availability of polycations [295]. Nevertheless, the deposition of greater number of layers also results in enhanced motility of a polycation which could lower the effect. A lower hydration of the thinner assemblies results in compactly packed structures (reduced mobility) that favour the interactions between the polycation and adhered bacterial cells, which could result in stronger effect. In this study, the (HA/ACsol)₁₀ coating was more hydrated with higher motility of the polyelectrolytes, which translates into less amino groups of AC available on the surface to interact with bacteria membranes, and consequently a lower antibacterial activity. Nevertheless, such phenomenon was not observed for the ACNSs coatings where the spheres preserve the polymer motility regardless of the number of deposited layers. In this case the effect may be also assigned to the large surface area and improved cationic character of ACNSs when compared to ACsol.

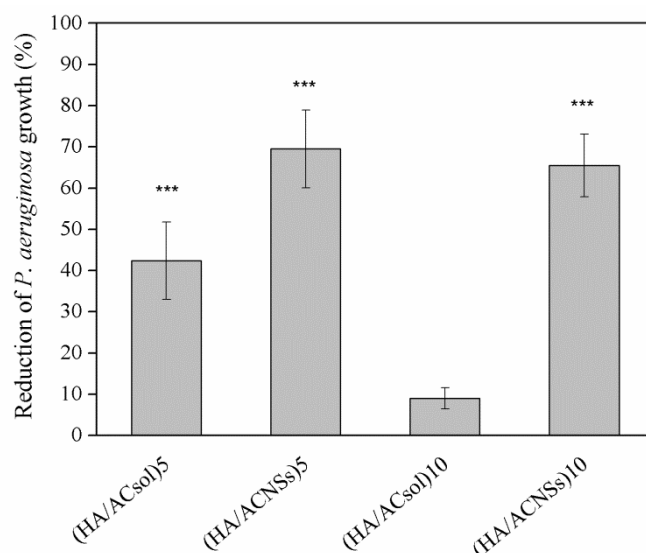


Figure 5.25 Antibacterial activity of silicone coated with HA/ACsol and HA/ACNSs against *P. aeruginosa* as compared to pristine silicone. Statistical differences are represented as ***p < 0.001.

Table 5.3 Antibacterial activity of silicone coated with HA/ACsol and HA/ACNSs against *P. aeruginosa*

	Sample	Number of colonies	Average number of colonies	Reduction of <i>P. aeruginosa</i> growth (%)
	Pristine silicone	59, 54, 57	56.7 ± 2.5	-
5-bilayer coating	(HA/ACsol) ₅	28, 39, 35	34	42.4 ± 9.4
	(HA/ACNSs) ₅	24, 13, 17	18	69.5 ± 9.4
10-bilayer coating	(HA/ACsol) ₁₀	54, 52, 55	53.7	9.0 ± 2.6
	(HA/ACNSs) ₁₀	25, 20, 16	20.3	65.5 ± 7.6

The integrity of the multilayer coatings after contact with *P. aeruginosa* was further evaluated in order to elucidate whether the antibacterial effect of the NSs was due to their release or they act from the surface. The incubation of (HA/ACNSs)₁₀ multilayer in *P. aeruginosa* suspension resulted in a partial collapse of the coating (Figure 5.26). After 6 h incubation the coating was still completely covering the silicone surface, although lower fluorescence indicate loss of upper layers of the structure. Further

incubation with the bacteria resulted in merely a partial silicone coverage. But even after 24 h the coating was found on the surface, revealing a gradual disintegration of the structure with the bacteria presence. The degradation was in contrast to the coating stability in water and the culture broth. The coating degradation by *P. aeruginosa* could be explained by the expressed hydrolytic activity and depolymerisation of the HA component. In such scenario, the antibacterial effect is a consequence of the release of the antibacterial ACsol and ACNSs upon triggered by bacteria degradation of the coating. Thus, the effective bacteria killing by (HA/ACsol)₁₀ and especially (HA/ACNSs)₁₀ coatings can be attributed to the locally high concentrations of polycationic antibacterials released. Release from the catheter coatings into a narrow space is relevant for urinary tract infections, where typically a small volume of urine surrounds the indwelling device surface. Even more important, a gradual collapse detected together with only a partial loss of the coating indicated a possible achieving of a days-long effect.

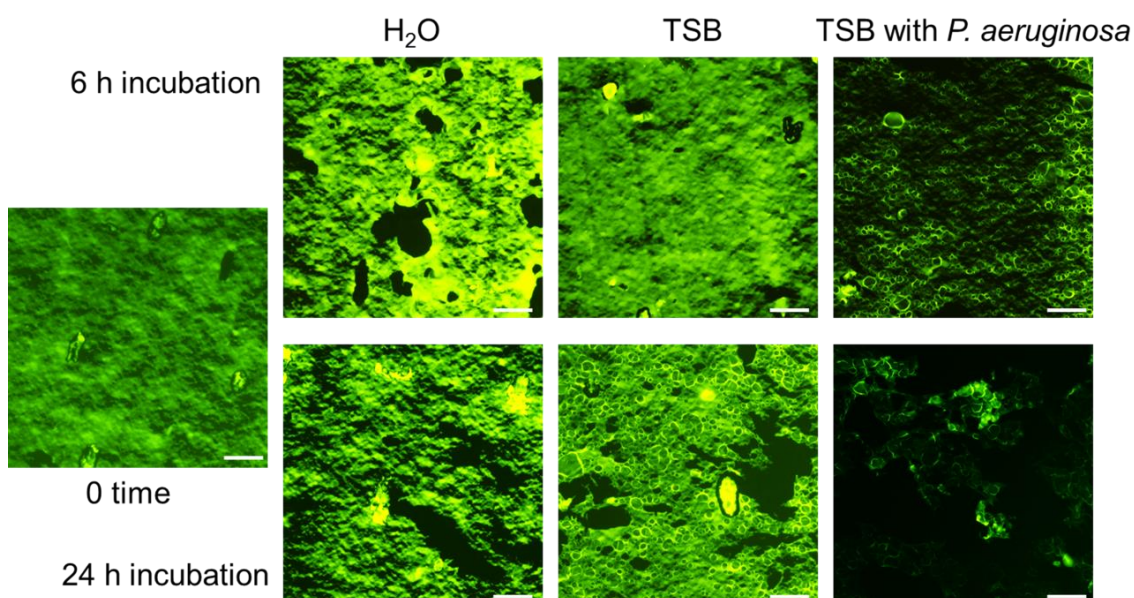


Figure 5.26 Fluorescence microscopy (20x magnification) of (HA/ACNSs)₁₀ coating incubated for 6 and 24 h in the absence and presence of *P. aeruginosa*. Scale bars 100 μ m.

5.3.4 Antibiofilm Properties of the Layered Assemblies

5.3.4.1 Under Static Conditions

The potential of HA/ACNSs and HA/ACsol coated silicones to prevent *P. aeruginosa* biofilm formation in static conditions was investigated using fluorescence microscopy.

Microscopy images after staining of live (green) and dead (red) bacteria attached to the surface showed that the bacteria develop well-established biofilms on the control material (untreated silicone), with several colonies merging into a continuous biofilm (Figure 5.27). The surfaces with deposited 5 bilayers were still colonised with bacteria, although the biofilm occurrence was considerably lower and represented with a smaller number of bacterial clusters. Despite the decrease in total biofilm growth for both ACNSs- and ACsol-based coatings, better antibiofilm effect was observed for the ACNSs coatings due to their stronger antibacterial effect. The *P. aeruginosa* cells were individually spread on the latter assemblies with limited number of aggregates that consisted mainly of dead cells (stained in red). Increasing number of layers brought about nearly total prevention of the biofilm formation, regardless of the shape of the AC polycation (free polymer vs. NSs): both 10 bilayers coatings showed higher biofilm inhibition efficiency compared to the 5 bilayer structures. Only few live bacteria were detected on (HA/ACsol)₁₀ coating, whereas the sporadic single cells on ACNSs-based surface were all dead. Nevertheless, it should be taken into account in this comparison that less material is deposited in the case of ACNSs (based on QCM-D and FTIR data), confirming that the embedded NSs also have stronger antibiofilm activity than the free AC macromolecules (deposited from solution). Interestingly, despite the negligible antibacterial effect observed for ACsol assemblies with 10 bilayer (less than 10 %, Figure 5.25), these coatings still effectively prevented the biofilm growth. Such observation could be explained with their relatively high hydrophilicity compared to the other multilayers (Figure 5.22). Hydrophobic interactions are suggested as one of the important factors promoting *P. aeruginosa* attachment and consequent biofilm development on silicone surfaces. This pathogen possesses a thin layer of glycoprotein covered by a thicker layer of lipoproteins and lipids that facilitate its interaction with hydrophobic surfaces such as silicone [346]. Thus, increased surface hydrophilicity is another way to prevent biofilm formation without affecting planktonic bacterial growth, as in the case of the (HA/ACsol)₁₀ coating.

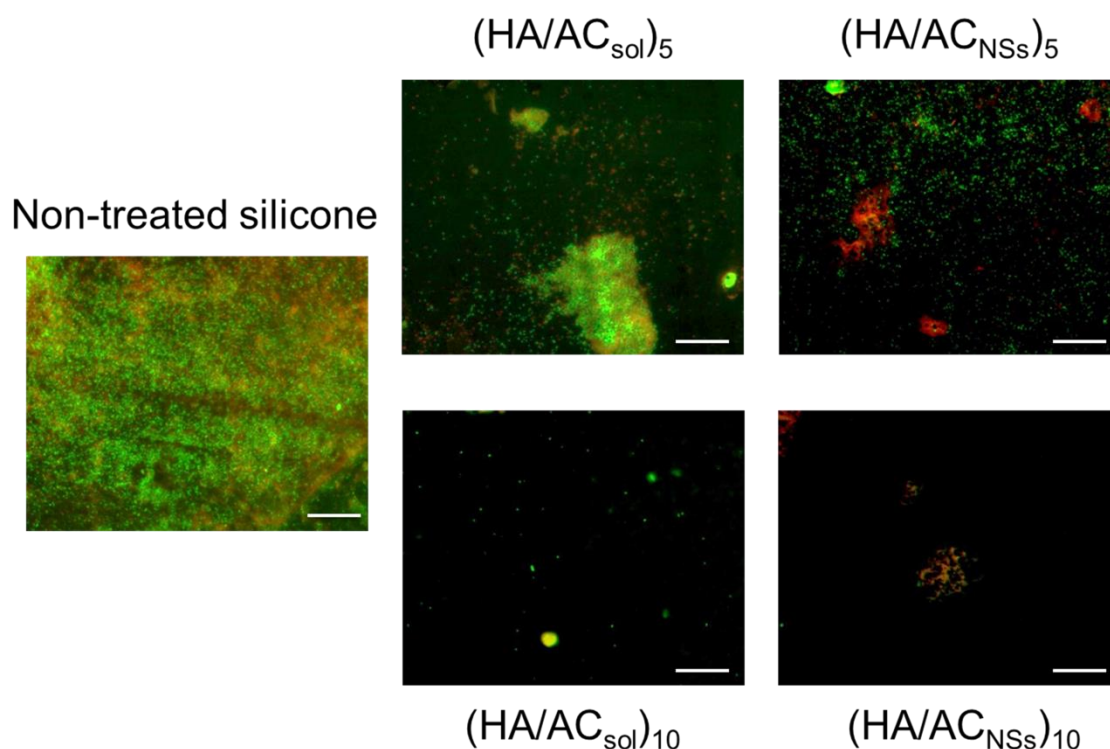


Figure 5.27 Fluorescence microscopy images (20x magnification) of *P. aeruginosa* biofilms on non-treated and silicone coated with HA/ACsol and HA/ACNSs, analysed after Live/Dead staining. Scale bars 100 μ m.

5.3.4.2 Under Dynamic Conditions – Catheterised Bladder Model

The biofilm inhibition capacity of urinary catheter coated with (HA/ACNSs)₁₀ was also assessed under dynamic conditions in an *in vitro* model of catheterized bladder (Section 4.3.2.7 Functional Characterisation of Catheters Coated With Antibiofilm Enzymes, *Dynamic Biofilm Inhibition Tests*). Prior to the assay, photos were taken of an untreated Foley catheter and the LbL-treated one. A clean surface is seen on the untreated catheter, whereas the immobilisation of ACNSs could be appreciated by a white colour on the catheter surface, typical for materials comprising this type of NSs (Figure 5.28, left side photo). Upon analysis, after 7 days in the catheterised bladder model, a bacterial biofilm is formed on the pristine catheter (especially visible on the catheter shaft), whereas the LbL-treated one was biofilm-free (Figure 5.28). Fluorescence images after staining of live and dead bacteria attached to the inner part of the catheter shaft confirmed the biofilm formation on the non-treated catheter and the absence of biofilm on the LbL-treated catheter (Figure 5.28). Unfortunately, the coatings were not as effective in inhibiting biofilm formation in the balloon section, although the effect is visible to a certain extent. Our investigation in catheterised

bladder model also suggested that the ACNSs-containing coating is effective in biofilm prevention on the commercially available Foley catheters, acting upon its degradation by *P. aeruginosa* and the consequent NSs release (the catheter displayed a clean surface after the incubation in the bladder model). The results obtained with the dynamic system showed the same tendency in inhibiting biofilm formation as in static conditions. These findings represent a proof-of-concept for antimicrobial effectiveness of the novel NSs-containing coatings evaluated during 7 days. Nevertheless, the stability, possible degradation and antibiofilm performance of the coatings over the time of use should be further considered for *in vivo* and evidence-based studies.

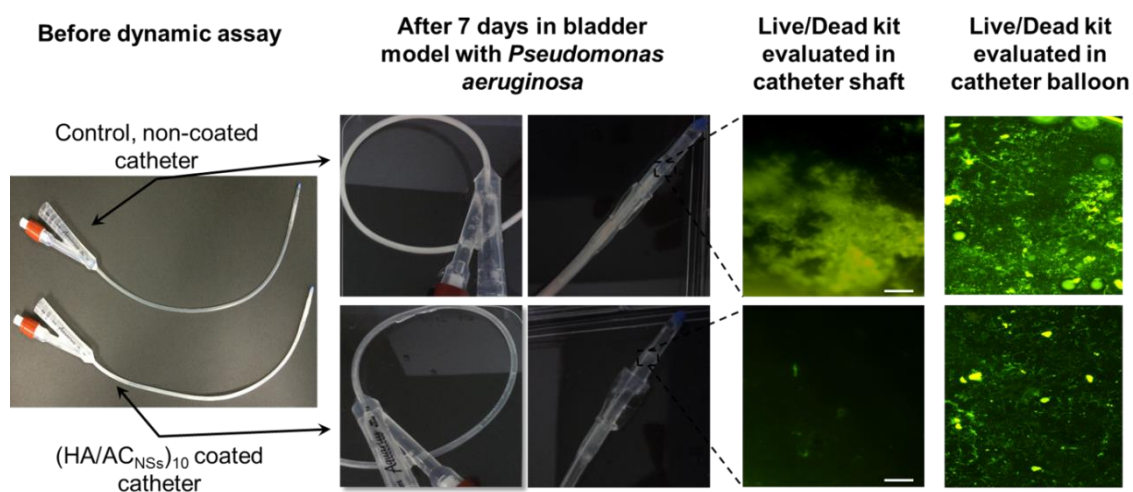


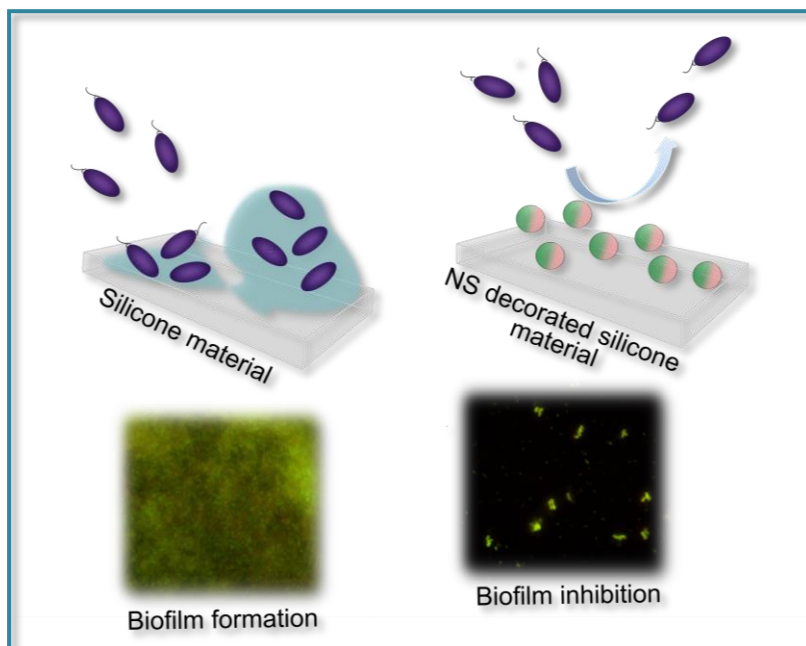
Figure 5.28 Photos and fluorescence microscopy images (20x magnification) of the shaft and balloon sections of untreated Foley catheter (top row) and catheter coated with (HA/ACNSs)₁₀ (bottom row) after a 7 day incubation in a dynamic bladder model system with *P. aeruginosa*. Scale bars 100 μ m.

5.3.5 Conclusions

In this study, cationic nanostructures were employed as powerful bactericides with great potential in suppressing biofilms. These were incorporated into catheter surface coatings in order to elicit their effect only in presence of pathogenic bacteria, e.g. upon release triggered by a certain stimuli, aiming to avoid unnecessary elution and rendering the coating inefficient. We demonstrated that the LbL deposition of HA and ACNSs resulted in inclusion of intact NSs within bacteria-responsive coating, as a key for effective prevention of bacterial biofilms. The coatings were non-eluting in physiological conditions, but gradually degraded in the presence of *P. aeruginosa* that causes most of the infections related to biofilm formation on urinary catheters. The responsiveness of the multilayers to the presence of bacteria leads to eradication of the biofilm upon release of the ACNSs. The antibiofilm properties were also demonstrated in a catheterised bladder model during seven days.

5.4 Covalent Grafting Of Aminocellulose Nanospheres onto Silicone Material

In this section, we used another strategy to impart silicone material with antibiofilm functionality against *E. coli*, a common Gram-negative pathogen related with UTIs. The approach is based on our previous findings that sonochemically processed ACNSs inhibit the growth and biofilm formation of *P.*



aeruginosa on urinary catheters when released in response to certain stimulus. Herein, we decorated silicone surface with epoxy functional groups for covalent immobilisation of ACNSs through the well-known epoxy-amine chemistry. The curing reactions of epoxy resins with aliphatic amines have been widely used for the development of coatings because they easily react at room temperature [147, 347-349]. The main goal of the study is to provide the proof of concept for permanent functionalisation of silicone-based material as an alternative strategy to counteract the *E. coli* attachment and avoid biofilm formation.

This section is based on the following publication:

Fernandes MM,^a Ivanova K,^a Francesko A, Mendonza E, Tzanov T. "Immobilization of antimicrobial core-shell nanospheres onto silicone for prevention of *Escherichia coli* biofilm", *Process Biochemistry*, 2016, 10.1016/j.procbio.2016.09.011.

5.4.1 Inhibition of *E. Coli* Biofilms – Proof of Concept

In order to obtain a silicone-based material with antibiofilm properties we developed a surface functionalised with ACNSs, previously shown to eradicate planktonic *E. coli* cells [147]. The use of ultrasound sonochemistry for the formation of ACNSs resulted in a stable dispersion with spheres of an average hydrodynamic diameter of 268 ± 7 nm, narrow size distribution and extremely high ζ -potential, $+103 \pm 2$ mV. Besides an extremely high stability, such high cationic charge was also found to be the main reason for the interaction with the negatively charged bacterial cell membrane and efficient bacterial eradication. This strategy presents other advantages in terms of overcoming the emergence of drug resistant strains. The NSs affect the membrane of bacteria, which is highly evolutionarily conserved and therefore unlikely to be changed by a single gene mutation. In fact, different macromolecules processed in the form of NSs and NPs were previously suggested as superior antibacterial agents against bacteria in both planktonic and biofilm forms because of their small size, high charge density and surface reactivity [350]. For that reason we also tested the ACNSs for their capacity to prevent biofilm formation and compared it with AC in solution (ACsol). The *E. coli* was grown on a polystyrene surface together with ACNSs or ACsol for 24h and then the biofilm formation was analysed. Characteristic biofilm structure of *E. coli* cells was observed when the biofilm grew in contact with ACsol, whereas few bacterial clusters were formed in the presence of bactericidal spheres (Figure 5.29B). The total biofilm mass decreased by up to 80 % in the presence of NSs, while almost no significant reduction was observed in the case of 0.5 mg/mL non-processed ACsol (Figure 5.29A). The spherical shape and large surface area of the ACNSs is believed to be the main reason for the prevention of bacterial biofilms.

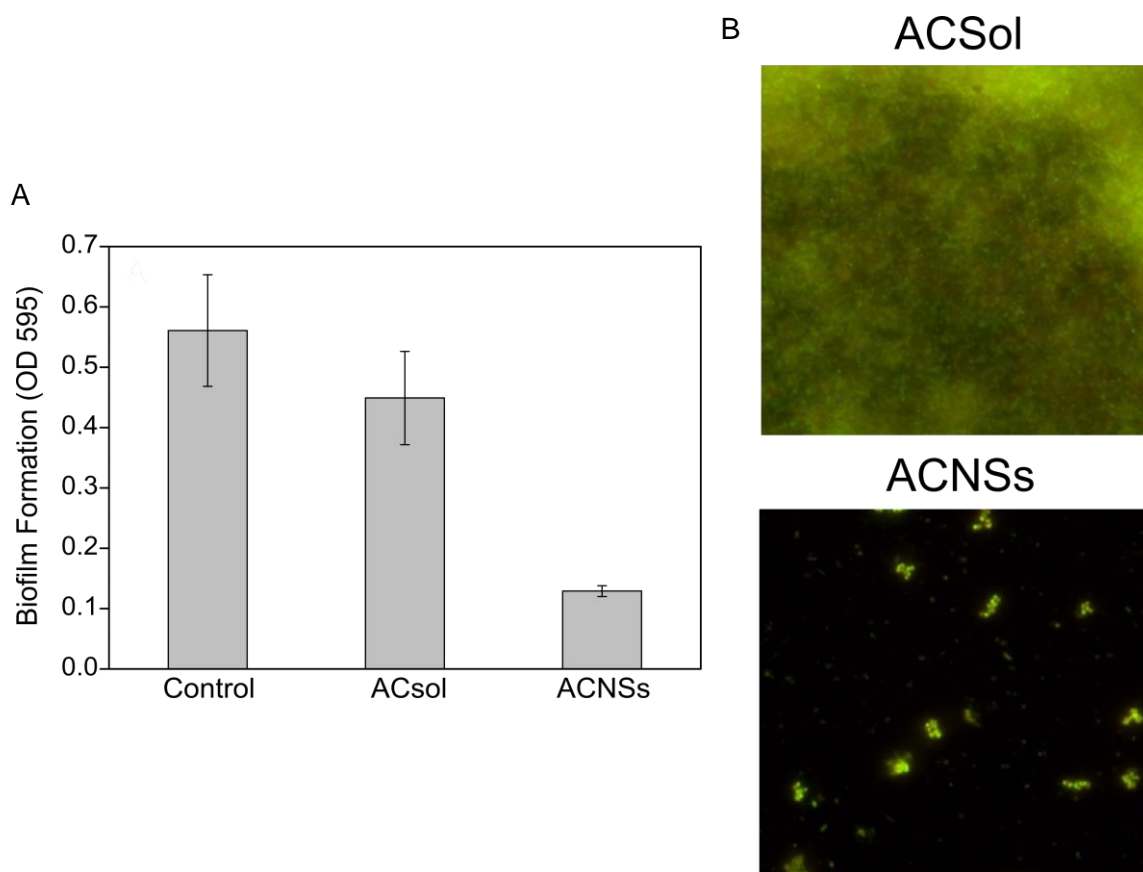


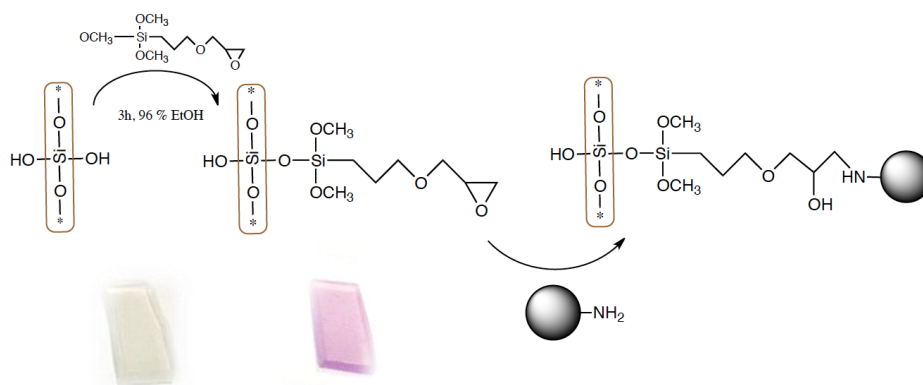
Figure 5.29 *E. coli* biofilm formation on polystyrene surface assessed by: A) crystal violet assay (the OD₅₉₅ is directly proportional to the amount of total biomass formed) and B) Live/dead cells viability kit (ACsol left and AC NS on the right). The green and red fluorescence are overlaid in for better comparison of live and dead cells. Scale bar indicate 100 μ m.

5.4.2 Incorporation of Cationic Nanospheres onto Silicone Material

This study further exploited the possibility for coating PDMS with the polycationic NSs in order to engineer novel antibiofilm surfaces. In the previous section we have proven the ability of these ACNSs within multilayer assemblies to impart antibiofilm and antibacterial functionalities onto the silicone/catheter surface. Herein, to develop biofilm resistant silicone material, the surface was initially functionalised with reactive epoxy groups that will interact with the amino bearing ACNSs.

Despite the fact that PDMS has been reported as an inert material for functionalisation, possessing scarcely distributed reactive hydroxyl groups on the surface, some authors have described a chemisorption phenomenon that allows for the formation of an oligomeric siloxane layer on the silicone surface. In this process both PDMS and GOPTS are hydrolysed in the presence of water, resulting in the generation of hydroxyl groups that further may interact via hydrogen bonding, leading to the

functionalisation of the PDMS with epoxy pendant groups (Scheme 5.1). Since the epoxy groups could not be identified by FTIR, the success of the used functionalisation strategy was confirmed by the development of characteristic pink colour after the interaction with p-NBP, a dye commonly used to spectrophotometrically identify the presence of epoxy groups [351].



Scheme 5.1 Strategy used to functionalise silicone material: chemisorption of GOPTS followed by the reaction of epoxy groups with ACNSs using the epoxy-amine curing method and evaluation of the colour of silicone after reaction with p-NBP to assess the efficiency of epoxy immobilisation.

The addition of epoxy functionalities provided a reactive site for further immobilisation of amino-containing compounds. This reaction occurs via a nucleophilic attack of the amine nitrogen on the terminal carbon of the epoxy function. The mechanism is a S_N^2 -type II, in which a primary amine can react twice with two epoxy group while a secondary amine can react only once [347, 349]. The amino groups from our AC biopolymer and within ACNSs are primary amines and thus able to react with the epoxy group on the functionalised surface through the active amine hydrogen (Scheme 5.1). The pre-functionalisation of silicone with epoxy groups was essential for the immobilisation of ACNSs. The infrared spectra of the epoxy-functionalised silicone treated with ACNSs, showed the characteristic for amine groups and the N-H stretching vibrations peaks at around 1650 cm^{-1} and 2900 cm^{-1} , suggesting that ACNSs were indeed present at the surface of silicone (Figure 5.30). Without the epoxy pre-treatment, the infrared spectra of the pristine and treated with ACNSs silicones are the same – no immobilisation of the biopolymer on the surface.

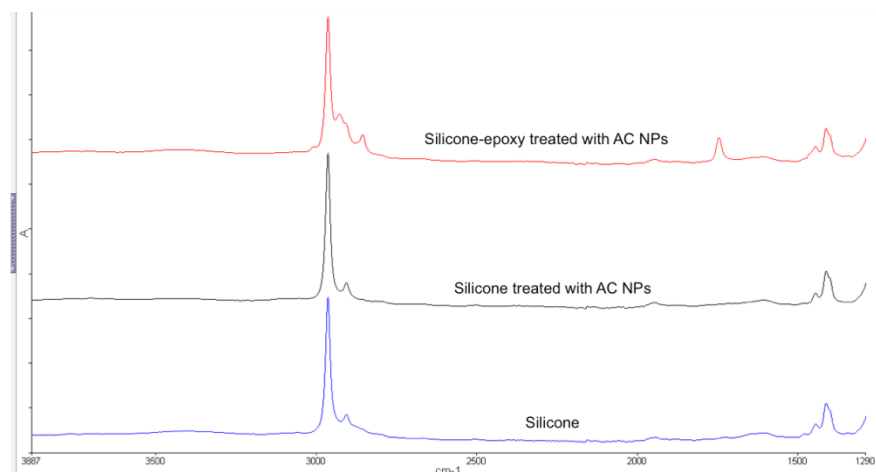


Figure 5.30 ATR-FTIR spectra of non-treated silicone (blue line), silicone (black line) epoxy silicone treated with ACNSs at pH 6 (red line).

Therefore, the epoxy-treated silicone was further functionalised with antimicrobial ACNSs previously dispersed in a solution at pH 3 and pH 6. These variations in pH were used to manipulate the properties of the amino groups of the spheres, namely: at pH 3 the amino groups are mainly protonated ($-\text{NH}_3^+$) and thus more reactive towards negatively charged surfaces, while at pH 6 the amino groups are more nucleophilic, which should favour the epoxy-amino curing reaction. SEM images have shown that the immobilisation of ACNSs was successful when both pHs were used, revealing the presence of intact spheres on the surface. The size of the spheres corresponds to the size measured in the dispersion. The bigger spheres that appear in the SEM images are air-filled microbubbles, shelled by oil-filled ACNSs (smaller spheres in the images). This pattern has been described to occur in sonochemically generated dispersions from polysaccharide conjugates (Figure 5.31) [352]. The immobilisation of intact nanostructures, e.g. core/shell NSs with a soft core, is advantageous, since the added value of processing polymers into nanostructures is transferred to the functional materials/surfaces. Important for our study observation is that considerably more NSs were fixed on the epoxy-treated silicone when the immobilisation reaction was performed at pH 6 because of the improved nucleophilicity of the amine groups at these conditions (Figure 5.31). For this reason, only the silicone treated with the spheres at pH 6 was used for further experiments.

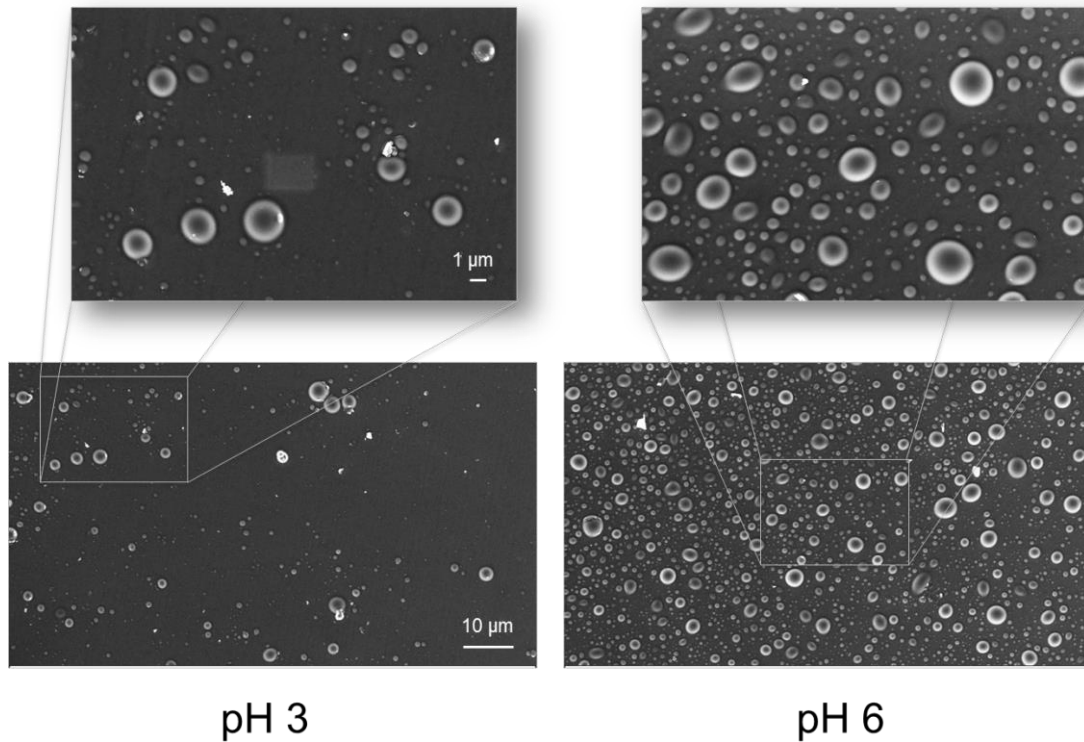


Figure 5.31 SEM images of ACNSs functionalised silicone surface at pH 3 and 6.

5.4.3 Functional Properties

The functionalised silicone surface was then tested for preventing *E. coli* biofilm formation. *E. coli* is one of the most frequently isolated microorganisms in catheter-associated UTIs [89]. It is a highly versatile bacterium ranging from harmless intestinal inhabitant to deadly pathogen, including common colonisers of medical devices, small intestine and the urethra [353]. On the surface of urinary catheters *E. coli* may establish biofilms and cause difficult to treat urogenital infections.

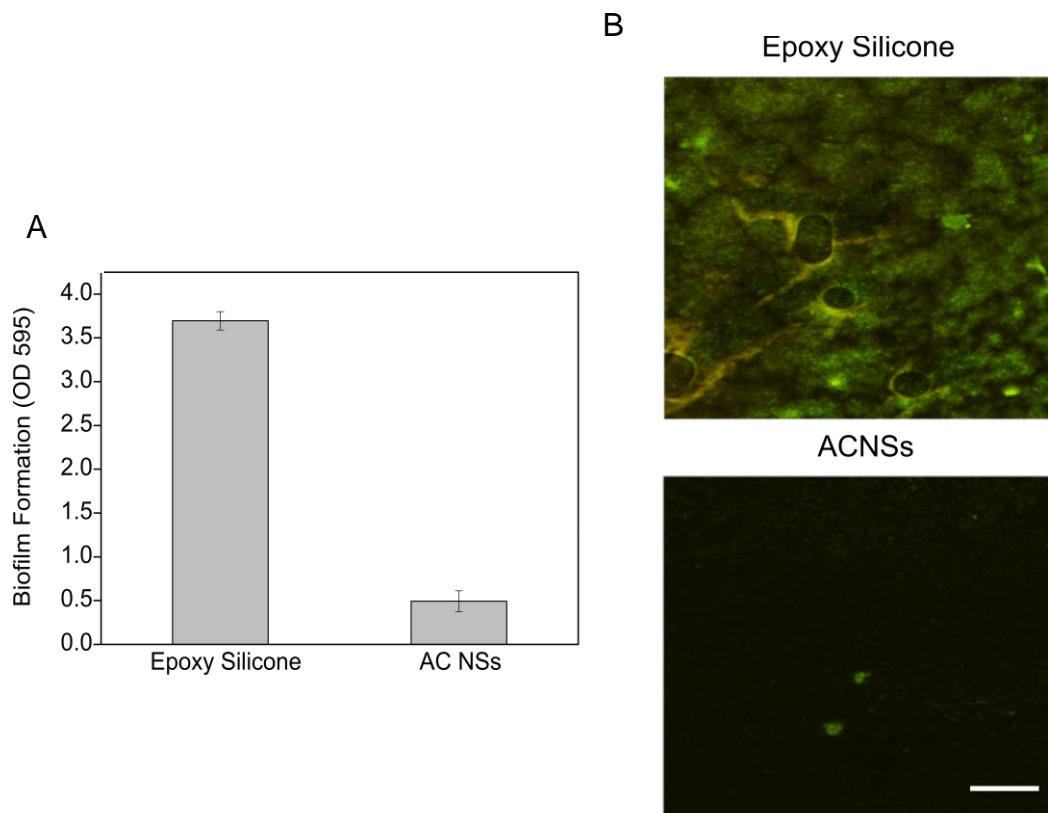


Figure 5.32 *E. coli* biofilm formation on epoxy-treated silicone decorated with ACNSs and unmodified silicone assessed by: A) crystal violet assay (the OD595 is directly proportional to the amount of total biomass formed) and B) Live/dead cells viability kit. The green and red fluorescence images are overlaid for better comparison of live and dead cells. Scale bar indicate 100 μm .

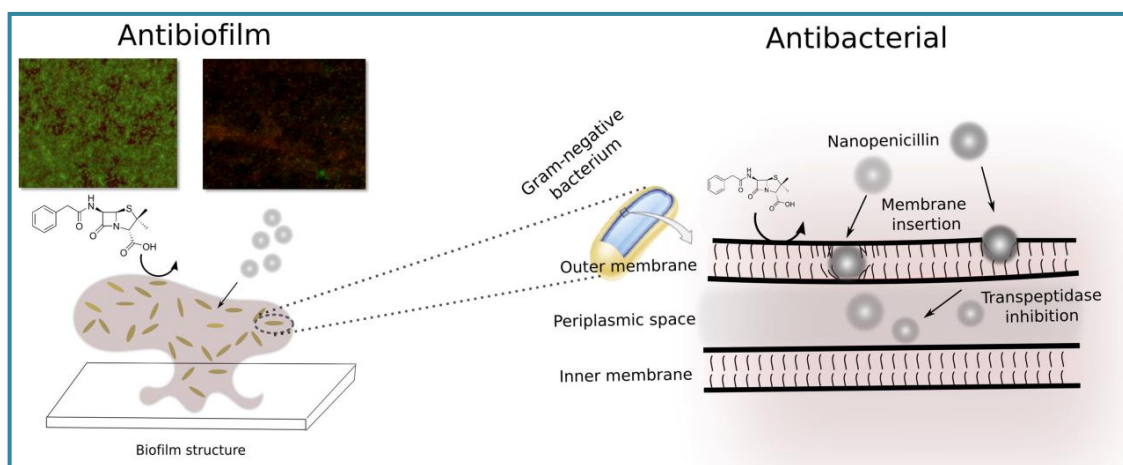
Since ACNSs were found to be efficient in preventing the *E. coli* biofilm growth on polystyrene surface, we assessed the ACNSs decorated silicone surface for their ability to prevent the biofilm growth. Similarly to the results shown above, the ACNSs on the surface of silicone were able to inhibit *E. coli* biofilm formation reducing the total mass of sessile bacteria up to 80 % when compared to the control epoxy treated silicone (Figure 5.32A). Furthermore, the fluorescence microscopy images after Live/Dead staining corroborated this finding and well-established biofilm of live (stained in green) and dead (stained in red) bacteria was visualised on the surface of the pristine silicone material. In contrast, the functionalisation with ACNSs resulted in significant reduction of drug resistant *E. coli* biofilm and only few cells individually spread on the surface were observed (Figure 5.32B). At that stage the individual cells are considered less virulent and even more susceptible to antibiotics at lower therapeutic dosages. Since the concentration of NSs used to immobilise the silicone surface was previously found to be innocuous towards fibroblasts cells [147], we believe the functionalisation

described herein may constitute an efficient approach to obtain a biocompatible and anti-biofilm surface for the prevention of *E. coli* associated infections and biofilms.

5.4.4 Conclusions

The inherent resistance of established biofilms to antibacterial drugs and their pervasive involvement in implant-related infections has prompted the search for surfaces/coatings that inhibit the initial stages of bacterial attachment, thus preventing or restricting the occurrence of biofilm formation. Herein, ACNSs were used to develop permanent antibiofilm coatings on silicone material. The NSs were grafted onto silicone surface using an epoxy/amine immobilisation reaction. The nanostructured surface was found to be efficient in preventing the *E. coli* biofilm growth. The sonochemically-induced nanospherisation of cationic biopolymer derivatives such as aminocellulose appears as a novel approach for improvement not only of their bactericidal activity towards free *E. coli* cells, but also their inhibition potential against biofilms. Further functionalisation of catheter surfaces with intact nanospheres may decrease the incidence of the *E. coli* biofilms and significantly reduce the urinary tract infections occurrence, increasing the usage time of the medical devices.

5.5 Nano-sized Penicillin G for Overcoming Gram- Negative Bacterial Resistance



In this section, we opted for altering the form and enhancing the interaction with the bacterial cell wall of an existing and already Food and Drug Administration approved antibiotic, e.g. penicillin G, as a facile method to create a broad-spectrum antibiotic, rather than undertaking a time- and resource-consuming screening for new drug entities. The strategy we propose would shorten the drug development process, because it does not alter the drug target, but simply adds a supporting mechanism to the main activity of penicillin G. Moreover, mostly Gram-positive spectrum agents are currently in clinical trials [354], while the hereby produced nano-size antibiotic will extend its activity also to Gram-negative species, relying on a mechanism of action that comprises additionally bacterial membrane disturbance and easy penetration into biofilms.

This section is based on the following publication:

Fernandes MM, **Ivanova K**, Francesko A, Rivera D, Torrent-Burgués J, Gedanken A, Mendonza E, Tzanov T. "Escherichia coli and Pseudomonas aeruginosa Eradication by Nano-Penicillin G", *Nanomedicine*, 2016, S1549-9634(16)30065-X. doi: 10.1016/j.nano.2016.05.018

5.5.1 Antibacterial Activity of Penicillin G towards Gram-negative Bacteria

Penicillin G is a beta-lactam antibiotic mainly used in the treatment of bacterial infections caused by Gram-positive organisms. The four-membered β -lactam ring binds and inhibits the transpeptidase enzymes involved in the synthesis of the peptidoglycan layer and hinder the synthesis of bacterial cell wall. An imbalance between cell wall production and degradation is thus created, leading to cell death [355]. Transpeptidases are located in the periplasmic space, which is easily accessible by antibiotics in Gram-positive bacteria [356]. In Gram-negative bacteria, β -lactams have to cross the outer membrane of bacteria either by passive diffusion or via porin channels. However, bacteria were able to create a resistance mechanism in which a permeability barrier to the antibiotic by porins modification, which explains the poor effect of penicillin against these pathogens [357, 358].

In fact, Gram-negative bacterial strains such as *E. coli* and *P. aeruginosa* used in this work were not susceptible to the action of the Penicillin G while the growth of Gram-positive *S. aureus* was completely inhibited at concentrations above 15 $\mu\text{g/mL}$ ($\text{O.D.}_{600} \approx 0$) (Figure 5.33). In order to extend the activity spectrum of penicillin G also to Gram-negative bacteria, a sonochemical nanospherization of the free antibiotic was carried out. This method has already been applied to boost the antibacterial activity of biopolymers such as aminocellulose and thiolated chitosan [147].

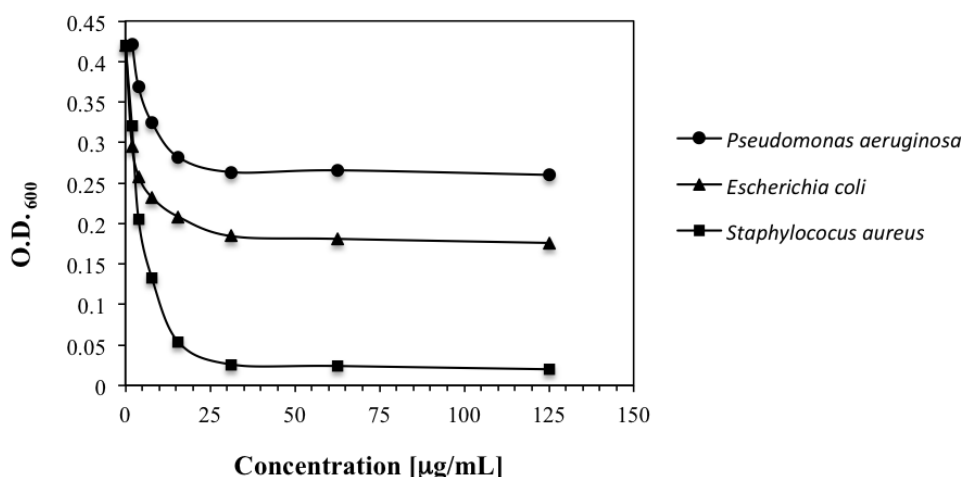


Figure 5.33 *P. aeruginosa*, *E. coli* and *S. aureus* growth after 24 h incubation with Penicillin G.

5.5.2 Penicillin Nanospheres Preparation and Characterisation

The use of nanotechnology to overcome bacteria resistance to β -lactams appears to hold significant promise as different biological modes of action towards cells are created. In fact, the nano-transformation has been considered as a novel tool to boost the antibacterial activity of materials. One common example is silver, which once transformed into NPs acquires a high antimicrobial activity due to the large surface area of the NPs and better contact with the microorganisms [359]. In this work, we sonochemically transformed the penicillin G into NSs as a novel tool for overcoming resistance in Gram-negative bacteria, aiming the improved interactions and penetration of the NSs with the bacterial membrane. The generation of penicillin nanoparticles using ultrasound has also been reported by Yariv *et al.* (although in absence of an organic phase or surfactant), as a way of enhancing the antimicrobial activity against a *S. aureus* clinical isolate [280]. However, the reported penicillin NPs did not kill Gram-negative bacteria. Herein, we obtained nano-sized, oil-filled, surfactant-containing spheres able to efficiently interact with the membrane of Gram-negative bacteria. The generated nanomaterials were spherical in shape (Figure 5.34B) with a mean size of 192 ± 6 nm, a polydispersity of 0.12 ± 0.04 (Figure 5.34FA) and a zeta potential of -12.8 ± 1.2 mV. Despite the relatively low zeta-potential (< -20 mV) the NSs were stable in aqueous solution for more than 6 months, i.e. did not aggregate in solution, related to the presence of poloxamer. Poloxamer is hydrophilic surfactant, comprised of polyethylene oxide (PEO) and polypropylene oxide (PPO), which is able to induce steric stabilization of the spheres. The hydrophobic PPO chains adsorb on the particle surfaces as the “anchor chain”, while the hydrophilic PEO chains pull out from the surface to the aqueous medium, producing a stabilizer layer [360]. This effect shifts the plane of shear to a farther distance from the particle surface thus reducing the measured zeta potential [361]. Poloxamers have been frequently applied for stabilisation of NPs, regardless of the method used for their synthesis. Pezeshki *et al.* have synthesized nanostructured lipid carriers with similar size as the one obtained in this study using 6 % Poloxamer while we used only 0.1 % (w/v) [360]. Vineeth *et al.* also suggested that not only the surfactant influences the size of particle, but also the choice of the organic solvent [362]. However, most of the organic solvents used in the cited studies are considered cytotoxic, while our NSs encapsulate edible sunflower oil as an organic phase in order to avoid harmful effects in humans. Besides poloxamers, other anionic, cationic and/or amphoteric surfactants have also been reported to efficiently stabilise nanoparticulate systems. The choice of the best surfactant for each formulation depends on the final application and several factors such as the type of stabilisation

required (electrostatic versus steric stabilisation) and the route of administration (for example, steric stabilisation is recommended because it is less susceptible to electrolytes in the gut or blood). Several studies have been carried out to determine the effect of different surfactants and organic solvents in nanoemulsions [363-366].

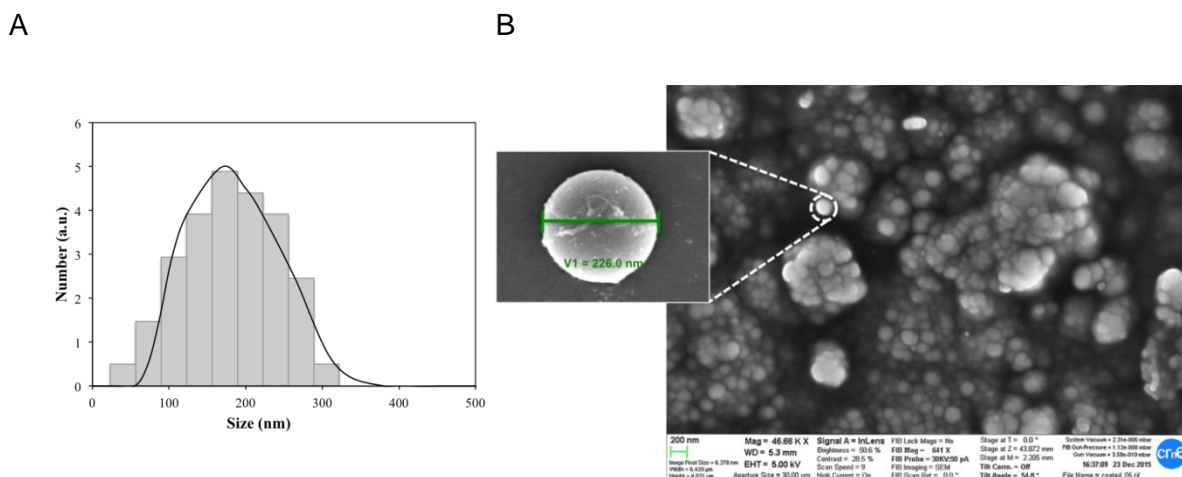


Figure 5.34 A) Dynamic light scattering, and B) scanning electron microscopy images of nanopenicillin.

The nano transformation of penicillin G induced some changes on the chemical structure of the antibiotic, confirmed by infrared spectroscopy. The most noticeable ones were the disappearance of the β -lactam carbonyl group band at 1790 cm^{-1} and the increase of the broad band at 3500 cm^{-1} , which corresponds to the -OH group from the carboxylic group ($-\text{CO}_2\text{H}$) due to the hydrogen bonding effect (Figure 5.35). The sonochemical-induced formation of nanopenicillin was accompanied by the creation of a hydrogen bond network between the hydroxyl group and the β -lactam carbonyl that contributed for the stabilization of the NSs. This effect has already been observed when tetracycline was formulated into NPs using the same sonochemical method [238]. Nevertheless, the peaks assigned to penicillin found at 1600 cm^{-1} and corresponding to amide I band were not significantly changed, suggesting that no major changes were induced in the structure of Penicillin G upon spherization. The remaining peaks were assigned to the surfactant and oil as could be seen in their spectra. On the other hand, the IR spectra of control NSs presented a combination of the surfactant, oil and hydrogen bonding peaks. The hydrogen bonding is present either in the spectra of nanopenicillin and control NSs, suggesting their important role in the formation of the spheres (Figure 5.35).

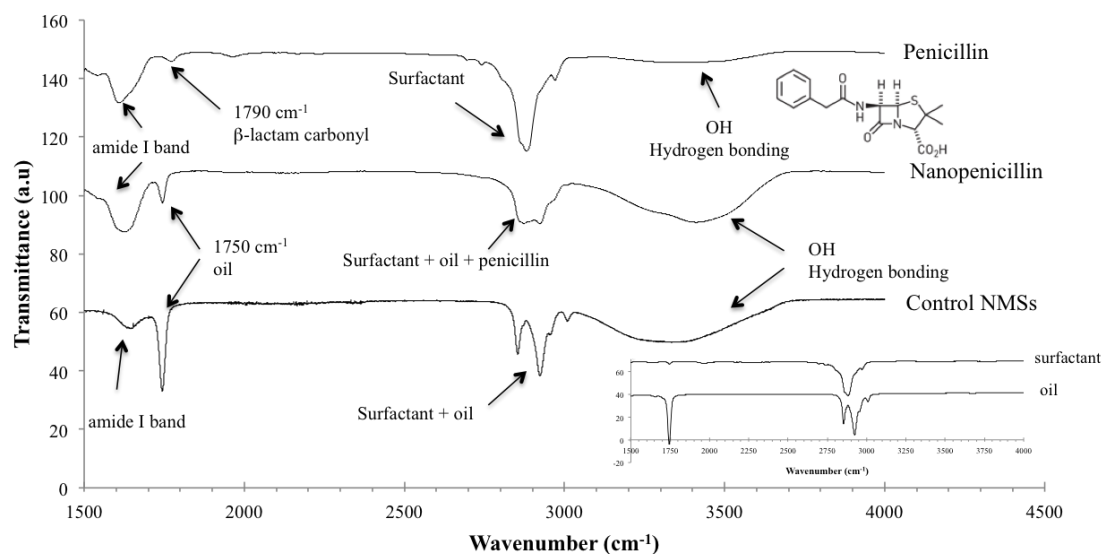


Figure 5.35 FTIR spectra of lyophilized penicillin, nanopenicillin, surfactant (poloxamer) and oil.

5.5.3 Antibacterial and Antibiofilm Activities

Penicillin and nanopenicillin were further evaluated for their antibacterial and antibiofilm activity against the Gram-negative *P. aeruginosa* and *E. coli*. Control NSs, i.e. spheres without penicillin comprised solely of surfactant and oil, were also produced in order to determine both the effect of the surfactant and the effect of the particle spherical shape on the interaction with planktonic bacteria and their biofilms.

Penicillin in solution, tested at the same concentration and under the same assay conditions, was less effective in killing both Gram-negative bacteria than nanopenicillin. The last induced a 3 log₁₀ reduction of *P. aeruginosa* and 1.2 log₁₀ reduction of *E. coli* while the penicillin in solution induced less than 0.3 log₁₀ reduction of both microorganisms (Figure 5.36). An improvement of 10- and 4-fold, respectively, in the inhibition of these planktonic Gram-negative bacteria was achieved.

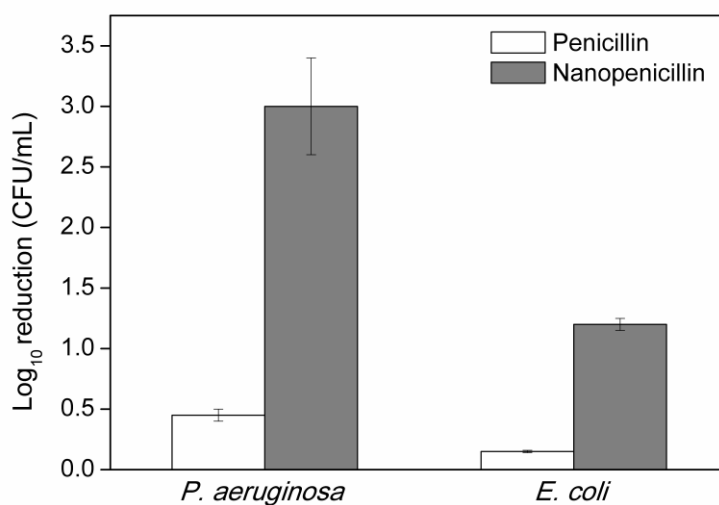


Figure 5.36 Antimicrobial activity of 125 µg/mL penicillin and nanopenicillin on *E. coli* and *P. aeruginosa* after 24 h contact.

The effect of the nanopenicillin on biofilms was also evaluated. A decrease of the total biomass was observed under fluorescence microscopy after Live/Dead staining when either penicillin or nanopenicillin was applied (concentration of 125 µg/mL) on previously formed and well-established biofilms (Control in Figure 5.37). Nevertheless, the effect was more pronounced when nanopenicillin was applied (Figure 5.37) and in the case of *P. aeruginosa*, red cells could also be observed which is indicative of a killing effect. The control NSs, on the other hand, did not produce a decrease on the biomass neither a killing effect, confirming that NSs lacking the antibiotic were not able to penetrate and prevent biofilm formation.

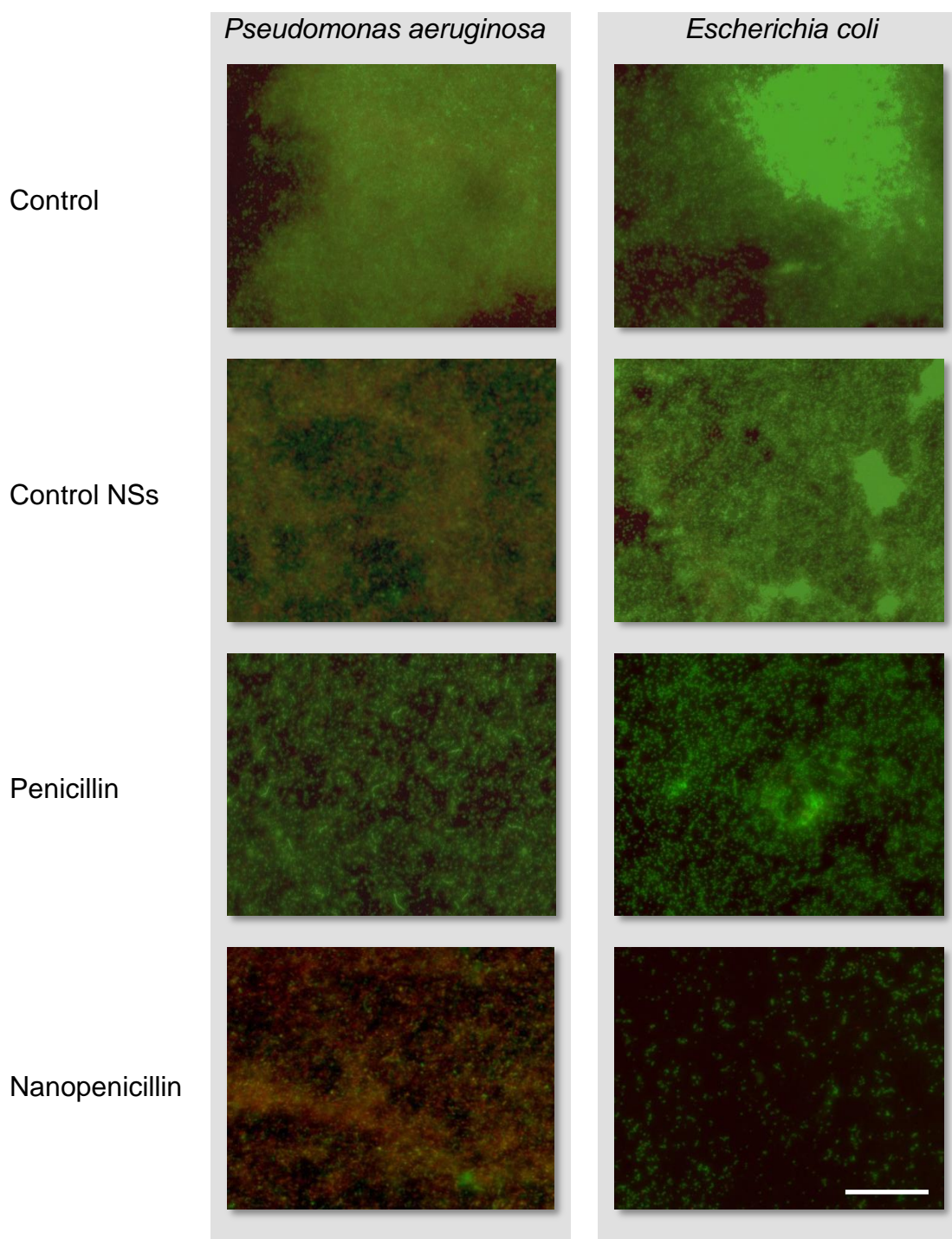


Figure 5.37 Fluorescence microscopy live/dead images of 24 h grown *P. aeruginosa* and *E. coli* biofilms incubated with 125 µg/mL penicillin, nanopenicillin and control NSs (live cells are represented in green and dead cells in red). Scale bars denote 100 micron.

To sustain these results, the quantification of viable microorganisms within the biofilms after application of the antimicrobial agents was also performed using the MBEC™ HTP assay. This technique allows microorganisms to grow on 96 identical pegs protruding down from a plastic lid to form a biofilm. Treating the established

biofilm with the antimicrobial compounds and further quantification of the survived bacteria assess the therapeutic potential of the NSs. Nanopenicillin was also able to kill more bacteria within *P. aeruginosa* and *E. coli* biofilms than Penicillin G. *P. aeruginosa* was more susceptible to the action of nanopenicillin being reduced in 2.5 log₁₀ while less effect was observed for *E. coli* biofilms, in which a 1.65 log₁₀ reduction was detected. Penicillin in solution was not effective against *P. aeruginosa* but it was able to induce a 0.8 log₁₀ reduction of *E. coli* in biofilms, corroborating the results found by fluorescence microscopy and antibacterial assays (Table 5.4).

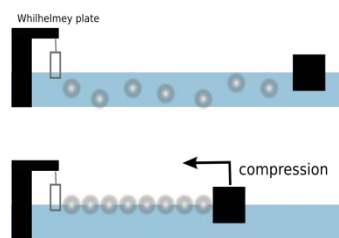
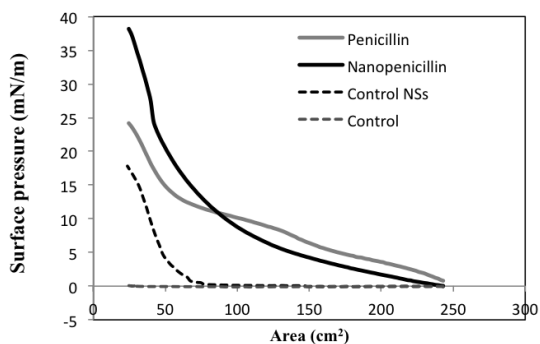
Table 5.4 Viable cells within *P. aeruginosa* and *E. coli* biofilms before (control) and after applying 125 µg/mL of penicillin, nanopenicillin and control NSs.

	Log ₁₀ of CFU/mL	
	<i>Escherichia coli</i>	<i>Pseudomonas aeruginosa</i>
Control	6.60 ± 1.2	7.52 ± 1.5
Control NSs	6.70 ± 0.9	7.50 ± 1.1
Penicillin	5.78 ± 1.7	7.51 ± 0.9
Nanopenicillin	4.95 ± 0.9	5.26 ± 1.6

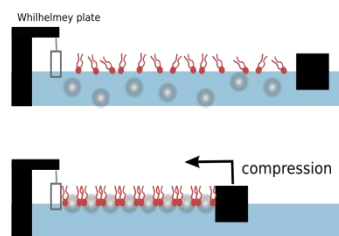
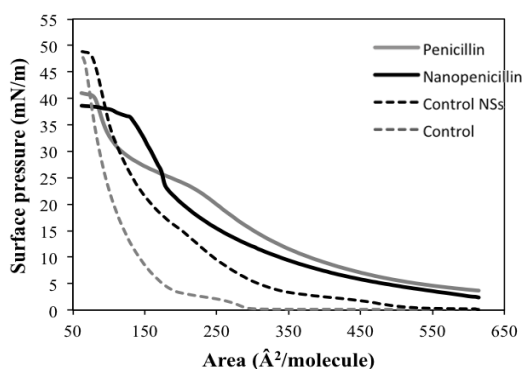
5.5.4 Interaction with Bacterial Cell Membrane

To understand the mechanism of action of the developed NSs, a Langmuir monolayer technique, used for mimicking bacterial membranes, was applied. This technique is commonly used as a supportive model to explain the interactions between different molecules and nanoparticulate systems with bacterial membranes even without considering the other constituents of the bacterial membrane. In a first assessment, both penicillin in solution and nanopenicillin were found to be surface active when analysed by Langmuir technique in the absence of phospholipid upon compression (Figure 5.38A). The movement of the spheres to the air-water interface indicated that they might be capable to interact with a membrane model and possibly with a bacterial membrane (Figure 5.38A right panel).

A



B



C

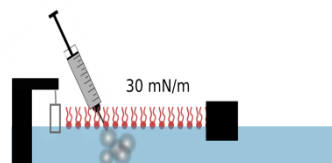
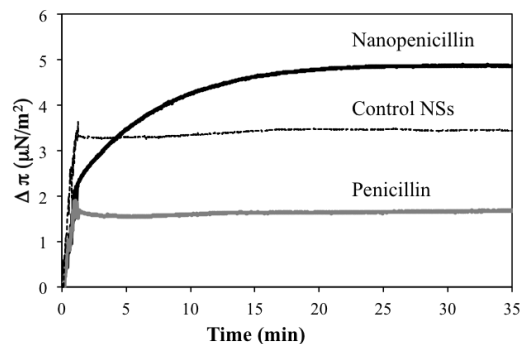


Figure 5.38 A) Surface pressure-area isotherms (or surface activity) and schematic representation of the nanospheres surface activity upon Langmuir compression; B) Surface pressure-area isotherm of *E. coli* PE monolayer (the area per molecule in X-axis refers to *E. coli* PE) in water with 0.5 µg/mL penicillin in solution, nanopenicillin and control NSs and schematic representation of the NSs interaction with the a Langmuir monolayer upon compression; and C) kinetic adsorption process resulting from the incorporation of 0.2 µg/mL (final concentration) penicillin, nanopenicillin and control NSs onto the air/water interface of *E. coli* PE monolayer at a surface pressure of 30 mN/m and schematic representation of the incorporation of the spheres in the subphase beneath the phospholipid monolayer built at 30 mN/m.

To prove this concept, the interaction and internalisation of nanopenicillin and penicillin in solution with a membrane model comprised of PE, the principal phospholipid extracted from *E. coli* was studied [367]. This technique has been commonly applied in our group to elucidate the interactions of antimicrobial agents with bacterial cell membranes at a molecular level, thus indirectly assessing their antimicrobial potential [147, 368]. The isotherms of *E. coli* PE with only water in the subphase presented a lift-off at molecular areas of around 300 Å²/molecule, while the others lifted-off at significantly higher molecular areas indicating a membrane disturbing effect (Figure 5.38). In fact, the same concentration of penicillin and nanopenicillin were able to efficiently interact with the PE membrane of *E. coli*, although at different extent, inducing a significant expansion of the monolayer at large areas per molecule of phospholipid (Figure 5.38B). This is mainly due to the penetration of the spheres and penicillin molecules within the monolayer when the molecules of phospholipids are not highly compressed as depicted in the right panel of Figure 5.38B (upper image). Regarding the control NSs, despite the fact that the effect was not as pronounced as the one observed for penicillin and nanopenicillin, a disturbing effect on the membrane model was also detected, indicating that the spherical shape and the surfactant indeed play an important role in the interaction with the membrane model.

After compression, at lower phospholipid molecular areas, the isotherm of the control NSs merged with the isotherm of the pure monolayer (water in the subphase), which means that these spheres were expelled from the monolayer after full Langmuir compression, indicating that they produce an insignificant effect on the established compressed monolayer [369]. Nevertheless, this did not occur with penicillin and especially with nanopenicillin, as the isotherms collapsed before reaching the monolayer highly compressed stage, demonstrating that even at smaller areas per phospholipid the nanopenicillin is inserted in between the phospholipid molecules, as depicted in the right panel of Figure 5.38B. This effect is called penetration and occurs when the compounds present in the subphase emerge to the air-water interface and penetrates in between the phospholipid molecules [369]. Moreover, by determining the maximum compression modulus of the isotherms it could be observed that they all experienced a unique phase transition, from gaseous to liquid-expanded state, represented by the $C_s^{-1},_{max}$ around 50 mN/m (Table 5.5). The inability of the monolayer to reach a condensed state, commonly represented by higher values of compression modulus (C_s^{-1}), is due to the fact that the *E. coli* PE phospholipid is a non-pure compound that impedes the monolayer to organise into a more packed structure. The presence of nanopenicillin, in particular, induced a significant increase of the

monolayer fluidity, lowering the $C_{s, \max}^{-1}$ value, corroborating the observed monolayer disturbing effect of the spheres (Table 5.5).

Table 5.5 Maximum compression modulus of *E. coli* PE monolayers with water, penicillin, nanopenicillin and control NSs in the subphase.

<i>E. coli</i> PE		
Sample	$C_{s, \max}^{-1}$ (mN/m)	Phase transitions
Control (H₂O)	55.8	Gaseous-liquid expanded
Penicillin	51.9	Gaseous-liquid expanded
Nanopenicillin	26.7	Gaseous-liquid expanded
Control NSs	48.1	Gaseous-liquid expanded

By analysing the behaviour of the isotherms on Figure 5.38B at a fixed surface pressure of 30 mN/m, which corresponds to the lateral pressure of naturally occurring cell membrane, we could also infer about how these spheres interact with the bacterial membrane [300, 370]. We observed that at this surface pressure, nanopenicillin highly increased the expansion (membrane fluidity) of the monolayer as one molecule of phospholipid occupied ≈ 190 Å (see straight line on Figure 5.38B). On the other hand, the phospholipid molecules only occupied ≈ 120 Å when either penicillin in solution or the control NSs were present in the subphase. These results demonstrated that by engineering penicillin into NSs we are indeed able to improve the interaction of penicillin with a bacterial membrane.

To further elucidate this behaviour, all tested compounds were also injected into the subphase beneath the *E. coli* PE monolayer, previously formed at 30 mN/m, and the variation in the surface tension of the monolayer was monitored as a function of time (Figure 5.38C). Nanopenicillin efficiently penetrated the membrane model, indicated by the higher increase of the surface tension in comparison to the penicillin molecules and control NSs inserted in the subphase. Nevertheless, the control NSs also induced a significant increase on the surface tension indicating that the spherical shape and nanosize play an important role in the interaction and penetration of nanopenicillin into the bacterial membrane (Figure 5.38C). The presence of the surfactant together with penicillin in the spheres played a key role on the interaction with the bacterial membrane, as suggested by the insertion capacity of the control NSs (solely comprised of surfactant) on the Langmuir monolayer. Indeed, surfactants such as poloxamer have been reported to be biomembrane active due to their relative ratio of hydrophobic versus hydrophilic building blocks [371].

Mainly cationic NPs have been reported to efficiently kill bacteria by disrupting the cell membrane due to electrostatic interaction between the positively charged particles and the negatively charge bacterial membrane, leading to cell leakage and death - an effect that we have already observed for other cationic NSs [147]. The herein generated NSs possessed negatively charged properties and it was therefore expected that they would not affect significantly the bacterial membrane. Nevertheless, these particles were surface active and able to penetrate the membrane model, providing the boosting effect compared to Penicillin G in solution for killing Gram-negative bacteria. In fact, negatively charged particles have been reported to efficiently penetrate the cells, without disrupting the membrane, through nonspecific binding and clustering of the particles on the cationic sites of the membrane followed by internalization via endocytosis [372].

5.5.5 Cytotoxicity with Mammalian Cells

Since NPs and nanomaterials become highly active at nanometre scale, illustrated here by the enhanced bactericidal capacity of nanopenicillin, nanotoxicology studies should be performed to determine whether these properties might pose a threat to humans. We used skin fibroblasts as a model for human cells and analysed the cytotoxicity of nanopenicillin and penicillin at the antimicrobial-effective concentrations. Nanopenicillin was cytotoxic at concentration of 250 $\mu\text{g}/\text{mL}$, but at the antibacterial-effective concentration of 125 $\mu\text{g}/\text{mL}$ the antibiotic NSs were fully biocompatible (Figure 5.39).

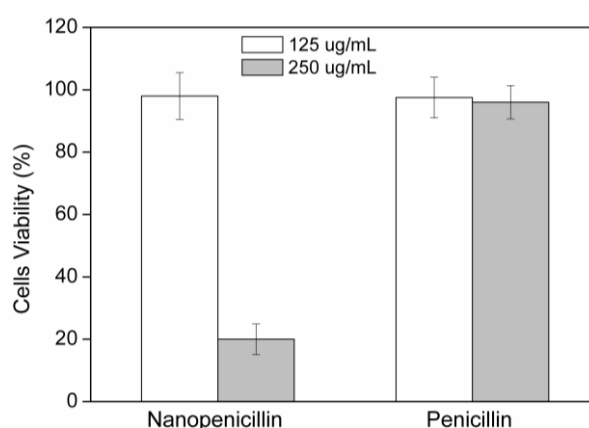


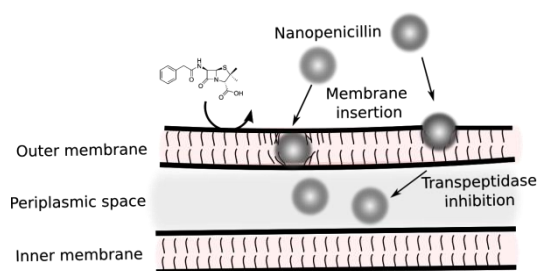
Figure 5.39 Relative viabilities (%) of human fibroblasts exposed to 250 $\mu\text{g}/\text{mL}$ and 125 $\mu\text{g}/\text{mL}$ penicillin and nanopenicillin for 24 h.

5.5.6 Conclusions

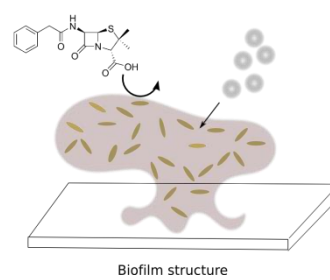
The results obtained from Langmuir monolayer studies suggested that by engineering penicillin G into NSs the interaction and penetration of otherwise less penetrable antibiotic molecules into the bacterial membrane is favoured. Since the resistance of Gram-negative bacteria to β -lactams is mainly due to the incapability of the penicillin molecules to penetrate the outer membrane and inhibit the transpeptidases in the periplasmic space, it is expected that nanopenicillin, in contrast, would be able to insert into the membrane and overcome this antibacterial-resistance mechanism (Scheme 5.2A). Combining NPs with antibiotics has already been proved to generate a synergy against bacterial resistance by reducing the toxicity of both agents towards human cells due to the decrease on the requirement for high dosages, but also to enhance their bactericidal properties [373]. Herein, the same enhanced killing effect was observed, however, in our case the antibiotic itself was formulated into the nanoform, instead of being encapsulated or combined with other particles, thereby combining both bactericidal and nanoscale effects.

The spherical shape and large surface area of the antibiotic NSs was further designated as the main reason for the successful eradication of bacterial biofilm by penetrating them more easily than the Penicillin G in solution and by providing better contact with microorganisms encased, thus allowing the eradication of Gram-negative biofilms and even induce a killing effect, mainly on *P. aeruginosa* (Scheme 5.2B). Treating biofilm infections remains a major challenge due to the fact that high doses of antimicrobial agents are required. It has also been reported that by packing the antibiotic into NPs increased killing of biofilm-encased bacteria could be achieved compared to the free antibiotic due to the protection effect that the NPs provide against enzymatic degradation of the antibiotic and its binding to matrix components. The nanoscale formulation of antibiotics could constitute a powerful tool for the treatment of antibiotic-resistant Gram-negative bacteria, which is particularly important due to the fact that this highly prevalent opportunistic pathogen is one of the most worrisome bacteria in clinical settings owing to its low antibiotic susceptibility, especially in the form of biofilms.

A



B



Scheme 5.2 Schematic representation of the interaction of nanopenicillin and penicillin G onto: A) the gram-negative bacterial cell wall and B) the biofilm structure.

6 Conclusions and Future Plans

6.1 Final conclusions

The accelerated emergence of drug resistant bacterial strains and their ability to form biofilms are one of the most serious problems of the modern medicine and the difficulties in finding cost-effective alternatives make it even more challenging. However, since the pathogenesis of implant-associated infections has become more clearly elucidated, the therapies and the biomaterials used to mitigate disease severity have also evolved. Approaches based on enzymes or antibacterial nanomaterials have been extensively investigated for the control of medically relevant biofilms, mainly because they offer the promise to decrease the need for high drug dosages and limit the acquisition and spread of resistance in bacteria. Based on the above, a platform of antibacterial and anti-biofilm nanomaterials and coatings was developed using:

A. Enzymatic approaches targeting the inhibition of biofilm establishment rather than killing the free floating bacterial cells. These comprise:

- QS inhibiting acylase in multilayer nanocoatings
 - QQ acylase within multilayers breaks down the QS signals in the surrounding imposing less selective pressure on the bacterial population for resistance occurrence. The pathogenic cells could not establish drug resistant biofilms on the silicone, therefore would be more susceptible to host immune defence and antibiotics.
 - Acylase multilayers were stable for seven days under conditions that mimic the real situation during catheterisation and significantly delayed the QS regulated biofilm formation of Gram-negative *P. aeruginosa*, without affecting the viability of human fibroblasts.
- QQ and matrix-degrading enzymes in hybrid LbL assemblies
 - QQ acylase and matrix-degrading amylase were assembled into stable and biocompatible hybrid multilayer coating able to interfere with bacterial QS process and degrade matrix polysaccharides.
 - The combination of both enzymes resulted in strong antibiofilm activity against medically relevant biofilms as a function of the enzyme position (acylase vs amylase) in the layers.

- *In vitro* and *in vivo* studies suggested the potential of these enzyme-integrated assemblies to reduce the biofilm growth on catheter surface and postpone device-related infections.

B. Nanomaterials aimed at controlling free floating bacterial growth and biofilm occurrence

- *Bacteria-responsive multilayer coatings comprising polycationic NSs*
 - Sonochemically generated polycationic ACNSs were incorporated into “smart” self-defensive LbL assemblies able to counteract planktonic and cooperative biofilm growth of bacteria.
 - The release of highly antibacterial ACNSs in response to bacterial stimuli resulted in a notable inhibition of biofilm development on catheter surface even after seven days of catheterisation in an *in vitro* model of human bladder.
- *Covalent grafting of antibacterial ACNSs onto silicone material*
 - The covalently immobilised on silicone NSs were able to counteract the bacterial attachment and biofilm formation, showing potential to prevent implant related infections.
- *Nano-sized Penicillin G for overcoming Gram-negative bacterial resistance*
 - Clinically relevant antibiotic penicillin G was sonochemically transformed into NSs with high antibacterial efficiency against Gram-negative pathogens in both planktonic and biofilm forms.
 - The NSs were shown to penetrate within model cell membrane, confirming their capacity to interact with bacterial cell wall and cause membrane damage. These spheres were innocuous towards human fibroblasts at the antibacterial/antibiofilm-effective concentrations and thus are valuable alternative to combat drug resistant phenotypes.

6.2 Future Perspectives

Overall, the development of materials and coatings that efficiently inhibit bacterial adhesion, while reducing the high incidence of antibiotic resistance, is one of the most difficult and challenging tasks. The results obtained during the realisation of this thesis demonstrated the feasibility of using enzymes and nanostructures to control bacterial growth and drug resistant biofilm occurrence on indwelling medical devices. The coatings comprising QQ and matrix degrading enzymes were able to delay biofilm growth on catheter surface *in vitro*, when inserted in a glass model of catheterised human bladder as well as *in vivo* in an animal model. A pilot study with urine collected from patients with UTIs is on-going at the Emergency Medicine department of George Washington University to validate the strategy prior to clinical trials. Furthermore, using simultaneously antibiotics and antibiofilm enzymes in the pilot system would provide the opportunity to assess the enzymes potential in enhancing the antibiotic effectiveness at lower therapeutic dosages.

The results obtained in this thesis open alternative avenues to design novel multifunctional nanostructured materials and coatings. The efficiency of commercially available and in some cases obsolete, antibiotics could be synergistically enhanced via the combination of the innovative approaches used herein: i) attenuation of bacterial virulence by enzymes interfering with bacterial QS process, ii) enzymatic degradation of biofilms adhesives, and iii) nanotransformation of antibiotics. The assemblies of the molecules into hybrid nano-sized antibacterials would improve their stability, durability and even increase the activity against multi-drug resistant strains and their biofilm phenotypes. The synergy of these innovative hybrid nanomaterials for counteracting biofilm formation of clinically relevant bacteria on catheters will be further investigated during the projects: “Hybrid nanocoatings on indwelling medical devices with enhanced antibacterial and antibiofilm efficiency” (MAT2015-67648-R) and “Investigating the mechanism of eradication of multi drug resistant bacteria by inorganic (mixed metal oxides), organic (antibiotic) and protein-based NPs” (AC14/00022)

These nano-modalities could also impart antibacterial functionalities to textiles, wound dressings materials, contact lenses and water treatment membranes. These applications will be further up-scaled to a pre-commercial level for coating of medical devices in the project “Pre-commercial lines for production of surface nanostructured antimicrobial and anti-biofilm textiles, medical devices and water treatment membranes” (H2020-720851). Besides of human care, these nanostructures and nanostructures surfaces could be considered for diseases prevention, increased production performance and improved animal welfare.

Bibliography

1. Rodney, M.D., *Biofilms: microbial life on surfaces*. Emerging Infectious Disease journal, 2002. **8**(9): p. 881-890.
2. Francolini, I. and G. Donelli, *Prevention and control of biofilm-based medical-device-related infections*. FEMS Immunology & Medical Microbiology, 2010. **59**(3): p. 227-238.
3. Hung, C.S. and J.P. Henderson, *Emerging concepts of biofilms in infectious diseases*. Mo Med, 2009. **106**(4): p. 292-6.
4. Bjarnsholt, T., et al., *Applying insights from biofilm biology to drug development - can a new approach be developed?* Nature Reviews Drug Discovery, 2013. **12**(10): p. 791-808.
5. Darouiche, R.O., *Treatment of infections associated with surgical implants*. New England Journal of Medicine, 2004. **350**(14): p. 1422-1429.
6. Hall-Stoodley, L., J.W. Costerton, and P. Stoodley, *Bacterial biofilms: from the Natural environment to infectious diseases*. Nat Rev Micro, 2004. **2**(2): p. 95-108.
7. Lebeaux, D., J.-M. Ghigo, and C. Beloin, *Biofilm-related infections: bridging the gap between clinical management and fundamental aspects of recalcitrance toward antibiotics*. Microbiology and Molecular Biology Reviews, 2014. **78**(3): p. 510-543.
8. Gu, H. and D. Ren, *Materials and surface engineering to control bacterial adhesion and biofilm formation: A review of recent advances*. Frontiers of Chemical Science and Engineering, 2014. **8**(1): p. 20-33.
9. Richards, J.J. and C. Melander, *Controlling bacterial biofilms*. ChemBioChem, 2009. **10**(14): p. 2287-2294.
10. Sadekuzzaman, M., et al., *Current and recent advanced strategies for combating biofilms*. Comprehensive Reviews in Food Science and Food Safety, 2015. **14**(4): p. 491-509.
11. Wu, H., et al., *Strategies for combating bacterial biofilm infections*. In J Oral Sci, 2015. **7**(1): p. 1-7.
12. Feneley, R.C.L., et al., *Developing alternative devices to the long-term urinary catheter for draining urine from the bladder*. Proceedings of the Institution of Mechanical Engineers, Part H: Journal of Engineering in Medicine, 2003. **217**(4): p. 297-303.
13. Khoo, X. and M.W. Grinstaff, *Novel infection-resistant surface coatings: A bioengineering approach*. MRS Bulletin, 2011. **36**(05): p. 357-366.
14. Römling, U. and C. Balsalobre, *Biofilm infections, their resilience to therapy and innovative treatment strategies*. Journal of Internal Medicine, 2012. **272**(6): p. 541-561.
15. Lellouche, J., et al., *Antibiofilm surface functionalization of catheters by magnesium fluoride nanoparticles*. International Journal of Nanomedicine, 2012. **7**: p. 1175-1188.
16. Srinivasan, A., et al., *A prospective trial of a novel, silicone-based, silver-coated Foley catheter for the prevention of nosocomial urinary tract infection*. Infect Control Hosp Epidemiol, 2006. **27**: p. 38 - 43.
17. Samuel, U. and J.P. Guggenbichler, *Prevention of catheter-related infections: the potential of a new nano-silver impregnated catheter*. International Journal of Antimicrobial Agents, 2004. **23**: p. 75-78.
18. Ha, U.S. and Y.-H. Cho, *Catheter-associated urinary tract infections: new aspects of novel urinary catheters*. International Journal of Antimicrobial Agents, 2006. **28**(6): p. 485-490.
19. Saini, R., S. Saini, and S. Sharma, *Biofilm: A dental microbial infection*. Journal of Natural Science, Biology, and Medicine, 2011. **2**(1): p. 71-75.
20. Wood, T.K., S.H. Hong, and Q. Ma, *Engineering biofilm formation and dispersal*. Trends in biotechnology. **29**(2): p. 87-94.

21. Davey, M.E. and G.A. O'Toole, *Microbial Biofilms: from Ecology to Molecular Genetics*. Microbiology and Molecular Biology Reviews, 2000. **64**(4): p. 847-867.
22. Bjarnsholt, T., *The role of bacterial biofilms in chronic infections*. APMIS, 2013. **121**: p. 1-58.
23. Donlan, R.M., *Biofilm Formation: A Clinically Relevant Microbiological Process*. Clinical Infectious Diseases, 2001. **33**(8): p. 1387-1392.
24. Jain, A., et al., *Biofilms: A Microbial Life Perspective: A Critical Review*. Critical Reviews in Therapeutic Drug Carrier Systems, 2007. **24**(5): p. 393-443.
25. Flemming, H.-C. and J. Wingender, *The biofilm matrix*. Nat. Rev. Micro., 2010. **8**(9): p. 623-633.
26. Høiby, N., et al., *Antibiotic resistance of bacterial biofilms*. International Journal of Antimicrobial Agents, 2010. **35**(4): p. 322-332.
27. Sauer, K., et al., *Pseudomonas aeruginosa displays multiple phenotypes during development as a biofilm*. Journal of Bacteriology, 2002. **184**(4): p. 1140-1154.
28. Limoli, D.H., C.J. Jones, and D.J. Wozniak, *Bacterial Extracellular Polysaccharides in Biofilm Formation and Function*. Microbiology Spectrum, 2015. **3**(3).
29. Rabin, N., et al., *Biofilm formation mechanisms and targets for developing antibiofilm agents*. Future Medicinal Chemistry, 2015. **7**(4): p. 493-512.
30. May, T.B., et al., *Alginate synthesis by Pseudomonas aeruginosa: a key pathogenic factor in chronic pulmonary infections of cystic fibrosis patients*. Clinical Microbiology Reviews, 1991. **4**(2): p. 191-206.
31. Sledjeski, D.D. and S. Gottesman, *Osmotic shock induction of capsule synthesis in Escherichia coli K-12*. Journal of Bacteriology, 1996. **178**(4): p. 1204-1206.
32. Colvin, K.M., et al., *The Pel and Psl polysaccharides provide Pseudomonas aeruginosa structural redundancy within the biofilm matrix*. Environmental Microbiology, 2012. **14**(8): p. 10.1111/j.1462-2920.2011.02657.x.
33. Tolker-Nielsen, T., et al., *Development and Dynamics of Pseudomonas spp. Biofilms*. Journal of Bacteriology, 2000. **182**(22): p. 6482-6489.
34. Cabarkapa, I., J. Levic, and O. Djuragic, *Biofilm*, in *Microbial pathogens and strategies for combating them: science, technology and education*, A. Mendez-Vilas, Editor 2013, Formatex Research Center: Badajoz (Spain).
35. Li, Y.-H. and X. Tian, *Quorum Sensing and Bacterial Social Interactions in Biofilms*. Sensors (Basel, Switzerland), 2012. **12**(3): p. 2519-2538.
36. Annous, B.A., P.M. Fratamico, and J.L. Smith, *Scientific status summary: Quorum sensing in biofilms: Why bacteria behave the way they do*. Journal of Food Science, 2009. **74**(1): p. R24-R37.
37. Cvitkovitch, D.G., Y.-H. Li, and R.P. Ellen, *Quorum sensing and biofilm formation in Streptococcal infections*. Journal of Clinical Investigation, 2003. **112**(11): p. 1626-1632.
38. Ivanova, K., M. Fernandes, and T. Tzanov, *Strategies for Silencing Bacterial Communication*, in *Quorum Sensing vs Quorum Quenching: A Battle with No End in Sight*, V.C. Kalia, Editor 2015, Springer India. p. 197-216.
39. Wang, W., et al., *Inhibition of Lux quorum-sensing system by synthetic N-acyl-L-homoserine lactone analogs*. Acta Biochimica et Biophysica Sinica, 2008. **40**(12): p. 1023-1028.
40. Galloway, W.R.J.D., et al., *Applications of small molecule activators and inhibitors of quorum sensing in Gram-negative bacteria*. Trends in Microbiology, 2012. **20**(9): p. 449-458.
41. Sifri, C.D., *Quorum Sensing: Bacteria Talk Sense*. Clinical Infectious Diseases, 2008. **47**(8): p. 1070-1076.
42. Watson, W.T., et al., *Structural basis and specificity of acyl-homoserine lactone signal production in bacterial quorum sensing*. Molecular Cell, 2002. **9**(3): p. 685-694.

43. Choudhary, S. and C. Schmidt-Dannert, *Applications of quorum sensing in biotechnology*. Applied Microbiology and Biotechnology, 2010. **86**(5): p. 1267-1279.
44. Tay, S. and W. Yew, *Development of Quorum-Based Anti-Virulence Therapeutics Targeting Gram-Negative Bacterial Pathogens*. International Journal of Molecular Sciences, 2013. **14**(8): p. 16570-16599.
45. Smith, R.S. and B.H. Iglewski, *P. aeruginosa quorum-sensing systems and virulence*. Current Opinion in Microbiology, 2003. **6**(1): p. 56-60.
46. Fux, C.A., et al., *Survival strategies of infectious biofilms*. Trends Microbiol, 2005. **13**(1): p. 34-40.
47. Moore, J.D., et al., *Active Efflux Influences the Potency of Quorum Sensing Inhibitors in Pseudomonas aeruginosa*. ChemBioChem, 2014. **15**(3): p. 435-442.
48. Lee, J., et al., *A cell-cell communication signal integrates quorum sensing and stress response*. Nat Chem Biol, 2013. **9**(5): p. 339-343.
49. Lee, J. and L. Zhang, *The hierarchy quorum sensing network in Pseudomonas aeruginosa*. Protein & Cell, 2015. **6**(1): p. 26-41.
50. S. Swift, A.V.K., L. Fish, E. L. Durant, M. K. Winson, S. R. Chhabra, P. Williams, S. Macintyre and G. S. Stewart. *Quorum sensing in Aeromonas hydrophila and Aeromonas salmonicida: identification of the LuxRI homologs AhyRI and AsaRI and their cognate N-acylhomoserine lactone signal molecules*. - Research Repository. 1997; Available from: <http://eprints.kingston.ac.uk/4461/>.
51. Cao, J.G. and E.A. Meighen, *Purification and structural identification of an autoinducer for the luminescence system of Vibrio harveyi*. The Journal of biological chemistry, 1989. **264**(36): p. 21670-21676.
52. Zhang, Z. and L.S. Pierson, *A second quorum-sensing system regulates cell surface properties but not phenazine antibiotic production in Pseudomonas aureofaciens*. Applied and Environmental Microbiology, 2001. **67**(9): p. 4305-4315.
53. McClean, K.H., et al., *Quorum sensing and Chromobacterium violaceum: exploitation of violacein production and inhibition for the detection of N-acylhomoserine lactones*. Microbiology (Reading, England), 1997. **143 (Pt 12)**: p. 3703-3711.
54. Atkinson, S., et al., *A hierarchical quorum-sensing system in Yersinia pseudotuberculosis is involved in the regulation of motility and clumping*. Molecular Microbiology, 1999. **33**(6): p. 1267-1277.
55. Lupp, C. and E.G. Ruby, *Vibrio fischeri uses two quorum-sensing systems for the regulation of early and late colonization factors*. Journal of bacteriology, 2005. **187**(11): p. 3620-3629.
56. Sokol, P.A., et al., *The CepIR quorum-sensing system contributes to the virulence of Burkholderia cenocepacia respiratory infections*. Microbiology (Reading, England), 2003. **149**(Pt 12): p. 3649-3658.
57. Welch, M., et al., *Structure activity relationships of Erwinia carotovora quorum sensing signaling molecules*. Bioorganic & Medicinal Chemistry Letters, 2005. **15**(19): p. 4235-4238.
58. Nasser, W., et al., *Characterization of the Erwinia chrysanthemi expl-expR locus directing the synthesis of two N-acyl-homoserine lactone signal molecules*. Molecular Microbiology, 1998. **29**(6): p. 1391-1405.
59. Haudecoeur, E. and D. Faure, *A fine control of quorum-sensing communication in Agrobacterium tumefaciens*. Communicative & integrative biology, 2010. **3**(2): p. 84-88.
60. Fekete, A., et al., *Dynamic regulation of N-acyl-homoserine lactone production and degradation in Pseudomonas putida IsoF*. FEMS Microbiology Ecology, 2010. **72**(1): p. 22-34.
61. Kirwan, J.P., et al., *Quorum-sensing signal synthesis by the Yersinia pestis acyl-homoserine lactone synthase Yspl*. Journal of bacteriology, 2006. **188**(2): p. 784-788.

62. Kalia, V.C. and H.J. Purohit, *Quenching the quorum sensing system: Potential antibacterial drug targets*. Critical Reviews in Microbiology, 2011. **37**(2): p. 121-140.
63. Rutherford, S.T. and B.L. Bassler, *Bacterial quorum sensing: its role in virulence and possibilities for its control*. Cold Spring Harbor perspectives in medicine, 2012. **2**(11): p. 1-25.
64. Parker, C.T. and V. Sperandio, *Cell-to-cell signalling during pathogenesis*. Cellular Microbiology, 2009. **11**(3): p. 363-369.
65. Wu, H., et al., *Synthetic furanones inhibit quorum-sensing and enhance bacterial clearance in Pseudomonas aeruginosa lung infection in mice*. The Journal of antimicrobial chemotherapy, 2004. **53**(6): p. 1054-1061.
66. Hume, E.B.H., et al., *The control of Staphylococcus epidermidis biofilm formation and in vivo infection rates by covalently bound furanones*. Biomaterials, 2004. **25**(20): p. 5023-5030.
67. Al-Bataineh, S.A., et al., *Covalent immobilization of antibacterial furanones via photochemical activation of perfluorophenylazide*. Langmuir, 2009. **25**(13): p. 7432-7437.
68. Thoendel, M. and A.R. Horswill, *Chapter 4 - Biosynthesis of Peptide Signals in Gram-Positive Bacteria*, in *Advances in Applied Microbiology*, I.L. Allen, S. Sima, and M.G. Geoffrey, Editors. 2010, Academic Press. p. 91-112.
69. Jarosz, L.M., et al., *Streptococcus mutans competence-stimulating peptide inhibits Candida albicans hypha formation*. Eukaryotic cell, 2009. **8**(11): p. 1658-1664.
70. Mah, T.-F.C. and G.A. O'Toole, *Mechanisms of biofilm resistance to antimicrobial agents*. Trends in Microbiology, 2001. **9**(1): p. 34-39.
71. Kumon, H., et al., *A sandwich cup method for the penetration assay of antimicrobial agents through Pseudomonas exopolysaccharides*. Microbiol Immunol, 1994. **38**(8): p. 615-9.
72. Nichols, W.W., et al., *Inhibition of tobramycin diffusion by binding to alginate*. Antimicrob Agents Chemother, 1988. **32**(4): p. 518-523.
73. Tanaka, G., et al., *Effect of the Growth Rate of <i>Pseudomonas aeruginosa </i> Biofilms on the Susceptibility to Antimicrobial Agents: β -Lactams and Fluoroquinolones*. Chemotherapy, 1999. **45**(1): p. 28-36.
74. Walters, M.C., et al., *Contributions of Antibiotic Penetration, Oxygen Limitation, and Low Metabolic Activity to Tolerance of Pseudomonas aeruginosa Biofilms to Ciprofloxacin and Tobramycin*. Antimicrob Agents Chemother, 2003. **47**(1): p. 317-323.
75. Trautner, B.W. and R.O. Darouiche, *Role of biofilm in catheter-associated urinary tract infection*. American Journal of Infection Control, 2004. **32**(3): p. 177-183.
76. Molin, S. and T. Tolker-Nielsen, *Gene transfer occurs with enhanced efficiency in biofilms and induces enhanced stabilisation of the biofilm structure*. Current Opinion in Biotechnology, 2003. **14**(3): p. 255-261.
77. Hoiby, N., et al., *Antibiotic resistance of bacterial biofilms*. International Journal of Antimicrobial Agents, 2010. **35**(4): p. 322-332.
78. Tenover, F.C., *Mechanisms of Antimicrobial Resistance in Bacteria*. The American journal of medicine, 2006. **119**(6): p. S3-S10.
79. Costerton, J.W., P.S. Stewart, and E.P. Greenberg, *Bacterial biofilms: a common cause of persistent infections*. Science (New York, N.Y.), 1999. **284**(5418): p. 1318-1322.
80. Peters, B.M., et al., *Polymicrobial Interactions: Impact on Pathogenesis and Human Disease*. Clinical Microbiology Reviews, 2012. **25**(1): p. 193-213.
81. Stacy, A., et al., *The biogeography of polymicrobial infection*. Nat Rev Micro, 2016. **14**(2): p. 93-105.
82. Percival, S.L., et al., *Healthcare-associated infections, medical devices and biofilms: risk, tolerance and control*. Journal of Medical Microbiology, 2015. **64**(4): p. 323-334.

83. Pritt, B., L. O'Brien, and W. Winn, *Mucoid Pseudomonas in Cystic Fibrosis*. American Journal of Clinical Pathology, 2007. **128**(1): p. 32-34.
84. Mulcahy, L.R., V.M. Isabella, and K. Lewis, *Pseudomonas aeruginosa Biofilms in Disease*. Microbial Ecology, 2014. **68**(1): p. 1-12.
85. Otto, M., *Staphylococcal Biofilms*. Current topics in microbiology and immunology, 2008. **322**: p. 207-228.
86. Shorr, A. and T. Lodise, *Burden of Methicillin-resistant Staphylococcus aureus on healthcare cost and resource utilization*. ISMR Update, 2006. **1**(2): p. 1-12.
87. Naber, C.K., *Staphylococcus aureus Bacteremia: Epidemiology, Pathophysiology, and Management Strategies*. Clinical Infectious Diseases, 2009. **48**(Supplement 4): p. S231-S237.
88. Jain, P., et al., *Overuse of the indwelling urinary tract catheter in hospitalized medical patients*. Archives of Internal Medicine, 1995. **155**(13): p. 1425-1429.
89. Jacobsen, S.M., et al., *Complicated Catheter-Associated Urinary Tract Infections Due to Escherichia coli and Proteus mirabilis*. Clinical Microbiology Reviews, 2008. **21**(1): p. 26-59.
90. Stamm, W.E., *Catheter-associated urinary tract infections: epidemiology, pathogenesis, and prevention*. Am J Med, 1991. **91**(3B): p. 65S-71S.
91. Warren, J.W., *CATHETER-ASSOCIATED URINARY TRACT INFECTIONS*. Infectious Disease Clinics of North America, 1997. **11**(3): p. 609-622.
92. Donlan, R.M. and J.W. Costerton, *Biofilms: Survival Mechanisms of Clinically Relevant Microorganisms*. Clinical Microbiology Reviews, 2002. **15**(2): p. 167-193.
93. Stickler, D.J., *Bacterial biofilms and the encrustation of urethral catheters*. Biofouling, 1996. **9**(4): p. 293-305.
94. McLean, R.J.C., J. C. Nickel, and M. E. Olson, *Biofilm associated urinary tract infections*, in *Microbial biofilms*, H.M.L.-S.a.J.W. Costerton, Editor 1995, Cambridge University Press: Cambridge. p. 261-273.
95. Stickler, D., *Bacterial biofilms in patients with indwelling urinary catheters*. Nat Clin Pract Urol, 2008. **5**(11): p. 598 - 608.
96. Morris, S.N., J.D. Stickler, and C.R.J. McLean, *The development of bacterial biofilms on indwelling urethral catheters*. World Journal of Urology, 1999. **17**(6): p. 345-350.
97. Nicolle, L., *Catheter associated urinary tract infections*. Antimicrobial Resistance and Infection Control, 2014. **3**(1): p. 23.
98. Rodney, M.D., *Biofilms and Device-Associated Infections*. Emerging Infectious Disease journal, 2001. **7**(2): p. 277.
99. Macleod, S.M. and D.J. Stickler, *Species interactions in mixed-community crystalline biofilms on urinary catheters*. Journal of Medical Microbiology, 2007. **56**(11): p. 1549-1557.
100. Holá, V., F. Ruzicka, and M. Horka, *Microbial diversity in biofilm infections of the urinary tract with the use of sonication techniques*. FEMS Immunology & Medical Microbiology, 2010. **59**(3): p. 525-528.
101. Burmølle, M., et al., *Interactions in multispecies biofilms: do they actually matter?* Trends in Microbiology. **22**(2): p. 84-91.
102. Lee, K.W.K., et al., *Biofilm development and enhanced stress resistance of a model, mixed-species community biofilm*. ISME J, 2014. **8**(4): p. 894-907.
103. Jacobsen, S.M. and M.E. Shirtliff, *Proteus mirabilis biofilms and catheter-associated urinary tract infections*. Virulence, 2011. **2**(5): p. 460-5.
104. Stickler, D.J. and J. Zimakoff, *Complications of urinary tract infections associated with devices used for long-term bladder management*. J Hosp Infect, 1994. **28**(3): p. 177-94.
105. Kwiecinska-Piróg, J., et al., *Proteus mirabilis biofilm - Qualitative and quantitative colorimetric methods-based evaluation*. Brazilian Journal of Microbiology, 2014. **45**(4): p. 1423-1431.

106. Stickler, D.J. and R.C.L. Feneley, *The encrustation and blockage of long-term indwelling bladder catheters: a way forward in prevention and control*. Spinal Cord, 2010. **48**(11): p. 784-790.
107. Jones, B.D. and H.L. Mobley, *Genetic and biochemical diversity of ureases of Proteus, Providencia, and Morganella species isolated from urinary tract infection*. Infect Immun, 1987. **55**(9): p. 2198-203.
108. Stickler, D., et al., *Studies on the formation of crystalline bacterial biofilms on urethral catheters*. Eur J Clin Microbiol Infect Dis, 1998. **17**(9): p. 649-52.
109. Cole, S.J., et al., *Catheter-associated urinary tract infection by Pseudomonas aeruginosa is mediated by exopolysaccharide independent biofilms*. Infection and Immunity, 2014.
110. Denstedt, J.D., T.A. Wollin, and G. Reid, *Biomaterials used in urology: current issues of biocompatibility, infection, and encrustation*. J Endourol, 1998. **12**(6): p. 493-500.
111. Evliyaoglu, Y., et al., *The efficacy of a novel antibacterial hydroxyapatite nanoparticle-coated indwelling urinary catheter in preventing biofilm formation and catheter-associated urinary tract infection in rabbits*. Urol Res, 2011. **39**(6): p. 443-9.
112. Li, X., et al., *Antimicrobial functionalization of silicone surfaces with engineered short peptides having broad spectrum antimicrobial and salt-resistant properties*. Acta Biomater, 2014. **10**(1): p. 258-66.
113. Dong, Y., et al., *Surface microstructure and antibacterial property of an active-screen plasma alloyed austenitic stainless steel surface with Cu and N*. Biomedical Materials, 2010. **5**(5): p. 054105.
114. Fadeeva, E., et al., *Bacterial Retention on Superhydrophobic Titanium Surfaces Fabricated by Femtosecond Laser Ablation*. Langmuir, 2011. **27**(6): p. 3012-3019.
115. Harris, C.A., et al., *Reduction of protein adsorption and macrophage and astrocyte adhesion on ventricular catheters by polyethylene glycol and N-acetyl-L-cysteine*. J Biomed Mater Res A, 2011. **98**(3): p. 425-33.
116. Li, M., et al., *Surface Modification of Silicone with Covalently Immobilized and Crosslinked Agarose for Potential Application in the Inhibition of Infection and Omental Wrapping*. Advanced Functional Materials, 2014. **24**(11): p. 1631-1643.
117. Zhou, J., et al., *Platelet adhesion and protein adsorption on silicone rubber surface by ozone-induced grafted polymerization with carboxybetaine monomer*. Colloids Surf B Biointerfaces, 2005. **41**(1): p. 55-62.
118. Morra, M. and C. Cassineli, *Non-fouling properties of polysaccharide-coated surfaces*. Journal of Biomaterials Science, Polymer Edition, 1999. **10**(10): p. 1107-1124.
119. Abu El-Asrar, A.M., et al., *Heparin and heparin-surface-modification reduce Staphylococcus epidermidis adhesion to intraocular lenses*. International Ophthalmology, 1997. **21**(2): p. 71-74.
120. Roosjen, A., et al., *Stability and effectiveness against bacterial adhesion of poly(ethylene oxide) coatings in biological fluids*. Journal of Biomedical Materials Research Part B: Applied Biomaterials, 2005. **73B**(2): p. 347-354.
121. Hickok, N.J. and I.M. Shapiro, *Immobilized antibiotics to prevent orthopaedic implant infections*. Advanced Drug Delivery Reviews, 2012. **64**(12): p. 1165-1176.
122. Tebbs, S.E. and T.S.J. Elliott, *A novel antimicrobial central venous catheter impregnated with benzalkonium chloride*. Journal of Antimicrobial Chemotherapy, 1993. **31**(2): p. 261-271.
123. Siedenbiedel, F. and J.C. Tiller, *Antimicrobial Polymers in Solution and on Surfaces: Overview and Functional Principles*. Polymers, 2012. **4**(1): p. 46.
124. He, W., et al., *A Novel Surface Structure Consisting of Contact-active Antibacterial Upper-layer and Antifouling Sub-layer Derived from Gemini Quaternary Ammonium Salt Polyurethanes*. Scientific Reports, 2016. **6**: p. 32140.

125. Minardi, D., et al., *Efficacy of Tigecycline and Rifampin Alone and in Combination against *Enterococcus faecalis* Biofilm Infection in a Rat Model of Ureteral Stent*. Journal of Surgical Research. **176**(1): p. 1-6.
126. Chew, B.H., et al., *Second Prize: In-Vitro Activity of Triclosan-Eluting Ureteral Stents against Common Bacterial Uropathogens*. Journal of Endourology, 2006. **20**(11): p. 949-958.
127. Roe, D., et al., *Antimicrobial surface functionalization of plastic catheters by silver nanoparticles*. Journal of Antimicrobial Chemotherapy, 2008. **61**(4): p. 869-876.
128. Desai, D.G., et al., *Silver or Nitrofurazone Impregnation of Urinary Catheters Has a Minimal Effect on Uropathogen Adherence*. The Journal of urology, 2010. **184**(6): p. 2565-2571.
129. Mathews, S.M., et al., *Prevention of bacterial colonization of contact lenses with covalently attached selenium and effects on the rabbit cornea*. Cornea, 2006. **25**(7): p. 806-14.
130. Glinel, K., et al., *Antibacterial surfaces developed from bio-inspired approaches*. Acta Biomaterialia, 2012. **8**: p. 1670-1684.
131. Lichter, J.A., K.J. Van Vliet, and M.F. Rubner, *Design of Antibacterial Surfaces and Interfaces: Polyelectrolyte Multilayers as a Multifunctional Platform*. Macromolecules, 2009. **42**(22): p. 8573-8586.
132. Crouzier, T., T. Boudou, and C. Picart, *Polysaccharide-based polyelectrolyte multilayers*. Current Opinion in Colloid & Interface Science, 2010. **15**(6): p. 417-426.
133. Caruso, F. and C. Schüller, *Enzyme Multilayers on Colloid Particles: Assembly, Stability, and Enzymatic Activity*. Langmuir, 2000. **16**(24): p. 9595-9603.
134. Berg, M.C., et al., *Controlled Drug Release from Porous Polyelectrolyte Multilayers*. Biomacromolecules, 2006. **7**(1): p. 357-364.
135. Kolasinska, M., T. Gutberlet, and R. Krastev, *Ordering of Fe₃O₄ Nanoparticles in Polyelectrolyte Multilayer Films*. Langmuir, 2009. **25**(17): p. 10292-10297.
136. Richardson, J.J., M. Björnmalm, and F. Caruso, *Technology-driven layer-by-layer assembly of nanofilms*. Science, 2015. **348**(6233).
137. Boudou, T., et al., *Multiple Functionalities of Polyelectrolyte Multilayer Films: New Biomedical Applications*. Advanced Materials, 2010. **22**(4): p. 441-467.
138. Séon, L., et al., *Polyelectrolyte Multilayers: A Versatile Tool for Preparing Antimicrobial Coatings*. Langmuir, 2015. **31**(47): p. 12856-12872.
139. Tang, K. and N.A.M. Besseling, *Formation of polyelectrolyte multilayers: ionic strengths and growth regimes*. Soft Matter, 2016. **12**(4): p. 1032-1040.
140. Jourdainne, L., et al., *Multiple Strata of Exponentially Growing Polyelectrolyte Multilayer Films*. Macromolecules, 2007. **40**(2): p. 316-321.
141. Sakr, O.S. and G. Borchard, *Encapsulation of Enzymes in Layer-by-Layer (LbL) Structures: Latest Advances and Applications*. Biomacromolecules, 2013. **14**(7): p. 2117-2135.
142. Cloutier, M., D. Mantovani, and F. Rosei, *Antibacterial Coatings: Challenges, Perspectives, and Opportunities*. Trends in biotechnology, 2015. **33**(11): p. 637-652.
143. Boulmedais, F., et al., *Polyelectrolyte multilayer films with pegylated polypeptides as a new type of anti-microbial protection for biomaterials*. Biomaterials, 2004. **25**(11): p. 2003-2011.
144. Saldarriaga Fernández, I.C., et al., *The inhibition of the adhesion of clinically isolated bacterial strains on multi-component cross-linked poly(ethylene glycol)-based polymer coatings*. Biomaterials, 2007. **28**(28): p. 4105-4112.
145. Fu, J., et al., *Construction of anti-adhesive and antibacterial multilayer films via layer-by-layer assembly of heparin and chitosan*. Biomaterials, 2005. **26**(33): p. 6684-6692.

146. Schmolke, H., et al., *Polyelectrolyte multilayer surface functionalization of poly(dimethylsiloxane) (PDMS) for reduction of yeast cell adhesion in microfluidic devices*. *Biomicrofluidics*, 2010. **4**(4): p. 044113.
147. Fernandes, M.M., et al., *Sonochemically processed cationic nanocapsules: efficient antimicrobials with membrane disturbing capacity*. *Biomacromolecules*, 2014. **15**(4): p. 1365-74.
148. Lichter, J.A. and M.F. Rubner, *Polyelectrolyte Multilayers with Intrinsic Antimicrobial Functionality: The Importance of Mobile Polycations*. *Langmuir*, 2009. **25**(13): p. 7686-7694.
149. Bratskaya, S., et al., *Adhesion and Viability of Two Enterococcal Strains on Covalently Grafted Chitosan and Chitosan/ κ -Carrageenan Multilayers*. *Biomacromolecules*, 2007. **8**(9): p. 2960-2968.
150. Wang, Y., et al., *Surface properties of polyurethanes modified by bioactive polysaccharide-based polyelectrolyte multilayers*. *Colloids and Surfaces B: Biointerfaces*, 2012. **100**: p. 77-83.
151. Gomes, A.P., et al., *Layer-by-Layer Deposition of Antibacterial Polyelectrolytes on Cotton Fibres*. *Journal of Polymers and the Environment*, 2012. **20**(4): p. 1084-1094.
152. Dubas, S.T., P. Kumlangduksana, and P. Potiyaraj, *Layer-by-layer deposition of antimicrobial silver nanoparticles on textile fibers*. *Colloids and Surfaces A: Physicochemical and Engineering Aspects*, 2006. **289**(1-3): p. 105-109.
153. Shirvan, A.R., N.H. Nejad, and A. Bashari, *Antibacterial finishing of cotton fabric via the chitosan/TPP self-assembled nano layers*. *Fibers and Polymers*, 2014. **15**(9): p. 1908-1914.
154. Carmona-Ribeiro, A.M. and L.D. de Melo Carrasco, *Cationic Antimicrobial Polymers and Their Assemblies*. *International journal of molecular sciences*, 2013. **14**(5): p. 9906-9946.
155. Tischer, M., et al., *Quaternary Ammonium Salts and Their Antimicrobial Potential: Targets or Nonspecific Interactions?* *ChemMedChem*, 2012. **7**(1): p. 22-31.
156. Graisuwan, W., et al., *Multilayer film assembled from charged derivatives of chitosan: Physical characteristics and biological responses*. *Journal of Colloid and Interface Science*, 2012. **376**(1): p. 177-188.
157. Wong, S.Y., et al., *Bactericidal and virucidal ultrathin films assembled layer by layer from polycationic N-alkylated polyethylenimines and polyanions*. *Biomaterials*, 2010. **31**(14): p. 4079-4087.
158. Obłąk, E., et al., *Antibacterial activity of gemini quaternary ammonium salts*. *FEMS Microbiology Letters*, 2014. **350**(2): p. 190-198.
159. Kayumov, A.R., et al., *New Derivatives of Pyridoxine Exhibit High Antibacterial Activity against Biofilm-Embedded Staphylococcus Cells*. *BioMed Research International*, 2015. **2015**: p. 890968.
160. Nikitina, E.V., et al., *Antibacterial effects of quaternary bis-phosphonium and ammonium salts of pyridoxine on Staphylococcus aureus cells: A single base hitting two distinct targets?* *World Journal of Microbiology and Biotechnology*, 2015. **32**(1): p. 5.
161. Bakhshi, H., et al., *Synthesis and characterization of antibacterial polyurethane coatings from quaternary ammonium salts functionalized soybean oil based polyols*. *Materials Science and Engineering: C*, 2013. **33**(1): p. 153-164.
162. Zhou, B., et al., *Antibacterial multilayer films fabricated by layer-by-layer immobilizing lysozyme and gold nanoparticles on nanofibers*. *Colloids and Surfaces B: Biointerfaces*, 2014. **116**: p. 432-438.
163. Nepal, D., et al., *Strong Antimicrobial Coatings: Single-Walled Carbon Nanotubes Armored with Biopolymers*. *Nano Letters*, 2008. **8**(7): p. 1896-1901.
164. Zhang, T., et al., *Pectin/lysozyme bilayers layer-by-layer deposited cellulose nanofibrous mats for antibacterial application*. *Carbohydrate Polymers*, 2015. **117**: p. 687-693.

165. Etienne, O., et al., *Multilayer Polyelectrolyte Films Functionalized by Insertion of Defensin: a New Approach to Protection of Implants from Bacterial Colonization*. *Antimicrob Agents Chemother*, 2004. **48**(10): p. 3662-3669.
166. Faure, E., et al., *Sustainable and bio-inspired chemistry for robust antibacterial activity of stainless steel*. *Journal of Materials Chemistry*, 2011. **21**(22): p. 7901-7904.
167. Zhu, X. and X. Jun Loh, *Layer-by-layer assemblies for antibacterial applications*. *Biomaterials Science*, 2015. **3**(12): p. 1505-1518.
168. Banerjee, I., R.C. Pangule, and R.S. Kane, *Antifouling Coatings: Recent Developments in the Design of Surfaces That Prevent Fouling by Proteins, Bacteria, and Marine Organisms*. *Advanced Materials*, 2011. **23**(6): p. 690-718.
169. Agarwal, A., et al., *Surfaces modified with nanometer-thick silver-impregnated polymeric films that kill bacteria but support growth of mammalian cells*. *Biomaterials*, 2010. **31**(4): p. 680-690.
170. Chuang, H.F., R.C. Smith, and P.T. Hammond, *Polyelectrolyte Multilayers for Tunable Release of Antibiotics*. *Biomacromolecules*, 2008. **9**(6): p. 1660-1668.
171. Taubes, G., *The Bacteria Fight Back*. *Science*, 2008. **321**(5887): p. 356-361.
172. Pavlukhina, S., et al., *Polymer Multilayers with pH-Triggered Release of Antibacterial Agents*. *Biomacromolecules*, 2010. **11**(12): p. 3448-3456.
173. Schmidt, D.J., J.S. Moskowitz, and P.T. Hammond, *Electrically Triggered Release of a Small Molecule Drug from a Polyelectrolyte Multilayer Coating*. *Chemistry of Materials*, 2010. **22**(23): p. 6416-6425.
174. Zhu, Z., et al., *Temperature-triggered on-demand drug release enabled by hydrogen-bonded multilayers of block copolymer micelles*. *Journal of Controlled Release*, 2013. **171**(1): p. 73-80.
175. Zhuk, I., et al., *Self-Defensive Layer-by-Layer Films with Bacteria-Triggered Antibiotic Release*. *ACS Nano*, 2014. **8**(8): p. 7733-7745.
176. Pavlukhina, S., et al., *Small-molecule-hosting nanocomposite films with multiple bacteria-triggered responses*. *NPG Asia Mater*, 2014. **6**: p. e121.
177. Pichavant, L., et al., *pH-controlled delivery of gentamicin sulfate from orthopedic devices preventing nosocomial infections*. *Journal of Controlled Release*, 2012. **162**(2): p. 373-381.
178. Cado, G., et al., *Self-Defensive Biomaterial Coating Against Bacteria and Yeasts: Polysaccharide Multilayer Film with Embedded Antimicrobial Peptide*. *Advanced Functional Materials*, 2013. **23**(38): p. 4801-4809.
179. Noble, M.L., P.D. Mourad, and B.D. Ratner, *Digital drug delivery: on-off ultrasound controlled antibiotic release from coated matrices with negligible background leaching*. *Biomaterials Science*, 2014. **2**(6): p. 893-902.
180. Fayaz, A.M., et al., *Biogenic synthesis of silver nanoparticles and their synergistic effect with antibiotics: a study against gram-positive and gram-negative bacteria*. *Nanomedicine: Nanotechnology, Biology and Medicine*, 2010. **6**(1): p. 103-109.
181. Weigang, W., et al., *A programmed release multi-drug implant fabricated by three-dimensional printing technology for bone tuberculosis therapy*. *Biomedical Materials*, 2009. **4**(6): p. 065005.
182. Jessel, N., et al., *Multiple and time-scheduled in situ DNA delivery mediated by β -cyclodextrin embedded in a polyelectrolyte multilayer*. *Proc Natl Acad Sci U S A*, 2006. **103**(23): p. 8618-8621.
183. Ho, C.H., et al., *Nanoseparated Polymeric Networks with Multiple Antimicrobial Properties*. *Advanced Materials*, 2004. **16**(12): p. 957-961.
184. Li, Z., et al., *Two-level antibacterial coating with both release-killing and contact-killing capabilities*. *Langmuir*, 2006. **22**(24): p. 9820-9823.

185. Frei, R., A.S. Breitbach, and H.E. Blackwell, *2-Aminobenzimidazole derivatives strongly inhibit and disperse Pseudomonas aeruginosa biofilms*. *Angewandte Chemie International Edition*, 2012. **51**(21): p. 5226-5229.
186. Broderick, A.H., et al., *Surface Coatings that Promote Rapid Release of Peptide-Based AgrC Inhibitors for Attenuation of Quorum Sensing in Staphylococcus aureus*. *Advanced Healthcare Materials*, 2014. **3**(1): p. 97-105.
187. Kratochvil, M.J., et al., *Nanoporous superhydrophobic coatings that promote the extended release of water-labile quorum sensing inhibitors and enable long-term modulation of quorum sensing in Staphylococcus aureus*. *ACS Biomaterials Science & Engineering*, 2015. **1**(10): p. 1039-1049.
188. Hentzer, M. and M. Givskov, *Pharmacological inhibition of quorum sensing for the treatment of chronic bacterial infections*. *The Journal of clinical investigation*, 2003. **112**(9): p. 1300-1307.
189. Ho, K.K.K., et al., *Quorum sensing inhibitory activities of surface immobilized antibacterial dihydropyrrolones via click chemistry*. *Biomaterials*, 2014. **35**(7): p. 2336-2345.
190. Rogers, S.A., R.W. Huigens Iii, and C. Melander, *A 2-Aminobenzimidazole That Inhibits and Disperses Gram-Positive Biofilms through a Zinc-Dependent Mechanism*. *Journal of the American Chemical Society*, 2009. **131**(29): p. 9868-9869.
191. Fulghesu, L., C. Giallorenzo, and D. Savoia, *Evaluation of Different Compounds as Quorum Sensing Inhibitors in Pseudomonas aeruginosa*. *Journal of Chemotherapy*, 2007. **19**(4): p. 388-390.
192. Lee, J.-H., M.H. Cho, and J. Lee, *3-Indolylacetonitrile Decreases Escherichia coli O157:H7 Biofilm Formation and Pseudomonas aeruginosa Virulence*. *Environmental Microbiology*, 2011. **13**(1): p. 62-73.
193. Frei, R. and H.E. Blackwell, *Small molecule macroarray construction via palladium-mediated carbon-carbon bond-forming reactions: highly efficient synthesis and screening of stilbene arrays*. *Chemistry – A European Journal*, 2010. **16**(9): p. 2692-2695.
194. Broderick, A.H., et al., *Surface-mediated release of a small-molecule modulator of bacterial biofilm formation: A non-bactericidal approach to inhibiting biofilm formation in Pseudomonas aeruginosa*. *Advanced Healthcare Materials*, 2013. **2**(7): p. 993-1000.
195. Roche, D.M., et al., *Communications blackout? Do N-acylhomoserine-lactone-degrading enzymes have any role in quorum sensing?* *Microbiology*, 2004. **150**(7): p. 2023-2028.
196. Hong, K.-W., et al., *Quorum quenching revisited—from signal decays to signalling confusion*. *Sensors*, 2012. **12**(4): p. 4661-4696.
197. Camps, J., et al., *Paraoxonases as potential antibiofilm agents: their relationship with quorum-sensing signals in Gram-negative bacteria*. *Antimicrob Agents Chemother*, 2011. **55**(4): p. 1325-31.
198. Draganov, D.I., et al., *Human paraoxonases (PON1, PON2, and PON3) are lactonases with overlapping and distinct substrate specificities*. *J Lipid Res*, 2005. **46**(6): p. 1239-47.
199. Teiber, J.F., et al., *Dominant role of paraoxonases in inactivation of the Pseudomonas aeruginosa quorum-sensing signal N-(3-oxododecanoyl)-L-homoserine lactone*. *Infection and Immunity*, 2008. **76**(6): p. 2512-2519.
200. Chan, K.-G., et al., *Characterization of N-acylhomoserine lactone-degrading bacteria associated with the Zingiber officinale (ginger) rhizosphere: Co-existence of quorum quenching and quorum sensing in Acinetobacter and Burkholderia*. *BMC Microbiology*, 2011. **11**(1): p. 51.

201. Dong, Y.-H., et al., *AiiA, an enzyme that inactivates the acylhomoserine lactone quorum-sensing signal and attenuates the virulence of Erwinia carotovora*. Proceedings of the National Academy of Sciences, 2000. **97**(7): p. 3526-3531.
202. Lin, Y.H., et al., *Acyl-homoserine lactone acylase from Ralstonia strain XJ12B represents a novel and potent class of quorum-quenching enzymes*. Molecular Microbiology, 2003. **47**(3): p. 849-860.
203. Xu, F., et al., *Degradation of N-acylhomoserine lactones, the bacterial quorum-sensing molecules, by acylase*. Journal of Biotechnology, 2003. **101**(1): p. 89-96.
204. Uroz, S., et al., *N-acylhomoserine lactone quorum-sensing molecules are modified and degraded by Rhodococcus erythropolis W2 by both amidolytic and novel oxidoreductase activities*. Microbiology, 2005. **151**(10): p. 3313-3322.
205. Lee, B., et al., *Effective antifouling using quorum-quenching acylase stabilized in magnetically-separable mesoporous silica*. Biomacromolecules, 2014. **15**(4): p. 1153-1159.
206. Kaplan, J.B., *Biofilm dispersal: mechanisms, clinical Implications, and potential therapeutic uses*. Journal of Dental Research, 2010. **89**(3): p. 205-218.
207. Izano, E.A., et al., *Detachment and Killing of Aggregatibacter actinomycetemcomitans Biofilms by Dispersin B and SDS*. Journal of Dental Research, 2007. **86**(7): p. 618-622.
208. Pavlukhina, S.V., et al., *Noneluting Enzymatic Antibiofilm Coatings*. ACS Applied Materials & Interfaces, 2012. **4**(9): p. 4708-4716.
209. Darouiche, R.O., et al., *Antimicrobial and antibiofilm efficacy of triclosan and DispersinB[®] combination*. Journal of Antimicrobial Chemotherapy, 2009. **64**(1): p. 88-93.
210. Swartjes, J.J.T.M., et al., *A functional DNase I coating to prevent adhesion of bacteria and the formation of biofilm*. Advanced Functional Materials, 2013. **23**(22): p. 2843-2849.
211. Boyd, A. and A.M. Chakrabarty, *Role of alginate lyase in cell detachment of Pseudomonas aeruginosa*. Applied and Environmental Microbiology, 1994. **60**(7): p. 2355-2359.
212. Alkawash, M.A., J.S. Soothill, and N.L. Schiller, *Alginate lyase enhances antibiotic killing of mucoid Pseudomonas aeruginosa in biofilms*. APMIS, 2006. **114**(2): p. 131-138.
213. Lamppa, J.W., et al., *Genetically engineered alginate lyase-PEG conjugates exhibit enhanced catalytic function and reduced immunoreactivity*. PLoS One, 2011. **6**(2): p. e17042.
214. Alipour, M., Z.E. Suntres, and A. Omri, *Importance of DNase and alginate lyase for enhancing free and liposome encapsulated aminoglycoside activity against Pseudomonas aeruginosa*. Journal of Antimicrobial Chemotherapy, 2009. **64**(2): p. 317-325.
215. Thallinger, B., et al., *Antimicrobial enzymes: An emerging strategy to fight microbes and microbial biofilms*. Biotechnology Journal, 2013. **8**(1): p. 97-109.
216. Molobela, I.P., T.E. Cloete, and M. Beukes, *Protease and amylase enzymes for biofilm removal and degradation of extracellular polymeric substances (EPS) produced by pseudomonas fluorescens bacteria*. African Journal of Microbiology Research, 2010. **4**(14): p. 1515-1524.
217. Yeroslavsky, G., et al., *Antibacterial and antibiofilm surfaces through polydopamine-assisted immobilization of lysostaphin as an antibacterial enzyme*. Langmuir, 2015. **31**(3): p. 1064-1073.
218. Pangule, R.C., et al., *Antistaphylococcal nanocomposite films based on enzyme-nanotube conjugates*. ACS Nano, 2010. **4**(7): p. 3993-4000.
219. Kokai-Kun, J.F., T. Chanturiya, and J.J. Mond, *Lysostaphin as a treatment for systemic Staphylococcus aureus infection in a mouse model*. Journal of Antimicrobial Chemotherapy, 2007. **60**(5): p. 1051-1059.

220. Placencia, F.X., L. Kong, and L.E. Weisman, *Treatment of Methicillin-Resistant Staphylococcus aureus in Neonatal Mice: Lysostaphin Versus Vancomycin*. *Pediatr Res*, 2009. **65**(4): p. 420-424.
221. Yuan, S., et al., *Lysozyme-coupled poly(poly(ethylene glycol) methacrylate)-stainless steel hybrids and their antifouling and antibacterial surfaces*. *Langmuir*, 2011. **27**(6): p. 2761-2774.
222. Muszanska, A.K., et al., *Pluronic-lysozyme conjugates as anti-adhesive and antibacterial bifunctional polymers for surface coating*. *Biomaterials*, 2011. **32**(26): p. 6333-6341.
223. Minier, M., et al., *Covalent immobilization of lysozyme on stainless steel. Interface spectroscopic characterization and measurement of enzymatic activity*. *Langmuir*, 2005. **21**(13): p. 5957-5965.
224. Rohde, H., et al., *Polysaccharide intercellular adhesin or protein factors in biofilm accumulation of Staphylococcus epidermidis and Staphylococcus aureus isolated from prosthetic hip and knee joint infections*. *Biomaterials*, 2007. **28**(9): p. 1711-1720.
225. Chen, M., Q. Yu, and H. Sun, *Novel strategies for the prevention and treatment of biofilm related infections*. *International journal of molecular sciences*, 2013. **14**(9): p. 18488-18501.
226. McDonnell, G. and A.D. Russell, *Antiseptics and disinfectants: activity, action, and resistance*. *Clinical Microbiology Reviews*, 1999. **12**(1): p. 147-179.
227. Walker, S.L., et al., *Removal of microbial biofilms from dispense equipment: The effect of enzymatic pre-digestion and detergent treatment*. *Journal of the Institute of Brewing*, 2007. **113**(1): p. 61-66.
228. Nyanhongo, G.S., et al., *An antioxidant regenerating system for continuous quenching of free radicals in chronic wounds*. *European Journal of Pharmaceutics and Biopharmaceutics*, 2013. **83**(3): p. 396-404.
229. Ge, L., et al., *Immobilization of glucose oxidase in electrospun nanofibrous membranes for food preservation*. *Food Control*, 2012. **26**(1): p. 188-193.
230. Thallinger, B., et al., *Preventing microbial colonisation of catheters: Antimicrobial and antibiofilm activities of cellobiose dehydrogenase*. *International Journal of Antimicrobial Agents*, 2014. **44**(5): p. 402-408.
231. Thallinger, B., et al., *Cellobiose dehydrogenase functionalized urinary catheter as novel antibiofilm system*. *Journal of Biomedical Materials Research Part B: Applied Biomaterials*, 2015: p. n/a-n/a.
232. Vaterrodt, A., et al., *Antifouling and Antibacterial Multifunctional Polyzwitterion/Enzyme Coating on Silicone Catheter Material Prepared by Electrostatic Layer-by-Layer Assembly*. *Langmuir*, 2016. **32**(5): p. 1347-1359.
233. Lipovsky, A., et al., *Ultrasound coating of polydimethylsiloxanes with antimicrobial enzymes*. *Journal of Materials Chemistry B*, 2015. **3**(35): p. 7014-7019.
234. Hansen, E.H., et al., *Curvularia haloperoxidase: antimicrobial activity and potential application as a surface disinfectant*. *Applied and Environmental Microbiology*, 2003. **69**(8): p. 4611-4617.
235. Amitai, G., et al., *Polyurethane-based leukocyte-inspired biocidal materials*. *Biomaterials*, 2009. **30**(33): p. 6522-9.
236. Wang, L.-S., A. Gupta, and V.M. Rotello, *Nanomaterials for the Treatment of Bacterial Biofilms*. *ACS Infectious Diseases*, 2016. **2**(1): p. 3-4.
237. Abeylath, S.C. and E. Turos, *Drug delivery approaches to overcome bacterial resistance to beta-lactam antibiotics*. *Expert Opin Drug Deliv*, 2008. **5**(9): p. 931-49.
238. Shimanovich, U., et al., *Tetracycline nanoparticles as antibacterial and gene-silencing agents*. *Adv Healthc Mater*, 2015. **4**(5): p. 723-8.
239. Verran, J., et al., *Variables affecting the antibacterial properties of nano and pigmentary titania particles in suspension*. *Dyes and Pigments*, 2007. **73**(3): p. 298-304.

240. Eshed, M., et al., *Sonochemical coatings of ZnO and CuO nanoparticles inhibit Streptococcus mutans biofilm formation on teeth model*. Langmuir, 2012. **28**(33): p. 12288-12295.
241. Michel, M., et al., *Deposition mechanisms in Layer-by-Layer or Step-by-Step deposition methods: from elastic and impermeable films to soft membranes with ion exchange properties*. ISRN Materials Science, 2012. **2012**: p. 13.
242. Rao, J.P. and K.E. Geckeler, *Polymer nanoparticles: Preparation techniques and size-control parameters*. Progress in Polymer Science, 2011. **36**(7): p. 887-913.
243. Shimanovich, U., et al., *Protein micro- and nano-capsules for biomedical applications*. Chemical Society Reviews, 2014. **43**(5): p. 1361-1371.
244. Huh, A.J. and Y.J. Kwon, *Nanoantibiotics : A new paradigm for treating infectious diseases using nanomaterials in the antibiotics resistant era*. 2011. **156**: p. 128-145.
245. Xu, H., B.W. Zeiger, and K.S. Suslick, *Sonochemical synthesis of nanomaterials*. Chemical Society Reviews, 2013. **42**(7): p. 2555-2567.
246. Skirtenko, N., et al., *One-Step Preparation of Multifunctional Chitosan Microspheres by a Simple Sonochemical Method*. Chemistry – A European Journal, 2010. **16**(2): p. 562-567.
247. Saleh, N.B., et al., *Mechanistic lessons learned from studies of planktonic bacteria with metallic nanomaterials: implications for interactions between nanomaterials and biofilm bacteria*. Frontiers in Microbiology, 2015. **6**: p. 677.
248. Gupta, A., R.F. Landis, and V.M. Rotello, *Nanoparticle-Based Antimicrobials: Surface Functionality is Critical*. F1000Research, 2016. **5**: p. F1000 Faculty Rev-364.
249. Li, X., et al., *Control of nanoparticle penetration into biofilms through surface design*. Chemical Communications, 2015. **51**(2): p. 282-285.
250. Lerner, R.N., et al., *The effects of biofilm on the transport of stabilized zerovalent iron nanoparticles in saturated porous media*. Water Research, 2012. **46**(4): p. 975-985.
251. Karatan, E. and P. Watnick, *Signals, regulatory networks, and materials that build and break bacterial biofilms*. Microbiology and Molecular Biology Reviews, 2009. **73**(2): p. 310-347.
252. Levard, C., et al., *Environmental transformations of silver nanoparticles: Impact on stability and toxicity*. Environmental Science and Technology, 2012. **46**(13): p. 6900-6914.
253. Allaker, R.P., *The use of nanoparticles to control oral biofilm formation*. Journal of Dental Research, 2010. **89**(11): p. 1175-1186.
254. Peulen, T.O. and K.J. Wilkinson, *Diffusion of nanoparticles in a biofilm*. Environmental Science and Technology, 2011. **45**: p. 3367-3373.
255. Hetrick, E.M., et al., *Anti-biofilm efficacy of nitric oxide-releasing silica nanoparticles*. Biomaterials, 2009. **30**(14): p. 2782-2789.
256. Richter, A.P., et al., *An environmentally benign antimicrobial nanoparticle based on a silver-infused lignin core*. Nat Nano, 2015. **10**(9): p. 817-823.
257. Radovic-Moreno, A.F., et al., *Surface Charge-Switching Polymeric Nanoparticles for Bacterial Cell Wall-Targeted Delivery of Antibiotics*. ACS Nano, 2012. **6**(5): p. 4279-4287.
258. Horev, B., et al., *pH-Activated Nanoparticles for Controlled Topical Delivery of Farnesol To Disrupt Oral Biofilm Virulence*. ACS Nano, 2015. **9**(3): p. 2390-2404.
259. Ikuma, K., A.W. Decho, and B.L.T. Lau, *When nanoparticles meet biofilms - Interactions guiding the environmental fate and accumulation of nanoparticles*. Frontiers in Microbiology, 2015. **6**.
260. Monopoli, M.P., et al., *Biomolecular coronas provide the biological identity of nanosized materials*. Nature Nanotechnology, 2012. **7**(12): p. 779-786.
261. Choi, O., et al., *Interactions of nanosilver with Escherichia coli cells in planktonic and biofilm cultures*. Water Research, 2010. **44**(20): p. 6095-6103.

262. Mohanty, S., et al., *An investigation on the antibacterial, cytotoxic, and antibiofilm efficacy of starch-stabilized silver nanoparticles*. *Nanomedicine: Nanotechnology, Biology and Medicine*. **8**(6): p. 916-924.
263. Vasilev, K., et al., *Antibacterial surfaces by adsorptive binding of polyvinyl-sulphonate-stabilized silver nanoparticles*. *Nanotechnology*, 2010. **21**(21): p. 215102-215102.
264. Körner, E., et al., *Surface topography, morphology and functionality of silver containing plasma polymer nanocomposites*. *Surface and Coatings Technology*, 2011. **205**(8-9): p. 2978-2984.
265. Secinti, K.D., et al., *Nanoparticle silver ion coatings inhibit biofilm formation on titanium implants*. *Journal of Clinical Neuroscience*, 2011. **18**(3): p. 391-395.
266. Feng, Q.L., et al., *A mechanistic study of the antibacterial effect of silver ions on Escherichia coli and Staphylococcus aureus*. *Journal of Biomedical Materials Research*, 2000. **52**: p. 662-668.
267. Sondi, I. and B. Salopek-Sondi, *Silver nanoparticles as antimicrobial agent: a case study on E. coli as a model for Gram-negative bacteria*. *Journal of Colloid and Interface Science*, 2004. **275**(1): p. 177-182.
268. Allahverdiyev, A.M., et al., *Antimicrobial effects of TiO(2) and Ag(2)O nanoparticles against drug-resistant bacteria and leishmania parasites*. *Future Microbiology*, 2011. **6**: p. 933-940.
269. Soenen, S.J., et al., *(Intra)cellular stability of inorganic nanoparticles: effects on cytotoxicity, particle functionality, and biomedical applications*. *Chemical Reviews*, 2015: p. 2109–2135.
270. Marambio-Jones, C. and E.V. Hoek, *A review of the antibacterial effects of silver nanomaterials and potential implications for human health and the environment*. *Journal of Nanoparticle Research*, 2010. **12**(5): p. 1531-1551.
271. Sambhy, V., et al., *Silver bromide nanoparticle/polymer composites: dual action tunable antimicrobial materials*. *Journal of the American Chemical Society*, 2006. **128**(30): p. 9798-9808.
272. Agnihotri, S., S. Mukherji, and S. Mukherji, *Antimicrobial chitosan–PVA hydrogel as a nanoreactor and immobilizing matrix for silver nanoparticles*. *Applied Nanoscience*, 2012. **2**(3): p. 179-188.
273. Francesko, A., et al., *Enzymatic functionalization of cork surface with antimicrobial hybrid biopolymer/silver nanoparticles*. *ACS Applied Materials & Interfaces*, 2015. **7**(18): p. 9792-9799.
274. Nair, S., et al., *Role of size scale of ZnO nanoparticles and microparticles on toxicity toward bacteria and osteoblast cancer cells*. *Journal of Materials Science: Materials in Medicine*, 2009. **20**(1): p. 235-241.
275. Kishen, A., et al., *An Investigation on the antibacterial and antibiofilm efficacy of cationic nanoparticulates for root canal disinfection*. *Journal of Endodontics*, 2008. **34**(12): p. 1515-1520.
276. Petkova, P., et al., *Simultaneous sonochemical-enzymatic coating of medical textiles with antibacterial ZnO nanoparticles*. *Ultrason Sonochem*, 2016. **29**: p. 244-50.
277. Petkova, P., et al., *Sonochemical coating of textiles with hybrid ZnO/chitosan antimicrobial nanoparticles*. *ACS Appl Mater Interfaces*, 2014. **6**(2): p. 1164-72.
278. Natan, M., et al., *Two are Better than One: Combining ZnO and MgF₂ Nanoparticles Reduces Streptococcus pneumoniae and Staphylococcus aureus Biofilm Formation on Cochlear Implants*. *Advanced Functional Materials*, 2016. **26**(15): p. 2473-2481.
279. Mishra, R.K., et al., *New life for an old antibiotic*. *ACS Appl Mater Interfaces*, 2015. **7**(13): p. 7324-33.
280. Yariv, I., et al., *Enhanced pharmacological activity of vitamin B₁(2) and penicillin as nanoparticles*. *Int J Nanomedicine*, 2015. **10**: p. 3593-601.

281. Melkoumov, A., et al., *Nystatin nanosizing enhances in vitro and in vivo antifungal activity against Candida albicans*. J Antimicrob Chemother, 2013. **68**(9): p. 2099-105.
282. Avivi, S., et al., *An easy sonochemical route for the encapsulation of tetracycline in bovine serum albumin microspheres*. J Am Chem Soc, 2003. **125**(51): p. 15712-3.
283. Okusanya, O.O., et al., *Pharmacokinetic and pharmacodynamic evaluation of liposomal amikacin for inhalation in cystic fibrosis patients with chronic pseudomonal infection*. Antimicrob Agents Chemother, 2009. **53**(9): p. 3847-54.
284. Gubernator, J., et al., *In vitro antimicrobial activity of liposomes containing ciprofloxacin, meropenem and gentamicin against Gram-negative clinical bacterial strains*. Letters in Drug Design & Discovery, 2007. **4**(4): p. 297-304.
285. Rahn, K., et al., *Homogeneous synthesis of cellulose p-toluenesulfonates in N,N-dimethylacetamide/LiCl solvent system*. Die Angewandte Makromolekulare Chemie, 1996. **238**(1): p. 143-163.
286. Steindler, L. and V. Venturi, *Detection of quorum-sensing N-acyl homoserine lactone signal molecules by bacterial biosensors*. FEMS Microbiol Lett, 2007. **266**(1): p. 1-9.
287. Ravn, L., et al., *Methods for detecting acylated homoserine lactones produced by Gram-negative bacteria and their application in studies of AHL-production kinetics*. J Microbiol Methods, 2001. **44**(3): p. 239-51.
288. Goncalves, C., et al., *Adaptation of dinitrosalicylic acid method to microtiter plates*. Analytical Methods, 2010. **2**(12): p. 2046-2048.
289. Diaz Blanco, C., et al., *Building an antifouling zwitterionic coating on urinary catheters using an enzymatically triggered bottom-up approach*. ACS Applied Materials & Interfaces, 2014. **6**(14): p. 11385-11393.
290. Horcas, I., et al., *WSXM: A software for scanning probe microscopy and a tool for nanotechnology*. Review of Scientific Instruments, 2007. **78**(1): p. -.
291. Blosser, R.S. and K.M. Gray, *Extraction of violacein from Chromobacterium violaceum provides a new quantitative bioassay for N-acyl homoserine lactone autoinducers*. Journal of Microbiological Methods, 2000. **40**(1): p. 47-55.
292. Liu, H. and H.H.P. Fang, *Extraction of extracellular polymeric substances (EPS) of sludges*. Journal of Biotechnology, 2002. **95**(3): p. 249-256.
293. Stickler, D.J., N.S. Morris, and C. Winters, *Simple physical model to study formation and physiology of biofilms on urethral catheters*, in *Methods in Enzymology* 1999, Academic Press. p. 494-501.
294. Suslick, K.S. and M.W. Grinstaff, *Protein microencapsulation of nonaqueous liquids*. Journal of the American Chemical Society, 1990. **112**(21): p. 7807-7809.
295. Francesko, A., et al., *One-step sonochemical preparation of redox-responsive nanocapsules for glutathione mediated RNA release*. Journal of Materials Chemistry B, 2014. **2**(36): p. 6020-6029.
296. Amorim, S., et al., *Interactions between Exogenous FGF-2 and Sulfonic Groups: in Situ Characterization and Impact on the Morphology of Human Adipose-Derived Stem Cells*. Langmuir, 2013. **29**(25): p. 7983-7992.
297. Hoyo, J., J. Torrent-Burgués, and E. Gaus, *Biomimetic monolayer films of monogalactosyldiacylglycerol incorporating ubiquinone*. Journal of Colloid and Interface Science, 2012. **384**(1): p. 189-197.
298. Torrent-Burgués, J., et al., *Synthesis, Langmuir and Langmuir-Blodgett films of a calix[7]arene ethyl ester*. Colloids and Surfaces A: Physicochemical and Engineering Aspects, 2012. **401**: p. 137-147.
299. Davies, J.T. and E.K. Rideal, *Interfacial Phenomena* 1963, New York: Academic Publisher.
300. Marsh, G.C.a.D., *Phospholipid bilayers physical principles and models.*, in *Cell Biochemistry and Function*, D. Chapman, Editor 1988, John Wiley & Sons, Ltd. p. 147-148.

301. Harmsen, M., et al., "An update on *Pseudomonas aeruginosa* biofilm formation, tolerance, and dispersal". FEMS Immunology & Medical Microbiology, 2010. **59**(3): p. 253-268.
302. Christensen, L.D., et al., *Impact of Pseudomonas aeruginosa quorum sensing on biofilm persistence in an in vivo intraperitoneal foreign-body infection model*. Microbiology, 2007. **153**(7): p. 2312-2320.
303. Davies, D.G., et al., *The Involvement of Cell-to-Cell Signals in the Development of a Bacterial Biofilm*. Science, 1998. **280**(5361): p. 295-298.
304. Sakuragi, Y. and R. Kolter, *Quorum-Sensing Regulation of the Biofilm Matrix Genes (pel) of Pseudomonas aeruginosa*. Journal of Bacteriology, 2007. **189**(14): p. 5383-5386.
305. Youshko, M.I., et al., *Application of aminoacylase I to the enantioselective resolution of α -amino acid esters and amides*. Tetrahedron: Asymmetry, 2004. **15**(12): p. 1933-1936.
306. Kalia, V.C., *Quorum sensing inhibitors: An overview*. Biotechnology Advances, 2013. **31**(2): p. 224-245.
307. Gilles, S., *Chemical Modification of Silicon Surfaces for the Application in Soft Lithography* 2007, University of Freiburg: Jülich, Germany.
308. Kim, J., et al., *Formation, structure, and reactivity of amino-terminated organic films on silicon substrates*. Journal of Colloid and Interface Science, 2009. **329**(1): p. 114-119.
309. Kong, J. and S. Yu, *Fourier transform infrared spectroscopic analysis of protein secondary structures*. Acta biochimica et biophysica Sinica, 2007. **39**(8): p. 549-559.
310. Richert, L., et al., *Layer by Layer Buildup of Polysaccharide Films: Physical Chemistry and Cellular Adhesion Aspects*. Langmuir, 2003. **20**(2): p. 448-458.
311. Follmann, H.D.M., et al., *Antiadhesive and Antibacterial Multilayer Films via Layer-by-Layer Assembly of TMC/Heparin Complexes*. Biomacromolecules, 2012. **13**(11): p. 3711-3722.
312. Caseli, L., et al., *Control of catalytic activity of glucose oxidase in layer-by-layer films of chitosan and glucose oxidase*. Materials Science and Engineering: C, 2007. **27**(5-8): p. 1108-1110.
313. Kong, W., et al., *A new kind of immobilized enzyme multilayer based on cationic and anionic interaction*. Macromolecular Rapid Communications, 1994. **15**(5): p. 405-409.
314. Onda, M., K. Ariga, and T. Kunitake, *Activity and stability of glucose oxidase in molecular films assembled alternately with polyions*. Journal of Bioscience and Bioengineering, 1999. **87**(1): p. 69-75.
315. Sio, C.F., et al., *Quorum Quenching by an N-Acyl-Homoserine Lactone Acylase from Pseudomonas aeruginosa PAO1*. Infection and Immunity, 2006. **74**(3): p. 1673-1682.
316. Palmer, J., S. Flint, and J. Brooks, *Bacterial cell attachment, the beginning of a biofilm*. Journal of industrial microbiology & biotechnology, 2007. **34**(9): p. 577-588.
317. Jeremy S. Webb, L.S.T., Sally James, Tim Charlton, Tim Tolker-Nielsen, Birgit Koch, Michael Givskov, and Staffan Kjelleberg, *Cell death in pseudomonas aeruginosa biofilm development - ePrints Soton*. 2003.
318. Sarkar, K. and P.P. Kundu, *Preparation of low molecular weight N-maleated chitosan-graft-PAMAM copolymer for enhanced DNA complexation*. International Journal of Biological Macromolecules, 2012. **51**(5): p. 859-867.
319. Lopez-Perez, P.M., et al., *Surface phosphorylation of chitosan significantly improves osteoblast cell viability, attachment and proliferation*. Journal of Materials Chemistry, 2010. **20**(3): p. 483-491.
320. Hong, S., et al., *Interaction of Polycationic Polymers with Supported Lipid Bilayers and Cells: Nanoscale Hole Formation and Enhanced Membrane Permeability*. Bioconjugate Chemistry, 2006. **17**(3): p. 728-734.

321. Mann, E.E. and D.J. Wozniak, *Pseudomonas biofilm matrix composition and niche biology*. FEMS Microbiology Reviews, 2012. **36**(4): p. 893-916.
322. Yadav, M.K., et al., *Hyaluronic Acid Derived from Other Streptococci Supports Streptococcus pneumoniae In Vitro Biofilm Formation*. BioMed Research International, 2013. **2013**: p. 7.
323. Ensor, L.A., S.K. Stosz, and R.M. Weiner, *Expression of multiple complex polysaccharide-degrading enzyme systems by marine bacterium strain 2-40*. Journal of Industrial Microbiology and Biotechnology, 1999. **23**(2): p. 123-126.
324. Sivaramakrishnan, S., et al., *α -Amylases from Microbial Sources – An Overview on Recent Developments*. Food Technol. Biotechnol, 2006. **44** (2)(173-184): p. 173-184.
325. Kulik, E.A., et al., *Trypsin immobilization on to polymer surface through grafted layer and its reaction with inhibitors*. Biomaterials, 1993. **14**(10): p. 763-769.
326. Picart, C., et al., *Molecular basis for the explanation of the exponential growth of polyelectrolyte multilayers*. Proceedings of the National Academy of Sciences, 2002. **99**(20): p. 12531-12535.
327. Disawal, S., et al., *Two-step sequential reaction catalyzed by layer-by-layer assembled urease and arginase multilayers*. Colloids and Surfaces B: Biointerfaces, 2003. **32**(2): p. 145-156.
328. Craigen, B., A. Dashiff, and D.E. Kadouri, *The use of commercially available alpha-amylase compounds to inhibit and remove Staphylococcus aureus biofilms*. Open Microbiology Journal, 2011. **5**: p. 21-31.
329. Kalpana, B., S. Aarthy, and S. Pandian, *Antibiofilm Activity of α -Amylase from Bacillus subtilis S8-18 Against Biofilm Forming Human Bacterial Pathogens*. Applied Biochemistry and Biotechnology, 2012. **167**(6): p. 1778-1794.
330. Azevedo, M.M., et al., *Polyethyleneimine and polyethyleneimine-based nanoparticles: novel bacterial and yeast biofilm inhibitors*. Journal of Medical Microbiology, 2014. **63**(9): p. 1167-1173.
331. Kiss, É., et al., *Membrane Affinity and Antibacterial Properties of Cationic Polyelectrolytes With Different Hydrophobicity*. Macromolecular Bioscience, 2012. **12**(9): p. 1181-1189.
332. De Kievit, T.R., *Quorum sensing in Pseudomonas aeruginosa biofilms*. Environmental Microbiology, 2009. **11**(2): p. 279-288.
333. Stepanovic, S., et al., *Influence of dynamic conditions on biofilm formation by staphylococci*. Eur J Clin Microbiol Infect Dis, 2001. **20**(7): p. 502-4.
334. Cerqueira, L., et al., *Biofilm formation with mixed cultures of Pseudomonas aeruginosa/Escherichia coli on silicone using artificial urine to mimic urinary catheters*. Biofouling, 2013. **29**(7): p. 829-840.
335. Fischer, D., et al., *In vitro cytotoxicity testing of polycations: influence of polymer structure on cell viability and hemolysis*. Biomaterials, 2003. **24**(7): p. 1121-1131.
336. Nolte, A., et al., *Impact of polyelectrolytes and their corresponding multilayers to human primary endothelial cells*. Journal of Biomaterials Applications, 2013. **28**(1): p. 84-99.
337. Hong, S., et al., *Interaction of Poly(amidoamine) Dendrimers with Supported Lipid Bilayers and Cells: Hole Formation and the Relation to Transport*. Bioconjugate Chemistry, 2004. **15**(4): p. 774-782.
338. Zintchenko, A., et al., *Simple Modifications of Branched PEI Lead to Highly Efficient siRNA Carriers with Low Toxicity*. Bioconjugate Chemistry, 2008. **19**(7): p. 1448-1455.
339. Barford, J.M.T., et al., *A model of catheter-associated urinary tract infection initiated by bacterial contamination of the catheter tip*. BJU International, 2008. **102**(1): p. 67-74.

340. Halthur, T.J. and U.M. Elofsson, *Multilayers of Charged Polypeptides As Studied by in Situ Ellipsometry and Quartz Crystal Microbalance with Dissipation*. *Langmuir*, 2004. **20**(5): p. 1739-1745.
341. Ozen, B.F., I. Weiss, and L.J. Mauer, *Dietary Supplement Oil Classification and Detection of Adulteration Using Fourier Transform Infrared Spectroscopy*. *Journal of Agricultural and Food Chemistry*, 2003. **51**(20): p. 5871-5876.
342. Rohman, A. and Y.B. Che Man, *Quantification and Classification of Corn and Sunflower Oils as Adulterants in Olive Oil Using Chemometrics and FTIR Spectra*. *The Scientific World Journal*, 2012. **2012**: p. 6.
343. Silva, J.M., et al., *Tailored Freestanding Multilayered Membranes Based on Chitosan and Alginate*. *Biomacromolecules*, 2014. **15**(10): p. 3817-3826.
344. Genco, T., et al., *Physicochemical Properties and Bioactivity of a Novel Class of Celluloses: 6-Deoxy-6-amino Cellulose Sulfate*. *Macromolecular Chemistry and Physics*, 2012. **213**(5): p. 539-548.
345. Gribova, V., R. Auzely-Velty, and C. Picart, *Polyelectrolyte Multilayer Assemblies on Materials Surfaces: From Cell Adhesion to Tissue Engineering*. *Chemistry of Materials*, 2012. **24**(5): p. 854-869.
346. Al-Tahhan, R.A., et al., *Rhamnolipid-Induced Removal of Lipopolysaccharide from Pseudomonas aeruginosa: Effect on Cell Surface Properties and Interaction with Hydrophobic Substrates*. *Applied and Environmental Microbiology*, 2000. **66**(8): p. 3262-3268.
347. Horie, K., et al., *Calorimetric investigation of polymerization reactions. III. Curing reaction of epoxides with amines*. *Journal of Polymer Science Part A-1: Polymer Chemistry*, 1970. **8**(6): p. 1357-1372.
348. Boey, F.Y.C. and B.H. Yap, *Microwave curing of an epoxy-amine system: effect of curing agent on the glass-transition temperature*. *Polymer Testing*, 2001. **20**(8): p. 837-845.
349. Ehlers, J.-E., et al., *Theoretical Study on Mechanisms of the Epoxy-Amine Curing Reaction*. *Macromolecules*, 2007. **40**(12): p. 4370-4377.
350. Beyth, N., et al., *Alternative Antimicrobial Approach: Nano-Antimicrobial Materials*. *Evidence-Based Complementary and Alternative Medicine*, 2015. **2015**: p. 16.
351. Cedrone, F., T. Bhatnagar, and J.C. Baratti, *Colorimetric assays for quantitative analysis and screening of epoxide hydrolase activity*. *Biotechnol Lett*, 2005. **27**(23-24): p. 1921-7.
352. Cavalieri, F., et al., *One-pot ultrasonic synthesis of multifunctional microbubbles and microcapsules using synthetic thiolated macromolecules*. *Chemical Communications*, 2011. **47**(14): p. 4096-4098.
353. Kaper, J.B., J.P. Nataro, and H.L.T. Mobley, *Pathogenic Escherichia coli*. *Nat Rev Micro*, 2004. **2**(2): p. 123-140.
354. Payne, D.J., et al., *Drugs for bad bugs: confronting the challenges of antibacterial discovery*. *Nat Rev Drug Discov*, 2007. **6**(1): p. 29-40.
355. Chain, B., *Penicillin and beyond*. *Nature*, 1991. **353**(6344): p. 492-494.
356. Cunha, B.A., *Aminopenicillins in urology*. *Urology*. **40**(2): p. 186-190.
357. Miller, E.L., *The penicillins: a review and update*. *The Journal of Midwifery & Women's Health*, 2002. **47**(6): p. 426-434.
358. Silhavy, T.J., D. Kahne, and S. Walker, *The Bacterial Cell Envelope*. *Cold Spring Harbor Perspectives in Biology*, 2010. **2**(5): p. a000414.
359. Ravishankar Rai V, J.B.A., *Biomimetic Synthesis of Silver Nanoparticles Using Endosymbiotic Bacterium Inhabiting Euphorbia hirta L. and Their Bactericidal Potential*, in *Science against microbial pathogens: communicating current research and technological advances*, M.-V. A, Editor 2011, Formatex Research Center. p. 197-209.

360. Pezeshki, A., et al., *Encapsulation of Vitamin A Palmitate in Nanostructured Lipid Carrier (NLC)-Effect of Surfactant Concentration on the Formulation Properties*. *Advanced Pharmaceutical Bulletin*, 2014. **4**(Suppl 2): p. 563-568.
361. Quaglia, F., et al., *The intracellular effects of non-ionic amphiphilic cyclodextrin nanoparticles in the delivery of anticancer drugs*. *Biomaterials*, 2009. **30**(3): p. 374-382.
362. Vineeth P, V.P., Kumar K, Babu D, Rao AV, Babu KS, *Influence of organic solvents on nanoparticle formation and surfactants on release behaviour in-vitro using costunolide as mode*. *Pharm Pharm Science*, 2014. **6**: p. 638-645.
363. Feczko, T., J. Tóth, and J. Gyenis, *Comparison of the preparation of PLGA-BSA nano- and microparticles by PVA, poloxamer and PVP*. *Colloids and Surfaces A: Physicochemical and Engineering Aspects*, 2008. **319**(1-3): p. 188-195.
364. Zhou, F., et al., *Influences of surfactant (PVA) concentration and pH on the preparation of copper nanoparticles by electron beam irradiation*. *Radiation Physics and Chemistry*, 2008. **77**(2): p. 169-173.
365. Mu, L. and P.H. Seow, *Application of TPGS in polymeric nanoparticulate drug delivery system*. *Colloids and Surfaces B: Biointerfaces*, 2006. **47**(1): p. 90-97.
366. Cohen-Sela, E., et al., *A new double emulsion solvent diffusion technique for encapsulating hydrophilic molecules in PLGA nanoparticles*. *Journal of Controlled Release*, 2009. **133**(2): p. 90-95.
367. Golovastov, V.V., N.I. Mikhaleva, and M.A. Nesmeyanova, *Depletion of phosphatidylethanolamine--the major membrane phospholipid of Escherichia coli--depresses posttranslocational modification of alkaline phosphatase in the periplasm*. *Biochemistry*, 2002. **67**(7): p. 765-9.
368. Fernandes, M.M., et al., *Effect of thiol-functionalisation on chitosan antibacterial activity: Interaction with a bacterial membrane model*. *Reactive and Functional Polymers*, 2013. **73**(10): p. 1384-1390.
369. Dynarowicz-Łątka, P., A. Dhanabalan, and O.N. Oliveira Jr, *Modern physicochemical research on Langmuir monolayers*. *Advances in Colloid and Interface Science*, 2001. **91**(2): p. 221-293.
370. Dennison, S.R., et al., *Investigations into the ability of the peptide, HAL18, to interact with bacterial membranes*. *Eur Biophys J*, 2008. **38**(1): p. 37-43.
371. Cheng, C.-Y., et al., *Nature of Interactions between PEO-PPO-PEO Triblock Copolymers and Lipid Membranes: (II) Role of Hydration Dynamics Revealed by Dynamic Nuclear Polarization*. *Biomacromolecules*, 2012. **13**(9): p. 2624-2633.
372. Verma, A. and F. Stellacci, *Effect of Surface Properties on Nanoparticle-Cell Interactions*. *Small*, 2010. **6**(1): p. 12-21.
373. Allahverdiyev, A.M., et al., *Coping with antibiotic resistance: combining nanoparticles with antibiotics and other antimicrobial agents*. *Expert review of anti-infective therapy*, 2011. **9**(11): p. 1035-1052.

Appendix: Scientific Contribution

Peer reviewed publications

Fernandes M M, **Ivanova K**, Francesko A, Mendoza E, Tzanov T. "Immobilization of antimicrobial core-shell nanospheres onto silicone for prevention of *Escherichia coli* biofilm formation". *Process Biochemistry*, 2016, doi: 10.1016/j.procbio.2016.09.011.

Fernandes M M, **Ivanova K**, Francesko A, River D, Torrent-Burgués J, Gedanken A, Mendonza E, Tzanov T. "Escherichia coli and Pseudomonas aeruginosa eradication by nano-penicillin G." *Nanomedicine: Nanotechnology, Biology and Medicine*, 2016, 12, 2061-2069, doi:10.1016/j.nano.2016.05.018

Francesko A, Fernandes M M, **Ivanova K**, Amorim S, Reis R L, Pashkuleva I, Mendoza E, Pfeifer A, Heinze T, Tzanov T. "Bacteria-responsive multilayer coatings comprising polycationic nanospheres for bacteria biofilm prevention on urinary catheters", *Acta Biomaterialia*, 2016, <http://dx.doi.org/10.1016/j.actbio.2016.01.020>

Ivanova K, Fernandes M M, Francesko A, Gueguez J, Burnet M, Mendonza E, Tzanov T. "Quorum quenching and matrix degrading enzymes in multilayer coatings synergistically prevent bacterial biofilm formation on urinary catheters", *ACS Applied Materials & Interfaces*, 2015, DOI: 10.1021/acsami.5b09489, <http://pubs.acs.org/articlesonrequest/AOR-C2ftuuKenNNQY6f4kPSS>.

Ivanova K, Fernandes M M, Mendonza E, Tzanov T. "Enzyme multilayer coatings inhibit Pseudomonas aeruginosa biofilm formation on urinary catheters", *Applied Microbiology and Biotechnology*, 2015, DOI: 10.1007/s00253-015-6378-7.

Thallinger B, Brandauer M, Burger P, Sygmund C, Ludwig R, **Ivanova K**, Kun J, Scaini D, Burnet M, Tzanov T, Nyanhongo G, Guebitz G. "Cellobiose dehydrogenase functionalized urinary catheter as novel antibiofilm system", *Journal of Biomedical Materials Research Part B: Applied Biomaterials*, 2015, DOI: 10.1002/jbm.b.33491.

Book chapters

Ivanova K, Ramon E, Hoyo J, Tzanov T. "Innovative Approaches for Controlling Clinically Relevant Biofilms: Current Trends and Future Prospects." In "*Current Topics in Medicinal Chemistry on Recent Advances in Anti-biofilm Strategies*". Vol. 17, No. 0, 2017

Ivanova K, Fernandes MM, Tzanov T. Strategies for silencing bacterial communication, in "*Quorum sensing vs quorum quenching: a battle with no end in sight*", edited by Kalia, VC, Springer India, 2015.

Ivanova K, Fernandes MM, Tzanov T. Current advances on bacterial pathogenesis inhibition and treatment strategies, in "*Microbial pathogens and strategies for combating them: science, technology and education*", edited by Mendez-Vilas, A, Formatex Research Center, 2013.

Communications to meetings

Tzanov T, **Ivanova K**, Petkova P, Ramon E, Fernandes M, Blanco C, "Antibacterial approaches from materials engineering perspective – enzymes on work" (oral), 251st American Chemical Society National Meeting & Exposition, March 13-17, 2016, San Diego (USA)

Ivanova K, Metieva M, Tzanov T, "Enzymatically-crosslinked multilayer antioxidant/nanoantibiotic coatings for prevention of bacterial biofilms" (oral), 251st American Chemical Society National Meeting & Exposition, March 13-17, 2016, San Diego (USA)

Ivanova K, Fernandes MM, Francesko A, Tzanov T. "Alternative approaches for prevention of *Pseudomonas aeruginosa* biofilm formation on urinary catheters" (oral), The international chemical congress of pacific basin societies (PACIFICHEM), December 15-20, 2015, Honolulu, Hawaii (USA)

Ivanova K, Fernandes MM, Francesko A, Tzanov T. "Quorum quenching and matrix degrading enzymes in multilayer coatings prevent bacterial biofilm formation on urinary catheters" (oral), Conference 2015 Advances in Functional Materials, June 29 - July 3, 2015, Stony Brook, USA

Ivanova K, Fernandes MM, Tzanov T. "Sonochemical coatings of acylase nanoparticles inhibit *Pseudomonas aeruginosa* biofilm formation and virulence factors production" (oral), International Symposium on Quorum Sensing Inhibition, June 3-5, 2015, Santiago de Compostela (Spain)

Ivanova K, Fernandes MM, Francesko A, Tzanov T. "Enzyme multilayer coatings prevent bacterial biofilm formation on urinary catheters" (oral), 249th ACS National Meeting & Exposition, March 22-26, 2015, Denver (USA)

Fernandes MM, **Ivanova K**, Francesko A, Tzanov T. "Convectonal antibiotics in form of nanospheres prevent biofilm formation and provide infection control" (oral), III International Conference on Antimicrobial Research (ICAR 2014), October 1-3, 2014, Madrid (Spain)

Ivanova K, Fernandes MM, Tzanov T. "Enzyme-based nanoparticles to inhibit bacterial biofilm formation in urinary catheters" (oral), 8th International Conference on Polymer and Fiber Biotechnology (IPFB 2014), May 25-27, 2014, Braga (Portugal)

Rocasalbas G, **Ivanova K**, Petkova P, Tzanov T. "Solid-liquid surface functionalization of biopolymeric platforms with plant-derived polyphenols" (poster), 245th ACS National Meeting, April 07-11, 2013, New Orleans (USA)

Ivanova K, Fernandes MM, Tzanov T. "Enzymes to control bacterial biofilm formation" (poster), 245th ACS National Meeting, April 07-11, 2013, New Orleans (USA)

Ivanova K, Fernandes MM., Tzanov T. "Enzymatic-induced degradation of bacterial biofilms" (oral), E-MRS 2012 Fall Meeting, September 17-21, 2012, Warsaw (Poland)

Awards

Best student oral communication to the contribution entitled "Sonochemical coatings of acylase nanoparticles inhibit *Pseudomonas aeruginosa* biofilm formation and virulence factors production", I International Symposium on Quorum Sensing Inhibition, June 3-5, 2015, Santiago de Compostela (Spain)